New Ultrasound Techniques for Detection and Management of Pulmonary Vascular Disease

By

Leah Wright

Submitted in fulfilment of the requirements for the Degree of Doctor of Philosophy (Medical Research)

Menzies Research Institute Tasmania

University of Tasmania

The research work presented in this thesis was supervised by:

Primary supervisor

Professor Thomas Hugh Marwick, MBBS, MPH,PhD

Baker Heart and Diabetes Institute

Melbourne, Australia

Co-supervisor

Dr Nathan Dwyer MBBS, PhD

School of Medicine

University of Tasmania

Hobart, Australia

Declaration of originality

This thesis contains no material which has been accepted for a degree or diploma by the University or any other institution, except by way of background information and duly acknowledged in the thesis, and to the best of my knowledge and belief no material previously published or written by another person except where due acknowledgement is made in the text of the thesis, nor does the thesis contain any material that infringes copyright.

Name: Leah Michelle Wright

Signed: …… Date:……30/12/2017……

Statement of authority of access

The publishers of the papers comprising Chapters 1, 4, 5 and 7 hold the copyright for that content, and it is likely that Chapters 3, 6, 8 and 9 will be published by the time that the thesis is examined. Access to the material should be sought from the respective journals. The remaining unpublished content of this thesis may be made available for loan and limited copying in accordance with the *Copyright Act 1968*.

Name: Leah Michelle Wright

Signed: …… … Date:30/12/2017……

Statement of ethical conduct

The research activities associated with this thesis complied with "Australian Code for the Responsible Conduct of Research", "National Statement of Ethical Conduct in Human Research", "Guidelines for the prevention, detection and management of Chronic heart failure in Australia 2011", and Regulator and the rulings of the Safety, Ethics and Institutional Biosafety Committees of the University.

The Tasmania Human Research Ethics Committee (HREC) approved this project (Approval number H0014899, Assessment of Subclinical Right Ventricular dysfunction in Pulmonary Hypertension), and Metro Health South (QLD) HREC (Approval number HREC/16/QPAH/008 Assessment of Subclinical Right Ventricular dysfunction in Pulmonary Hypertension). Chapter 11 was approved by the Tasmania HREC (Approval number H0014031, Peripheral Endothelial Function Assessment in Scleroderma Patients).We obtained written participant informed consent from all participants.

Name: Leah Michelle Wright

Signed: … Date: 30/12/2017……

Abstract

Background. Pulmonary arterial hypertension (PAH), a rare condition of raised blood pressure in the lungs, is a debilitating disease with considerable morbidity and mortality. Clinical diagnosis is through an assessment of pulmonary artery pressures. The condition is treatable, but medications are expensive and not always practical, thus echocardiographic evidence of treatment response is used to rationalise ongoing therapy. However, outcome studies have now shown that invasive and echocardiographic pressures do not strongly associate with outcome.

Aims. The thesis proposes that a variety of echocardiographic markers, including those of right ventricular (RV) systolic function, are more indicative of patients' clinical status than currently used methods for assessing pressures, and six-minute walk (6MW) distance. Assessment of myocardial deformation (strain) is now accessible at the bedside using echocardiographic speckle tracking. I seek to determine how to use this measure throughout the treatment course, and how RV free wall strain relates to outcome in a clinical setting. The goal of this thesis is to determine where and how strain (especially RV strain) fits in the clinical decision process.

Methods. A review of echocardiographic methods in regards to RV assessment with echocardiography was undertaken. Following ethics clearance, the majority of patient recruitment was from the Tasmanian Pulmonary Hypertension Registry (Hobart, Australia) Tasmanian Scleroderma Database (Hobart, Australia), and the Princess Alexandra Hospital (Brisbane, Australia). All echocardiographic measurements were performed in accordance with recommended echocardiographic guidelines. Statistical analysis was performed primarily with SPSS (version 21, IBM,

Chicago, IL) and MedCalc software version 16.8.4 (MedCalc Software bvba, Ostend, Belgium).

Results. **First**, in PAH, baseline RV function (RVFWS) is a strong predictor of outcome, independent of PASP. Changes throughout therapy appear minimal, and the prognostic value of change appears limited. **Second**, Afterload changes should be taken into account in the evaluation of RVFWS during PAH follow-up, with the relationship to PASP likely to be linear. **Third**, RVFWS is more predictive than RVEDA and less variable than FAC in distinguishing acute from chronic RV pressure overload. RVFWS adds incremental and independent information to standard measures of RV function in assessing the acuity of PH. **Fourth**, RVFWS is strongly associated with exercise capacity in PAH and ise a useful adjunct to the assessment of treatment response. **Fifth,** RV dysfunction was associated with adverse outcome, independent of and incremental to clinical and LV deformation parameters in SSc. Subclinical LV dysfunction appears to have less prognostic relevance than RV dysfunction. **Sixth**, the detection of post-capillary PH appears to be better predicted with LV markers than recently recommended algorithms for detecting raised PCWP. **Seventh**, right atrial strain was significantly different between those with normal versus raised pressure, but it did not identify those with an incorrect echocardiographic assessment of RAP. **Eighth**, LV markers were associated with changes in PCWP after fluid loading. RV function showed a weak association with raises in PAPm. Myocardial deformation was not associated with a rise in filling pressure after fluid loading. **Ninth**, microvascular disease appears to be related to be related to RV function in PAH. Macrovascular disease appears to relate to traditional heart disease factors such as LV mass. Endothelial function markers do not appear to be interchangeable in assessing patient outcome.

Conclusions:

New echocardiographic markers of RV systolic function offer a significant increment of prognostic information in PAH. The measurement of RV free wall strain aids in clinical decision-making and integration daily clinical practice is needed. We have found that in a group with a high rate of PAH, current guidelines do not offer strong guidance on the differentiation of LV and pulmonary vascular aetiologies for PH. Although RA speckle tracking is associated with RAP, it did not appear to add in the correction of pressure assessment. Speckle tracking imaging also shows potential in systemic CTD, exposing unique fibrosis patterns in the LV. Vascular function had associations with echocardiographic LV and RV parameters, but heterogeneity in this population hinder its use as a robust discriminative marker. Speckle tracking echocardiography does not appear to detect elevations of invasive PCWP. This work shows that RV free wall strain is now ready for prime time and integration into the clinical decision-making process.

Acknowledgments

This research was kindly supported by the National Heart Foundation of Australia, through their Health Professional Scholarship. I would also like to thank the American Society of Echocardiography, Cardiac Society of Australia and New Zealand and Professionals in Cardiac Science for awards, which have helped me to fund conference travel.

This thesis has had the help of many different departments and organisations. Initially, the University of Queensland Centre for Cardiac Imaging, where I initially trained in echocardiography and research skills, and the Princess Alexandra Echocardiography Department for their assistance in learning clinical echocardiography.

Staff, and other PhD students at the Menzies Institute for Medical Research for their assistance with starting my thesis. A very big thank you to Dr Kazuaki Negishi, for always offering his assistance when needed. Hilda Yang, for being my comrade sonography/PhD student throughout this experience. A big thank you to the Royal Hobart Hospital Department of Cardiology, specifically Dr Paul McIntyre and Janette Power, for always being supportive of mixing research and clinical work. My co-supervisor Dr Nathan Dwyer, for all of his experience and clinical knowledge of the pulmonary hypertension cohort, and help with formatting papers and this thesis.

Finally, I would like to thank Baker Heart and Diabetes Institute for enabling me to complete my thesis while being based in Melbourne. A massive thankyou to Lisa Riddell, who helped for many years with coordinating supervisor meetings, conference travel, and poster printing amongst many other things.

A big thank you to my primary supervisor Professor Tom Marwick, for encouraging me to enrol, and (patiently!) guiding me through the process.

Finally, thank you to my friends and family for their encouragement and support throughout.

Table of Contents

List of Tables

List of Figures

Abbreviations

3DE- three dimensional echocardiography

6MW - Six minute walk

AF – atrial fibrillation

BSA – body surface area

CAD – coronary artery disease

CCBs - Calcium channel blockers

CHD- Congenital heart disease

CMR – cardiac magnetic resonance imaging

CO – cardiac output

CTD – connective tissue disease

CTEPH – chronic thromboembolic pulmonary hypertension

DICOM - digital imaging and communication in media

EF – Ejection fraction

Ea- arterial elastance

MV E - mitral valve early peak velocity

Mv A - mitral valve atrial contraction velocity

MV e' - Peak mitral early contraction velocity

Ees- end-systolic elastance

ESP - end systolic pressure

ESV- end systolic volume

FAC – fractional area change

HR – heart rate

IVCT - isovolumetric contraction

IVV - isovolumetric contraction velocity

IVRT - isovolumetric relaxation time

IVS - interventricular septum

IVC – inferior vena cava

JVP – jugular venous pressure

LAV - left atrial volume

LV – left ventricle

PAPm-mean pulmonary artery pressure (invasively derived)

mRAP- mean right atrial pressure (invasively derived)

PAPs- pulmonary artery systolic pressure

PAH – Pulmonary arterial hypertension

PASP- pulmonary artery systolic pressure

PCWP- pulmonary capillary wedge pressure

PH – Pulmonary hypertension

PV – pulmonary valve

PVR – Pulmonary vascular resistance

RA – right atrium

RA ƐCT- RA contraction strain

RA ƐR- RA reservoir strain

RA ƐCD -RA conduit function

RAP – right atrial pressure

RHC – right heart catheterisation

RHH - Royal Hobart Hospital

RV – Right ventricular

RV IVA- right ventricular isovolumetric acceleration

RVS'- Right ventricular peak systolic velocity

RVEDA – right ventricular end diastolic area

RVESA – right ventricular end systolic area

RVFWS - RV free wall strain

RVOT VTI- right ventricular outflow tract velocity time integral, equivalent to RV stroke volume

sPAP- systolic pulmonary artery pressure (invasively derived)

SSC- systemic sclerosis

stroke volume - SV

TPG – transpulmonary gradient

TR – tricuspid regurgitation

WU – Wood Units

Publications and presentations relating to thesis

Published/accepted/submitted papers to peer-reviewed journals

Chapter	Publication	Status
1. Introduction	Wright LM, Dwyer N, Celermajer D, Kritharides L, Marwick TH. Follow-Up of Pulmonary Hypertension With Echocardiography. JACC Cardiovasc Imaging. 2016 Jun;9(6):733-46.	Published 2016
2. Methods	N/A	
3. RV strain and prognosis	Relative Importance of Baseline and Longitudinal Evaluation in the Follow-up of Vasodilator Therapy in Pulmonary Arterial Hypertension	Submitted JACCi 2017
4. Load-dependence of RV strain	Wright L, Negishi K, Dwyer N, Wahi S, Marwick TH. Afterload Dependence of Right Ventricular Myocardial Strain. J Am Soc Echo 2017 Jul;30(7):676-684.	Published 2017
5. Acute and chronic PHT and remodelling	Wright et al. Right Ventricular Systolic Function Responses to Acute and Chronic Pulmonary Hypertension: Assessment with Myocardial Deformation. J Am Soc Echocardiogr. 2016 Mar;29(3):259-66.	Published 2016
6. RV strain and 6MW	Association of Right Ventricular Strain with Exercise Capacity in	Submission Journal of the American Society of

	Pulmonary Arterial Hypertension	Echocardiography 2017. Response to reviewer comments sent.
7. Post-capillary PHT and LV strain	Saito M. Mechanics and prognostic value of left and right ventricular dysfunction in patients with systemic sclerosis. JACC Cardiovasc Imaging. 2016	Published 2016
8. Post-capillary PHT and LV diastology	Echocardiographic Evaluation of Dyspnoea in the Context of Diastolic Evaluation Guidelines: Implications for Evaluation of Pulmonary Arterial Hypertension	Submission Heart Lung Circulation 2017 Response to reviewer comments sent
9. PA pressure and RA strain	Association with Right Atrial Strain with Right Atrial Pressure: An Invasive Validation Study	Under review Echo research and practice 2017 Response to reviewer comments sent
10. RV strain vs fluid response in preclinical disease		
11. Vascular markers and preclinical disease		
12. Conclusion		

Statement of authorship

This thesis includes several papers, in which Leah Wright (LW) is not the sole author. LW took the lead in this research. She designed the studies, collecting the data, measuring echo parameters, performed analyses, interpreted the findings and prepared the manuscripts, with contributions from the co-authors.

The contributions of each of the authors are detailed as follows.

Chapter 1

Wright LM, Dwyer N, Celermajer D, Kritharides L, Marwick TH. Follow-Up of Pulmonary Hypertension with Echocardiography. JACC Cardiovasc Imaging. 2016 Jun;9(6):733-46.

- LW contributed to narrative review concept design, performing analyses, composed the drafts of manuscript and revisions of the manuscript.
- ND contributed to concept input and revised the manuscript
- JP contributed to concept input and revised the manuscript
- LK contributed to concept input and revised the manuscript
- DC contributed to concept input and revised the manuscript
- THM contributed to the design of the review, critical revision and final approval.

Chapter 3.

Wright LM, Dwyer N, Wahi S,, Marwick TH. Importance of Baseline and Longitudinal Evaluation in the Follow-up of Vasodilator Therapy in Pulmonary Arterial Hypertension.

- LW contributed to narrative review concept design, performing analyses, composed the drafts of manuscript and revisions of the manuscript.
- ND contributed to data acquisition and revised the manuscript
- SW contributed to data acquisition and revised the manuscript
- THM contributed to the design of the study, interpreting findings, critical revision and final approval.

Chapter 4:

Leah Wright, Kazuaki Negishi, Nathan Dwyer, Sudhir Wahi; Thomas H Marwick. Afterload-Dependence of Right Ventricular Myocardial Strain. J Am Soc Echo 2017 (30(7)676-684 e1)

The contributions of each author are as following:

- LW contributed to study design, data extraction, performing analyses, interpreting findings, composed the drafts of manuscript and revisions of the manuscript.
- KN contributed to , interpretation of finding and revised the manuscript
- ND contributed to data extraction, provided statistical expertise analysis and revised the manuscript
- SW contributed to data acquisition and revised the manuscript
- THM contributed to the design of the study, interpreting findings, critical revision and final approval.

Chapter 5

Wright L, Dwyer N, Power J, Kritharides L, Celermajer D, Marwick TH. "Right Ventricular Systolic Function Responses to Acute and Chronic Pulmonary Hypertension: Assessment with Myocardial Deformation". J Am Soc Echocardiogr. 2016 Mar;29(3):259-66. doi: 10.1016/j.echo.2015.11.010.

The contributions of each author are as following:

- LW contributed to study design, data extraction, performing analyses, interpreting findings, composed the drafts of manuscript and revisions of the manuscript.
- ND contributed to data acquisition and revised the manuscript
- JP contributed to data acquisition and revised the manuscript
- LK contributed to , interpretation of finding and revised the manuscript
- DC contributed to interpretation of finding and revised the manuscript
- THM contributed to the design of the study, interpreting findings, critically revision and final approval.

Chapter 6

Wright LM, Dwyer N, Wahi S, Marwick TH. Importance of Baseline and Longitudinal Evaluation in the Follow-up of Vasodilator Therapy in Pulmonary Arterial Hypertension. Association of Right Ventricular Strain with Exercise Capacity in Pulmonary Arterial Hypertension

- LW contributed to narrative review concept design, performing analyses, composed the drafts of manuscript and revisions of the manuscript.
- ND contributed to data acquisition and revised the manuscript

- SW contributed to data acquisition and revised the manuscript
- THM contributed to the design of the study, interpreting findings, critical revision and final approval.

Chapter 7

Makoto Saito, Leah Wright *, Kazuaki Negishi MD, PhD[1], Nathan Dwyer, Thomas H Marwick. Mechanics and Prognostic Value of Left and Right Ventricular Dysfunction in Patients with Systemic Sclerosis*Joint first authors. Journal of the American College of Cardiology; Imaging; Aug; 2017*

The contributions of each author are as following:

- LW contributed to study design, data extraction, performing analyses, interpreting findings, composed the drafts of manuscript and revisions of the manuscript.
- MS contributed to study design, data extraction, performing analyses, interpreting findings, composed the drafts of manuscript and revisions of the manuscript.
- KN contributed to , interpretation of finding and revised the manuscript
- ND contributed to data acquisition, interpretation of finding and revised the manuscript
- THM contributed to the design of the study, interpreting findings, critical revision and final approval

Chapter 8

Wright LM, Dwyer N, Wahi S, Marwick TH.PAH differential diagnosis; Echocardiography for the Differential diagnosis of pre versus post capillary pulmonary arterial hypertension

- LW contributed to narrative review concept design, performing analyses, composed the drafts of manuscript and revisions of the manuscript.
- ND contributed to data acquisition and revised the manuscript
- SW contributed to data acquisition and revised the manuscript
- THM contributed to the design of the study, interpreting findings, critical revision and final approval.

Chapter 9

Wright LM, Dwyer N, Wahi S, Marwick TH . Right atrial pressure estimation with echocardiography

- LW contributed to narrative review concept design, performing analyses, composed the drafts of manuscript and revisions of the manuscript.
- ND contributed to data acquisition and revised the manuscript
- SW contributed to data acquisition and revised the manuscript
- THM contributed to the design of the study, interpreting findings, critical revision and final approval.

Abstracts/ Presentations at national or international conferences

Cardiac Society of Australia and New Zealand 2017

- Oral presentation "*Pulmonary Arterial Hypertension and outcome; How does baseline RV function compare to sequential follow up for predicting outcome?*"

American Society of Echocardiography 2017

- Oral presentation "*Progression of Pulmonary Artery Pressure and RV Function as Predictors of Outcome in Pulmonary Arterial Hypertension*"

American College of Cardiology 2016

- *Determinants of Overt and Masked Pulmonary Hypertension in Scleroderma*
- *Distinction of Pre- versus Post-capillary Pulmonary Arterial hypertension*
- *Importance of Right Atrial Conduit Function to Right Atrial Pressure Estimation with Echocardiography: A Role for Atrial Strain Assessment*

American Heart Association 2016

- *Are All Diastolic Parameters Equal***?**

American Society of Echocardiography 2016

- *Brachial Flow-Mediated Dilatation is Associated with Pulmonary Artery Pressure in Scleroderma*
- *Endothelial Function as a Potential Marker for Pulmonary Hypertension in Scleroderma*
- *Use of Isovolumetric Acceleration as an Afterload-Independent Marker of RV Dysfunction in Scleroderma*

Cardiac Society of Australia and New Zealand 2016

Is Provocative Testing Necessary for Diagnosis of Heart Failure with Preserved Ejection Fraction? A Comparison with Non-invasive Haemodynamics and Myocardial Mechanics

Cardiac Society of Australia and New Zealand 2015

- *Baseline RV Function is a stronger predictor of Response to Vasodilators in Pulmonary Hypertension than Six-Minute Walk*

European Society of Cardiology 2015

- *Independent Association of Right Ventricular Strain with Functional Strain with Functional Capacity in Pulmonary Arterial Hypertension*

American Society of Echocardiography 2014

- *Right Ventricular Free Wall Strain can Discriminate Acute Pressure Overload from Chronic Conditions*

European Society of Cardiology 2014 (moderated Poster)

- *Right Ventricular Free Wall Strain can Discriminate Acute Pressure Overload from Chronic Conditions*

World Congress of Cardiology 2014

- *Nonlinear Afterload Dependence of RV Strain: A Follow-up Study During Vasodilator Therapy*

American Heart Association 2013

- *Nonlinear Afterload-dependence of RV strain: A Follow-up Study During Pulmonary Vasodilator Therapy*

Structure of the thesis

Chapter 1 reviews the use of echocardiography in the clinical follow-up of pulmonary arterial hypertension. A review is performed of papers documenting the response of echocardiographic parameters to the initiation of PAH therapy, and current evidence relating to RV parameters and outcome. Considerations in the clinical use of different haemodynamic and RV size and systolic function measurements are assessed. This section introduces the concept that using RV free wall strain for follow-up in pulmonary arterial hypertension is clinically appropriate, and offers substantial benefit over non-invasive haemodynamic assessment, as well as traditional measures of right ventricular systolic function.

Chapter 2 provides a review of the methods. A comprehensive explanation is given of standard 2D echocardiographic performance of right heart size, systolic function and haemodynamic assessment. Left ventricular systolic and diastolic assessment measurement are summarised. A review of speckle tracking imaging of left and right ventricles and right and left atria follow. Statistical techniques are detailed, with specific details on techniques used in each chapter.

The cohort of patients recruited for this thesis are from two primary referral centres the Royal Hobart Hospital (Tasmania) and the Princess Alexandra (Queensland). From the Royal Hobart Hospital four cohorts were recruited; Tasmanian Pulmonary Hypertension registry (PAH Tas), Tasmanian scleroderma database (TAS SSC, the Royal Hobart Hospital Echocardiographic database and the Royal Hobart Hospital catherisation lab database. The Queensland cohort was identified from the Pulmonary Hypertension database required for PBS supplied therapy.

The central tenet of this thesis is that decision-making in pulmonary hypertension requires more than an assessment of pulmonary pressure. **Chapter 3** documents the association of baseline RV free wall strain with mortality in PAH, but also shows the limitations of attempting to follow changes in echocardiographic parameters in follow-up. Finding this limitation is an essential observation because some studies measuring outcome in PAH have come under criticism for using poorly defined endpoints. There can be significant learning effects with functional tests, with often overlooked complex interactions that lead to reductions in exercise capacity.

Myocardial strain is afterload-dependent. Establishment of the relationship between RV afterload and systolic function is required to integrate RV strain into clinical practice. **Chapter 4** addresses this concern in a clinical cohort and demonstrates how best to adjust for the relationship through follow-up.

The chronicity of afterload increase (e.g. chronically elevated afterload in pulmonary arterial hypertension, as opposed to the acute elevation as seen in pulmonary embolism) may influence the RV response to loading. **Chapter 5** demonstrates the value of RV free wall strain in differentiating in these two conditions.

Exercise capacity – measured as 6MW distance – has been a cornerstone of assessing pulmonary vasodilator responses. Recent work has cast doubt on the value of 6-minute walk (6MW) distance as an outcome marker to determine treatment efficacy. The use of haemodynamics as a surrogate for functional status simplifies the determinants of exercise capacity in PAH patients. Cardiopulmonary exercise testing shows an only moderate correlation between exercise capacity and invasive haemodynamics. **Chapter 6** examines the associations of RV free wall strain and 6MW distance.

Pulmonary hypertension may have several potential aetiologies – an important distinction being pre- and post-capillary pulmonary hypertension, because patients with post-capillary pulmonary hypertension do not respond to pulmonary arterial vasodilators. Patients with connective tissue disease may have left- or right-sided pathophysiology. **Chapter 7** explores the use of not only RV but also LV strain in patients with systemic sclerosis and shows that an abnormal LV myocardial signal provides a source of information regarding post-capillary disease, that is separate from the usual haemodynamic measures. Moreover, **chapter 8** emphasises the limitations of the current guidelines for the diagnosis of diastolic dysfunction, especially as it pertains to the distinction of post-capillary pulmonary hypertension. This chapter involves a cohort in which pulmonary hypertension groups are distinguished with right heart catheterisation.

Part of the problem with echocardiographic measurement of pulmonary artery systolic pressure (PASP) is that it is obtained by combining RV and estimated right atrial (RA) pressure. Inferior vena cava (IVC) size is traditionally used to calculate right atrial pressure. The IVC method has inaccuracies which can compromise the accuracy of estimation of pulmonary a (PA) pressure. **Chapter 9** explores whether RA strain can improve the accuracy of echocardiographic assessment of RA pressure. Unfortunately, this chapter shows that this novel tool is unable to adjust for errors in the echocardiographic assessment of right atrial pressure (RAP).

Having shown that RV assessment provides incremental prognostic information and is robust to small changes in afterload, we next sought whether this could be used for the identification of early disease. **Chapter 10** evaluates the response to echocardiographic predictors of response to fluid loading during right heart catheterisation in an at-risk population, with particular attention to the information

provided by measurement of left ventricular strain. The results suggest that while RV strain is a marker of clinical disease, provocative testing identifies abnormal responses in patients with preserved RV strain.

Apart from fluid loading, tests of the peripheral vasculature might be another means of detection of early disease in pulmonary arterial hypertension, in some disease entities that involve both the pulmonary and systemic vasculature. It is possible that the small vessel disease in the lungs associated with small vessel disease elsewhere – in which case the measurement of this parameter may help with diagnosis and following response to therapy. **Chapter 11** establishes the correlates of novel vascular markers in patients with and without established PAH.

The thesis shows the limitations of PASP measurements, the robustness of RV strain (especially relative to afterload) and the association of RV strain with functional capacity, and emphasises the utility of considering not only RV but also LV strain responses.

Figure xxxix.1. Flowchart of cohorts involved in thesis chapters.

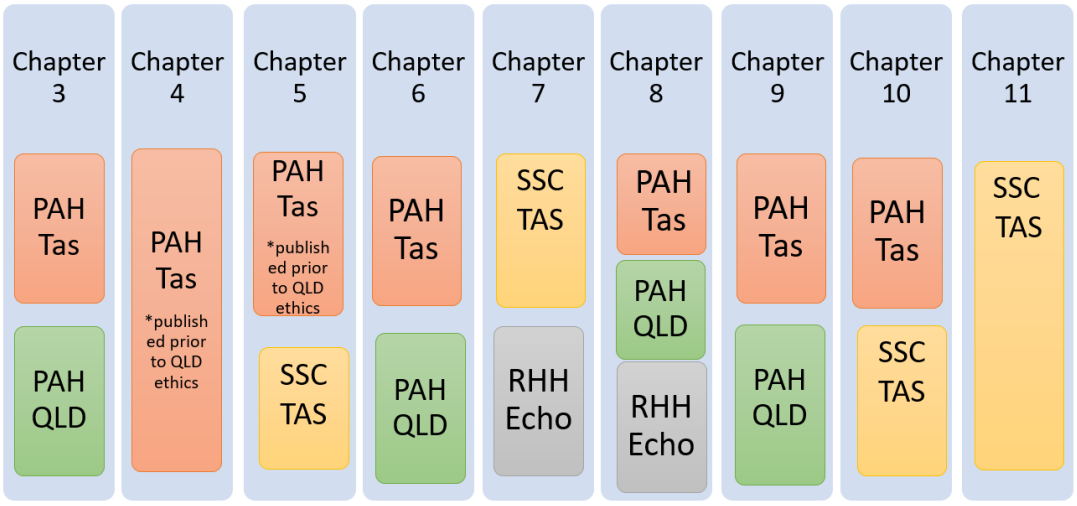

The majority of studies focused on the Pulmonary Hypertension cohort of Tasmania (PAH Tas), Tasmanian scleroderma database (TAS SSC), the Royal Hobart Hospital Echocardiographic database and the Royal Hobart Hospital catherisation lab database. A second cohort was collected from the Princess Alexandra Hospital (PAH QLD).

Aims

The aims of this thesis are:

- To define the optimal method for follow-up in pulmonary hypertension. We propose that the use of right ventricular strain will add substantially to traditional right ventricular function markers.
- Examine whether right atrial strain measurements can be used to improve the diagnostic accuracy of RAP estimation using the IVC method for estimation of pressure
- Determine how RV free wall strain can be used to track systolic function over a range of afterload conditions
- Examine how global and regional systolic strain can be used to differentiate acute versus chronic increases in afterload
- Determine the frequency and prognostic relevance of RV dysfunction at baseline in PAH
- Determine the frequency of change in RV parameters in follow-up and their prognostic relevance
- Discover whether RV myocardial deformation is incrementally predictive of functional capacity above haemodynamic measures
- Determine the predictive ability of left ventricular versus right ventricular myocardial deformation in a connective tissue disease cohort
- Determine the effectiveness of current guidelines for prediction of Pre versus post-capillary pulmonary arterial hypertension within a substantial connective tissue disease cohort.
- Determine whether microvascular function testing results in SSC is a surrogate for disease endpoints in pulmonary hypertension

The goal of this thesis is to determine the role of right ventricular strain in the clinical management of pulmonary hypertension

Chapter 1

Introduction

Article “Follow-Up of Pulmonary Hypertension With Echocardiography” was published in

Journal of the American College of Cardiology; Cardiovascular Imaging 2016 Jun;9(6):733-46

Wright LM, Dwyer N, Celermajer D, Kritharides L, Marwick TH.

1 Introduction

1.1.1 Basic physiology

The heart is designed to be a conduit and a pump, with the right heart acting as an intermediary between the venous system and lungs. For this purpose, the right ventricle (RV) is designed to act as a conduit for venous blood, and pump against the low resistance within the pulmonary arteries, where blood is oxygenated and then delivered to the left heart. Pulmonary hypertension (PH) an increase in pressure within the pulmonary arteries, which opposes the RV's inherent design of a low resistance pump. This rise in pressure can come from diverse pathologic origins, described in the WHO classification system, in which there are five groups of PH. Post-capillary PH (Group 2) is due to left heart changes, with a transfer of hydrostatic pressure causing an elevation in the pulmonary arteries. The characteristics of PAH (Group 1) are intimal proliferation, smooth muscle hypertrophy, in-situ thrombosis and the development of plexiform lesions in the small pulmonary arterioles. Generally regarded as idiopathic, there are conditions associated with an increased risk of developing PAH, such as the connective tissue disease (CTD) related more commonly with systemic sclerosis (SSC), as well as human immunodeficiency virus (HIV) related, congenital heart disease (CHD) related, and heritable forms. Until a decade ago, limited treatment options existed, with median life expectancy being 2.8 years from diagnosis [1], but current registry data show increases to 7 years [2]. There have been three primary pathways identified for treatment, endothelin receptor antagonism, prostacyclin augmentation and nitric oxide augmentation. The diagnosis and follow-up of pulmonary arterial hypertension (PAH) involves the use of echocardiography, right heart catheterisation (RHC) and patient functional status with 6-minute walk testing (6MW).

Invasively, the response of the RV to changes in pressure are documented by RV pressure-volume loop studies. The RV responds with high compliance (as compared to the left ventricle

(LV)). To accommodate load changes, the RV dilates to increase stroke volume, in agreeance with the Frank-Starling. Larger volumes are required to stimulate this than the LV. This curve underpins the RV response to loading.

A clinical classification[3] has been established, with groupings based on pathological and hemodynamic characteristics. 5 groups with the term "pulmonary hypertension" are defined; Group 1 PAH, Group 2, PH due to left heart disease, Group 3, PH due to chronic lung disease and/or hypoxia, Group 4, PH due to chronic thromboembolic pulmonary hypertension (CTEPH), and Group 5, PH due to unclear or multifactorial mechanisms

This thesis will mainly focus on two groups, Group 1 PAH and Group 2 PH. Group 2 PH consists of patients with left heart disease-related pathogenesis. Classically PH is associated with advanced heart failure (both heart failure with reduced and preserved systolic function), and mitral valve disease. Downstream pulmonary venous congestion leads to increases in pulmonary pressures and progression to right heart disease. The association between development of PH and mortality in the left heart failure cohort [4] is an established concept.

1.1.2 Epidemiology

Within Group 1 PAH, the epidemiologic data presented by different registries vary slightly. The French registry describes the populations as 40% idiopathic PAH, CTD associated ~ 15%, and ~11% with CHD related PH. Another potent clinical influence on survival is the concomitant of interstitial lung disease. Although the cost-effectiveness of screening CTD patients routinely has been argued, treating patients in WHO class 2 with PAH-specific therapies has been shown to be beneficial in this cohort, with patients deriving symptomatic benefit[5]. An argument for early screening is made for those at risk of PAH, for example, CTD patients or people with a family history of PAH.

The insidious onset of PAH (non-specific feelings of breathlessness, fatigue or exercise impairment) means patients are diagnosed in late stages. Tracking disease development in PAH is more difficult than in LV disease progression, as patients often already present in overt right heart failure. Another cohort which is of interest concerns those with SSC. SSC is a disease manifested by fibrosis and thickening of the skin, which is associated with endothelial dysfunction and organ disease. There is an increased risk of developing PAH within this cohort (~ 15% prevalence). In contrast to CHD-associated, SSC-associated PAH has higher mortality rates. Guidelines recommend routine echocardiographic screening the SSC cohort, but current methods of early diagnosis do not appear to be sufficient. The tricuspid regurgitant (TR) jet, required for the echocardiographic estimation of PASP, is unmeasurable in ~20-40%[6,7] of people, and these pressured are only elevated when ~ 65-70[8]% of the pulmonary capillary bed has been affected.

The heterogeneity of the CTD group makes heart disease progression difficult to follow, in particular, the rates of development of LV associated disease. Ventricular-vascular uncoupling can lead to the development of LV associated PH. Pre-capillary PH is differentiated through invasive assessment of wedge pressure (PCWP). The classical definition of LV dysfunction (an ejection fraction (EF) of <55%) is present in <6% of SSc patients[9]. The prior classification does not include heart failure with preserved EF, which is a consequence of chronic LV dysfunction and has been reported to be as high as 50%. Importantly, treatment of Group 2 PH with PAH-specific drugs has not been clinically proven and may lead to clinical worsening.

Limitations of the current approach

Currently, the Pharmaceutical Benefits Scheme in Australia is undergoing a review with regards to inconsistencies with current international treatment guidelines, these being:

- Requiring failure to respond to six or more weeks of appropriate vasodilator treatment for WHO class III patients with mean right atrial pressure (mRAP) 8 mmHg or less
- Failing to allow treatment of functional class II patients
- Failing to allow combination therapy

To define if the "failure to respond" criteria have been met, this can include a RHC, echocardiography and 6MW test. Two of these criteria must be evaluated every six months to qualify for continuation or change in therapy. The echo composite assessment is defined as "an ECHO result demonstrating stability of improvement of disease, as assessed by a physician", which is not well defined. The 6MW test must also demonstrate "disease stability" defined by less than a 20% decline from baseline values. Although pharmaceutical intervention has shown mortality reduction with for a variety of drugs, common endpoints, are used as surrogates including, RHC haemodynamics, echocardiographic parameters and 6MW tests. [1 2]

1.2 Echocardiography to infer PAH diagnosis

The ESC taskforce has determined criteria that should raise suspicion of the presence of PH. Initial screening involves Doppler echocardiography [10], followed by the presence of secondary echocardiographic PAH signs (e.g. D-Shaped flattening of the interventricular septum). An estimation of right atrial pressure (RAP) is not included in the criteria, due to inaccuracies in this estimation. Related echocardiographic signs can be broken down into three criteria; the ventricles, pulmonary artery, and the inferior vena cava (IVC). The ventricle component includes a ratio of the RV to LV base of >1.0 and LV eccentricity index of >1.1. The pulmonary artery right ventricular outflow Doppler acceleration time <105 m/sec, and presence of mid-systolic notching is also supportive, as is an early diastolic pulmonary regurgitation velocity of >2.2 m/sec. Although RAP is not included, this is a secondary marker, with a RAP estimate of > 15 mmHg or a right atrial area >18 cm^2 suggestive of PH. The probability of PH is low if TR

max velocity is ≤2.8 or not measurable, with no other echocardiographic signs of PH. Echocardiographic techniques will be discussed further on in this chapter.

1.3 Echocardiographic follow-up of PAH

In patients with PAH treated with pulmonary vasodilators, continuation of therapy is conditional on the demonstration of treatment effect. Early clinical trials used PASP in the assessment of pulmonary vasodilator treatment response; these trials were limited by small sample size, with often limited follow-up [11]. The assumption that pressure changes reflect mortality is disputed by clinical trials and systematic reviews, it is recognised that PASP responses to PAH-specific drugs are heterogeneous, with differences related to sex, race and disease patterns [12]. Mortality rates in PAH trials have improved, with an average five-year survival of 61%, increasing to 75% in those aged under 50 years [13]. Hence, the endpoints of PAH trials are under review; invasive haemodynamics are recommended as secondary, not primary endpoints[14].

As the risk and cost of performing RHC make this test unsuitable for six monthly follow-up, Doppler is used to document changes in cardiac function, and 6MW distance is used to assess functional performance. Recommendations are based on level C evidence, supported by expert opinion and small retrospective studies and registries [15]. Moreover, there are considerable differences between echocardiographic and invasive measurements [15]. Clinical trials have established clinical correlates of mortality in PAH patients. These range from subjective measures such as baseline WHO functional class, 6MW distance, echocardiographic measures, to invasive measures of mixed venous O_2 saturation. The National Institutes of Health registry shows that changes in the cardiac index, mRAP and mean pulmonary artery pressure (mPAP) have a substantial influence on survival. However, RV impairment has significant prognostic

implications, and the presence of RV myocardial disease cannot be distinguished from RV impairment due to pressure overload unless RV afterload can be estimated.

1.3.1 Haemodynamic assessment for diagnosis and follow-up

1.3.1.1 Resting haemodynamics

The use of RHC to document a PAPm >25mmHg is required for PAH diagnosis (Table 1.1), although this is also supported by only level C evidence [15].

Complete haemodynamic assessment includes measurements of the RA, right ventricular (RV) and pulmonary capillary wedge pressure (PCWP), cardiac output (CO) (Fick or thermodilution) and mixed venous oxygen saturation. The normal pulmonary circulation is characterised by low pulmonary vascular resistance (PVR), with compliant vessels. Calculation of PVR (in dynes or Wood units) is the ratio of diastolic pulmonary gradient or transpulmonary gradient (TPG) and CO, and this is especially important for the diagnosis of left heart-derived PH.

Table 1-1. Invasive variables in the diagnosis of pulmonary hypertension and its subgroups

Pulmonary hypertension type	**Measurement**	**Clinical Group**
Pulmonary hypertension	Mean PAP >25 mmHg	All
Pre Capillary	Mean PAP >25 mmHg PCWP <15 mmHg CO normal or reduced	• Pulmonary arterial hypertension • PH due to lung disease • CTEPH • PH with unclear and multifactorial origins.
Post Capillary	Mean PAP> 25 mmHg PCWP>15 mmHg Passive TPG < 12 mmHg Reactive TPG >12 mmHg	PH due to left heart disease

PAP, pulmonary artery pressure; PCWP, pulmonary capillary wedge pressure; CO, cardiac output; PH, pulmonary hypertension, CTEPH, chronic thromboembolic pulmonary hypertension; TPG, trans pulmonary gradient

Some clinical trials have shown that PASP is unrelated to clinical endpoints [16]. Medications available for PAH therapy show differing results in regards to changes in haemodynamic parameters;

Calcium channel blockers (CCBs) - Acute pulmonary vasodilator testing can detect responders to CCB treatment. A >10 mmHg reduction of PAPm defines responders to <40 mmHg in the setting of unchanged or increased CO. However, as only about 5% of patients with idiopathic PAH are CCB-responders, and as very few patients related to CTD respond [17], the value of this step is limited.

Prostanoids- Invasive assessment has shown improvement of RV stroke work index (the product of mean PAP-mean RAP with CI/HR in g.m/m^2/beat) and invasively-measured pulmonary capacitance in response to intravenous or inhaled prostanoids [18]. PASP reductions at follow-up are documented as secondary outcomes in trials.

Endothelin receptor antagonists- Most studies with endothelin antagonists have used 6MW as the primary outcome. Assessment of RHC derived haemodynamics in clinical trials [5,19-21] show reductions of mRAP and PVR [5,19-22].

Phosphodiesterase type 5-inhibitors- One of two studies comparing sildenafil versus placebo used Doppler echocardiography [23], showing an improvement in CO but not PASP [23]. However, in another study of mixed PAH and Eisenmenger's Syndrome, there was a significant fall in PASP [24].

1.3.1.2 Dynamic haemodynamic testing.

In healthy subjects, pulmonary artery vasodilation permits the increased stroke volume associated with exercise, without an increment in PASP. An increase in stroke volume can unmask masked PH (reduced CO). However, stress protocols used to achieve this vary between centres, with modalities including supine and arm cycle ergometry, and arm and leg press, as well as dobutamine. Moreover, normal ranges are variable, especially in athletes and normal elderly subjects, a rise in PAPm >30 mmHg is not necessarily pathological [25]. Consequently, exercise responses are not part of current guidelines [15]. Incorporating multiple components of the PVR equation (PAPm, LAP and flow) in the haemodynamic assessment of exercise response would improve this. A fluid challenge of ~500 ml saline is thought to be safe for the diagnosis of masked PAH. Pulmonary venous hypertension is distinguished on the stability of wedge pressure following infusion, with an increment of >15 mmHg suggesting pulmonary venous hypertension. However, fluid loading and dynamic testing are not validated for clinical use.

1.3.1.3 Imaging assessment of haemodynamics.

The echocardiographic evaluation of haemodynamics in PAH should not be limited to PASP, although PASP and PVR are central to the evaluation of RV dysfunction (Figure 1.1) [13]. Critical

components in the accurate quantification of preload and afterload should include mRAP, PAPm, PA diastolic pressure, LV filling pressure, RV stroke volume (RVOT VTI) and PVR.

Figure 1-1. Echocardiographic evaluation for pulmonary hypertension follow-up

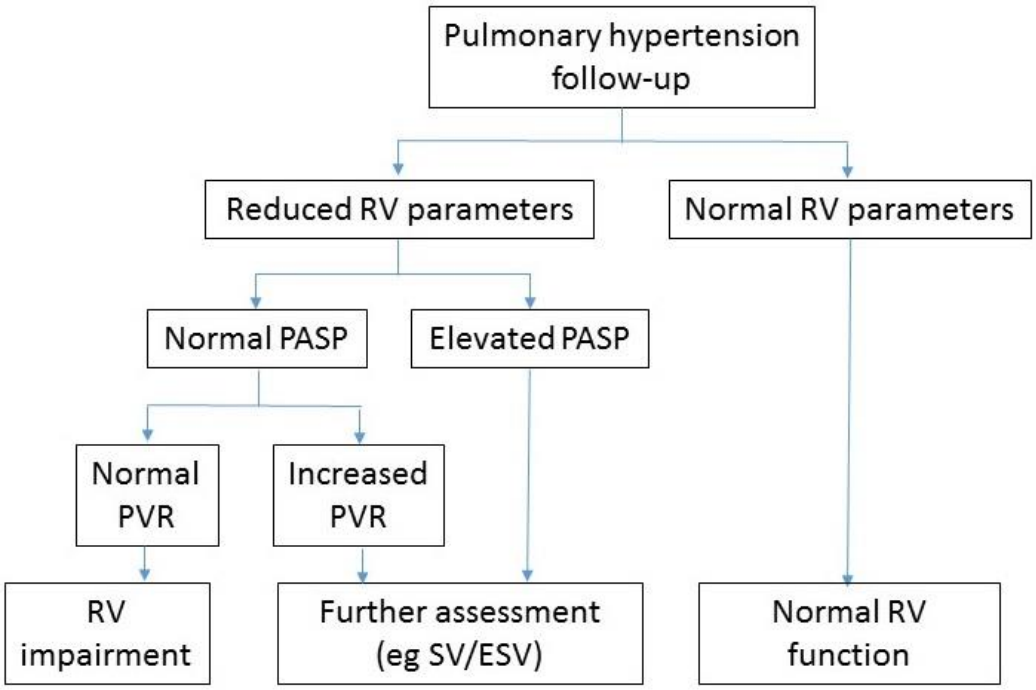

1.3.1.4 Pulmonary artery systolic pressure.

The measurement of pulmonary artery systolic pressure (PASP) from the addition of estimated RA pressure to RV systolic pressure derived from application of the Bernoulli equation to the TR maximum velocity (with or without contrast enhancement) has been a cornerstone of non-invasive Doppler assessment since the 1980's [26,27].

This tricuspid gradient method of PASP estimation has been validated by numerous studies [28,29], but not all validations have been favourable [30], and accuracy appears to vary depending on centre and population. PASP may be over- and under-estimated by Doppler [31], with Doppler being >10 mmHg different than RHC in 48% of cases, potentially leading to inaccurate diagnosis. While Doppler assessment of PASP may be accurate for population-based studies, individual patient diagnosis may be problematic [32].

Figure 1.2 summarises main causes of inaccuracies. An incomplete TR signal from mild TR (Figure 1.2a) or Doppler angle errors are likely the most common sources of underestimation of PASP. Severe TR may lead to rapid equalisation of RV and RA pressures, with underestimation of PASP (Figure 1.2c). Another factor, which is especially relevant in PH, is the impact of reduced stroke volume due to RV dysfunction. Studies of bosentan have shown a reduction of invasive measures of PVR and PASP over a wide range of PAH severity [5,22], but this does not seem to be consistent across all studies [33]. Moreover, PASP values plateau after initial changes. Follow-up of PASP responses to therapy requires contextualisation with changes of stroke volume (or as PVR, Figure 1.3).

To optimise imaging of the tricuspid regurgitation jet, sonographers should image from multiple windows, have sweep speed optimised for HR, and avoid measurement on beats which are post ectopic (atrial fibrillation (AF) beats should be averaged). Spectral Doppler gain signals should also be optimised, decreasing the signal to noise ratio. Disease setting could also affect the accuracy of echocardiographic prediction ability (for example, advanced lung disease, severe tricuspid regurgitation) [34].

1.3.1.5 Secondary markers of pulmonary hypertension.

Pulmonary valve (PV) acceleration time is measured from pulsed-wave Doppler at the level of the PV leaflets, with a measurement of time from baseline to peak modal velocity. Echocardiographic-invasive correlations have led to the proposal of a 100ms cut-off for detection of sPAP of 38 mmHg [35]. Although this is an attractive alternative to PASP in the ~25% of patients who lack an adequate tricuspid regurgitation signal, the correlation of PV acceleration time <90 ms with PVR >3 wood units (W.U) is only modest [36]. In the absence of an evidence base in patients undergoing PAH therapy, we do not use it in this setting.

Mid- and late systolic notching in the RVOT outflow tracing is a qualitative marker for PH. However, this is insufficiently sensitive to "rule out" PH, with studies reporting this in only 53% of PAH patients. However, this marker may provide insight into the underlying physiology of elevated PASP; it is believed to be affected by large artery stiffness and transient flow deceleration related to early systolic pulmonary artery wave reflection. Increased vascular resistance is thought to play a crucial role, with the early arrival of wave reflection denoting a more constricted and less compliant vascular bed. Late systolic notching is more likely to be present in PH due to left heart disease [37].

A number of echocardiographic measures are used to estimate Mean PAP. Most common are planimetry of the TR jet (RV-RA gradient), application of the Bernoulli equation to the opening maximum pulmonary regurgitation velocity when a full pulmonary valve regurgitation signal is available [38], and from the combination of PASP with diastolic PA pressure, obtained from the end-diastolic PR velocity [39]. Increased mPAP his shown to predict NYHA status, elevated LV mass and all-cause mortality [40,41] in stable coronary artery disease (CAD), it is obtainable in a large number of patients. It is not part of our routine clinical practice in following up PAH patients but has strengths for internal consistency and validation of measurements.

Figure 1-2. Tricuspid regurgitant jet measurement and common problems with signal interpretation.

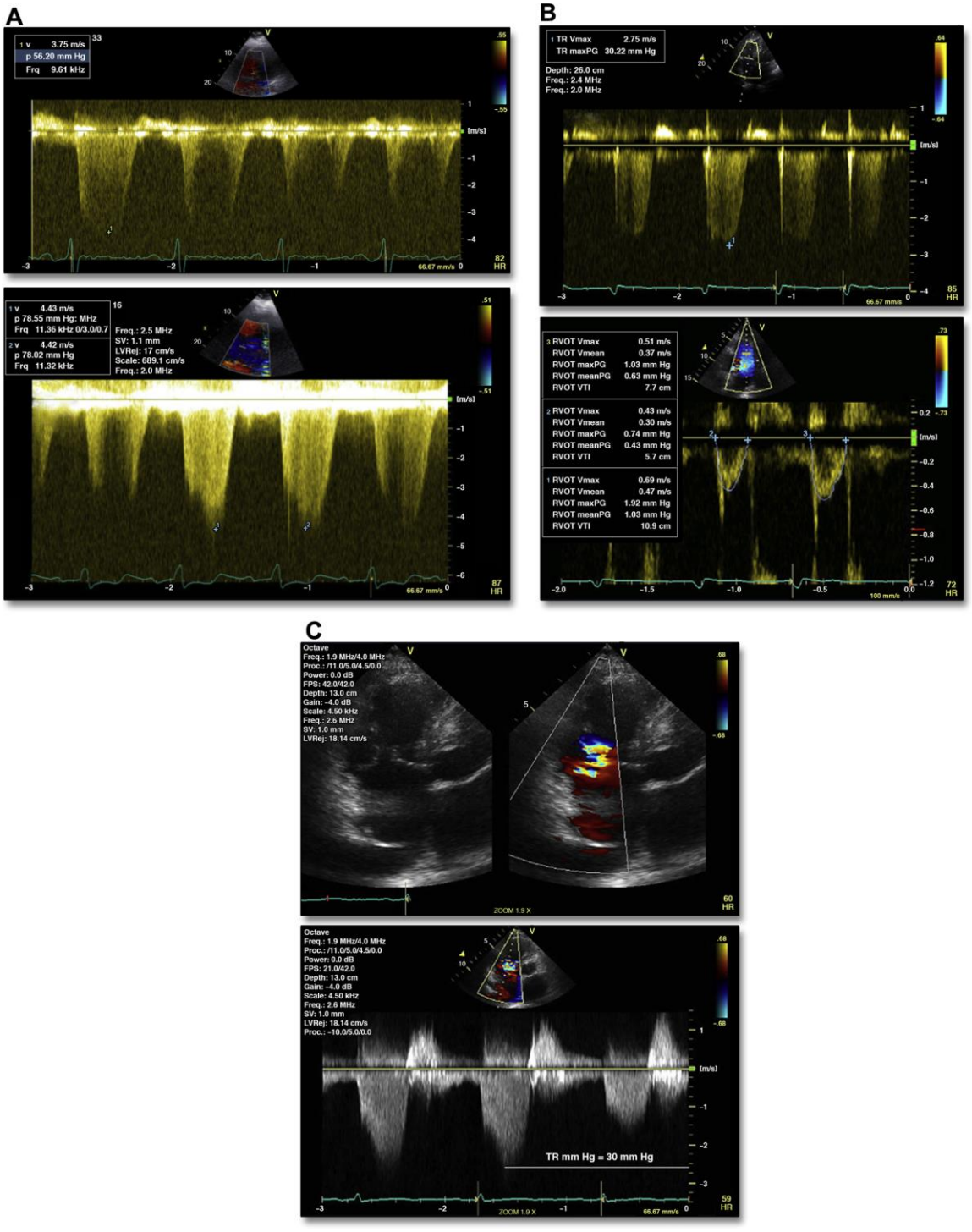

a) Mild Tricuspid Regurgitation, an increase of signal using agitated saline; b) Stroke volume dependence of tricuspid regurgitation); c) PASP may be underestimated when severe TR leads to high RAP (TR velocity <3 m/s)

1.3.1.5.1 Right atrial pressure.

RAP has shown to be a valuable diagnostic marker in outcome studies [1,42]. Early in the history of echocardiography, RAP was derived from clinical jugular venous pressure (JVP) assessment. The use of an assumed RAP of 10 mmHg leads to under- and over-estimation of PASP, and more importantly, ignores the striking correlation RAP with mortality in PAH [16,43]. Echocardiography has value as the intermediate between invasive RHC assessment and clinical evaluation of central venous pressure (which is unreliable). We use a combination of IVC assessment and Doppler waveform analysis of the hepatic veins or superior vena cava.

Measurement of IVC dimension is from the subcostal view, 1-2 cm from the junction of the right atrium (RA) (from a long-axis view). We still routinely assess IVC distensibility in response to respiratory measures that alter intra-thoracic pressure [44]; 50% collapsibility provides optimal sensitivity and specificity for detecting RAP greater or less than ten mmHg. In a study of over 4000 participants, a non-dilated and collapsible IVC associated with survival and survival free of admission [45]. This measurement has strong links to outcomes [16,43] but is underestimated when values exceeded 12 mmHg. Diastolic flow prominence is appreciated by assessment of velocity-time integrals (VTI) of the hepatic veins (or superior vena cava) and indicates elevated RAP. Hepatic vein systolic filling fraction (VTI systolic/ (VTI systolic +VTI diastolic) provide a semi-quantitative assessment of RAP[46], with a measurement of <55% predicting RAP>8 mmHg with good sensitivity and specificity. This technique offers advantages over IVC measurements in patients with falsely elevated IVC diameters (athletes, large BSA, mechanically ventilated patients). However, in AF there can be a reduction of hepatic vein systolic flow, regardless of RAP.

Although the ratio of the early tricuspid inflow to annular diastolic velocity (RV-E/e') may be used to estimate RA filling pressures, we rarely use this. An E/e' >4 is a marker of RAP>10 mmHg and is associated with cardiac events in a PH cohort.

1.3.1.5.2 **Estimated Pulmonary Vascular Resistance**

The assessment of PVR is a means of compensating for changes in stroke volume. The most widely used echocardiographic technique involves indexing the peak TR velocity for RV outflow velocity-time integral (VTI) (Figure 1.2b) and has been validated against RHC, using the equation 10 x TRV/RVOT-VTI [47]. Echocardiographic estimation of PVR may not track changes of PVR assessed by RHC [48]. Work from five validation studies has been combined to generate a new equation for elevated PVR (TRV^2/RVOT-VTI), for use when PVR is likely >6 WU [49].

Nonetheless, evidence shows PVR improves post prostacyclin treatment [50,51], although this seems to be therapy-specific [20]. The underestimation of PVR using echocardiography is independently associated with RV systolic dysfunction [48]. We use this routinely as a screening tool for identifying patients with PVR >2 Wood units (WU), but it is less useful in follow-up as it underestimates the degree of elevated PVR in the presence of high PASP [48,52]

Figure 1-3. RV dysfunction with near-normal PASP.

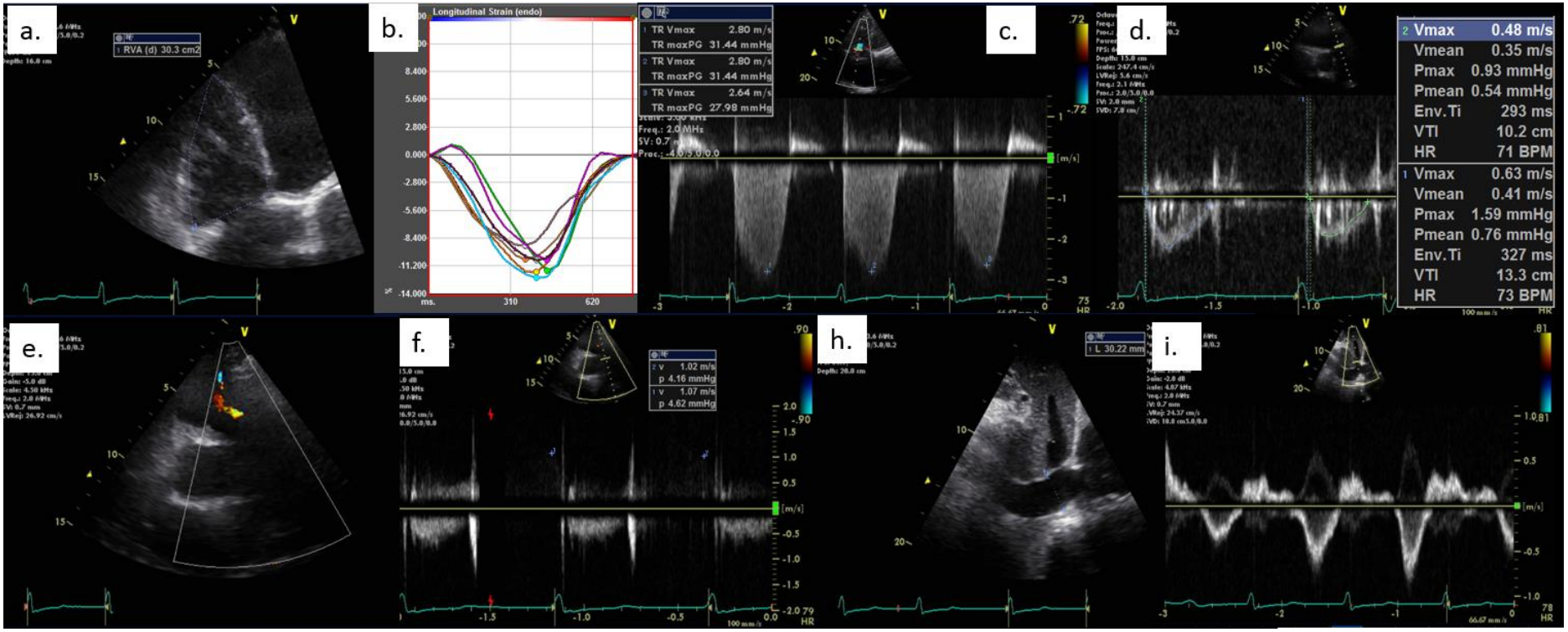

In this case, the RV is enlarged (a) and RV strain is reduced to <12% (1.3b). Although PASP is considered near-normal (1.3c) (TR velocity 2.8 m/s); RAP elevated as demonstrated by IVC size (1.3h) (3.0 cm) and hepatic s wave blunting, with a predominance of the diastolic filling (1.3i). A reduction in stroke volumes produces a decreased right ventricular outflow tract VTI (1.3d), leading to an elevated PVR (~ 2.5 w.u). Thus, despite near-normal PASP, other features point to increased afterload, so RV dysfunction should be interpreted in this context

1.3.2 Quantification of RV performance

Measures of RV function (Figure 1.4 and 1.5) are well known to be associated with outcome in PAH (Table 1.2) and improve in response to therapy (Table 1.3**).** The assessment of PASP and PVR are central to the evaluation of RV dysfunction, and if ambiguous, invasive measurement of PA pressure may be required. The reversibility of pressure-overload induced RV dysfunction is well –illustrated in patients after lung transplantation or pulmonary artery thrombo-endarterectomy. Nonetheless, those with higher baseline PASP values displayed significantly less remodelling [53]. There are at least 20 available echocardiographic variables for RV assessment, although not all have are associated with mortality in PH. The reference standard for RV assessment is cardiac magnetic resonance imaging (CMR), but cost and limited availability somewhat outweigh the high specificity and sensitivity of this test[54]. 3DE is now increasing in popularity for RV assessment and can add incrementally to the prediction of pre versus postcapillary PH [54].

1.4 Stroke Volume and Cardiac Output

Cardiac stroke volume (amount of blood ejected from the heart in one contraction) is routinely performed using the left ventricle. Cardiac output is the product of SV by HR. Ideally, 3D ultrasound measures are preferred, but 2D echocardiography is an acceptable surrogate[55] with cardiac CMR the gold standard. The Simpsons biplane is a 2D method of estimating both the systolic and end-diastolic chamber sizes in the 2 and 4 chamber view. LV stroke volume = LV EDV- LV ESV. The second manner with echocardiography is the Doppler VTI method; Cross-sectional area of the LV outflow tract during mid-diastole is multiplied by the VTI measurement at the level of the aortic valve leaflet tips. There are caveats to each method. The biplane estimation of the volume is dependent on image quality and accurate tracing of the myocardium. In PH dilatation of the RV causes significant LV compression. The

accuracy of tracing to calculate cardiac volumes is contingent on normal LV geometry[56]. Tracing of the biplane volumes becomes technically challenging due to the inability to acquire images from a true LV apex as shown in figure 1.4. The Doppler measurement of SV involves assumptions which can create errors. Measurement of the CSA is $adiuis = \pi r^2$; any errors in measurement are squared. The CSA of the outflow tract is considered to be circular but in reality in many patients it is elliptical. Overall, small bias exists with a high percentage error in the Doppler calculation as compared to thermodilution [57]. Using CMR a clinically meaningful change of SV in PH is 10 ml[58], but the echocardiographic range for this measures has not been calculated.

Cardiac output has a strong correlation with 6MW performance in PAH[59]. A failure to augment output for increasing cardiac demand[60] exists likely mediated by a decreased chronotropic response[59].

Figure 1-4. Technical challenges of LV volume measurement in a dilated Right Ventricle

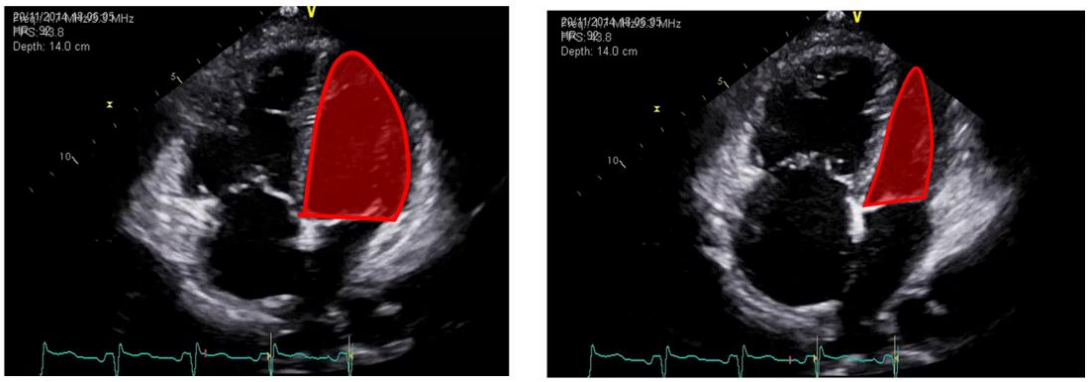

As the RV dilates it becomes apex forming and the LV is compressed. Correct alignment for a Simpson's biplane measurement is difficult due to foreshortening of the LV

Table 1-2 . Changes of RV parameters in response to treatment of PAH

Medication	Specific drug	Imaging tool	Study design	N	Parameter
Prostacyclins and prostanoids	Parenteral prostacyclin analogues [50]	Echo	1 year follow-up Not placebo-controlled	48	Significant improvement in: RVEDA, RVED mid cavity, TAPSE, RAA, PVR
	Epoprostenol [22]	Echo	12 week	81	NA
	Epoprostenol [61]	Echo	1 year	7	Significant changes in: RA size, Diastolic eccentricity index, Pericardial effusion score
	Epoprostenol [62]	Echo	Follow-up 5.9±4.6 months	16	Significant change in RV MPI (p=0.05). RV size and TR severity did not significantly change
Endothelin receptor antagonist	Bosentan	Echo			Significant change in RV size (qualitatively assessed) No significant change in RV MPI & TR Vmax
	Bosentan BREATH-1 study [33]	Echo	16 weeks of treatment	85 (56 treated)	Change in RV systolic eccentricity (p=0.03) No change in TRV, RVEDA, RV diastolic eccentricity
Combined therapy	Bosentan & prostanoid [63]	Echo	8 ± 3 months Not placebo-controlled	37	Significant changes in TAPSE, RV strain, RV strain rate, RV MPI index
	Conventional therapy+ prostacyclin [64]	Echo	12 week	N=81, N=40 on combined therapy	Significantly greater change in RVEDA, systolic and diastolic eccentricity index in the combined arm. No comment on combined group changes between baseline and follow-up
	Sildenafil versus Bosentan [65]	CMR & echo	16 weeks	25 (13 sildenafil, 12 bosentan)	A significant change in RV mass with sildenafil, not shown with bosentan No significant change in RV MPI index
	Predominantly ERA [66]	CMR & echo	12 months	91	Significant change in ejection fraction (p=0.0001). No significant change in RVEDVI (p=0.22) or RV mass (p=0.68)

RVEDA, right ventricular end diastolic area; TAPSE, tricuspid annular plane systolic excursion; RAA, right atrial area; PVR, pulmonary vascular resistance; RV MPI, Right ventricular myocardial performance index; CMR, cardiac magnetic resonance imaging.

1.4.1.1 Right ventricular size and structure

1.4.1.1.1 RV ejection fraction.

Echocardiographic assessment of this parameter is completed by calculation of volumes using geometric assumptions from the traced right ventricular end-diastolic area (RVEDA) and right ventricular end-systolic area (RVESA), or by direct measurement of RV volumes by 3D. Impaired RV (EF) is a manifestation of right heart failure, and linked to outcome [16,67], possibly through its association with RA size and TR. Fractional area change (FAC) is a widely-used surrogate of EF, calculated from diastolic and systolic areas (Figure 1.5a) [44]. Both 2-dimensional techniques are particularly affected by the non-geometric nature of the RV and potentially off-axis imaging planes. Some investigators have reported no significant change in RV size and EF, despite treatment with a spectrum of medication types [33,66,68,69]. Mortality in PAH also does not have a strong relationship with these variables [67,70,71], although there are some favourable reports [64]. For these reasons, we do not use RVEF and FAC in serial follow-up. CMR can measure EF more accurately than echocardiography, as the RV is traced in the appropriate imaging plane. However, the cost and potential access limitations of CMR are barriers to its use as a follow-up test.

1.4.1.1.1 RV size.

RV remodelling is indicative of long-term outcomes [72]. RVEDV (RV end-diastolic volume, measured by CMR) or RVEDA by 2DE have been proposed as prognostic markers [50] in uncontrolled studies that record the prognostic effects of a slower progression of dilatation or reduced systolic function. This process is a complex interplay of factors, RVEDA was only indicative of poor outcome when RV wall thickness (RV free wall thickness measured from the subcostal view) had not increased [73], potentially showing an adaptive remodelling process.

Table 1-3. Association of PAH therapy and Echocardiographic RV parameters

Study First Author	Population	N	Treatment	Results
Raymond[16]	Initial data also published[64]	N=81	Follow-up 37 months (SD 15.4 months) Survival	RA area index (5 cm2/m) 1.54 (1.13–2.10) 0.005 Pericardial effusion (Y/N) 3.89 (1.49–10.14) 0.003 Maximum TR velocity (0.5 m/s) 0.90 (0.62–1.31) 0.591
Forfia [43]	Initial data also published[74]	N=63	Survival	Baseline TAPSE predicted survival (sensitivity, specificity AUC .87, p<.0001)
Esymann [67]	NHLBI PPH registry	N=26	Survival	FAC, pericardial effusion, independently associated variable(p=0.006)
Yeo [75]	PAH	N=53	Survival	RV MPI index (HR 1.3, CI 1.09-1.56, p=.004) TR severity not significant
Brierre[76]	PAH	N=89	Survival	RV MPI >.98 (5.411.12-26.1, p=.035 TAPSE .84 _.72-.98) p=.024 Pericardial effusion 5.18(1.85-14.5), p=.002 Abnormal septal curve 5.33(1.21-23.5),p=.027
Fine[77]	PAH	N=575 (406 PH)	Survival	RV free wall strain (HR 1.46 (1.05-2.12, p<.001) (multivariable model) Univariate HR 2.59(CI 1.89-3.57, p<.001) cut off of 6.7% used. Sig for other RV echo parameters
Sachdev[78]	PAH	N=80	Survival	RV free wall strain (<12.5%) significant in Kaplan Meir for survival (p<.005)
Sano [72]	PAH	N=51	Survival	RV free wall of patients with events was significantly lower (17.8 vs 23%, p=.02). RV free wall strain added significantly to haemodynamic predictors. RV reverse remodelling was associated with improved survival (p=.001)
Ghio[73]	PAH	N=72	Survival	In patients with RV wall thickness <.66 dilated RV (>36.5) was associated with poorer survival.
Fijalkowska[71]	PAH	N=55	Survival	RV area change NS, RAA NS, RV MPI NS; Pericardial effusion significant
Mahapatra[79]	PAH	N=54	Survival	RV MPI RR 1.66 (1.05-2.6), p=.04 RVSP RR1.07 (1.02-1.12), p=.032 RAP via echo NS Invasive RAP RR 1.13 (1.04-1.23),P=.004
Nagaya[80]	PAH	N=53	Survival	Pericardial effusion RR 2.37(1.317-4.3), p=.04 LV deformity index RR1.88 (1.010-3.53), p=.0463 Neither sig in multivariate
Mathai[74]	SSC associated PAH	N=50	Survival	N=50 TAPSE <1.7 HR 3.81 (1.31-11.1) p=.01. As continuous variable HR .87(.078-.96)p<.002. RAA index HR 1.11(1.02-1.19)p=.01

				Pericardial effusion 1.11(.75-1.64), p=.59
Tonelli[50]	PAH	N=48	Survival	Significant associations with mortality TRV HR .58(.37-.89) RV mid cavity dimension, HR .76 (.57-.93) RVEDA HR .73(.57-.93) RVOT VTI HR .90 (.83-.98) RVSP HR.79(.63-1.0) Qualitatively measured RV function HR .55(.31-.96)

RA, right atrium; TR V max, tricuspid regurgitation maximum velocity; PAH, pulmonary arterial hypertension; NHLBI, national heart, lung and brain institute; PPH, primary pulmonary hypertension; FAC, fractional area change; TAPSE, tricuspid annular plane systolic excursion; RVEDA, Right ventricular end-diastolic area; RVOT VTI, right ventricular outflow tract velocity time integral; RVSP, right ventricular systolic pressure; HR, hazard ration.

The RV eccentricity index [16] (which measures the RV diameter as a ratio to the LV) is a simple method to assess the "D-shaped" flattening of the septum quantitatively; a ratio of >1.0 [44] is abnormal. Although changes are documented in response to therapy [61], and associations with outcome shown [76], its prognostic role does not seem to be independent of other features [80]. Studies done with prostacyclin suggest changes in this parameter could reflect improvement in LV filling.

RV thickness- The traditional 2DE measurement of the RV free wall from the subcostal view is subject to tangential measurements, and three-dimensional echocardiography (3DE) is likely more accurate as compared to CMR [81]. However, CMR measurements of baseline RV mass do not associate with survival [69], and follow-up CMR shows no significant change in RV mass with treatment [66,68,69], although this may be dependent on medication type [65]. Consequently, we do not follow RV mass to assess treatment response.

1.4.1.1.1 Myocardial Performance Index (MPI).

Myocardial Performance Index is the ratio between the sum of isovolumetric contraction time (IVCT) and isovolumetric relaxation time (IVRT) and RV ejection time. Standard measurement is with pulsed Doppler, or from tissue Doppler of the TV lateral annulus [82]. MPI is a prognostic marker [75,79]; measures >0.98 are associated with mortality in PAH [76]. Nonetheless, MPI is load-dependent, and may not reflect contractility – for example, elevated RAP causes a shortening of IVRT (due to early equalisation of pressures), so that MPI underestimates the severity of RV dysfunction [83], accounting for its inconsistent association with outcome [71]. MPI use in PAH has level C evidence [84]. Responses of MPI to medication changes have been reported with epoprostenol [62] or combined bosentan and iloprost [63], but other studies have shown no

significant change [65], even over 2-year follow-up [51]. Because of these inconsistencies, we do not use it in serial follow-up.

Figure 1-5. Common RV systolic Function measures; Fractional Area Change (1.4a) and Tricuspid Annular Plane Systolic Excursion (1.4b)

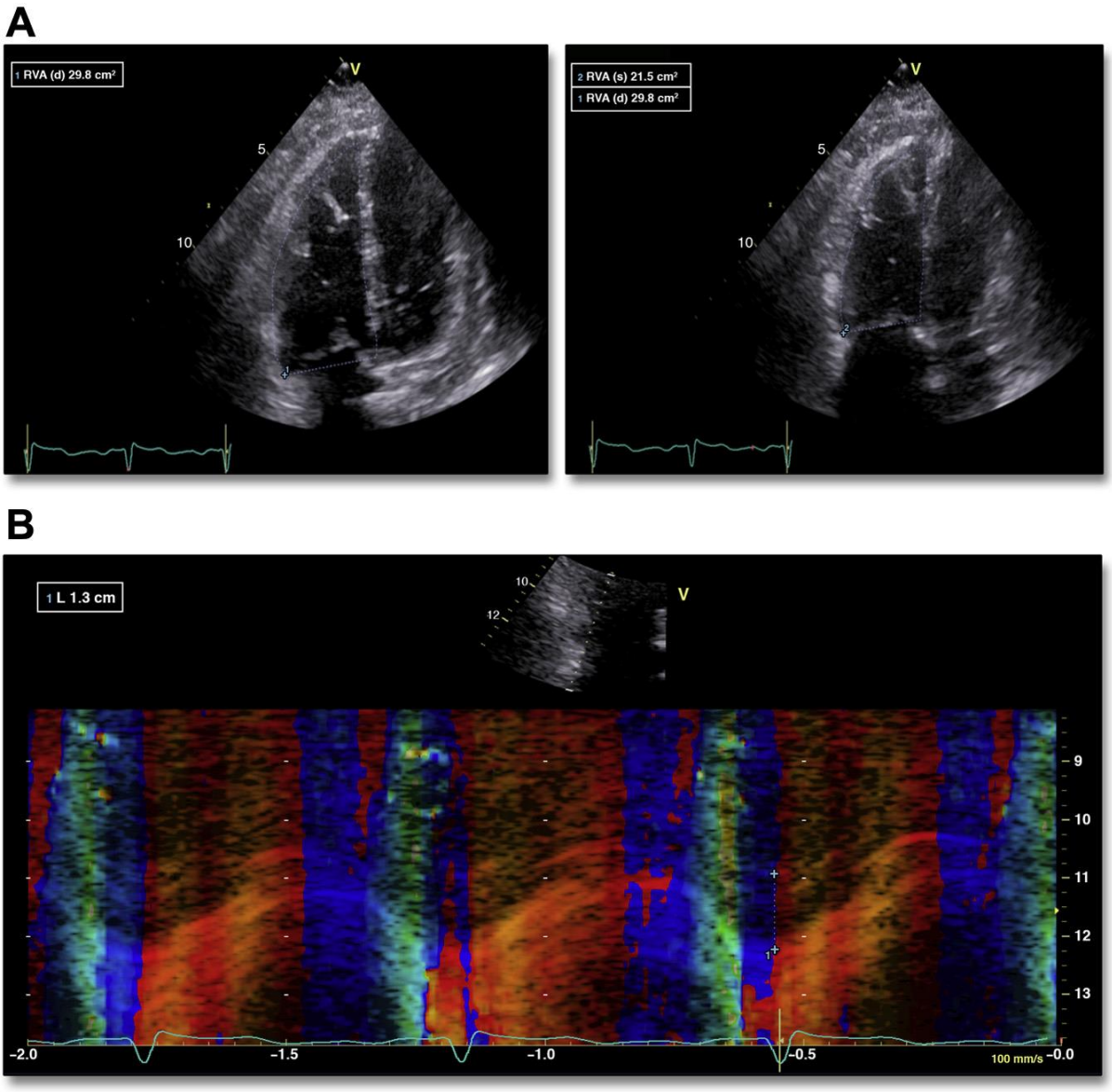

a) Measurement of RV systolic function with Fractional Area Change. Figure 1.4b. Tricuspid annular systolic plane excursion. Conventional parameters including FAC and TAPSE are supplemented or replaced with RV tissue Doppler and free wall strain.

1.4.1.1.2 Tricuspid annular plane systolic excursion (TAPSE).

TAPSE is the M-mode measurement of tricuspid annular motion in the apical 4 chamber view (Figure 1.5b). The measurement of displacement relative to the transducer makes this parameter susceptible to angle dependence, translational motion

and changes in LV systolic function. Although a relationship between TAPSE <1.8cm and survival are reported [43,74,76], a recent meta-analysis showed TAPSE results from clinical trials to be too inconsistent to determine relevance with mortality outcomes [70]. Nonetheless, the response to changes in TAPSE and PVR has a strong linear correlation [85], and TAPSE has been successfully used as a marker to document changes in response to therapy [50].

1.4.1.1.3 **Right ventricular systolic velocity (RVs')**

Right ventricular systolic velocity is the Doppler measurement of TV annular motion, obtained in the RV apical 4 chamber view. It recommended in current guidelines [82], widely available and well-validated [86]. A value of <9.5 cm/sec on the RV free wall is considered abnormal. Similar to TAPSE, angle dependency can lead to under-estimation, and susceptibility to translational motion may cause over-estimation. Although echocardiographic cut-offs are described [44], there are limited data on the use of this method in the follow-up of PAH therapy.

1.4.1.1.1 RV Isovolumic acceleration (RV IVA).

This parameter, acquired from the same tissue Doppler trace as the RVs', is measured as the isovolumetric contraction velocity (IVV), divided by the acceleration time [87]. As it is a pre-ejection parameter, it may be especially useful for RV evaluation in PAH [88]. The normal range is >1.1m/s^2, but limited data on normal ranges and poor reproducibility make the clinical utility of this parameter limited in our experience.

1.4.1.1.1 **Right ventricular strain**.

Deformation (strain) of the myocardium is a strong predictor of outcome in left heart disease [89]. The current measurement technique (speckle-tracking), is widely available as an "on-cart" feature and can be performed at the bedside. In recent guidelines normal ranges have been included to facilitate application in routine practice [82]. RV free wall strain measurement is from the RV-focused apical 4-chamber view. The

inclusion of the septal wall incorporates the LV contribution to RV function, so we favour RV free wall strain (RVFWS) as a marker of RV performance.

Figure 1-6. Right ventricular free wall strain (Figure 1.5a); Measurement of isovolumetric acceleration (Figure 1.5b).

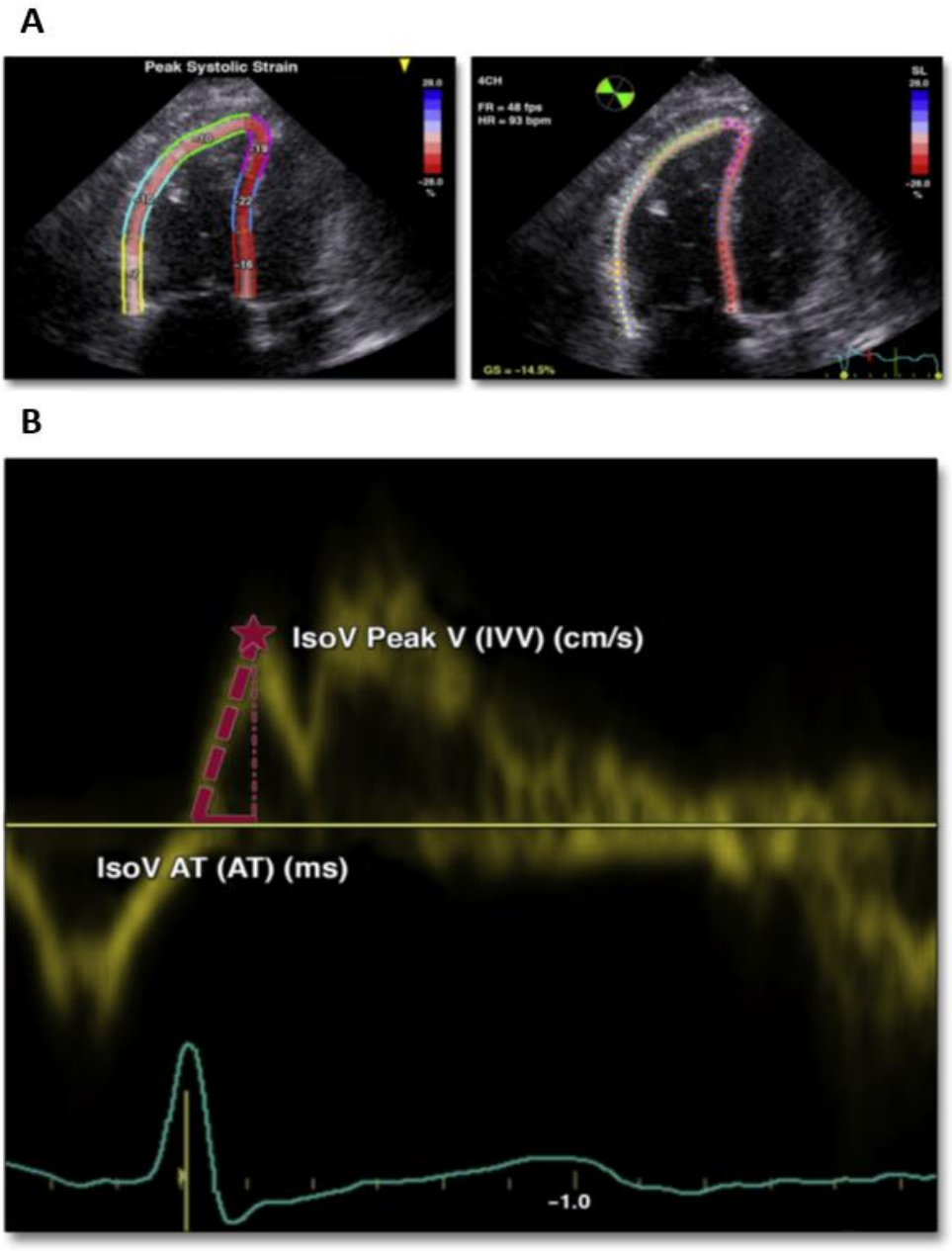

1.5a. Right ventricular free wall strain measured in the RV free wall, and RV septum. The free wall constitutes the basal, mid and apical segments. 1.5b shows Isovolumetric acceleration time (measured with PW Tissue Doppler) quantified as the isovolumetric contraction velocity, divided by the acceleration time

This measurement is validated against CMR [90], and RV strain has been shown to predict outcome in PH [77,78]. RV deformation parameters change in response to

haemodynamic changes [91], RV strain has been shown to respond to medical therapy [63] as the only independent echocardiographic predictor of secondary endpoints. Although 3D strain is correlated with clinical outcome in small studies, its feasibility (~75% in experienced hands) remains a barrier [92].

1.4.2 Markers of RV failure

1.4.2.1 Right atrial size.

Right atrial area or volume is obtained from a single plane area-length measurement in the 2D apical 4 chamber view. Right atrial size is an important measurement, with links to outcome in PAH. A measurement of RA area >27 cm^2 is predictive of increased risk of mortality or transplantation [73,93]. RA size has also been shown to respond to PAH therapy [50,61].

1.4.2.2 Severity of tricuspid regurgitation.

The quantification of severity of the tricuspid regurgitation jet is linked to mortality in studies [50,93], but this finding is inconsistent [75]. Severe TR is identified through a V-shaped cut-off of the TR spectral Doppler, or hepatic vein flow reversal (TR jet density is a weak indicator).TR severity has also not shown a change in response to bosentan [33].

1.4.2.3 Pericardial Effusion.

The presence of pericardial effusion (often graded categorically in small, moderate and large) associates with adverse outcomes in PAH [43,76,94]. Development of effusion is related to mean RAP, mediated by decreased lymphatic and subepicardial venous drainage. The diagnosis of tamponade in PAH presents difficulties; RA and RV collapse may not occur due to increased right-sided pressures, and the non-compliant RV limits RV inflow at all stages of respiration, so pulses paradoxus may not be evident

1.4.3 Integration of RV markers with afterload status

1.4.3.1 Pressure-volume loops.

Pressure-volume loops may be obtained using capacitance catheters or by combining an RV micromanometer-tipped catheter with another means of assessing RV volume. RV contractility is quantified using maximal end-systolic elastance (Ees=end systolic pressure (ESP)/end systolic volume (ESV)), defined from the slope through the end-systolic pressure volume points under different levels of flow induced by IVC balloon occlusion [95]. Afterload is assessed as arterial elastance (Ea=ESP/ stroke volume (SV)). Although this approach provides information regarding RV-PA coupling (the ventricular performance matched with arterial load), it is not amenable to clinical use.

1.4.3.2 Stroke volume/end-systolic volume ratio.

End-systolic elastance (Ees) is the ratio of end systolic pressure to ESV-V0 (V0 being the theoretical volume of the unstressed ventricle, which is assumed to be negligible in the RV). The ratio between stroke volume and RV end-systolic volume is a vital RV marker that is sensitive to impaired RV function in the setting of raised afterload [96]**.** V0 is assumed as 0, but it is likely ~ 8 ml/m2 [97]. Thus Emax is likely systematically overestimated. This ratio can be applied non-invasively [98], using RHC and CMR, or with CMR or 3DE alone [99]. Optimal RV-arterial coupling is an Ees/Ea between 1.5-2. In a small cohort, this was a reliable marker of outcome [96], with a value of SV/ESV<0.52 predicting a higher risk of death or transplant. The use of 3DE is becoming a viable alternative to CMR for the measurement of RV volume and stroke volume, with good correlations and agreements between measurements between 3DE and CMR [100]. However, it is constrained by technical difficulties [81] and can underestimate 3D volumes as compared to MRI, which is critical in the measurement of elastance.

1.5 Conclusion

Pulmonary vasodilator therapy is expensive, and its continuation in the Australian setting requires evidence of responsiveness. Echocardiography is an appropriate screening method for PH, although underestimation of PASP may arise due to inadequate signal, reduced stroke volume, and equalisation of RA and RV pressure due to severe TR. Reverse RV remodelling occurs as a result of vasodilator responses to treatment in PAH (as opposed to direct effects on the myocardium), and it is the RV responses that determine patient outcome. Reliable echocardiographic assessment of RV function has become more feasible and provides valuable prognostic information. The following points are important:

- The goals of therapy include not only the reduction of PA pressure but also decrease in PVR, improvements in CO and tricuspid regurgitation. These should be highlighted in the report, with attention on RV function, which is the primary determinant of outcome.
- As management decisions require repeat studies, laboratory processes for quality control are essential for controlling test-retest variation, and quantification is a critical component of this process.
- RV-focused windows are key. RV dilation causes a change in cardiac orientation, and optimal probe positions may be non-standard. Side-by-side comparison with previous studies is important to limit inter-study variation.
- A respirometer is often of value in Doppler assessment, especially if pulmonary HT is related to chronic pulmonary disease. The capture of long cycles (~10 beats) may be required to follow the response of the interventricular septum (IVS) during the breathing cycle especially in patients with pericardial effusion.

- Consideration of RV pressure overload etiology is required. Likewise, RV volume overload does not necessarily pertain to RV failure (other causes that warrant consideration include shunts and regurgitant valve lesions).
- Research work needs to focus on the applicability of novel echocardiographic techniques, in particular RV free wall strain and 3D techniques. Long-term follow up of patients is required with validation of traditional markers against the gold standard.

Chapter 2

Methods

2 Methodology

2.1 Echocardiographic equipment

Echocardiographic studies were performed on a number of machines (GE Vivid 7, Vivid I and Vivid e9, Horten, Norway; Philips ie33, Bothell, WA). Measures were performed by a single reader, on vendor-independent measurement software for all 2D DICOM measures (GE Health Medical, Horten, Norway)

2.2 Standard 2D echocardiography protocol

All left and right ventricular measurements were performed according to standard guidelines presented by the American Society of Echocardiography (ASE) [101]. These included parasternal long axis and short axis views of the LV, RV apical focused views and subcostal images. Pulse and continuous wave spectral Doppler was performed on all patients. Spectral Doppler signal-noise ratio was optimised to ensure a clear window. Measurements were not performed on beats which were post ectopic. In AF recordings were averaged, with three beats measured. Measurements used the modal velocity.

2.2.1.1 Left side quantification

LV mass calculation was performed according to the ASE 2D linear formula[101] in the parasternal long axis view, and values indexed to body surface area (BSA) (DuBois equation). LVEF was measured from the Simpson's biplane method from the apical 4- and 2-chamber views. The endocardial border was manually traced in systole and diastole. Stroke volume was calculated as the LV ESV subtracted from the LV EDV.

Left atrial volume (LAV) measurements were from the apical 2- and 4- chambers (area-length method) in ventricular systole [101]. Spectral Doppler measures used pulsed wave Doppler, with the sample volume placed at the mitral valve leaflets. Peak velocities of the mitral valve early (E) and late (A) diastolic filling were derived from

the transmitral inflow pattern. Mitral valve deceleration time was measured as the modal velocity from the peak E wave, to the end of the flow of early diastole.

Tissue Doppler imaging using the colour Doppler method with a pulse wave sample volume (2D guided) used to determine the peak diastolic early velocity (e') of the lateral and septal mitral annulus from the apical 4-chamber view. LV filling pressures (E/e') were estimated by calculating the mitral inflow E wave, divided by the average of the septal e' wave, and lateral e' wave.

2.2.1.2 Right ventricular measures

RV end-diastolic (RVEDA) and end-systolic area (RVESA) were calculated from the apical RV focused view; FAC was calculated as the percentage change in RVEDA and RVESA [101] (Figure 1.4a).

2.2.1.3 Tricuspid annular plane systolic excursion

TAPSE was measured from M-Mode and calculated as the distance travelled by the TV annulus between systole and diastole (cm) (Figure 1.4a). Care was taken to ensure M-Mode alignment was parallel to the movement TV annulus.

2.2.2 Right Atrial Area

Right atrial area measurements were traced in the RV apical focused view, with the maximal size during ventricular end systole identified.

2.2.3 Right-sided Spectral Doppler

2.2.3.1 Tricuspid regurgitation maximum velocity

Continuous wave Doppler measurement of TR was assessed from multiple windows to ensure optimal Doppler alignment with maximum velocity of the recorded traces used. Saline enhancement was not routinely used to optimise the Doppler signal.

2.2.3.2 Pulmonary vascular resistance

To determine PVR, the RVOT VTI was acquired through placing a pulsed wave sample volume proximal to the PV insertion point. PVR was calculated from the

RVOT VTI, and TR signal using the Abbas method (PVR echo=TRV/TVI_{RVOT} × 10 + 0.16) [47].

2.2.3.3 Right ventricular systolic velocity

Right ventricular systolic velocity (RVS') was measured using pulse wave tissue Doppler imaging, with the sample volume placed at the tricuspid annulus. RVS' was measured as the peak after QRS on the ECG.

2.2.3.4 Right atrial pressure

RAP assessment was with 2D echocardiography of the IVC from the subcostal view. 2D linear measurements were performed in the long axis view with a change in diameter throughout the respiratory cycle assessed. Patients were categorised as follows:

- IVC diameter <2.1 cm, with >50% collapsibility; RAP= 3 mmHg
- IVC diameter >2.1 cm, with >50% collapsibility; RAP =8 mmHg
- IVC diameter >2.1 cm, with <50% collapsibility; RAP= 15 mmHg

2.2.4 Myocardial deformation imaging

Myocardial deformation imaging was performed using wall motion tracking software (Image-Arena, Version 4.6.3.9 TomTec Gmbh, Unterschleissheim, Germany) to analyse 2D echocardiographic images. Frame rates of >30 fps were required for data analysis. Endocardial borders were manually traced during diastole. Borders were then tracked automatically frame-by-frame throughout the cardiac cycle. Manual adjustments were performed when necessary, and regions excluded if excessive noise or inadequate tracking was present.

2.2.4.1 Left ventricular strain

Optimal LV cavity views were selected, with the LV end-diastolic endocardial border manually traced along the myocardium (borders automatically tracked frame-by-

frame). Manual adjustments were performed when necessary, and regions excluded as required (e.g. inadequate tracking). Apical 4, 2 and 3 chamber views with optimal wall definition were selected for analysis (Figure 2.1), each wall was split into 3 segments. Peak global strain was defined as the average of 18 segments.

Figure 2-1. Left ventricular global longitudinal (LV GLS) strain measurement of the apical long axis, apical 4 chamber and apical 2 chamber

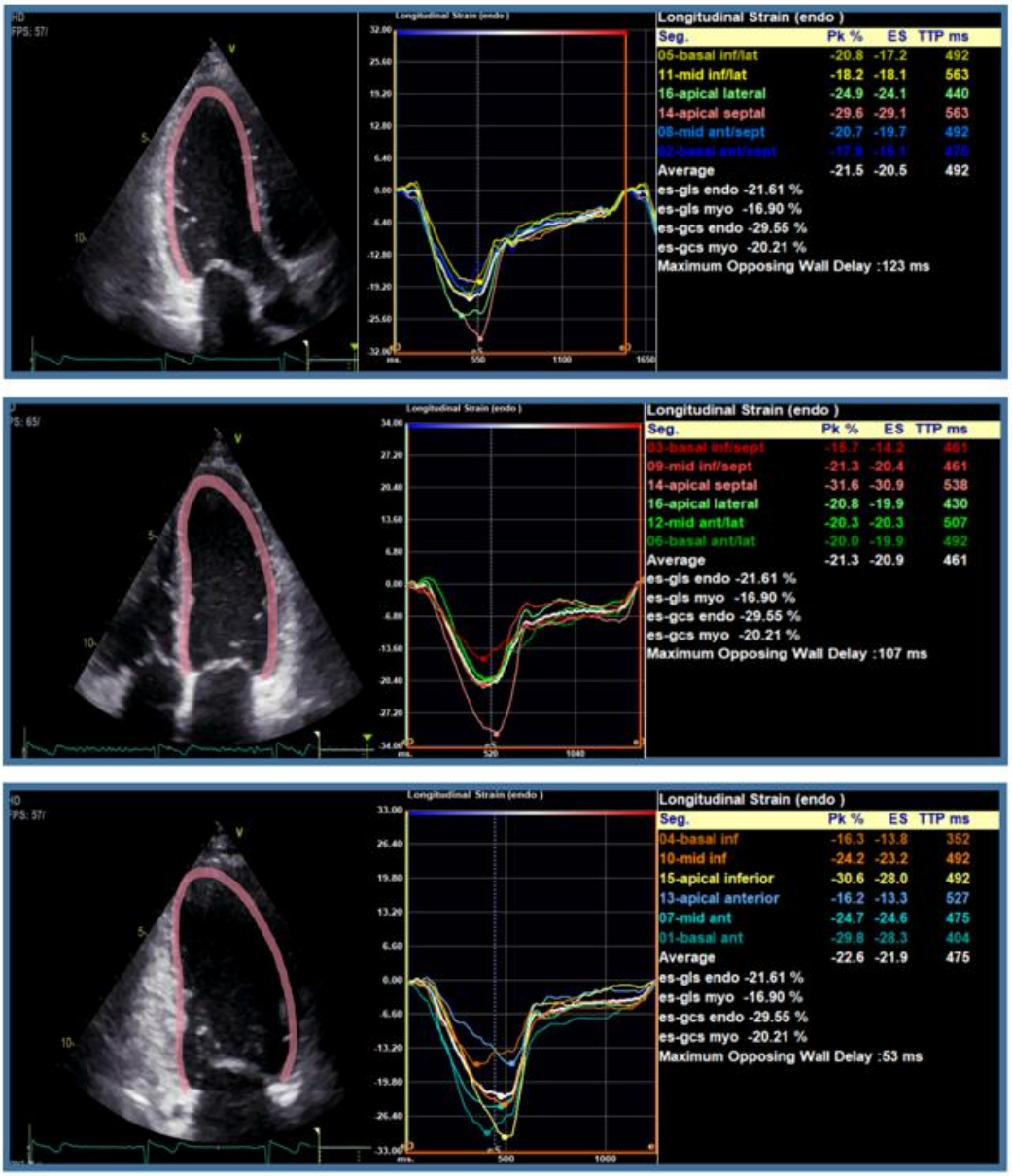

2.2.4.2 Right ventricular strain

RVFWS measurement was from the modified RV apical view (Figure 2.2). Specific RV algorithms for tracking were not available thus the LV program was manually

adjusted to track the RV border. The RV end-diastolic endocardial border was manually traced along the RV septal and RV free wall. For mean values, the basal, mid and apical segments of the free wall are included. Manual adjustments were performed when necessary, and regions excluded as required.

Figure 2-2. Right ventricular free wall strain

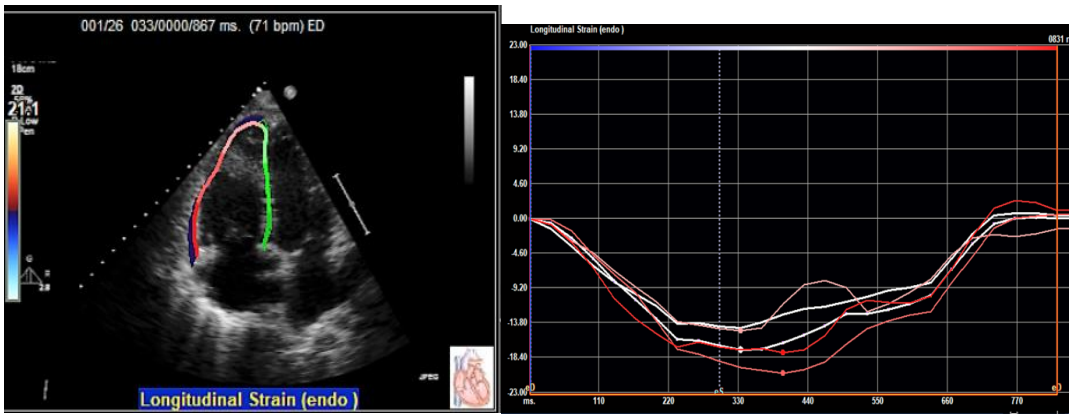

The RV free wall and the septal border were traced. The basal, mid and apical free wall segments were average.

2.2.4.3 Right atrial strain

Right atrial strain was performed using the left ventricular strain package, with borders manually altered to track the atrial walls. For each chamber, manual adjustments were performed when necessary, and regions excluded if excessive noise or poor tracking were present. For RA strain, P-P gating was used from the RV apical-focused view. RA measurement points (Figure 2.2), peak RA reservoir (RA ℇR) was measured as the mean peak of 6 segments of the RA, RA contraction (ℇCT) was measured as 6 segments at peak RA ℇCT. RA conduit function (ℇCD) was the difference between RA ℇR and RA ℇCD.

Figure 2-3. Measurement of right atrial strain. RA reservoir, RA contraction and RA conduit function

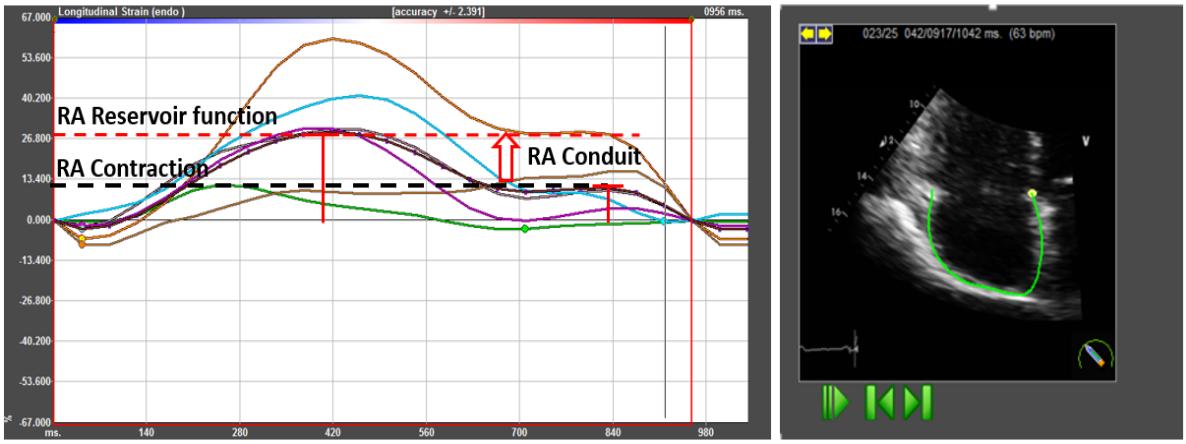

2.2.4.4 Left atrial strain

Left atrial a strain was measured using R-R gating (Figure 2.4) utilising the left ventricular strain package. The first peak (between the R wave and T wave corresponds) to the reservoir function (LA ƐR), while the second peak (starting on the P wave) is the atrial contraction phase (LA ƐCT). The difference between the reservoir and atrial contraction strain relates to the LA conduit function (LA ƐCD).

Figure 2-4. Measurement of left atrial strain.

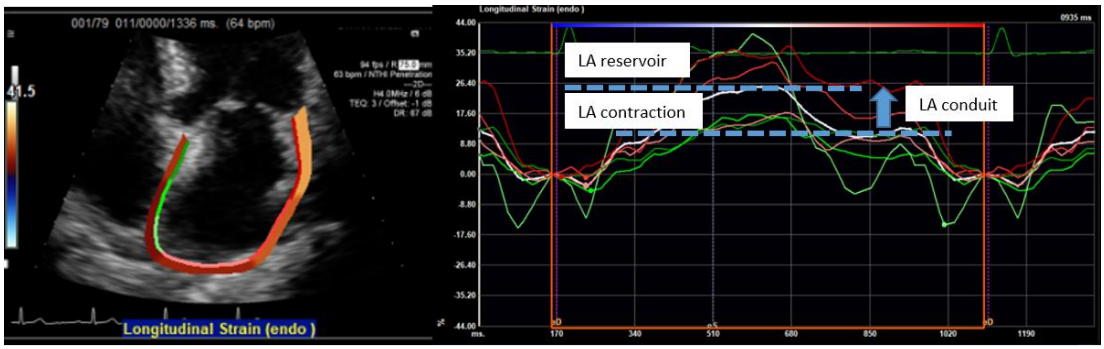

After tracing the atrial border, the strain curves are given. The LA reservoir is defined as the peak strain post T wave, the LA conduit is the peak deformation prior to termination of the P wave. LA conduit is LA reservoir with LA conduit subtracted.

2.3 Vascular function

2.3.1 Brachial Flow-mediated dilatation (Brachial FMD)

The peripheral vascular function was assessed using distensibility of the brachial artery with ultrasound. Endothelial response to shear stress was the change in diameter after a 5 minute occlusion period [102]. Mediation of this response is through the endothelial-derived nitric oxide. The second method of assessment, performed through an exogenous dose of nitric oxide through nitroglycerin spray or tablet (0.4 mg) was not performed for this study.

Studies were performed according to published guidelines [103], using standard equipment (Philips iu22, Phillips Healthcare, Bothell, WA and Vivid I, General Electric Medical Systems, Milwaukee, WI). All studies were performed by a single expert sonographer. A cuff was placed on the forearm, an ECG tracing obtained, and 3 beat acquisitions were used (Figure 2.5). A cuff was pumped up to 220 mmHg (or >50 mmHg systolic), and longitudinal plane imaging was performed distal to the antecubital fossa, with the probe baseline position marked. Pulsed Doppler recordings were performed before cuff occlusion, and this was used to calculate baseline flow. Brachial flow readings were performed immediately post cuff release, and diameter readings were performed 1-minute post cuff release.

2.3.2 Peripheral artery tonometry

Peripheral artery tonometry is the non-invasive measurement of arterial tone changes in the peripheral artery beds. Probes placed on contralateral fingertips measure finger -arterial pulse volume changes in response to a 5-minute occlusion stimulus. Similar to brachial flow-mediated dilation, the surge in blood flow causes an endothelium-dependent vasodilation response.

Peripheral artery tonometry (PAT) measurements were obtained with plethysmography (Endopat 2000, Haifa, Israel). After probe placement on the fingertips, a digital pulse wave is created, reflecting the peripheral arterial tone.

Figure 2-5 Brachial artery flow-mediated dilatation

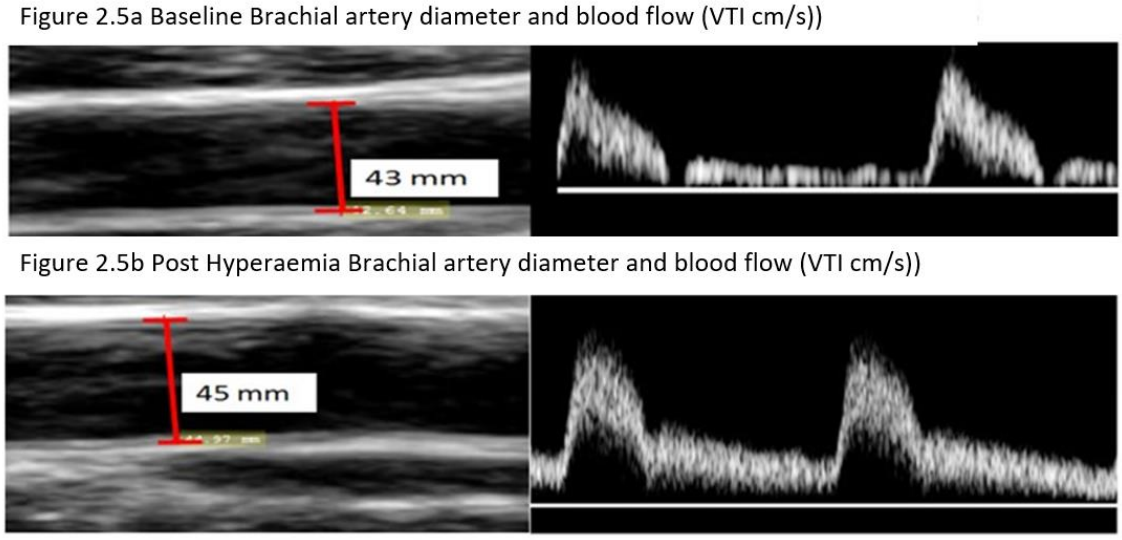

Measurement of brachial flow-mediated dilation at baseline (2.5a). Post-Hyperaemia measurement of brachial artery size and blood flow (2.5b).

All jewellery was removed before testing. Testing followed recommend guidelines [104], and hyperemic measurements were performed simultaneously with brachial FMD measurements. The index finger was used for the majority of testing (94%); if this finger was not available (due to digit amputation, or open wounds), the next finger with no open wounds was used-usually the ring finger (3.4%). The 3rd and 5th digit was used for 1 patient each. Blood pressure measurement occurred on the control arm, and the cuff placed in the same position for brachial FMD. Patients achieved a haemodynamically stable steady state (at least 15 minutes resting supine, no talking). Automated readings and measurements were performed (Figure 2.6). The EndoPAT score was calculated as the ratio of the average amplitude of the PAT signal over a 1 minute period, 1.5 minutes after cuff deflation [105], measured as the log reactive hyperemia index (log PAT).

Figure 2-6. Measurement of endothelial function with Peripheral artery tonometry with EndoPAT2000 showing normal versus abnormal response

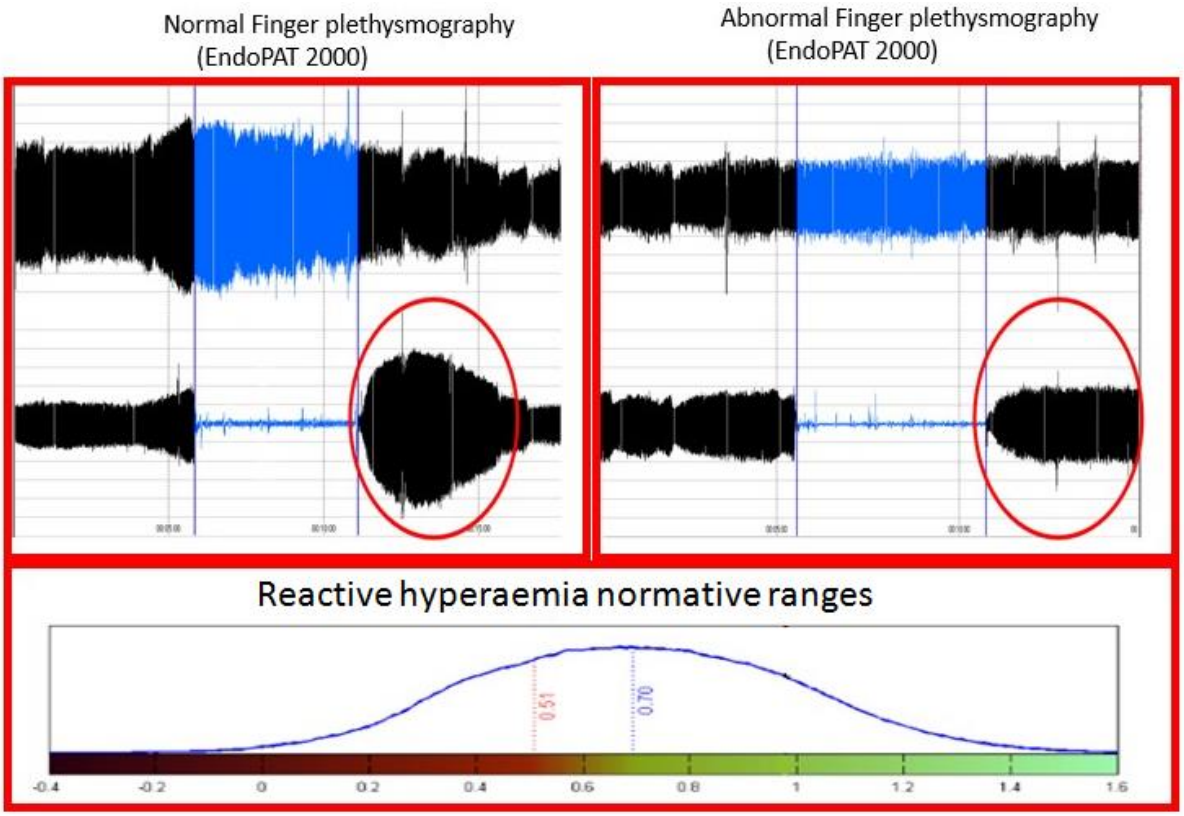

2.3.3 Laser Doppler flowmetry

Laser Doppler probes (CP1, Moor Instruments, UK) were placed on the subcutaneous tissues on the dorsal side of the forearm. Participants skin was shaved and wiped with alcohol. Probes were fixed lightly with medical tape to the same arm as was used for brachial FMD and Endopat-2000. Measurement of data was performed according to the methodology of Roustit et al. [106]. Figure 2.7 details measurement of baseline, peak and peak-baseline measurements, and time to peak (time from cuff release to peak hyperemia).

Figure2-7 Laser Doppler flowmetry.

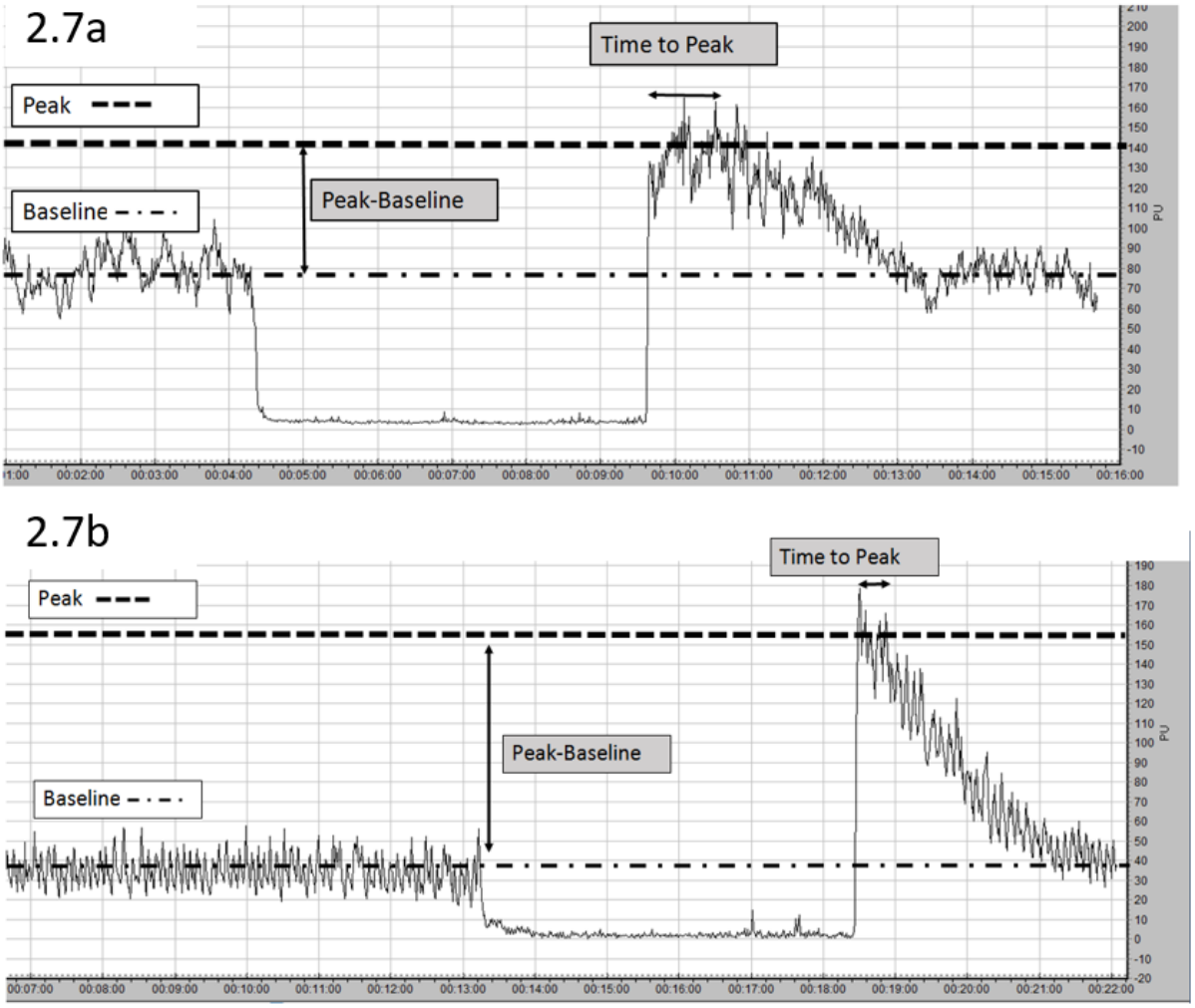

Figure2.7a-Abnormal Laser Doppler hyperaemia response. Figure 2.7b-Normal Laser Doppler hyperaemia response.

2.4 Study patients

PAH patients were recruited from two separate hospital sites, the Royal Hobart Hospital and The Princess Alexandra database. These patients were included in chapters 3, 4, 5(Hobart site only), 6, 7 (Hobart site only), 8, 9, 10. Patients were registered in nurse databases, for prescription of Medicare subsidised medications. Once patient details were retrieved, respective echocardiographic databases were queried with data stored in DICOM compliant format.

In chapter 4, the control cohort of pulmonary embolism patients was recruited from discharge summaries from the RHH. SSC patients in chapters 7 and 11 were recruited from the Tasmanian Scleroderma Registry. Postcapillary PH patients included in chapter 8 were recruited from patients undergoing invasive testing in the RHH cardiac catheterisation laboratory.

2.5 Clinical data

Clinical data were retrospectively acquired through PH tracking databases maintained by dedicated PAH nurses for chapters 3, 4, 5, 6, 7, 8, 9, 10 and 11. Clinical control groups included in chapters 5, 7, 8, 10 and 11 had clinical information gained from clinical chart reviews. Clinical data for study 11 was taken at the time of study by LW, history on SSC was acquired from nurse run database for the Tasmanian scleroderma cohort. All patients were defined as having PH through invasive measures as required in clinical guidelines.

2.6 Right heart catheterisation.

RHC studies were undertaken after premedication and local anesthesia. A 4-lumen 110 cm 7-Fr Swan-Ganz catheter (Edwards Lifesciences, Irvine, CA, USA) was floated to the right heart, and resting measurements of mRAP, RVSP, PAPs, PAPm and PCWP were made at end-expiration using a pressure transducer (21BB, ITL Healthcare, Chelsea Heights, Australia). The transducer was calibrated to atmospheric pressure at the level of the RA (1/3 chest height) and re-checked at intervals to avoid zero drift. CO was determined by thermodilution, using an average of four consecutive values that varied less than 10%. Electrocardiographic (ECG) leads were connected to both arms and the left leg, allowing three ECG channels for the timing of signals. All haemodynamic monitoring was recorded using a Horizon SE Haemodynamic System (Mennen Medical Ltd., Yavne, Israel) and subsequently analysed off-line.

Chapter 3

Importance of Baseline and Longitudinal Evaluation in the Follow-up of Vasodilator Therapy in Pulmonary Arterial Hypertension

Paper under review "Relative importance of baseline and longitudinal evaluation in the follow up of vasodilator therapy in Pulmonary arterial hypertension"

Journal of the American College of Cardiology; Cardiovascular Imaging

Leah Wright; Nathan Dwyer; Sudhir Wahi; Thomas Marwick.

3 Importance of Baseline and Longitudinal Evaluation in the Follow-up of Vasodilator Therapy in Pulmonary Arterial Hypertension

3.1 Preface

Classically, assessment of PH patients during clinical follow-up is with the echocardiographic evaluation of PASP. Quantification of disease severity is through a calculation of the tricuspid valve regurgitation signal with the peak value obtained used to determine RVSP. RVSP is added to assumed RAP, measured as IVC diameter, and its collapsibility. Pressure assessment with echocardiography was initially the primary measure for follow-up in outcome studies of PAH. As technology has advanced, our ability to quantify right ventricular function has improved, and the importance of RV systolic function in patient outcome is now better appreciated.

In Australia, PAH diagnosis is confirmed with RHC, patients then undergo a routine clinical assessment to determine the efficacy of treatment. Clinical status is assessed using functional performance measures (6MW distance), RHC, or echocardiographic assessment of PASP. Two of three of these assessments are required.

Right ventricular function is a robust baseline predictor of outcome. There has been limited work on long-term follow-up of patients and outcome predictors. As patients undergo mandated assessments, the benefits of this need to be elucidated.

3.2 Abstract

Background: PASP and right ventricular (RV) evaluation with echocardiography is used in the assessment of therapeutic response to vasodilator therapy in PAH. We sought the relative value of baseline and follow-up evaluation to risk assessment with standard clinical markers.

Methods. Of 162 prospectively recruited patients with PAH, with 96 included in the analysis with ≥3 sequential echocardiographic studies. PASP and RV function (including RVFWS) were measured at baseline and follow-up 2D echocardiograms. Univariable and multivariable Cox regression, with nested models, used to determine incremental and independent predictors of all-cause mortality.

Results. Changes between visits were minimal for all parameters (RVWFS (p=0.46), RVEDA (p=0.48), PASP (p=0.66), TAPSE (p=0.32), RAA (p=0.39) and IVC (p=0.25)). Over 3 years follow-up, 29 patients died. Baseline RVFWS was an independent (HR 0.90 [95%CI 0.83-0.97], p=0.007), and incremental predictor (p<0.001) of outcome when accounting for PASP and other clinical covariates (C statistic 0.74, p=0.001). Those who died showed no differences in RVFWS (p= 0.50), PASP (p=0.90), and TAPSE (p=0.83) between visits. Patients were split into those who improved vs. declined over time, no changes in RVFWS (HR 1.3[0.59-2.70], p=0.55), or PASP (p=0.78) predicted outcome. When baseline measures and follow up time were accounted for RVFWS (0.78[95%0.63-0.96], p=0.002), RAA (1.2[1.07; 1.4],p=0.003) and IVC (66.5[8.5;520.5],p<0.001) mean change over follow up were significant in predicting outcome.

Conclusion. In PAH, baseline RV function (RVFWS) is a strong predictor of outcome, independent of PASP. Changes throughout therapy appear minimal, and the prognostic value of change appears limited.

3.3 Background

While a decade of improving mortality rates [13] attests to the benefit of pulmonary vasodilator therapy in PAH, these treatments remain expensive, with inter-individual differences in efficacy. In Australia, the continuation of therapy is conditional on the demonstration of a treatment effect, and lack of an effect should lead to consideration of additional therapy. In Europe and USA, patients remain on treatment even without a marked improvement because, as this is believed to delay progression of the disease. Therefore, the treatment goals of normalisation or near-normalisation of right ventricular (RV) size and function [107], require sequential follow-up by RHC, 6MWD or echocardiographic parameters and, if accessible, by CMR. Clinical evaluation of PAH is through an assessment of functional class, combined with non-invasive tests including 6MWD and echocardiography [25]. Because clinical trials of pulmonary vasodilators used PASP response as a primary outcome measure, PASP evaluation using echocardiography acts as a surrogate for invasive hemodynamic assessment. However, hemodynamic and RV function changes do not necessarily follow the same trajectory as PASP [108]. RV function has also been shown to decline, even in patients deemed clinically stable [109].

RVWFS is a novel marker of myocardial deformation, which has a growing body of evidence as to its utility in predicting outcome in PAH [77]. In this current study, we sought to determine predictors of mortality. Our hypothesis was that baseline, and follow-up RV dysfunction would be a stronger marker than PASP for predicting outcome in PAH. The primary aims were to determine the severity and prognostic relevance of baseline PH and RV dysfunction, and its change in follow-up.

3.4 Methods.

3.4.1 Patient selection.

We prospectively enrolled 162 patients at two Australian regional centres (92 at Royal Hobart Hospital, Tasmania, and 70 at Princess Alexandra Hospital, Brisbane, Queensland), who were evaluated for pulmonary vasodilator therapy after invasive diagnosis of PAH (PAPm ≥25mmHg with PCWP ≤15 mmHg). We included 96 patients (age 62±14) years, 73% women) who had ≥3 echocardiographic studies available. Patients were placed on a variety of treatments, 38 (40%) on endothelin receptor antagonists (ERA) and phosphodiesterase type 5 inhibitors (PDE-5), 32 (33%) on ERA only, 15 (16%) on PDE-5 only, 7 (7%) on ERA+PDE-5+prostacyclin, and 4 (4%) on no treatment.

The patient follow-up protocol involved re-evaluation at intervals of 6-12 months. After the baseline study (treatment initiation), the 2nd visit was after a median time frame of 9 months (4-14), the 3rd visit at 16 (10-26) and 4th at 27 months (16-36). There were 96 patients followed over 3 visits (n=96), with 62 patients assessed over 4 visits.

3.4.2 Echocardiographic assessment.

Echocardiography was performed using standard commercial equipment (Vivid 7, Vivid i and Vivid e9, GE Medical Systems Horten, Norway; ie33, Philips, Bothell, WA). A standard imaging protocol was obtained, including RV-focused views.

Conventional measurements were performed by a single reader, according to ASE guidelines [101] by a single reader for all studies. PASP was measured from the peak tricuspid regurgitation velocity using the modified Bernoulli equation [29]. RAP was derived from the IVC dimension and distensibility from the subcostal view [44]. LV EF was measured from the Simpson's biplane method from the apical 4- and 2-chamber views. Peak velocities of the early (E) and late (A) diastolic filling were derived from

the transmitral inflow pattern. Tissue Doppler imaging using the pulsed Doppler method was used to determine the peak diastolic early velocity (e') of the lateral and septal mitral annulus from the apical 4-chamber view. RV end-diastolic area (RVEDA) and RV end-systolic area (RVESA) calculation was from an apical RV focused view. Fractional area change (FAC) was calculated as the percentage change between the RVEDA and RVESA. Tricuspid annular plane systolic excursion (TAPSE) was measured as the displacement (cm) of the lateral tricuspid annulus towards the RV apex in the RV 4-chamber view. Right atrial area (RAA) was measured from the RV apical focused view, with the largest maximal area traced in end-systole. The echocardiographic calculation of RV to PA coupling was calculated as the TAPSE/PASP ratio (mm/Hg). A second method, the RVFWS/PASP was calculated to elucidate the RV coupling process.

Categorization of normal echocardiography ranges; Dichotomization of echocardiographic values were based on ASE ranges and are as follow; PASP>35 mmHg, IVC>2.1, RVEDA >25 cm^2, TAPSE <1.6cm, RAP>8 mmHg, FAC <35%, RVFWS <19%, PVR>3 Wood, RAA>18 cm^2,

Standard software (Image-Arena, TomTec Gmbh, Unterschleissheim, Germany) was used to analyse 2D speckle-tracking. Image selection included the optimal image in which the whole RV cavity was visualised. The RV end-diastolic endocardial border was manually traced along the RV septal and RV free wall. These borders were then tracked automatically frame-by-frame throughout the cardiac cycle. Manual adjustments were performed when necessary, and regions excluded if excessive noise or poor tracking was present. RVFWS was calculated from an average of three segmental RVFWS traces.

3.4.3 Functional testing.

A 6MW test was performed at the time of the echocardiogram by a research nurse. Testing was done in a quiet corridor and followed a standard protocol [110].

3.4.4 Follow-up.

The cohort consisted of 96 patients with at least 3 follow-up scans (3 visits follow up time median 13 (11-23), 4 visits median follow up 23 months (18-32), 29 (30%) died. 66 patients were excluded because of <3 scans (follow up time median 0 months (0-14), 12 (18%) died. In 7, death was attributed to CVD, in 5 there was a final presentation with respiratory failure, in 2 the cause of death was liver failure related to right heart failure, and in a further 11, no other cause of death was identified, so it was attributed to PAH. One patient died from a stroke, and there were three cancer deaths.

3.4.5 Statistical analysis.

Statistical analysis was performed using standard software (SPSS 20.0, IBM, Chicago, IL) with statistical significance set to $p<0.05$. All-cause mortality was the primary outcome. Univariable and multivariable Cox regression used was used to determine a prediction of outcome. The first visit was used as the baseline. The average between-visit changes were calculated from the mean difference $((Visit_1-Visit_0)+(Visit_2-Visit_1)+(Visit_3-Visit_2)/3)$, and final visit change was included in those with 4 visits. Follow up time was included as months from first to final echocardiographic study. Patients were then categorised into those who displayed an overall improvement or decline as compared to baseline. Kaplan-Meier curves were used to illustrate outcome based on standard cut-offs [82], with differences sought using the log-rank p-value. In models of the progression of each parameter, the risk associated with age and sex was summarised in three groups, created according to REVEAL registry data [111]. The three tertiles of risk were i) men and women <60

years (n=34, 35%), ii) women >60 years (n=43, 45%), and men >60 years (n=19, 20%). Harrell C statistic was used to determine model strength.

3.5 Results.

3.5.1 Patient characteristics.

Baseline variables are shown in Table 3.1. RV systolic function (measured by TAPSE and RVFWS) was decreased by 73% and 38% of patients respectively. Measures of right ventricular filling pressures (RAA and RVEDA) were increased by 44% and 34% of patients, respectively. Primary PAH etiology was idiopathic (47%), with a large proportion having connective tissue disease (40%), portal pulmonary hypertension (6%), congenital heart disease (3%), undetermined (3%).

Table 3-1. Baseline echocardiographic and clinical parameters

		Mean (SD)	Proportion abnormal
Clinical features	Age (years)	62 (14.0)	
	BSA	1.8 (0.24)	
	6MWD (meters)	320 (134)	
	HR	75 (15)	
Right heart parameters	RVFWS (%)	17 (5.7)	38%
	RVEDA (cm^2)	23 (8.3)	34%
	FAC (%)	32 (14.2)	55%
	TAPSE (cm)	1.8 (0.50)	73%
	RVSP (mmHg)	52 (23)	74%
	IVC (cm)	1.9 (0.60)	56%
	PASP (mmHg)	57 (24.1)	79%
	PVR (w.u)	3.7(1.8)	54%
	RAA (cm^2)	20.3(7.6)	50%
Left heart parameters	LV mass (gm)	150 (51)	
	EF (%)	62 (9.8)	
	LV EDV (ml)	84 (35)	
	LV ESV (ml)	35 (26.4)	
	SV (ml)	39 (14)	
	LA volume (ml)	61 (26.0)	
	MV DT (cm/s)	227 (52)	
	E' septal (cm/s)	6 (2.3)	

E' lateral (cm/s)	9 (2.4)
E/e' septal (cm/s)	13 (6.9)
E/e' lateral (cm/s)	9 (4.7)

BSA, Body surface area; 6MWD, six-minute walk distance; HR, heart rate; RVFWS, right ventricular free wall strain; RVEDA, right ventricular end diastolic area; FAC, fractional area change; TAPSE, tricuspid annular plane systolic excursion; RVSP, right ventricular systolic pressure; IVC, inferior vena cava; PASP, pulmonary artery systolic pressure, PVR, pulmonary vascular resistance; LV, left ventricular; EDV, end diastolic volume; end systolic volume; LA, left atrium; MV DT, mitral valve deceleration time.

3.5.2 Baseline predictors of outcome.

Table 3.2 summarises the prediction of outcome from baseline variables. Mortality was predicted by increasing age, lower functional capacity, RV size and function, and evidence of right heart failure. Baseline PASP was not independently associated with outcome. However, TAPSE/PASP (p=0.02) and RVFWS/PASP (p=0.006) were significant univariable predictors of outcome. Adjustment of echocardiographic variables for age and sex showed RVFWS to be an independent predictor of outcome (HR 0.89 [0.83-0.96], p=0.001), as were the measures of RV coupling (TAPSE/PASP, p=0.03; RVFWS/PASP p=0.007). Cumulative survival is shown in appendix figure 3.8.

Figure 3-1. ROC curves with echocardiographic markers and outcome. Quartiles of RVfree wall strain

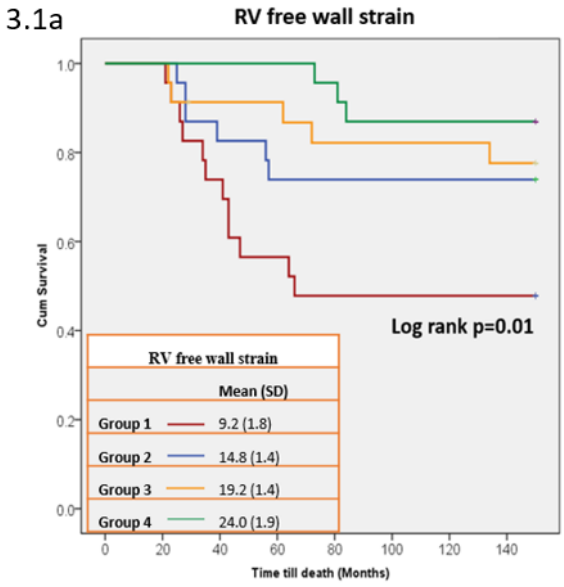

Based on categorization of normal ranges from clinical guidelines, RVFWS of ≤19% (p=0.03), RVEDA >25 cm^2 (p=0.005), and PASP >35 mmHg (p=0.05) were associated with mortality. In Kaplan-Meier curves of quartiles of RVFWS, PASP and TAPSE (Figure

3.1, 3.2, 3.3), only RVFWS quartiles were significantly different in regards to outcome (log rank p=0.03). RVFWS/PASP tertiles showed a significant difference in log-rank test between groups (p=0.023), but TAPSE/PASP tertiles did not show a significant difference between the groups (p=0.10). Nested Cox models showed that although PASP did not add incrementally to clinical features, RVFWS showed an incremental prognostic effect of RV function additional to the risk determined from age and sex groups (C statistic 0.74, p=0.001) (Figure 3.4).

Figure 3-2. ROC curves with echocardiographic markers and outcome. Quartiles of Pulmonary Artery Systolic Pressure

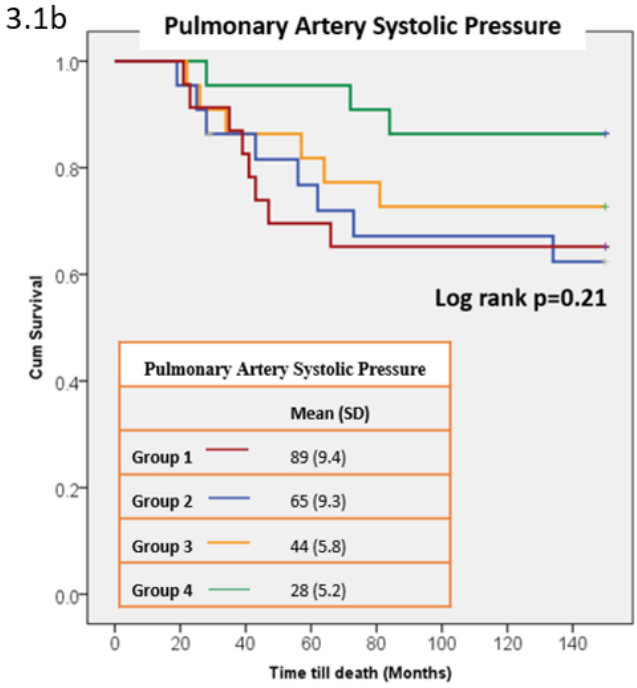

Figure 3-3. ROC curves with echocardiographic markers and outcome. Quartiles of Tricuspid Annular Plane Systolic Excursion.

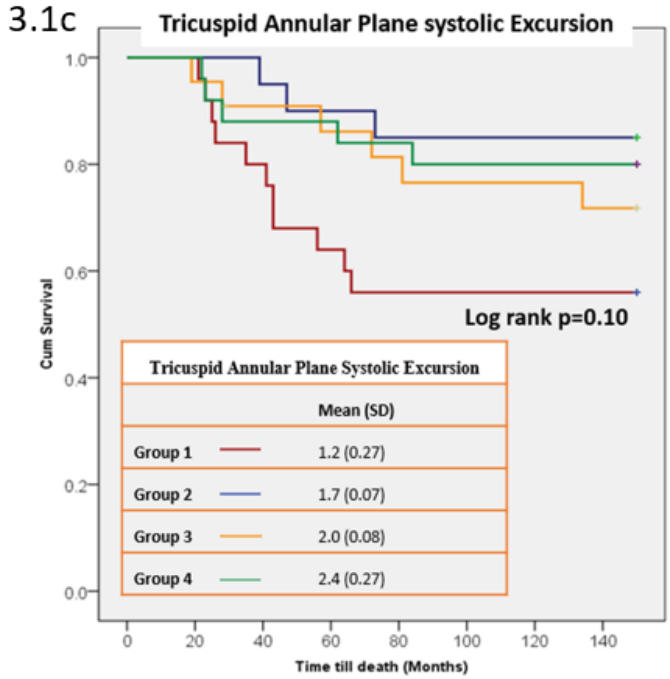

3.5.3 Sequential measurement and outcome

Sequential measurements of echocardiographic parameters (Figure 3.5) showed no significant changes in the group as a whole. When groups were split according to survival status (Figure 3.6), survivors were associated with significantly better function at all time points for RVFWS, PASP, RAA, IVC, RVEDA and TAPSE. The association of change in RVFWS, TAPSE and PASP with survival is shown in Figure 3.7. Standard deviations were large, indicating a large amount of individual variation present in the degree of change. The average change of RVFWS (p=0.46), RVEDA (p=0.48), PASP (p=0.66), TAPSE (p=0.32), RAA (p=0.39) and IVC (p=0.25) in the course of therapy was not significantly associated with outcome. Due to the time-varying nature of follow up, we created two additional variables to add into models, follow up time between first and final echo, and the mean delta over the course of the three or four visits (Table 3.3). Time was not a predictor of the outcome within our model Traditional RV function markers such as TAPSE and PASP showed significant

baseline predictors of outcome, but the change over time was not. RAA size and IVC showed change over time, and baseline size to be predictive of outcome. RVFWS was significant at baseline and also showed change over time to be significant.

Table 3.2. Baseline univariable and multivariable predictors of outcome

	Univariable		**Age/sex adjusted Variables**	
	HR (95%CI)	**P value**		
Age (years)	1.06(1.02;1.10)	0.002		
Male sex	0.45 (0.21;0.93)	0.03		
Age+Sex (female >60)	0.20(0.07;0.57)	0.003		
Age +Sex (Male >60)	0.49(0.22;1.09)	0.08		
6MWD (meters)	0.99(0.99;0.996)	<0.001		
RVEDA (cm^2)	1.08 (1.04;1.1)	<0.001		
FAC (%)	0.97 (0.94;0.99)	0.01		
TAPSE (cm)	0.47(0.21;1.03)	0.06	0.46(0.20;1.04)	0.06
RVFWS (%)	0.89(0.83;0.96)	0.001	0.89(0.83;0.96)	0.001
IVC (cm)	3.5 (1.9;6.6)	<0.001		
RAA (cm^2)	1.07 (1.03;1.1)	0.001		
PASP (mmHg)	1.02 (1.0;1.03)	0.05	1.02(1.0;1.03)	0.08
PVR (w.u)	1.1(0.90;1.4)	0.34	1.04(0.83;1.3)	0.72
TAPSE/PASP	0.09(0.01;0.70)	0.021	0.10(0.01;0.79)	0.03
RVFWS/PASP	0.04(0.004;0.39)	0.006	0.04(0.003;0.41)	0.007

IVC, inferior vena cava size; RVFWS, right ventricular free wall strain; RVEDA, right ventricular end diastolic area; RAA, right atrial area; FAC, fractional area change; 6MWD, six-minute walk distance; TAPSE, tricuspid annular plane systolic excursion; PASP, pulmonary artery systolic pressure; PVR, pulmonary vascular resistance

Table 3.3. Cox regression of RV echocardiographic markers

Dependent Variable: All-cause mortality	**Univariable analysis**				**Multivariable cox regression.**			
	Mean change over visits		**Time**		**Baseline Variable**		**Mean Change over time**	
	HR(95%CI)	**P**	**HR(95%CI)**	**P**	**HR(95%CI)**	**P**	**HR(95%CI)**	**P**
RVFWS (%)	0.91(0.76;1.09)	0.30	0.99(0.95;1.03)	0.65	**0.86 (0.79;0.93)**	**<0.001**	**0.78(0.63;0.96)**	**0.02**
RAA (cm^2)	1.2(1.04;1.4)	0.01	1.005(0.97;1.05)	0.81	**1.08(1.03;1.13)**	**0.001**	**1.2(1.07;1.4)**	**0.003**
TAPSE (cm)	1.5(0.24;9.0)	0.68	0.98(0.94;1.02)	0.24	0.35(0.15;0.85)	0.02	0.39(0.05;3.2)	0.38
PASP (mmHg)	1.01(0.97;1.05)	0.58	0.99(0.95;1.03)	0.54	1.02(1.003;1.04)	0.02	1.03(0.98;1.08)	0.24
IVC (cm)	3.2(0.71;14.8)	0.13	0.98(0.94;1.03)	0.41	**10.1(4.3;23.7)**	**<0.001**	**66.5(8.5;520.5)**	**<0.001**
6MWD (metres)	1.009(0.99;1.02)	0.09	0.97(0.93;1.01)	0.16	0.99(0.991;0.998)	0.001	1.005(0.996;1.01)	0.30
TAPSE/PASP	0.34(0.005;23.4)	0.61	0.99(0.95;1.03)	0.55	0.03(0.002;0.33)	0.005	0.07(0.0001;38.9)	0.40
RVFWS/PASP	0.04(0.004;0.39)	0.006	1.0(0.96;1.04)	0.99	**0.009(0.001;0.14)**	**0.001**	**0.003(0.00002;0.50)**	**0.003**

IVC, inferior vena cava size; RVFWS, right ventricular free wall strain; RVEDA, right ventricular end diastolic area; RAA, right atrial area; FAC, fractional area change; 6MWD, six-minute walk distance; TAPSE, tricuspid annular plane systolic excursion; PASP, pulmonary artery systolic pressure; PVR, pulmonary vascular resistance

Figure 3-4. Incremental value of baseline RV function to the estimation of PASP for prediction of outcome. Nested Cox model analysis.

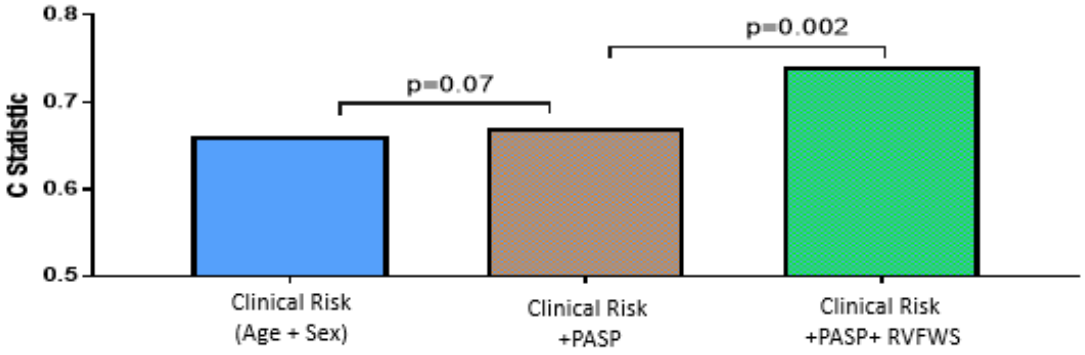

	HR (95%CI)	P value	HR (95%CI)	P value	HR (95%CI)	P value
Age +Sex 1	0.26(0.08;0.83)	0.02	0.29(0.09;0.92)	0.04	0.28(0.09;0.89)	0.03
Age +Sex 2	0.59(0.23;1.5)	0.26	0.64(0.25;1.6)	0.34	0.85(0.32;2.3)	0.75
PASP			1.02(1.0;1.03)	0.07	1.009(0.99;1.03)	0.29
RVFWS					0.89(0.82;0.96)	0.003

Figure 3-5. The longitudinal follow up of echocardiographic markers over the time course of the study

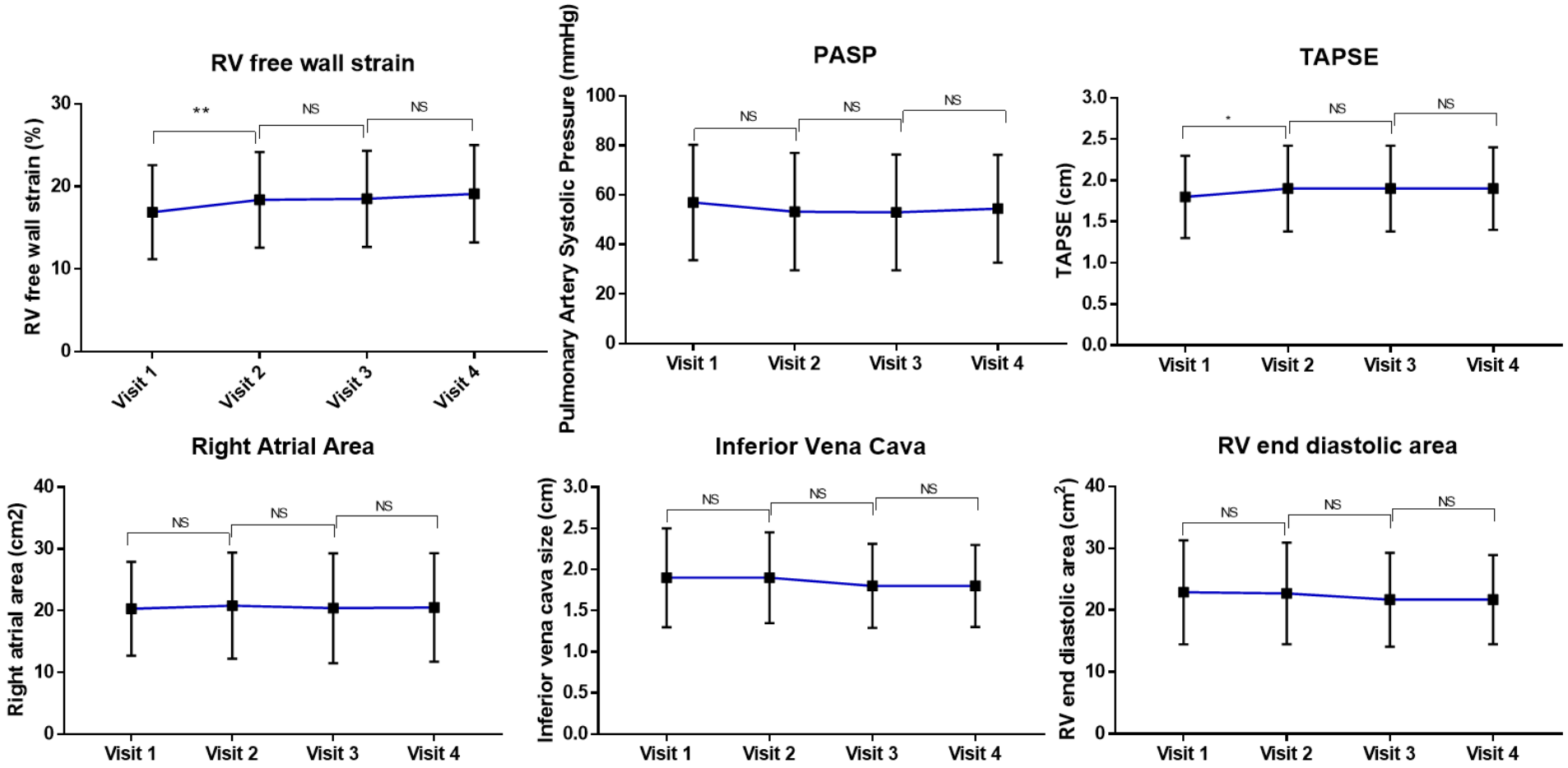

***,p<0.05; **, p<0.01, ***, p<0.001**

Figure 3-6. Differences over time in surviors versus non survivors for echocardiographic parameters

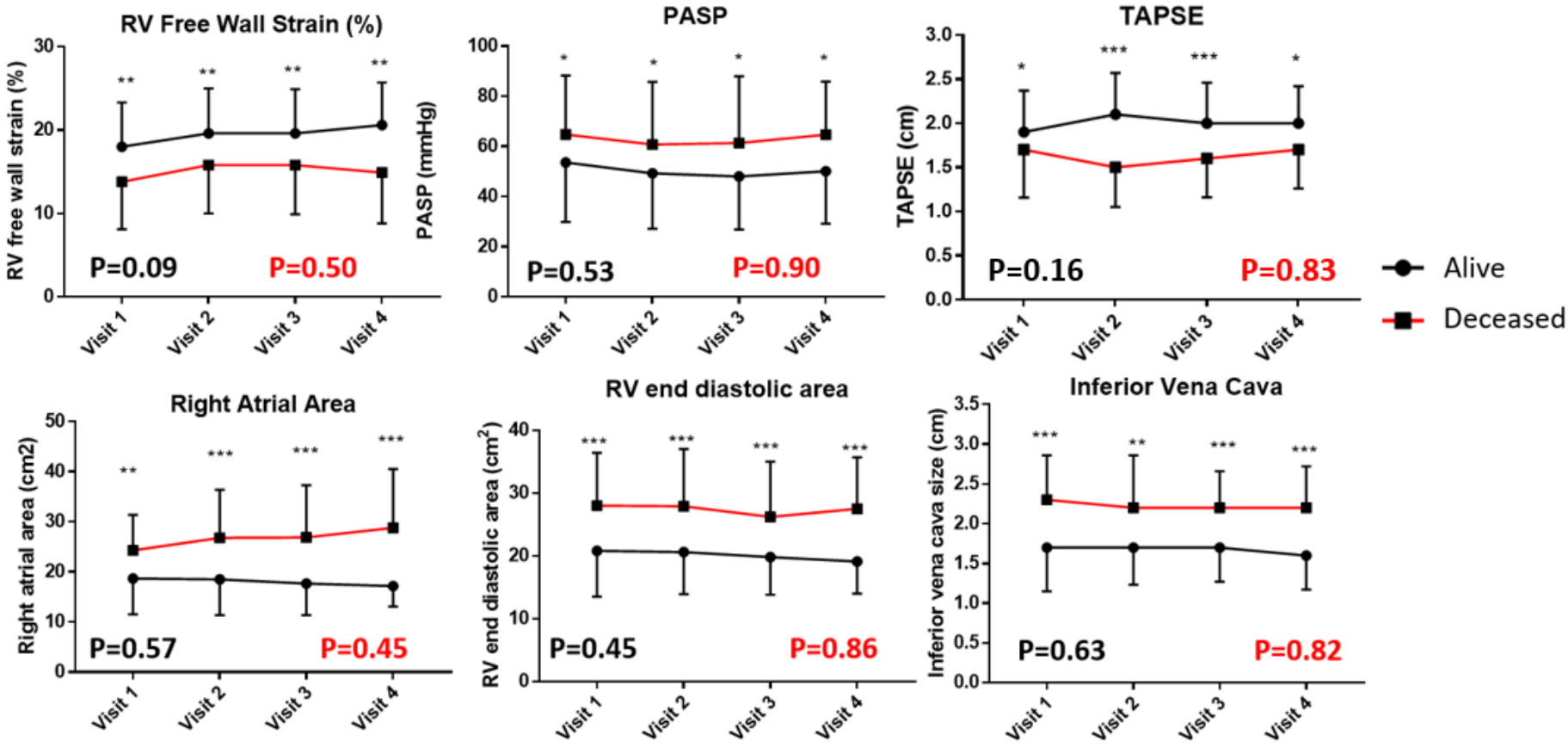

***,p<0.05; **, p<0.01, ***, p<0.001**

Figure 3-7. Comparison of the delta's between time points for RVFWS, TAPSE and PASP.

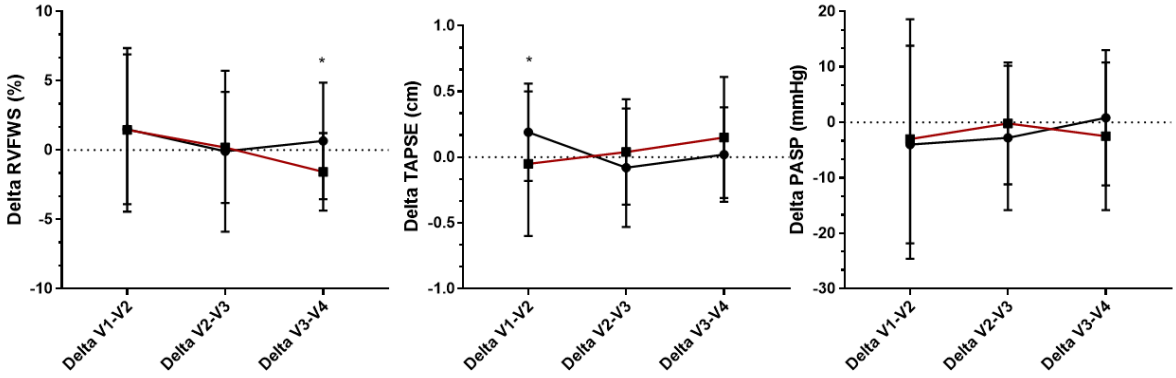

***,p<0.05**

3.6 Discussion

The results of this study show that baseline RV markers have a strong and independent association with outcome in PAH. Mortality is associated with reduced RV function across all time points, although changes throughout therapy were minimal for both RV systolic function and RV pressure markers, and these were unrelated to outcome. When accounting for follow up time and baseline function, RVFWS, IVC size and RAA change were associated with outcome

3.6.1 RV function in PAH

The initial response to PAH is an increment in RV contractility and wall thickness, but eventually, the RV dilates to preserve stroke volume in the face of increasing afterload [112]. The progressive disease course of PAH leads to uncoupling between the RV and PA in late-stage disease [113]. However, due to the vague and non-specific symptoms of PAH, patients can be diagnosed at any time point in the evolution of RV dysfunction. Pericardial effusion has long been established as a reliable outcome marker [114], but due to its association with right heart failure, this signal is of limited value to guide therapy. Markers of RV function may give greater insight into a patient's current clinical status.

Echocardiography is widely used to guide the initiation of therapy for PAH, and follow patient response. Current guidelines [115] acknowledge that clinicians often rely on the subjective appearance of the RA and RV to make clinical decisions, even without formal size measurements. This stance reflected the difficulty in quantifying RV dysfunction, but the availability of objective measures as allowed quantification to be incorporated into current follow-up. Therefore, in addition to the primary focus on hemodynamic parameters, the strength of baseline RV dysfunction as a prognostic marker in this study support a meticulous baseline imaging work-up, including all aspects of the PA-RV uncoupling process.

A variety of measures of RV function have been used. TAPSE has also shown associations with outcome [43] and has been used to assess PAH progression [116]. The limitations of this technique are that it may not perform as a global marker of RV dysfunction, as basal segment translation is only measured. Falsely elevated values are also possible, as TAPSE does not take into account rocking of the RV [117]. Previous work from our group has shown that RV strain is a sensitive parameter over small variations in PASP[118], and appears to be more significant to changes than traditional measures such as RV FAC. Pivotal work by Fine *et al.* showed the importance of RVFWS to outcome in 575 echocardiographic studies, of which 406 had a diagnosis of PAH either via RHC or echocardiographic parameters. Results showed poorer baseline RVFWS associated with shorter 6MWD, higher BNP and presence of right heart failure. (6). RVFWS predicted survival when adjusted for age and sex.

An essential aspect of our study is the use of sequential visits, over extended follow-up time. We also selectively included participants with RHC confirmed PAH. We have shown that patients appear to plateau after an initial improvement. If the initial patient trajectories do not continue over an extended period, treatment effects over long-term

are overestimated. Guidelines recommend the use of echocardiography for follow up, but there has not been guidance on the value of echocardiographic markers, or a clear consensus on how these data could improve outcome.

3.6.2 Sequential assessment.

Echocardiography is an attractive tool for the follow-up assessment of PAH patients. How to make the most out of this imaging technique is not well known. Pulmonary pressures are generally used, but these are not a strong predictor of outcome at baseline, and we have shown that changes over time do not account for outcome. The right ventricle is a notoriously tricky chamber to follow over time; the non-geometric shape leads to discrepancies in size, and lack of consistency when reporting RV size and function [119]. A goal of treatment should be to achieve "normal of near-normal size and function" [119], quantitative markers are thus not defined. A test must have sufficient reliability to detect a clinically significant change sensitively. A major problem with 2D echocardiography of the RV is the discrepancies in size which come with probe positioning (due to the non-geometric shape of the RV). Variability data on right ventricular 2D markers over time is lacking. Newer techniques must justify performance, for example, the validation of 3DE against CMR [120,121] and speckle-tracking imaging [122]. Some of the difficulties encountered in this work can also be applied to 2D echocardiographic follow up. Firstly, the RV is thin-walled and can be heavily trabeculated, (especially so in PAH), making border delineation a difficult task. Previously, we have published the reproducibility of traditional 2D RV function markers as compared to speckle tracking of the RV free wall [118], with speckle tracking imaging showing improvements over RV FAC% in variability. Within this paper, we show the strength of RVFWS to predict outcome at baseline, with changes over the course of follow up sensitive for predicting outcome.

Although strong outcome changes after therapy are seen with improvements in WHO functional class, these are not mirrored in parameters such as 6-minute walk distance [123]. A goal of >380 meters has been defined [119], but in meta-analysis, no relationship with change in six-minute walk distance and outcome were seen [124]. Perhaps a more sensitive tool such as cardiopulmonary exercise testing should be routinely performed in patients to quantify functional capacity.

3.6.3 Limitations

Due to the complexity of the RV's structure, CMR is considered a gold standard for RV quantification. Echocardiographic parameters have been compared to CMR measures for longitudinal follow up [125], and although a significant correlation was present, echocardiography was not able to detect changes in CMRI-derived RVEF (a change in CMR RVEF of >3%). Our cohort derived from 2 referral hospitals, with multiple sonographers used for image acquisition (with a single sonographer performing measures). Over the time course of therapy, there will be alterations of type and doses of therapy, and this has not been accounted for in the final analysis. The exclusion of patients with <3 subsequent visits could lead to survival bias. PH trials identify sex as a reliable outcome marker [126,127], and a determinant of treatment response [128], so RVFWS could have been dichotomised based on sex-specific ranges [122].

3.7 Conclusion

In PAH, RVFWS is a robust prognostic marker of all-cause mortality, independent of clinical and other echocardiographic parameters. Baseline echocardiographic parameters, rather than interval changes observed during therapy, are more strongly associated with mortality.

3.8 Postscript

New tools to track patient clinical status in PAH are required, although the development of these has been slow for a number of reasons. Firstly, as a rare condition, PAH patient numbers in studies are often small, with a diverse patient population displaying small treatment effects. Most outcome studies have short follow-up periods, with single measures used to predict the outcome. There is also criticism that endpoints may not be representative of the severity of disease [129].

Follow-up of PAH patient status with echocardiography should incorporate an assessment of cardiac pressure, structure and function. Although RHC is the gold standard for pressure assessment, there are still pitfalls for using this as a follow-up method. Attention to detail is important. One issue has been differences in the level of zeroing of the pressure transducer [130]. Another is the consistent performance of measurements at end-expiration. The test is also invasive.

Primarily, echocardiography is used to assess changes in cardiac structure and function. The lower variability studies on speckle tracking imaging support its use over traditional systolic function markers for sequential follow-up. RVFWS appears to be a reliable prognostic marker at baseline, with strengths over traditional 2D systolic function parameters. However, the use of RV markers to define treatment response brings some questions:

- Afterload dependence
- Responses in acute versus chronic PHT
- How to identify early disease (provocative testing)
- Could a myocardial approach replace the current haemodynamic approach to distinguishing categories of PHT, including the recognition of LV dysfunction?

- Could improvements in the haemodynamic approach be achieved with other measures? e.g., better RAP assessment.

The remainder of this thesis pertains to gathering evidence regarding these aspects.

3.9 Appendix

Figure 3-8. Median Cumulative survival

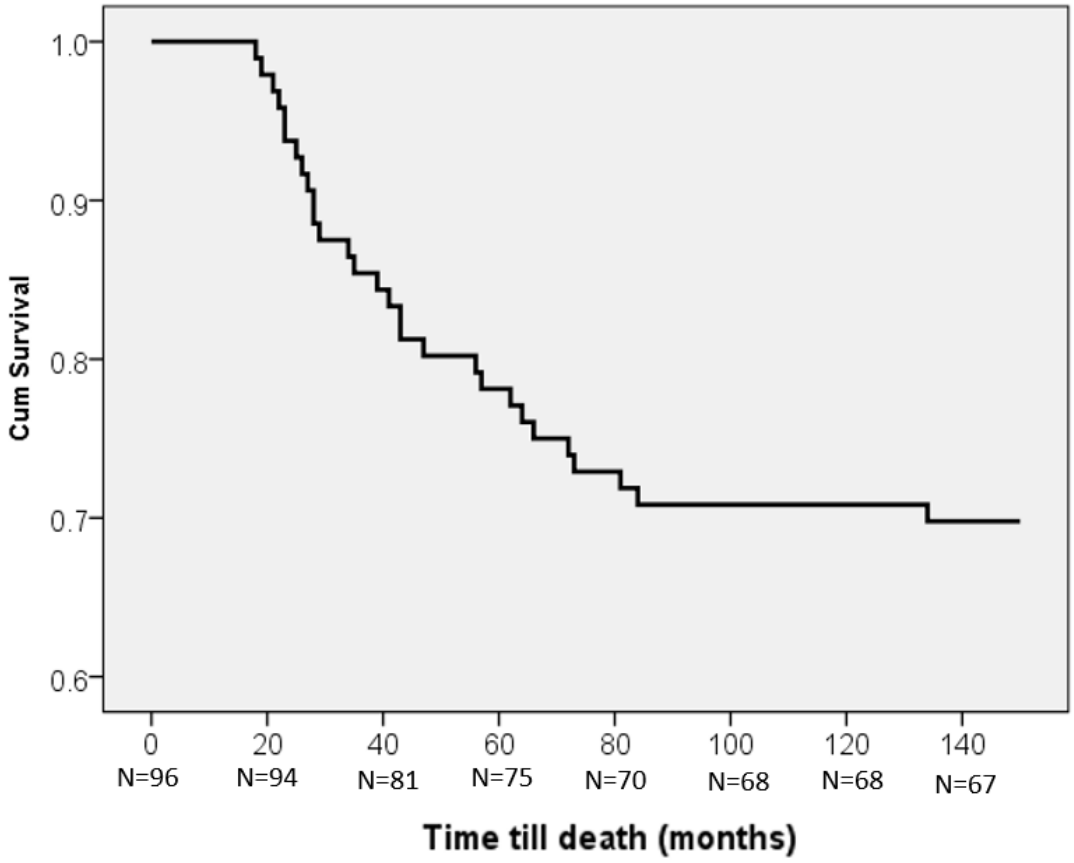

Cumulative survival of the entire cohort over time

Chapter 4

The Afterload dependence of RV Free Wall Strain in PAH

Published as "Afterload-Dependence of Right Ventricular Myocardial Strain" was accepted for publication in 2017

Journal of the American Society of Echocardiography

Leah Wright, Kazuaki Negishi, Nathan Dwyer, Sudhir Wahi MD[3];

Thomas H Marwick.

4 The Afterload dependence of RV free wall strain in PAH

4.1 Preface

Our previous chapter details the use of echocardiography as a follow-up tool in sequential PAH follow-up. Although we have separated PASP and right ventricular free wall function, in reality, these two parameters are intrinsically linked. Over the course of PAH treatment, variations occur in RV loading conditions. As mentioned previously, any new follow-up marker must display appropriate validity to be of clinical use. Afterload directly impacts our interpretation of systolic function.

Ideally, PASP and RV systolic function should be considered together, rather than in isolation. The relationship between changes in ventricular function and afterload is directly measured with invasive sure-volume loop studies; significant differences between left and right ventricular responses to load are present. The load relationship is very difficult to consider non-invasively, research work shows in E_{max} can be quantified with cardiac MRI and 3DE. Assessment of myocardial contraction is a cornerstone of echocardiographic follow-up, and RV dysfunction is a strong predictor of outcome [77].

There has been an acknowledgment of the impact of afterload on the LV [131], but there are limited data about sequential RV assessment. In particular, some oncology patients undergo sequential echocardiography, and afterload assessment is recommended in protocol guidelines [132]. As patients with PAH are followed up over time, the measurement of systolic function to load needs to be considered. It is critical to understand how physiological variables impinge on our understanding of RV strain.

4.2 Abstract

Background: RVFWS is a feasible method for quantitation and follow-up of RV function, and may have benefits over traditional markers such as FAC. However, like all ejection phase parameters, RVFWS is challenging to assess in the presence of changing afterload. We sought to compare RVFWS and traditional RV function parameters for tracking the progress of RV function in PAH over a range of PASP.

Methods: Sequential echocardiograms were collected retrospectively at two-time points between years 2005-2015 in 186 patients (71% female, 63±14 years) undergoing pulmonary vasodilator therapy for Group 1PAH. Patients were either studied during PAH therapy (n=111) or before and after treatment initiation (n=76). Standard measurements of RV and LV function and PASP were performed, and speckle tracking strain was used to calculate RVFWS. The linear response of RVFWS to afterload (PASP) was assessed with standard regression equation. As it is unclear if the response might be non-linear, a quadratic association (PASP squared) was included in the regression model.

Results: At visit 1, PAH patients showed impaired functional capacity (6MWD 371±131 meters), raised PASP (54±26 mmHg), and borderline RVFWS (18±6%). Patients before PAH therapy showed a more pronounced reduction in 6MWD (302±136) and RVFWS (16±5%). RVFWS at baseline was associated with PASP (R^2=0.25, p=0.001), RVEDA (R^2=0.36, p<0.001) and FAC (R^2=0.21, p<0.001). Change in RVFWS was more strongly associated with ΔPASP (Std β-0.20, p=0.02) than ΔPASP squared (Std β 0.11, p=0.20). RVFWS showed strength over FAC for sequential RV assessment over a range of PASP changes.

Conclusion: Afterload changes should be taken into account in the evaluation of RVFWS during PAH follow-up, with the relationship to PASP likely to be linear.

4.3 Background

Following the invasive diagnosis of PAH (PAPm ≥25 mmHg, with a pulmonary artery capillary wedge pressure (PCWP) ≤15 mmHg) [133], the efficacy of pulmonary vasodilator treatment is assessed by echocardiographic estimation of PASP. Echocardiographic derived PASP has shown adequate correlation with RHC[134]) although some have questioned its reliability [31]. Echocardiography continues to be recommended to assess treatment efficacy at 6-12 month intervals over long-term follow-up of treated patients. However, although much attention is paid to following PASP, the most robust echocardiographic markers of outcome in PAH are right atrial size, and pericardial effusion, both of which are related to late-stage disease [94].

There is increasing evidence of the importance of RV systolic markers in PAH [77]. The measurement of right ventricular (RV) strain using speckle tracking echocardiography is feasible for the quantification of RV function in PAH [135-137], with RVFWS shown to predict clinical deterioration and mortality [78]. However, despite the longstanding appreciation of the role of afterload in the assessment of RV function [138], and the load dependence of traditional RV functional indices in PAH [139], there has been little attention paid to the importance of afterload on RV strain. Sequential changes in RV strain are challenging to interpret in the follow-up of treated PAH patients due to fluctuations in PVR. In a clinical cohort, follow-up of patients taking pulmonary vasodilator therapy is a proposed method to track afterload changes over time. The RVFWS to afterload response is assumed to be linear. Invasive animal (with artificial creation of PAH through pulmonary artery banding [140]) studies have found mixed results, with a linear association found, but only when the "severe" category is removed. The non-association of the "severe" category indicates a "quadratic" relationship with PASP having differing effects on RV strain at increasing afterload

levels. The quadratic relationship has implications about how we adjust for afterload. Statistically, this might be best represented by a quadratic equation, which is the dependent variable (PASP) squared. We hypothesised that RVFWS would be a strong echocardiographic marker to track the progress of RV function in PAH over a range of ΔPASP, with changes in RVFWS showing a linear relationship to ΔPASP.

4.4 Methods

4.4.1 Patient selection.

Recruitment of patients with idiopathic PAH and CTD-related PH was from the Tasmanian Pulmonary Hypertension Registry (Hobart, Australia), and the Princess Alexandra Hospital (Brisbane, Australia) (Figure 4.1). After the initial search, 206 patients were identified, but five patients did not have adequate tricuspid regurgitation traces at either baseline or follow-up. A further 14 patients had poor strain images at baseline or follow-up, precluding the calculation of the change in the relevant parameters. Retrospective data collection occurred between years 2005-2015 in 186 patients (71% female, 63±14 years) at two-time points (median time between scans 6 months) during treatment with either endothelin receptor antagonists, phosphodiesterase-5 inhibitors, intravenous/inhaled prostacyclin analogs, or their combination, according to current guidelines

There were two groups of patients, the first being treatment naïve (in whom the baseline echocardiogram was available before treatment and repeated on therapy; n=76), and the second on therapy, who had echocardiograms performed to assess treatment response (n=110). This design was selected to provide a spectrum of change in PASP – our interest was the relationship of RV function to PA pressure rather than the response to particular treatments. Ethics approval was obtained from the Human

Research Ethics committee (Tasmania) Network (approval number H0013333) and the Metro South Human Research Ethics Committee (HREC 16/QPAH/008).

Figure 4-1. Study flow chart, with patient exclusions.

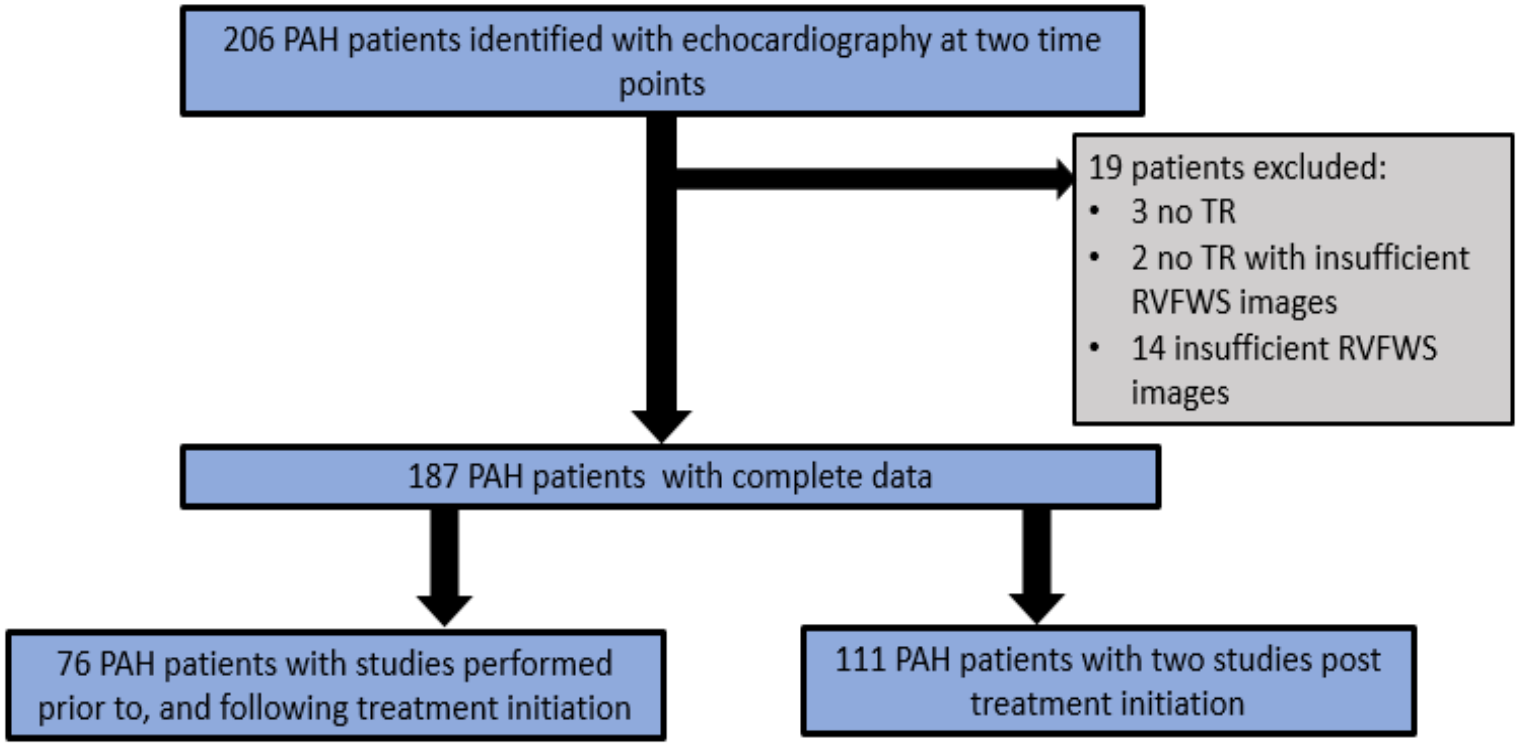

4.4.2 Echocardiographic measurements.

Echocardiography was performed using standard commercial equipment (GE Vivid 7, Vivid i and Vivid e9, Horten, Norway; Philips ie33, Bothell, WA). RV-focused views were obtained in addition to a standard imaging protocol. All measurements were performed by a single reader, using standard views.

Speckle-tracking strain analysis. Wall motion tracking software (Image-Arena, TomTec Gmbh, Unterschleissheim, Germany) was used to analyse 2D echocardiographic images. The optimal image in which the whole RV cavity was visualised was selected from each study. The RV end-diastolic endocardial border was manually traced along the RV septal and RV free wall. These borders were then tracked automatically frame-by-frame throughout the cardiac cycle. Endocardial borders were manually adjusted when necessary, and regions excluded if excessive noise or poor tracking was present. RVFWS was calculated from an average of three segmental RVFWS traces.

4.4.3 Right heart catheterisation.

RHC studies were undertaken after premedication and local anesthesia. A 4-lumen 110 cm 7-Fr Swan-Ganz catheter (Edwards Lifesciences, Irvine, CA, USA) was floated to the right heart, and resting measurements of right atrial, right ventricular, pulmonary arterial and PCWP were made at end-expiration using a pressure transducer (21BB, ITL Healthcare, Chelsea Heights, Australia). The transducer was calibrated to atmospheric pressure at the level of the RA and re-checked at intervals to avoid zero drift. CO was determined by thermodilution, using an average of four consecutive values that varied less than 10%. Electrocardiographic (ECG) leads were connected to both arms and the left leg, allowing three ECG channels for the timing of signals. All

haemodynamic monitoring was recorded using a Horizon SE Haemodynamic System (Mennen Medical Ltd., Yavne, Israel) and subsequently analysed off-line.

4.4.4 Functional testing.

A 6MW test was performed at the time of the echocardiogram by a research nurse. Testing occurred in a quiet hospital corridor and followed a standard protocol [110].

4.4.5 Statistical analysis.

Statistical analysis was performed using standard software (SPSS 20.0, IBM, Chicago, IL) with statistical significance set to $p<0.05$. Calculation of the delta between visits was the final visit values subtracted from visit 1. The change between baseline and follow-up was then plotted using linear and quadratic regression models. To understand which model showed the strongest relationship between variables, the ΔPASP $mmHg^2$ (for the quadratic model) was added using sequential linear regression model, to assess whether there was a significant reduction in the mean of the squared errors. A relative change in LV GLS of 10% has been defined as being clinically relevant [141], based on the reproducibility of strain. We, therefore, used cut-offs of the relative change of 10% for FAC (%) and RVFWS (%) to evaluate the relationship between ΔPASP (mmHg) and ΔRVFWS. One-way ANOVA with Tukey HSD was used to compare groups. Actual ΔRVFWS was compared with predicted ΔRVFWS from linear and quadratic models. 20 patients were randomly selected for inter and intra-variability analysis. Readers were blinded to originally measurement results. Bland Altman plots were used to asses level of agreement between measures, with the intra class correlation used to determine the reliability of measures. ICC readings of <0.5 classify as poor, 0.5-0.75 as moderate, 0.75-0.90 good, and >0.9 as excellent[142]

4.5 Results

4.5.1 Patient characteristics.

Baseline demographic details (Table 4.1) were similar to other PAH cohorts (age 63±14 years, 134 females (72%), with most patients having idiopathic PAH (52%) followed by CTD (36%). The majority of patients were treated with endothelin receptor antagonists (57%) or phosphodiesterase type-5 inhibitors (28%), and some participants on multiple therapies (14%).

4.5.2 Associations of baseline measurements

Baseline PASP (mmHg) was significantly related to 6MWD (r -0.37, $p<0.001$) and RV function (Table 4.2). 6MWD had a significant relationship with RV function and LV diastolic markers, but not LV EF.

4.5.3 Baseline vs follow-up.

At visit 1, 76 patients had echocardiography available for analysis before initiation of medication, and another 110 had sequential echocardiograms performed on PAH therapy. Between baseline and follow-up (Table 4.3), there was a decrease in PASP and an improvement in RV strain, with no significant difference in 6MWD, LV systolic function or estimated LV filling pressures. In the subgroup studied before and after initiation of pulmonary vasodilators (Appendix Table 4.6), there were no significant improvements in 6MWD, but the intervention group displayed a borderline improvement in RVFWS ($p=0.06$), and pulmonary artery systolic pressure ($p=0.02$)

Table 4-1. Baseline characteristics (n=187)

	Mean (SD)
Age (years)	63±14
HR (bpm)	76±14
BMI	28.1±7.0
Female (%)	134 (72%)
PAH Subtype	
- Connective Tissue Disease	66 (35%)
- Idiopathic PAH	97 (52%)
- Congenital	8 (4%)
- COPD	3 (2%)
- Unclear	9 (5%)
Treatment	
- Any ERA	139 (74%)
- PDE 5	70 (37%)
- Iloprost	9 (5%)
Multi Therapy	26 (14%)

HR, Heart rate; BMI, body mass index; PAH, pulmonary arterial hypertension; COPD, chronic obstructive pulmonary disease; ERA, endothelin receptor antagonist; PDE5; phosphodiesterase type 5 inhibitor;

4.5.4 Invasive measurements.

A subset of patients (n=64) had invasive measurements performed at two-time points (Table 4.3). PA pressure showed a significant reduction after therapy initiation, but there was no significant change in PCWP. At visit 1, the time difference between RHC and echocardiography was at a median interval of 0 days (interquartile range 167 days), with invasive PASP and Doppler-derived PASP showing a moderate significant correlation ($r=0.71$, $p<0.001$). The inter-class correlation coefficient at visit 1 was 0.71(0.59-0.79), $p<0.001$. At visit 2 median interval 0 days (mean 11±101.2) the inter-class correlation coefficient was 0.67 (0.50-0.78), $p<0.001$, with a moderate correlation ($r=0.67$, $p<0.001$). Similar to echocardiographic measures, there were modest significant correlations with invasive markers and echocardiographic variables (Table 4.4).

Table 4-2. Baseline associations of Doppler PASP and 6MWD

	PASP		6MW	
	R	**P**	**r**	**p**
RVFWS (%)	-0.45	<0.001	0.36	<0.001
FAC (%)	-0.45	<0.001	0.24	0.002
RVEDA (cm^2)	-0.46	<0.001	-0.31	<0.001
PAPs (invasive) (mmHg)	0.53	<0.001	-0.15	0.18
HR (bpm)	-0.17	0.01	-0.14	0.08
EF (%)	0.08	0.29	0.06	0.46
e' septal (cm/s)	-0.35	<0.001	0.39	<0.001
e' lateral (cm/s)	-0.18	0.02	0.45	<0.001
E/e' septal	0.005	0.95	-0.19	0.03
E/e' lat	-0.09	0.26	-0.19	0.03
BMI	0.03	0.69	-0.16	0.06

RVFWS, right ventricular free wall strain; FAC, fractional area change; RVEDA, right ventricular end diastolic area; PAPs, pulmonary artery systolic pressure; HR, heart rate; EF, ejection fraction; BMI, body mass index

4.5.5 Afterload dependence and RV function markers.

The decrease in PASP over follow-up in the group as a whole was associated with changes in 6MWD (r=-0.26, p=0.003), RV function with RVFWS (r=-0.25, p=0.001), but not FAC (r=-0.12, p=0.10), and heart-rate (r=0.16, p=0.03). A regression equation was then developed to predicted ΔRVFWS from the linear regression model (ΔRVFWS =0.75+-0.06*ΔPASP). The quadratic regression was (ΔRVFWS = 0.60 + [-0.047 * ΔPASP] + [0.0007 * ΔPASP* ΔPASP]). Both of these regression lines are shown in Figure 4.2. Figure 4.3a shows the actual versus predicted ΔRVWFS (derived from the regression equation; ΔRVFWS = 0.99+[-0.11*ΔPASP]+[0.0006*ΔPASP*ΔPASP]) for the entire group (r=0.26, p=0.001), Figure 4.3b shows those restricted to the treatment intervention group (r=0.44,p<0.001).

Figure 4.3c shows the linear and actual plotted against each other for the whole group (r=0.25, p=0.001) and for the treatment intervention group (ΔRVFWS=1.12+[-0.12*ΔPASP]) (r=0.44, p<0.001). When models based on ΔPASP and ΔPASP squared were compared, this showed the linear model to show the stronger association (Std β-

0.20, p=0.02, vs. Std β 0.11, p=0.20). ΔFAC showed no significant association for the linear or quadratic model (std β 0.12 p=0.10 vs. std β 0.14 p=0.34) (Figure 4.3c). Results were similar in a group restricted to pre and post-treatment only (std β-0.24,p=0.09 vs. std β -0.10, p=0.49) (Figure 4.3d).

Figure 4-1. Quadratic and linear regression models in all patients (left) and patients tested before and after treatment (right). The linear and quadratic regression lines are shown.

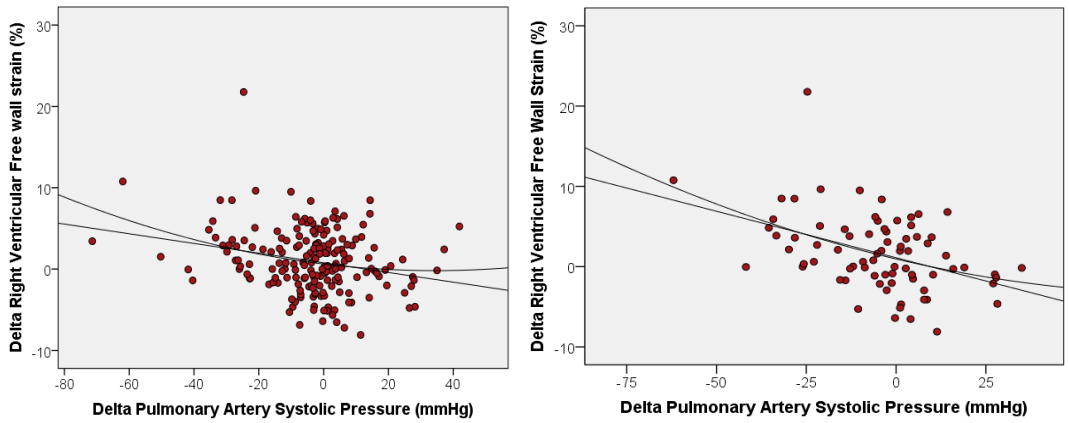

Figure 4-2. Actual change in RVFWS versus predicted change based on change of RV afterload.

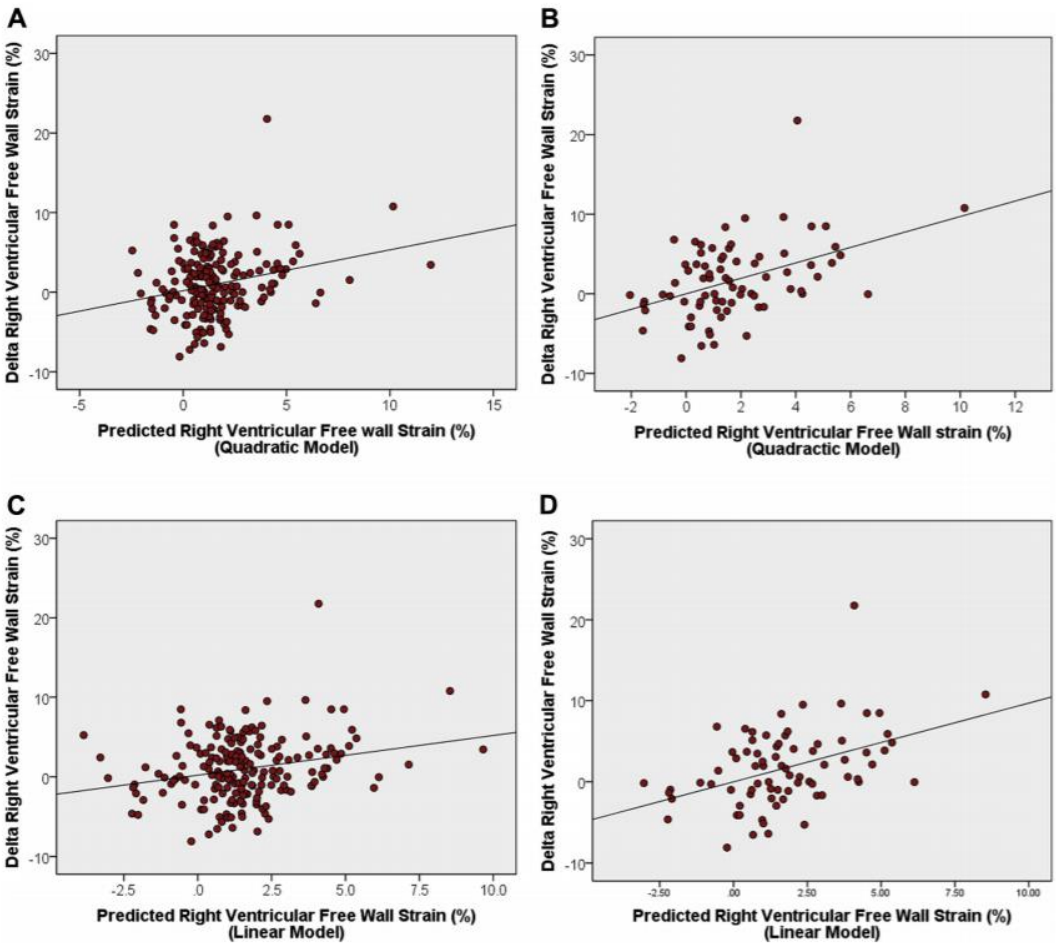

The overall and pre (4.2a) - and post-treatment groups (4.2b) for the Quadratic model. Figure 4.2c and 4.2d shows the predicted change based on RV afterload for the linear model in the pre (4.2c) and post-treatment groups (4.2d).

Figure 4-3. ΔPASP and common ΔRV variables

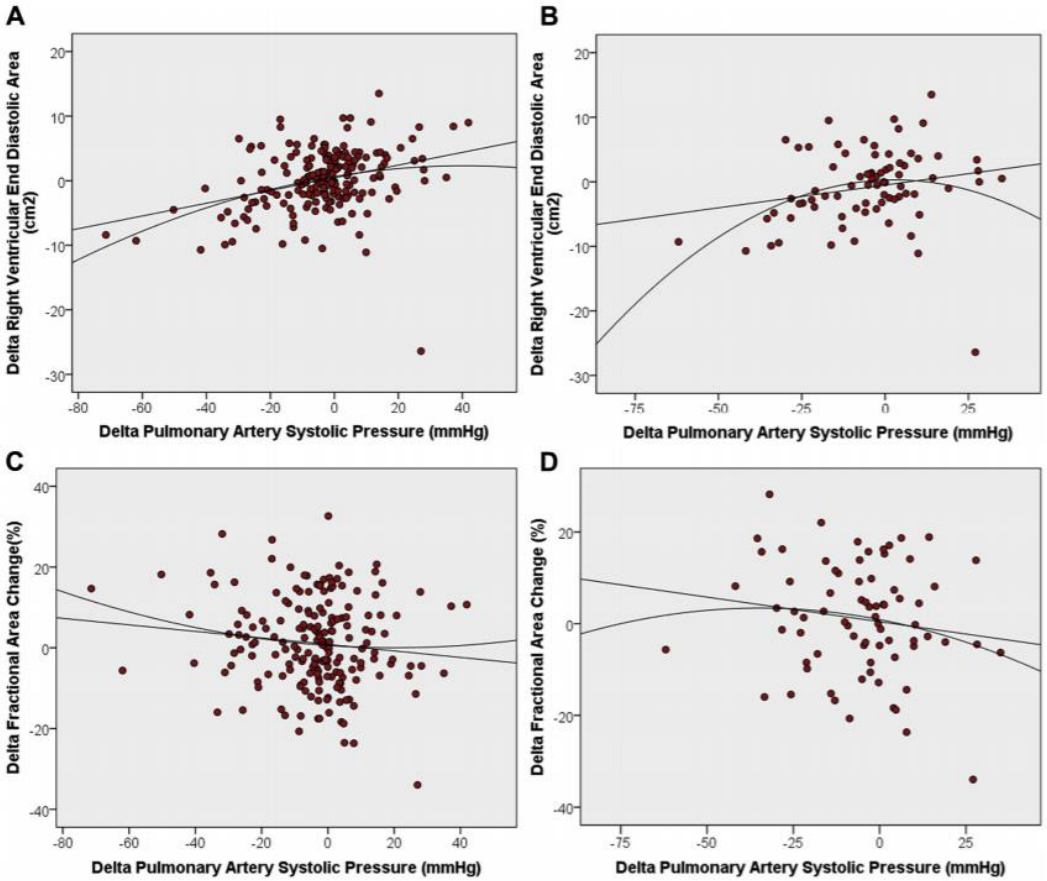

4.3a and those studies both pre and post treatment (4.3b) with both linear and quadratic regression lines. ΔFAC and ΔPASP for the whole group (4.3c) and restricted to pre and post-treatment (4.3d) with linear and quadratic regression.

Table 4-3. Baseline and follow-up* clinical and echocardiographic markers

Variable	Visit 1 (n=187)	Visit 2 (n=187)	Delta	p
Six-minute walk (m)	371±130.8	380±130.6	9.7±71.2	0.12
Heart rate (bpm)	76±13.8	75±14.2	-0.7±12.0	0.42
Left ventricle				
-Ejection fraction (%)	62±9.1	63±8.0	0.65±9.6	0.40
-LVEDV (ml)	72.3±24.8	73.9±24.2	1.6±17.1	0.22
-LVESV (ml)	27.9 ±13.2	28.2±12.3	0.35±10.2	0.64
-LV diastolic dimension (cm^2)	4.6±0.70	4.6±0.73	0.02±0.70	0.65
-PW (cm)	0.96±0.34	0.94±0.16	-0.02±0.32	0.42
- e' septal (cm/s)	6.2±2.3	6.2±2.2	-0.04±1.8	0.83
-E/e' avg	10.8±4.8	11.6±6.2	0.8±5.1	0.07
- E/e' lateral	9.3±4.5	9.0±5.0	-0.22±3.6	0.50
-E/e' septal	12.4±6.2	13.8 ±7.0	0.04±1.8	0.01
Right ventricle				
-Estimated PASP (RVSP+RAP, mmHg)	53.8±25.8	50.2±24.7	-3.6±15.8	0.001
- End-diastolic area (cm^2)	21.4±8.4	21.6±8.3	-0.02±0.32	0.71
- Fractional area change (%)	33.3±12.0	34.2±11.2	0.92±11.0	0.24
-TAPSE (cm)	1.9±0.53	2.0±0.55	0.10±0.48	0.006
-RVS' (cm) (n=75)	9.7±2.9	9.5±3.2	-0.16±2.6	0.59
- RVFWS (%)	18.0±5.7	18.9±5.4	0.94±3.9	0.001
-IVC (cm)	1.7±0.81	1.5±0.85	-0.2±0.93	0.002
-RVFWS/PASP	0.44±0.30	0.49±0.31	-0.05±0.19	<0.001
Invasive pressures				
- PAPs (n=58)	79.9±20.5	66.2±19.9	-3.7±14.7	0.06
- PAPm (n=64)	43.8±13.1	40.2±13.2	-3.5±10.3	0.008
- PCWP (n=58)	12.3±6.0	11.8±4.6	-0.57±6.1	0.48

LVEDV, left ventricular end diastolic volume; LV ESV, left ventricular end systolic volume; PW posterior wall; PASP, pulmonary artery systolic pressure; RVSP, right ventricular systolic pressure, RAP, right atrial pressure; TAPSE, tricuspid annular plane systolic excursion; RVS', right ventricular systolic peak velocity; Right ventricular free wall strain; IVC, inferior vena cava; PAPs, pulmonary artery peak systolic pressure; PAPm, mean pulmonary artery pressure; PCWP, pulmonary capillary wedge pressure.

4.5.6 Differences in echocardiographic measurements.

FAC change within 10% (n=48) showed a Doppler-derived PASP change of -4.1±12.2 mmHg. In those showing 10% improvement of FAC (n=79), the mean ΔPASP was -4.8±17.6, for those who FAC declined by >10% (n=65), mean change in PASP was -2.2±16.2 mmHg (Figure 4.5a). There was no significant within-group change (p=0.62) (Figure 4.5b). For the RVFWS group who had a change within 10% (n=76), the PASP mean change was -4.4±14.6 mmHg. For those who improved RVFWS by 10% (n=72), mean PASP change was-6.7± mmHg. Finally, those who RVFWS who declined by

10% (n=38) the mean change in PASP was 3.5±12.4mmHg. The between-group differences were highly significant (p=0.007).

In 61 patients with a TAPSE change <10% the mean change in echocardiographic PASP was -2.3±13.0 mmHg, compared with 36 with a >10% reduction (n=36) in whom the mean ΔPASP was -5.2±20.3 mmHg. In 80 patients with a >10% improvement in TAPSE, the mean ΔPASP was -2.3±14.0 mmHg. There was no significant difference between groups (p=0.59).

Table 4-4. Association of invasive PASP with echocardiographic variables

	Invasive PASP baseline visit 1		**Invasive PASP visit 2**	
	R	**P**	**r**	**P**
RVWFS (%)	-0.32	0.001	-0.23	0.08
FAC (%)	-0.17	0.19	-0.28	0.03
RVEDA (cm^2)	-0.26	0.01	0.29	0.02
TAPSE (cm)	-0.32	0.002	-0.24	0.06
PASP (mmHg)	0.71	<0.001	0.67	<0.001

RVFWS, Right ventricular free wall strain; FAC, fractional area change, RVEDA, right ventricular end diastolic area; TAPSE, tricuspid annular plane systolic excursion; PASP, pulmonary artery systolic pressure

4.5.7 Predictors of change in RV function.

The associations of the response of RV function to change in PASP, independent of age, sex, HR and PAH therapy, are shown in Table 4.5. ΔPASP was the strongest predictor of ΔRVFWS (Std β -0.24, p=0.001), independent of whether there was initiation of therapy between baseline and follow-up. There was no significant relationship between ΔPASP and ΔFAC (r=-0.1, p=0.09), in either the treated or untreated group (treated Std β -0.07, p=0.48 versus untreated Std β 0.19, p=0.11).

Table 4-5. Independent associations of the response of RV function (RVFWS) to change in PASP (R^2=0.09, p=0.007

	Std β (95%CI)	P
Age	0.03(-0.03;0.05)	0.73
Sex	-0.03(-1.5;1.0)	0.67
HR	-0.09(-0.07;0.02)	0.20
PAH therapy	0.14(-0.003;2.3)	0.05
ΔEcho PASP	-0.24(-0.09;-0.02)	0.001

HR, heart rate; PAH, pulmonary arterial hypertension, PASP, pulmonary artery systolic pressure

4.5.8 Intra- and inter-observer variability.

The intra-observer variability for RVFWS showed an intra-class correlation coefficient of 0.73 (95% CI 0.44-0.88, p<0.001), and a mean difference of 1.3±3.2%. The inter-observer variability showed an intra-class correlation coefficient of 0.62 (95% CI 0.26-0.83, p<0.001, mean difference of 4.5±4.7%.

4.6 Discussion

This study shows that there is a highly significant correlation between ΔRVFWS and ΔPASP. Over the modest range of ΔPASP, this relationship appears linear. RV FWS appears to have superiority over traditional RV function measures when tracking patients during variations in PASP.

4.6.1 Afterload and RV function measurement.

The impact of afterload changes on the measurement of RV systolic function is routinely overlooked. In general, a pressure load on the RV is less tolerated than a volume load [143]. Volume load toleration is well-exemplified in the preservation of RV function in tricuspid regurgitation. Remarkable differences between LV and RV physiology preclude the use of the same assumptions about afterload-dependence [144]. The RV has an intrinsically different mechanical function to the LV, with lower afterload [145] and a substantial proportion of systolic function occurring in the longitudinal plane [146]. Differences between LV and RV are readily apparent from a comparison of RV pressure-volume loops [147], with the myocardial response of the LV

[148]. An animal model showed a linear association of increasing RV pressure on RV circumferential strain, but only when the severe category was removed [140]. There was no significant change in RVFWS & RV FAC at increasing degrees of pulmonary artery banding [140]. It is possible that among "normal" variations of PASP, the response may be linear, but after a specified increase is reached, this relationship increases exponentially, as would be best represented with a quadratic model. Although, this does not appear to occur throughout ranges generally encountered during the clinical follow-up of PAH patients.

This study used PASP as the sole measure of RV afterload. In reality, a number of facets influence the RV response to afterload. These include resistance from the pulmonary valve, wave reflections in the main pulmonary artery and early bifurcations as well as impedance of the proximal pulmonary arteries and arterioles [149,150]. In an animal model, proximal PA pressure loading caused greater diastolic dysfunction than increased peripheral resistance [151]. Wall stress itself has many different components; resistance to blood flow during steady state, compliance of the vascular system, arterial wave reflections and inertia of blood during ejection [152].

A number of caveats need consideration during patient follow-up with echocardiography. There is not only the variability that exists in the measurement of Doppler-derived PASP but also individual variation in the degree of RV structural remodelling. RV remodelling occurs after prolonged exposure to afterload [153], but there are differences in this process in PAH and congenital heart disease. Changes in RV function at increasing afterloads are maintained through structural remodelling, as opposed to modifying myocardial function [153].

Figure 4-4. Degree of change in RV systolic function variables, and relation with ΔPASP

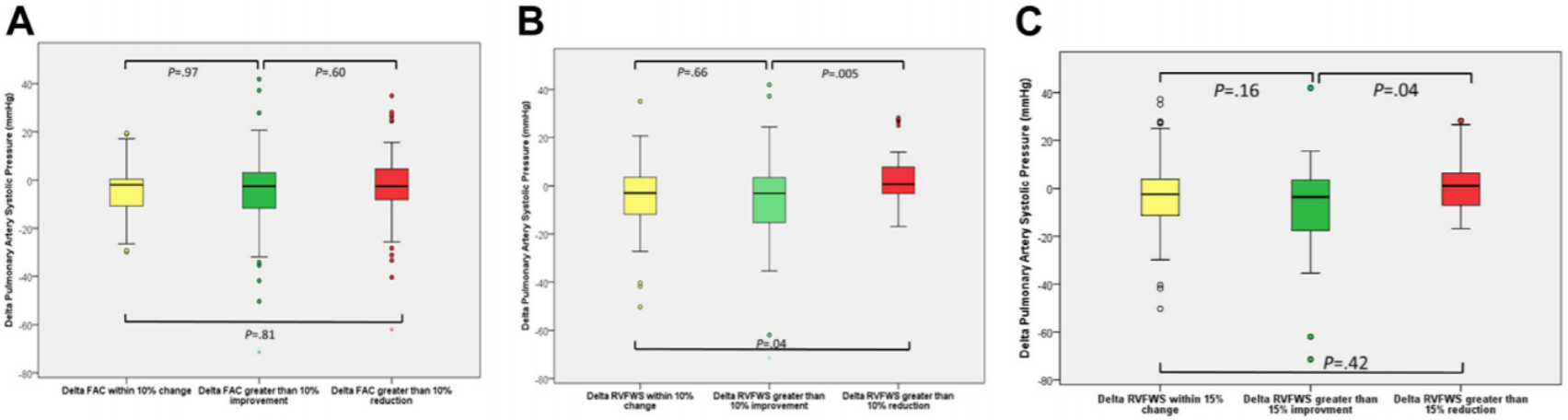

4.4a shows participants within 10% FAC change; FAC increased by >10% or FAC reduced by 10% and the mean PASP for each group. Figure 4.4b shows ΔRVFWS groups and corresponding PASP changes. 4.4c shows ΔRVFWS with 15% cut off ranges

Variability impacts the utility of 2D-derived RV FAC as a tool for longitudinal follow-up, as this measure of RV systolic function is based on RV cavity size. RV FWS and TAPSE may, therefore, have benefits over this method. Minor degrees of RV recovery are shown after initiation of sildenafil to bosentan therapy [154] over a 12 month period. Invasive procedures such as pulmonary artery endarterectomy and lung transplantation provide evidence that the RV has capacity to remodel over short periods after dramatic afterload changes[155]. The six month period chosen in this study eliminates some of the variations produced by RV reverse remodelling. The chronicity of afterload elevation is also important, with acute changes (such as pulmonary embolism) leading to RV enlargement and RV decompensation. The amount of remodelling that has occurred within the ventricle, before afterload increases, affects the ability of the RV to maintain function through heterometric autoregulation [156]

After combined efforts from industry and academia, the concordance of speckle tracking echocardiography strain has improved [157], and may even be superior to traditional 2D echocardiographic measures. The performance of vendor independent software, which can be used to measure retrospective data using DICOM images at frame rates of >30 frames/second, has been shown to be acceptable for strain analysis [158], as well as providing results comparable to online software [157]. Velocity vector imaging is based on speckle tracking echocardiography, and angle dependence (which was a limitation of previous tissue Doppler-based techniques), is not an issue.

The ability to define RV function in the presence of altered loading conditions may help the successful application of echocardiography to track RV status. This response has not been accurately defined in the past, with pulmonary artery constriction studies showing mixed results in the linear association of PASP to RVFWS [140,159].

4.6.2 Clinical implications.

Outcome studies have shown the importance of RV function in determining outcome in PAH. Routine studies of RV function and PASP are required when tracking therapeutic response in patients. RV systolic function is a significant predictor of patient outcome, but interpretation needs to consider changes in afterload. Perhaps the two most common situations of changing pulmonary afterload are in the evaluation of patients undergoing pulmonary vasodilator therapy, and in post-cardiopulmonary bypass patients, where PH may be transient.

The results of this study show that changes in RV afterload have a modest impact on changes in RV function and that this is linear within commonly observed changes in pulmonary artery systolic pressure with pulmonary vasodilator treatment afterload [160]. These considerations are essential because longitudinal measurements of RV function and dynamic changes in afterload can influence clinical management.

4.6.3 Study limitations.

The number of studies in which patients displayed a significant change in afterload was limited. The original studies did not include assessment of tricuspid annular e' or isovolumic acceleration (which is afterload independent), which could have strengthened the assessment of the RV-PASP relationship. Patient clinical status and etiology of PAH are possible confounding factors. A prospective longitudinal study design, with simultaneous RHC and echocardiography, would have been an ideal study design. Nonetheless, a 6-12 month follow-up time would still be desirable as this period is the one that is usually used to assess response to pulmonary vasodilator therapy, and therefore corresponds to the clinical question about the afterload-dependence of RV change. Use of a more extended timeframe would also increase the likelihood of confounding by RV remodelling.

4.7 Conclusions.

RVFWS is superior to FAC for tracking RV response to changes in PASP. The linear association of RVFWS with RV afterload has significant implications for the assessment of RV strain over long-term patient follow-up.

4.8 Postscript

As discussed in the previous chapter, afterload and sequential follow up are intrinsically linked when quantifying RV systolic function. As studied from a PAH cohort afterload entails a lasting impact on the heart. Patients with adult congenital heart disease constitute a well-defined cohort with chronically increased afterload and have a different outcome than idiopathic PAH[161]. Registry outcome data primarily focus on clinical variables and traditional 2D markers. RV free wall strain is measurable retrospectively but requires adequate imaging of the RV free wall and access to specialised imaging software. For this reason, our data set is unique and adds significantly to current literature. In Australia, unless symptom status changes, patients are routinely follow up with echocardiography. Limited data were available on sequential right heart catherisation and echocardiography thus were unable to validate findings with an invasive cohort.

Aside from this, presentations of afterload stress can also occur acutely, primarily, as an acute pulmonary embolism. A pulmonary embolism is associated with high morbidity and mortality rates[162]. Generally, this group presents with raised afterload, with the insult primarily occurring to a healthy myocardium (one that has not been exposed to chronically increased afterload). As the RV is not accustomed to this increment of pulmonary pressure, its response involves increases in RV size, and reductions in systolic function, despite the lower levels of PASP as compared to chronic PAH. Speckle tracking is an underutilised tool for RV tissue characterisation, which could be helpful in this acute clinical setting.

We have evaluated the effect of afterload on RV strain, in the next chapter we will address chronicity of afterload

4.9 Appendix

Table 4-6. Baseline and follow-up clinical and echocardiographic findings in patients on treatment

Variable	Visit 1	Visit 2	Delta	p
Six-minute walk (m)	302±135.7	315±139.8	12.6±50.0	0.39
Heart rate (bpm)	77±14.3	77±17.2	0.41±14.9	0.81
Left ventricle				
-Ejection fraction (%)	62±9.9	63±7.4	1.0±9.9	0.42
-LVEDV	71.7±25.3	75.1±25.3	3.3±18.4	0.12
-LV diastolic dimension (cm)	4.4±0.74	4.4±0.83	0.04±1.0	0.70
-PW (cm)	1.0±0.50	0.97±0.17	-0.06±0.48	0.23
- e' septal (cm/s)	5.3±1.8	5.6±2.4	0.30±1.8	0.25
-E/e'	10.7±5.0	12.8±8.4	2.02±6.8	0.03
-E/e' septal	12.3±6.0	14.9±8.7	0.30±1.8	0.02
-E/e' lat	9.2±5.1	9.7±6.2	0.54±4.0	0.34
Right ventricle				
- Estimated PASP (RVSP+RAP, mmHg)	60±23.3	55.5±23.0	-4.6±17.0	0.02
- End-diastolic area (cm^2)	24.2±8.2	23.6±7.7	-0.63±6.1	0.37
- Fractional area change (%)	29.5±13.5	30.2±12.0	0.70±12.1	0.62
- RVFWS (%)	15.5±5.3	17.1±5.3	1.65±4.7	0.003
-RVFWS/PASP	0.31±0.19	0.38±0.21	-0.06±0.18	0.003

LVEDV, left ventricular end diastolic volume; PW, posterior wall; PASP, pulmonary artery systolic pressure; RVSP, right ventricular systolic pressure; RAP, right atrial pressure; RVFWS, right ventricular free wall strain;

Chapter 5

Acute versus chronic afterload increase and the RV myocardium

Article "Right Ventricular Systolic Function Responses to Acute and Chronic Pulmonary Hypertension: Assessment with Myocardial Deformation" accepted for publication in March 2016

Journal of the American Society of Echocardiography

Wright L, Dwyer N, Power J, Kritharides L, Celermajer D, Marwick TH.

5 Acute vs chronic afterload increases and the RV myocardium

5.1 Preface

The interaction between afterload and systolic contraction underpins our understanding of cardiac function. Increases in afterload can arise from varying clinical conditions. There are frequent delays in the diagnosis of PAH, due to the non-specificity of symptoms, as well as failure to recognise due to its rarity, so patients may not be started on afterload reducing therapy until late in the disease course. Substantial remodelling is often present at the initial imaging visit. This remodelling is manifest by a dilated RV, with reduced systolic function.

A rapid increase in afterload may occur during an acute pulmonary embolism, leading to acute RV dilation, and significant reduction of systolic function. As the right ventricular pressure increases, the shape of the pressure-volume loop alters and tends to resemble the LV, with maximal elastance ($E_{max)}$ occurring at end-systolic pressure (ESP).

The morphology of the RV is similar in acute versus chronic RV afterload with significant RV dilatation present. The question is how the reasons for afterload increase affects the RV function. Prior methods of right ventricular assessment using 2D ultrasound can be hampered by the crescentic shape of the RV, or by translational motion. In patients with chronic pressure overload, speckle tracking may aid with the differential diagnosis.

5.2 Abstract

Background: The distinction between right ventricular (RV) dysfunction due to an acute etiology (pulmonary embolism, PE) or chronic afterload (pulmonary arterial hypertension, PAH) has significant therapeutic implications. We hypothesised that RV remodelling would alter RVFWS and differentiate chronic from acute RV afterload.

Methods. In this retrospective study, PE patients (n=45) with echocardiography within 48 hours of computed tomography pulmonary angiography were matched 1:1 for age, gender and PASP with PAH patients (n=45), and a larger un-matched PAH control group (n=116). RV function was evaluated with RVEDA, FAC, and RVFWS by 2D speckle-tracking. The ability of RVFWS to distinguish acute versus chronic RV dysfunction was assessed using receiver operating characteristic curves (ROC), and its incremental value sought with stepwise models.

Results. RVEDA, FAC and RVFWS were significantly impaired in PE ($p<0.001$) with no significant differences in other clinical variables. In matched patients, ROC analysis revealed RVFWS had a significantly better discriminative power than the McConnell sign ($p=0.02$), with a cut-off of -17.9%, sensitivity 87.5%, specificity 62.5%, AUC 0.76. Sequential logistic regression demonstrated an incremental and independent benefit of using RVFWS to predict acute PE versus chronic PAH ($p=0.01$). Interclass concordance was superior in RVFWS compared to FAC ($p<0.01$).

Conclusions: RVFWS is more predictive than RVEDA and less variable than FAC in distinguishing acute from chronic RV pressure overload. RVFWS adds incremental and independent information to standard measures of RV function in assessing the acuity of PH.

5.3 Background

The distinction between pulmonary embolism (PE) and chronic PAH may have significant therapeutic implications. Although right ventricular (RV) function and size are important prognostic markers in both patients with PE [163] and chronic PAH,[69,73] RV function may differ between these entities. In chronic pressure overload, the myocardium can adapt and remodel to compensate and maintain CO[164] evidenced by previous experimental models using pulmonary artery banding.[165] In contrast, the RV myocardium has limited time to increase contractility in acute pressure overload, resulting in RV dilation and impaired function.

The distinction between these causes might be facilitated by a technique which can quantify RV dysfunction, to the degree that has not been feasible with standard imaging.[166] This information is not readily gathered from computed tomographic pulmonary angiography (CTPA). PA systolic pressure (PASP) will only increase if >30-50% of the pulmonary artery bed is occluded,[167] and generally, echocardiography has limited value in submassive PE(negative predictive value of 40-50%). Historically, subjective markers (such as the McConnell sign, the "apical sparing" in the RV) have been used to diagnose acute pulmonary embolism,[168] but this is limited by a sensitivity of 70% and specificity of 33%.[169] Strain imaging using speckle tracking of the RV free wall (RVFWS) is an emerging technique to measure myocardial deformation, which has been validated using sonomicrometry,[159] and is now readily available – on most echocardiography machines, even at the bedside allowing clinical utility. Previous work has shown the ability of RVFWS to identify RV dysfunction in PAH.[136] However, the load dependency of functional measurements can complicate the evaluation of systolic dysfunction.[138] We sought to

determine whether RV global and regional strain could be used in a clinical context to differentiate acute versus chronic increases in RV afterload

5.4 .Methods

5.4.1 Study design.

In this cross-sectional study of RV function, patients with acute PE were compared with control patients with PAH. Patients with acute PE (n=45) were retrospectively identified from administrative records and were eligible for the study if echocardiography was performed within 48 hours of computed tomography pulmonary angiogram. These patients were anticoagulated; none underwent thrombolysis. Most were haemodynamically stable, although two had documented systolic blood pressure <90 mmHg. Patients with documented CTEPH were excluded. Control patients were obtained from a chronic PAH registry cohort from the Royal Hobart and Launceston General Hospitals between years 2005-2013 with diagnosis through RHC. Patients were treated with an endothelin receptor antagonist, a phosphodiesterase-5 inhibitor, intravenous/inhaled prostacyclin analogues, or their combination, in accordance with current guidelines. The primary control group comprised of PAH patients matched for age, gender and PASP (as derived from transthoracic echocardiography, TTE) (n=45). As matching is rarely perfect, an unmatched group from the same patient cohort (n=116) was run as a sensitivity analysis.

5.4.2 Standard echocardiography.

Studies were performed on commercially available GE (Vivid E9, Vivid 7 and Vivid I, General Electric, Milwaukee, WI) and Philips (IE33 and EPIQ, Philips, Andover, MA) equipment. The acquisition followed a standard protocol, including RV-focused views, and measurement of pulsed-wave Doppler of the RV outflow tract for estimation of PVR.[166]. Full details are provided in the methods section (3.0)

5.4.3 Speckle tracking strain analysis.

RVFWS was performed from an apical RV focused view, using speckle tracking (Image arena, Tomtec, Unterschlessheim, Germany).

5.4.4 Statistics.

Data were assessed for normality using the Shapiro-Wilk W test and transformed if necessary. For PVR values the "linear trend at point" method was used for missing data. Patients were placed into equal tertiles for PVR due to inability to normalise. Comparison of patients and controls was performed by matching 1:1 for age, gender, and PASP, as well as the inclusion of all controls into statistical models. Acuity of afterload increase was assessed as a binary variable (PAH versus PE). Associations of RV systolic function were determined using univariable and multivariable logistic regression. Anticipated associations were placed into the model (age, sex, gender and PASP). The incremental benefit was assessed by comparing the global chi-square value for each model. Receiver operating characteristic (ROC) curves were created to determine the diagnostic ability of RV functional measurements to distinguish those with and without acute increases in RV afterload with an area under the curve (AUC) calculated. Cut-off values were obtained using the Youden index. Inter-operator variability was performed in both the chronic PAH (n=30) and pulmonary embolism (n=25) studies. Variability studies were randomly selected, with the second reader not aware of reader 1's results, or which cardiac cycle and image window were measured.

Bland Altman analysis was used to assess the mean difference and limits of agreement, and the intra-class correlation coefficient was calculated.

5.5 Results

5.5.1 Patient characteristics

Patients in the PAH group were divided into 81 (50%) with idiopathic PAH, 68 (42%) with CTD-related PAH, 7 with congenital heart disease (3%), 4 with chronic

obstructive pulmonary disease (2.5%) and 1 with Porto-pulmonary hypertension (0.6%) (Table 5.1). The primary clinical differences between PE and the PHT controls were in BMI, HR, SBP and renal function. AF was present in 4 of the PE cohort (9%) and 5 in the PAH group (3%). The severity of tricuspid regurgitation in PAH patients was mild in 119 (74%), moderate in 27 (17%), and severe in 15 (9%).

5.5.2 Echocardiography

Comparison between PE and controls showed differences in echo estimated PVR (higher in PE) and all RV function indices (reduced in PE) (Table 5.1). RV size (RVEDA) was increased in PE patients. Figure 5.1 shows the pattern of right ventricular regional strain. LV EF showed a significant difference with the matched group (59±10% vs. 64±7, p=0.03). Diastolic function between groups was similar.

Figure 5-1. Strain patterns of the segments and whole right ventricular free wall in PAH compared in PE. Strain is consistently impaired in the PE than the PAH patients.

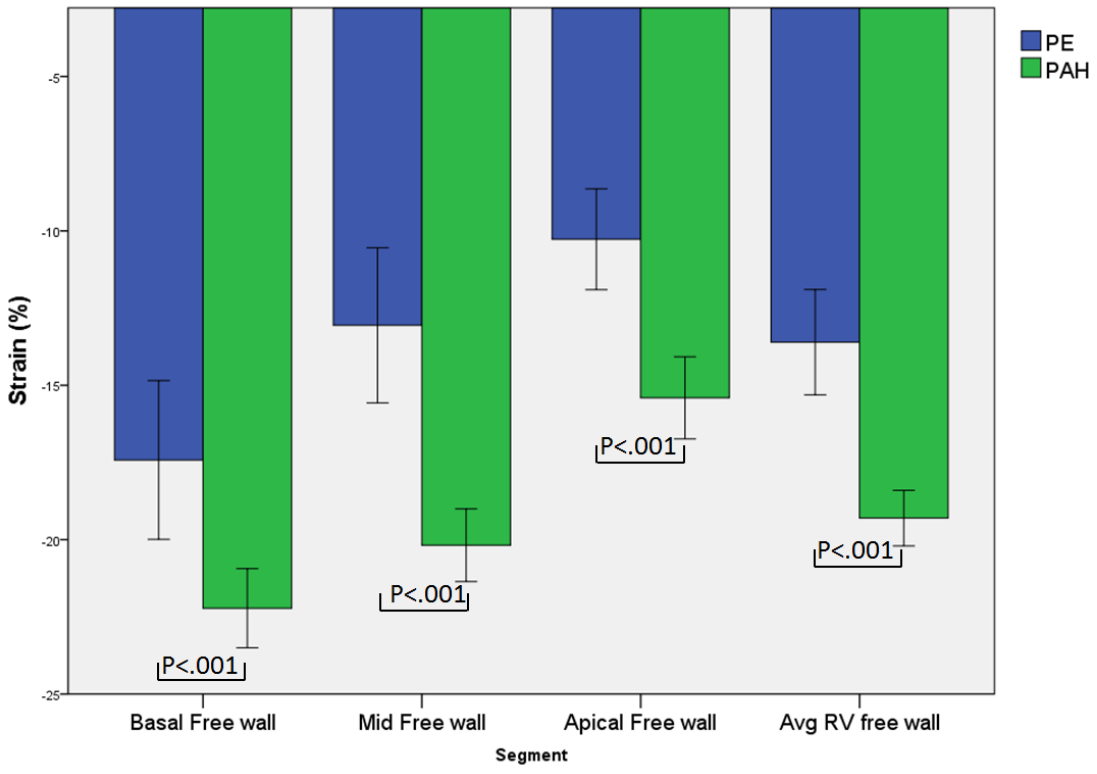

Table 5-1. *Clinical characteristics of PE patients, matched and unmatched PHT controls*

	Matched		
Variable	**PE (n=45)**	**PAH (n=45)**	**P value**
Age	64±15	62±13	0.57
Sex (F)	69%	69%	
BMI	34.5±8.3	28.5±9.1	0.01
SBP	115±32	126±18	0.09
DBP	69±19	69±8	0.90
HR (bpm)	92±16	71±12	<0.001
eGFR	58±17	66±15	0.07
BUN	7.7±3.6	6.7±2.9	0.24
Creatinine	97±36	83±27	0.06
PASP (mmHg)	48.2±18.2	46.3±17.1	0.61
PVR (W.u.)	4.1±1.7	2.9±.90	0.001
EF%	59±10	64±7	0.03
E/e’	10±4	11±5	0.29
Basal RV FWS (%)	-17.4±8.6	-22.8±7.6	0.002
Mid RV FWS (%)	-13.1±8.4	-19.6±4.7	<0.001
Apical RV FWS (%)	-10.3±5.4	-14.4±8.3	<0.007
RV FWS (%)	-13.6±5.7	-19.6±4.7	<0.001
FAC (%)	25.6±11.8	37.7±11.8	<0.001
RVEDA (cm^2)	24.8±6.1	21.02±7.1	0.01

BMI, body mass index; SBP, systolic blood pressure; DBP, diastolic blood pressure; HR, heart rate; eGFR, estimated Glomerular Filtration Rate; BUN, blood urea nitrogen; PASP, pulmonary artery systolic pressure; PVR, pulmonary vascular resistance; EF, ejection fraction; RV, right ventricle; FWS, free wall strain; FAC, fractional area change; RVEDA, right ventricle end diastolic area

5.5.3 McConnell sign.

Both PE and PAH groups were evaluated for the presence of the McConnell sign. This sign was identified in 41 patients, 18 (40%) with PE and 23 (14%) of PAH (**Table 5.2**). Generally, those presenting with the McConnell sign had higher HR, PVR, lower RVFWS, higher RVEDA, and lower FAC. Figure 5.2 shows the regional variation in strain between positive and negative McConnell sign patients. We created a ratio of RV free wall basal-mid/ apical free wall ratio (RV apex/[average basal + mid]*100). Patients who demonstrated the McConnell sign showed similar RV apical strain compared to those without this sign (59±54% vs 52±36%, p=0.27), with the same finding when restricted to PE patients (64±78% vs 47±25%, p=0.33). The RV strain showed the same pattern of reduction from base to apex, irrespective of afterload.

Figure5-2. Positive McConnell versus negative McConnell sign and regional strain patterns.

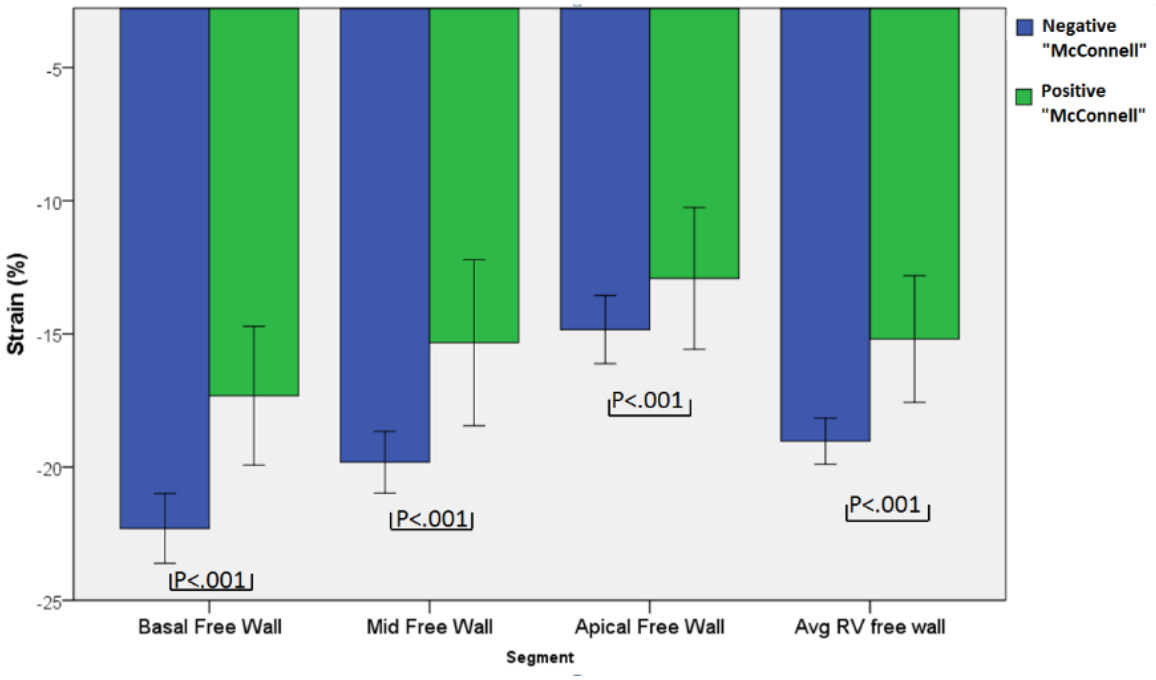

5.5.4 RV longitudinal function.

RVFWS was significantly decreased in the PE as compared to the unmatched ($p<0.001$), and the matched groups ($p<0.001$). This pattern was noted in all segments

of the RV free wall, with highly significant differences between the basal, mid and apical segments (p<0.001).

Table 5-2. . Clinical characteristics of positive versus negative McConnell sign

Variable	Positive	Negative	p
HR	89±19.5	76±13.2	<0.001
PASP (mmHg)	53.9±21	46.8±22.5	0.07
EF	61±8.8	65±9.6	0.07
e’	6.0±1.8	6.8±2.3	0.13
E/e’	12.5±7.2	11.6±4.8	0.45
PVR	4.3±2.3	3.2±1.4	0.007
Basal RVFWS (%)	-17.3±8.3	-22.3±8.4	0.001
Mid RVFWS (%)	-15.3±9.9	-19.8±7.4	0.009
Apical RVFWS (%)	-12.9±8.4	-14.8±8.2	0.18
RVFWS (%)	-15.2±7.5	-19.0±5.5	0.004
RVEDA	24.2±7.0	20.0±7.1±	0.001
FAC	27.4±10.9	36.2±11.2	<0.001
RV apical-/mid ratio	59.4±54.2	51.6±36.4	0.27

HR, heart rate; PASP, pulmonary artery systolic pressure; EF, Ejection fraction; PVR, pulmonary vascular; RVFWS right ventricle free wall strain; RVEDA, right ventricle end diastolic area; FAC, fractional area change.

The associations of RV dysfunction are shown in Table 5.3. Univariable analysis showed that age, sex, PASP, acuity of afterload, RVEDA and PVR were significantly associated with RVFWS. In multivariable models, even when taking into account PASP, acuity of afterload was still significantly associated with RV strain (OR -5.7 [95% CI:-7.4 to 4.0, p<0.001]). When PVR replaced PASP, this association still held true (OR -4.4 (95% CI: -6.0 to 2.1, p<0.001).

Acuity remained a significant association of GLS when RVEDA was taken into account (OR-3.9 [95% CI: -5.7 to 2.2], p<0.001).

The incremental value of each factor for discrimination of acuity using sequential logistic regression is shown in a series of models in Table 5.4. Using standard clinical predictors, HR, PASP and RVEDA were significantly associated with acuity (model X^2=60.5, p<0.001). The addition of PVR did not significantly increase the association (X^2=63.0, p=0.12), and PVR itself was not significant in the model (OR 0.80 [0.60-1.06), p=0.12). However, the addition of RVFWS was significant (p<0.001), and significantly increased the strength of the model (X^2 70, p=0.008).

5.5.5 The validity of RV function markers over a spectrum of measurements.

The diagnostic strength of different RV systolic function parameters may depend on the magnitude of RV failure. ROC analysis was performed, with groups divided based on quantification of RV systolic function; Group 1 contained those with mildly reduced/normal FAC values (>35%)[101], whereas group 2 contained those with moderate/severely reduced FAC (Figure 5a and b). If FAC is normal, discriminative power between variables is poor (Table 5.5a). When RV systolic function is at least moderately reduced, RVFWS retains its predictive ability (AUC 0.77). A second analysis was performed, with groups created based on RVFWS values (Normal/mildly reduced<-20% [101] or moderate/severely RVFWS). Similar results are seen, with RVFWS the most reliable predictor (AUC .69) (Table 5.5b), although some diagnostic strength is lost.

Table 5-3. Associations of right ventricular longitudinal strain (standardised OR)

	Univariable		**PASP model**		**PVR model**		**RVEDA**	
Variable	**OR(95% CI)**	**P**	**OR(95% CI)**	**P**	**OR(95% CI)**	**P**	**OR(95% CI)**	**P**
Age (yrs)	-0.06 (-0.12, -0.003)	0.04	-0.06 (-0.11, -0.01)	0.01	-0.05 (-0.10, -0.002)	0.06	-0.06 (-0.11, -0.01)	0.01
Sex	2.10 (0.21, 3.99)	0.030	1.50 (-0.06, 3.07)	0.06	1.85 (0.27, -3.44)	0.02	0.37 (-1.27, 2.01)	0.66
PASP (mmHg)	0.12 (0.08, 0.15)	<0.001	0.11 (0.08, 0.15)	<0.001				
PE (vs PAH)	-5.7 (-7.61 to -0.38)	<0.001	-5.7 (-7.4, -4.0)	<0.001	-4.4 (-6.1, -2.1)	<0.001	-3.9 (-5.7, -2.15)	<0.001
RVEDA (cm^2)	0.45 (0.35, 0.56)	<0.001					0.38 (0.28, 0.49)	<0.001
PVR	1.81 (1.35, 2.27)	<0.001			1.49 (1.04, 1.93)	<0.001		

PASP, Pulmonary artery systolic pressure; PE, pulmonary embolism; PAH, pulmonary arterial hypertension; RVEDA, right ventricular end diastolic area; PVR, pulmonary vascular resistance.

Table 5-4. Incremental and independent value of RV free wall strain for acute vs. chronic afterload

	Model 1 **Global X^2 60.5** **(p<0.001)**		**Model 2 (+PVR)** **Global X^2 63.0 (p<0.001)** **Increment p=0.12**		**Model 3 (+RVGLS)** **Global X^2 70.0 (p<0.001)** **Increment p=0.008**	
	OR	**p**	**OR**	**p**	**OR**	**p**
HR(bpm)	0.92 (0.89-0.95)	<0.001	0.92 (0.89-0.95)	<0.001	0.93 (0.90-0.97)	<0.001
Age (yrs)	0.99 (0.95-1.01)	0.159	0.97 (0.94-1.01)	0.12	0.97 (0.93-1.00)	0.05
Sex	1.74 (0.67-4.52)	0.252	1.69 (0.64-4.45)	0.29	1.87 (0.70-5.05)	0.214
PASP (mmHg)	1.04 (1.02-1.07)	0.002	1.05 (1.02-1.08)	0.001	1.05 (1.02-1.09)	0.001
RVEDA (cm^2)	0.88 (0.81-0.94)	<0.001	0.88 (0.81-0.94)	<0.001	0.90 (0.83-0.97)	0.01
PVR			0.80 (0.60-1.06)	0.12	0.86 (0.64-1.15)	0.29
RVFWS					0.89 (0.81-0.97)	0.01

PASP, pulmonary artery systolic pressure; PE, pulmonary embolism; PAH, pulmonary arterial hypertension; RVEDA, right ventricular end diastolic area; PVR, pulmonary vascular resistance; RVFWS, right ventricular free wall strain.

5.5.6 Comparison of RVFWS with standard echo for prediction of acuity.

ROC curves were used to evaluate the diagnostic potential of RV functional measurements to differentiate chronic from acute pressure overload (Figure 5.3).

Table 5.5 summarises the AUC, cut-offs, sensitivity and specificity of RVS, RVEDS, FAC and PVR. RV strain was similar to FAC, PVR, RVEDA, for the distinction between PE and chronic PAH. RVFWS was significantly better than McConnell sign ($p=0.016$) and PASP ($p<0.001$) for distinguishing between acute and chronic increases in afterload.

Figure 5-3. ROC curves for prediction of acute versus chronic increase in afterload

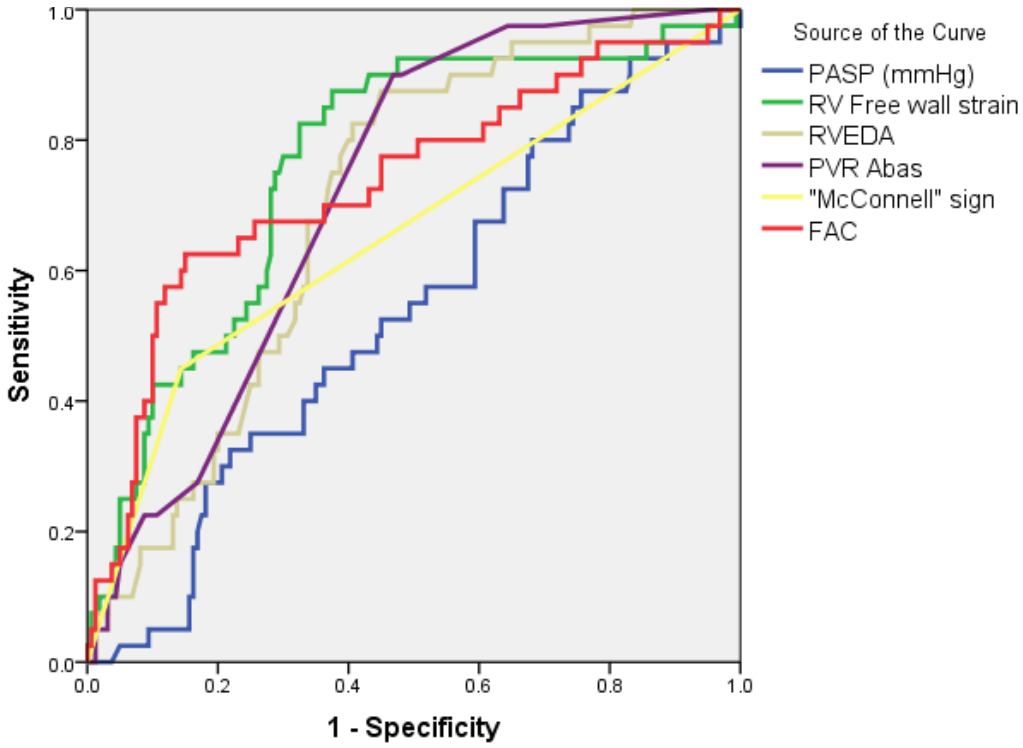

RVFWS (green) showed significantly greater discriminative power than the McConnell sign (yellow) ($p=0.016$), or PASP (blue) ($p<0.001$)

Table 5-5. The diagnostic ability of RV measurements to predict acuity of pulmonary hypertension

Variable	Cut off	Sensitivity	Specificity	AUC	p (vs RVFWS)
RV free wall strain	**-17.9**	**88%**	**63%**	**0.76**	
RVEDA	18.7	88%	55%	0.70	0.21
FAC	26.3	63%	85%	0.74	0.55
PVR	3.34	90%	53%	0.72	0.33
PASP	32.5	80%	32%	0.54	<0.001
McConnell Sign		45%	86%	0.65	0.02

RVEDA, right ventricular end diastolic area; FAC, fractional area change, PVR, pulmonary vascular resistance; PVR, pulmonary vascular resistance; PASP, pulmonary artery systolic pressure.

5.5.7 Combination of parameters.

To evaluate the combined effect of RVFWS and FAC, four groups were created, combining RV systolic function markers. Groups were split into median values for FAC (FAC< 34% vs FAC >34%); and RVFWS (RVFWS<18%, RVFWS >18%).

Most PE patients fell into groups 3 and 4 (RV strain abnormality the predominant feature). Interestingly, the PAH group had higher FAC in group 4, despite higher PASP.

Also, patients were split into two groups: normal RV strain (irrespective of FAC being normal or abnormal) and abnormal RV strain (irrespective of FAC being normal or abnormal).

In group 1 (RVFWS preserved), only FAC showed a difference between PE and PAH. PAH patients in Group 2 (RVFWS reduced) maintained higher FAC values (31.5±11.4 vs 24.2±10.5%, p=0.001) and significantly higher PASP (61.3±27.4 vs 50.3±17.7, p=0.015) (Table 5.6) than those with acute afterload increases.

Table 5-6. The relationship between the diagnostic strength of different RV systolic function parameters and the magnitude of RV failure

Table 5.6	FAC normal/mild			FAC abnormal		
Variable	AUC	95% CI	p	AUC	95%CI	p
FAC	0.54	0.37-0.71	0.65	0.43	0.28-0.57	0.29
RV free wall strain	0.49	0.31-0.67	0.89	0.76	0.62-0.90	<0.001
RVEDA	0.40	0.23-0.57	0.25	0.77	0.69-0.85	<0.001

	RVFWS normal (<-20%)			RVFWS abnormal (>-20%)		
Variable	AUC	95% CI	p	AUC	95%CI	p
FAC	0.70	0.26-1.0	0.25	0.28	0.18-0.37	<.001
RV free wall strain	0.20	0.03-0.36	0.076	0.69	0.59-0.78	0.001
RVEDA	0.81	0.68-0.94	0.07	0.60	0.50-0.70	0.06

FAC, fractional area change; RVEDA, right ventricular end diastolic area.

In a series of ROC analyses, separation by FAC (Table 5.6a) or RVFWS (Table 5.6b) showed that if RV function was normal, discriminative power of the variables was poor.

Table 5.6 shows the results. On the basis of RV strain abnormality being the predominant feature, most PE patients fell into groups 3 and 4. Interestingly, the PAH group had improved FAC (25.3±8.0 vs 19.2±6.4), p=0.001) in group 4, despite higher PASP (65.5±23.3 vs 50±18.2 mmHg, p=0.006).

Finally, groups were split into two groups, based on FAC values being above or below the group median.:

Group 1: FAC strain normal, RVFWS normal/abnormal

Group 2: FAC strain abnormal, RVFWS normal/ abnormal

In the normal FAC group, PE patients displayed significantly lower RVFWS (21.4±4.5 vs 16.8±6.7%, p=0.04) at similar FAC values, with no significant difference in PASP (41.3±19.2 vs 48.5±16.8% mmHg, p=0.19). In group 2 (FAC values below median), PE patients displayed significantly worse RVFWS (16.5±6.2 vs. 12.5±4.8%, p=0.001), FAC (26.7±7.0 vs 19.7±6.6%,

p<0.001). Interestingly, PASP values in the PAH group were trending towards being significantly higher (57.6±25.1 vs 48.1±18.9 mmHg, p=0.059))

5.5.8 Reproducibility.

Reproducibility of RVFWS, RVEDA and FAC were sought in randomly selected patients in both the PE and PAH (n=55) (Figure 5.4), with Bland-Altman analyses to examine bias and variability. RVFWS showed an interclass coefficient (ICC) of 0.85, (R=0.78) which was significantly better than FAC with an ICC of 0.66, (R=0.57) (RVFWS vs FAC, p<0.001). RVEDA showed an ICC 0.81, (R=0.82) which was not statistically different from RV strain. The variability of RVFWS was less than FAC (p<0.01), but comparable to RVEDA (p=0.14).

5.6 Discussion

The results of this study confirm the value of echocardiographic measurements into differentiating chronic from acute changes in RV afterload. While both RVFWS and FAC were helpful for detecting the acuity of RV pressure overload, RVFWS was more reproducible. Finally, the addition of RVFWS provided incremental value to clinical and traditional echocardiographic variables.

5.6.1 Acute vs chronic PAH.

The determination between acute from chronic RV overload has immediate consequences for patient management in critical settings. The standard echocardiographic approach to assessing RV dysfunction in patients with pulmonary embolism is based on subjective indices such as the McConnell and 60/60 signs (Pulmonary valve acceleration time ≤60ms and tricuspid regurgitation pressure gradient ≤60mmHg) [170] which demonstrate high specificity and low sensitivity. In addition, these fail to quantitate RV systolic function, which is most strongly linked with mortality.[171]

Figure 5-4. Bland-Altman plots and between reader correlation for RVFWS, FAC and RVEDA

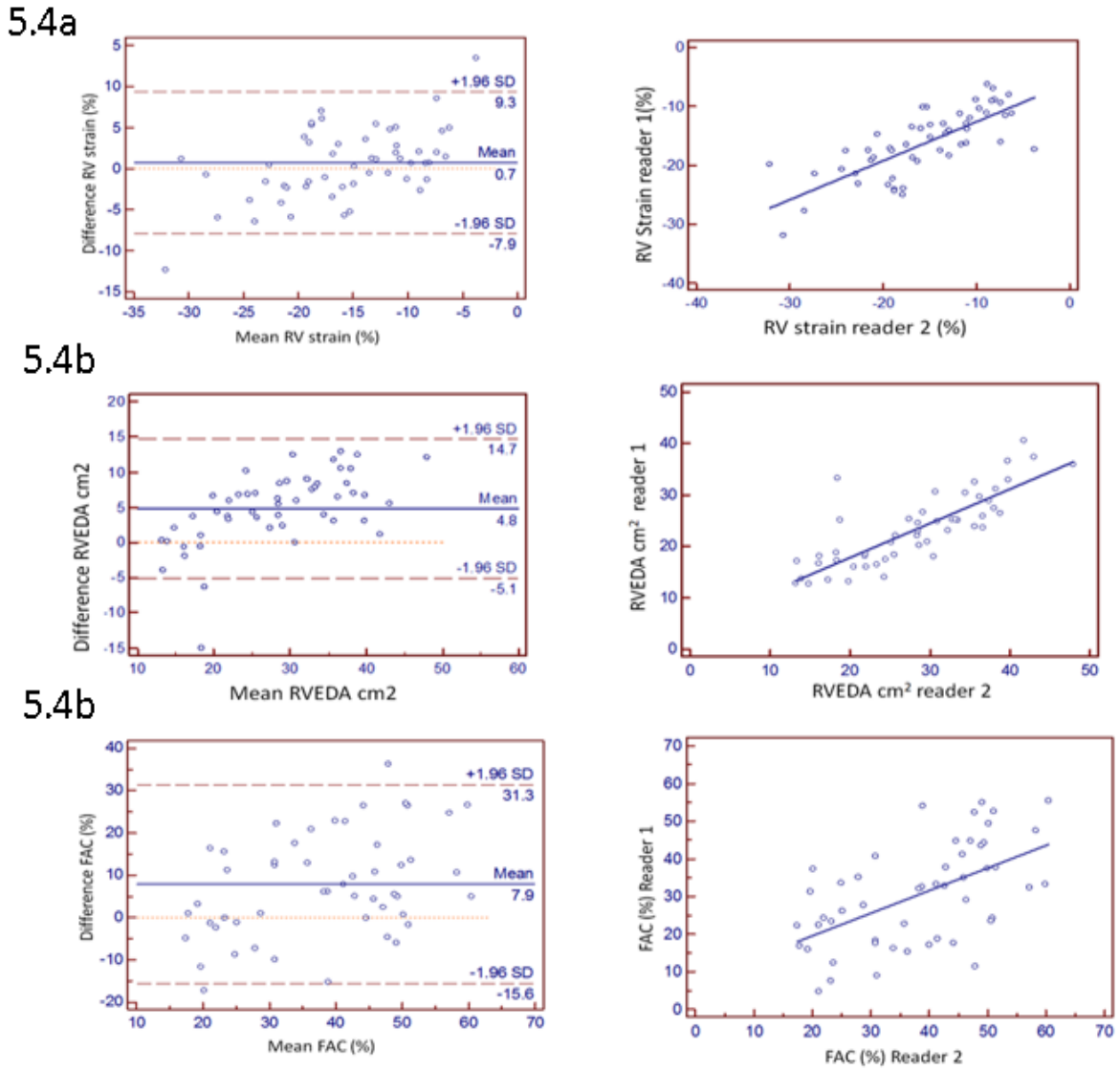

Figure 5.4a shows the variation in RVFWS, with an ICC of .851 & r=0.78. (Mean= 0.7 95% CI ; 9.3 - -7.9). Figure 5.4b shows RVEDA variability, with an ICC of .814, r=0.82 (mean=4.8, 95% CI: 14.7- -5.1). FAC is shown in Figure 5.4c, ICC is 0.66, r=0.57 (mean= 7.9, 95% CI: 31.3- -15.6).

Historically, RV hypertrophy assessed from RV free wall thickness in the subcostal view has been used to identify chronic PAH. In addition to the standard angle- dependence of M-mode calculations, increases in RV thickness are not specific to chronic pressure overload, also being seen in infiltrative and hypertrophic cardiomyopathy, and in patients with established LV hypertrophy. Strain has been used to distinguish normal from abnormal RV function in a

number of settings,[159,172] with work done in a PH cohort to support its clinical utility.[136,172] Echocardiography has the advantage of being a bedside diagnostic tool.

5.6.2 RV assessment in PAH.

The RV has a non-geometric shape that presents challenges to the quantitation of size and function. The clinical uptake of RV strain has lagged the measurement of strain for LV evaluation, especially for assessment of subclinical RV dysfunction. Limited evidence about RV strain variability was cited as a significant limitation in recent guidelines.[166] In this study, RVFWS outperformed most currently recommended measurement techniques.[173]

RV dysfunction in PE is due to a combination of factors, including the extent of the embolic obstruction, the severity of pre-existing cardiopulmonary dysfunction, the impact of hypoxia and the presence of RVH. The most common cause of death at 90 days is RV failure. In a study specifically examining echocardiographic markers of 6 -month patient outcome and recovery of RV function, the time course of recovery showed that RV dilatation improved after three weeks, but subclinical RV dysfunction persisted for up to 3 months.[174] We found that RVEDA was the weakest discriminator of chronic versus acute pressure overload.

The subjective evaluation of apical sparing of the RV, known as the "McConnell Index"[168], is thought to reflect a hyperdynamic LV. Previous work Lopez Candales demonstrated that basal strain exceeded apical strain, but there was no significant difference in strain in the apical segments between PAH and PE in small numbers of patients.[175] This change in strain from base to mid ventricle was observed in our study, with impaired strain being less prominent in the apex.[176]. The RV hyperdynamic apical contraction has been postulated to occur through tethering to the LV apex. This movement could result in translational, as opposed to deformation of the apex, which is calculated with strain imaging. A more robust way to detect these changes could be through a technique proposed by Rajagopal *et al*[177], with right ventricular strain measured from 3 RV focused views. This technique can detect regional patterns, which adds substantially to what is visually identified during the "McConnell sign".

5.6.3 Limitations.

Out of plane motion remains a potential limitation of 2D segmental strain, which may be overcome by 3-dimensional imaging. However, recent reports of 3D strain in PH emphasise the susceptibility of this approach to suboptimal image quality.[178] The availability of a reference method such as cardiac MRI would have been helpful but is usually not considered in acute pulmonary embolism. For the current studies, patients were treated for PAH, which could have affected the impact of right ventricular size as remodelling may have occurred. The heterogeneity of the PAH group could have affected results here, potentially resulting in an underestimation of RVEDA. CTEPH patients represent an interesting subgroup which we were unable to investigate. Those treatable with pulmonary artery endarterectomy (PEA) may have complete resolution of PAH. Studies have been performed looking at RV function pre and post PEA and have shown that right ventricular mass changes in response to PVR alterations[155]. This change in resistance also seems to alter the efficiency of cardiac contraction, with improvements in left to right dyssynchrony.[179].

5.7 Conclusions

RV strain is feasible and useful to help distinguish chronic versus acute pressure overload by differences in RV remodelling. The results show that echocardiography can diagnose different clinical RV loading conditions, and that echocardiography has a good discriminative ability within a clinical cohort. RV remodelling is an essential aspect of the adaptation process to increased afterload, but before afterload increases are detected with echocardiography, there is a gradual increase in PASP, which may progress over an extended period.

This ability to quantify remodelling is an important capability of strain echocardiography. Other methods which may quantify remodelling, including RV free wall thickness and RV end-diastolic volume, may not have adequate sensitivity to detect change. Due to the non-geometric nature of the RV, both of these methods carry substantial error, as probe placement can drastically change values, this suggests that RVFWS is more appropriate to use for sequential

follow-up of patients. The last two chapters have established the effect of afterload and its time course on RV strain. Another aspect of establishing the role of RV strain is to understand its place relative to functional testing, such as 6MW, which has a traditional role in the assessment of PAH.

Chapter 6

Determinants of Change in Functional Capacity

Under review as "Association of Right Ventricular Strain with Exercise Capacity in Pulmonary Arterial Hypertension"

Journal of the American Society of Echocardiography

Leah Wright, Nathan Dwyer, Sudhir Wahi, Thomas H Marwick

6 Determinants of change in functional capacity

6.1 Preface

PAH patients classically present with insidious declines in functional capacity. Cardiopulmonary fitness can be assessed quantitatively with cardiopulmonary exercise testing (CPET). CPET testing gives an accurate assessment of aerobic capacity, determination of sustained exercise performance (ventilator/anaerobic threshold), and assessment of ventilatory efficiency. Declines in functional capacity in PAH may originate from problems in the cardiac, pulmonary and skeletal systems[180]. For the test to be accurate, patients must exercise to exhaustion. Historically, maximal exercise testing has been considered a contraindication in PAH.

Functional status is routinely assessed using either the New York Heart Association or World Health Organisation scales, with patients placed into 4 or to 5 categories of increasing severity [181], respectfully this is essentially is a qualitative measure, with a significant degree of variation in grading between clinicians [181]. The sensitivity of class assessment to track the decline in status over time is limited.

The 6MW distance fits between these two parameters (functional class and VO2). It is a low-cost procedure, safe in the majority of patients, and provides a quantitative gauge of exercise capacity. Since the introduction of specific pharmacotherapy, 6MW has been established as a marker to track functional status and outcome in PAH. It has also shown better reliability than CPET in a PAH cohort [182].

Follow-up of patients for continued treatment under Australian PBS reimbursement guidelines requires the ongoing demonstration of echocardiographic and functional stability every six months. Interestingly, the strength of the relationship between pulmonary pressure and exercise capacity is not well established in PAH. Small studies are looking at cardiopulmonary exercise testing in combination with invasive pressure studies, finding an

only moderate correlation with PVR and max V02[183]. Both 6MW and NYHA have been used as outcome markers in clinical PAH trials. The associations between outcome, functional capacity and echocardiographic markers need to be established. Work performed in this chapters seeks to establish the relationship between novel RV markers and 6MW performance in our PAH cohort.

6.2 Abstract

Background. The continuation of pulmonary vasodilator therapy for pulmonary arterial hypertension (PAH) is based on responses of echocardiographic or exercise markers. As right ventricular (RV) function is a powerful prognostic marker in PAH, we compared the association of RV free wall strain (FWS) with conventional indices before and after initialisation of PAH therapy.

Methods. The study was a retrospective analysis of prospectively acquired data. 121 patients had exercise capacity (measured as 6-minute walk distance, 6MWDD) performed at baseline with echocardiography (including RV-FWS by speckle tracking), with a further subgroup analysis of 79 patients with baseline assessment available before PAH therapy initiation. 119 patients had measures performed at two-time points (21±15 months), follow up of the 79 patients having the initial visit before treatment was 19±15 months.

Results. 6MWD and RV-FWS improved after treatment ($p=0.003$ and $p<0.001$ respectively). Age, RV-FWS, RV end-diastolic area, RV fractional area change and LV E/e' showed univariable association with 6MWD distance. RV-FWS was the only RV function parameter to show association with 6MWD distance, independent of clinical variables ($R^2=0.38$, $p<0.001$, f change $p=0.005$). Change in RV-FWS showed a weak but significant association with change in the 6MWD distance before and after therapy($r=0.27$ $p=0.02$), or throughout therapy regardless of treatment initiation ($r=0.25$ $p=0.007$). In all patients throughout therapy, there was a weak association with delta pulmonary artery systolic pressure (PASP) and 6MWD ($r=-0.21$, $p=0.03$), but this was not apparent in the group before and after treatment initiation ($r=-0.12$, $p=0.31$). In a secondary analysis, those with higher baseline PASP are also more likely to show a decline in 6MWDD (58 ±18.9 vs 41±20 $p=0.004$).

Conclusion. RV-FWS is strongly associated with exercise capacity in PAH and is a useful adjunct to the assessment of treatment response.

Keywords: Right ventricle, strain, exercise capacity; pulmonary arterial hypertension

Although the echocardiographic assessment of pulmonary artery systolic pressure (PASP) has been the primary indicator of response in the management of pulmonary arterial hypertension (PAH), recent guidelines suggest that changes in PASP do not necessarily correspond to a change in clinical status [10]. Assessment of right ventricular (RV) performance has a potential role in predicting patient outcome, but traditional measures of RV function (e.g. tricuspid annular displacement and RV peak systolic velocity) can be affected by translational movement. Speckle tracking has improved RV function assessment. The measurement of RV free wall strain (RV-FWS) - which measures the contribution of longitudinal myocardial deformation – has been recommended over global RV strain in recently published guidelines [101]. RV-FWS is a significant predictor of outcome in pulmonary hypertension [77], but the guidelines do not recognise RV-FWS as superior to other markers of RV function [101].

Exercise limitation is a primary symptom of PAH [184], and the baseline, follow-up and change of exercise capacity represent another means of following PAH response. Although novel drugs have had substantial mortality benefits [2,185], improvement of exercise capacity is a crucial outcome goal in the treatment of PAH. Scoring systems such as the NYHA and WHO scales are used to assess symptom status and titrate therapy. The 6-minute walk test (6MWD) test is a quantitative measure of exercise capacity. It is a submaximal test that is significantly related to peak VO_2, anaerobic threshold and VE/VO_2 slope [186] in primary PAH. A baseline low 6MWD distance is an independent predictor of survival [187], and those who do not improve their 6MWD distance after therapy are at higher risk [187,188]. In our previous work on changes in PASP over time, the association with changes in RV-FWS was more significant than traditional 2D RV systolic function parameters [118]. This study will determine the clinical utility of change in RV-FWS in PAH patients over sequential visits. We aimed to determine whether RV function markers correlated with changes over time in patient exercise capacity as measured with 6MWD. We hypothesised that RV dysfunction is associated with a measure of submaximal exercise capacity (6MWD), with RV-FWS the best correlate over time.

6.3 Methods

6.3.1 Patient selection.

Study design was a retrospective analysis of a prospectively acquired dataset. Patients were recruited from Pulmonary Hypertension Registries at Royal Hobart Hospital, Hobart and Princess Alexandra Hospital, Brisbane, Australia, from August 2005 to October 2015. All patients had PAH confirmed using invasive right heart catheterisation, as recommended by treatment guidelines [10]. Of 143 patients in the registries, 22 were excluded due to insufficient baseline 6MWD data, leaving 121 with baseline 6MWD and echocardiography, 79 of whom were PAH treatment naïve during the echocardiography and 6MWD test. Of the 42 patients on therapy, mean treatment time before visit 1 was 12±16 months. Ongoing treatment access during follow-up required 2 of 3 tests (invasive RHC, echocardiography or 6MWD), so most patients underwent echocardiography and 6MWD (if RHC was acquired, 6MWD was not performed). Thus, although 119 patients attended echocardiographic follow-up after 21±15 months, a further 26 patients did not perform the 6MWD test at follow up. An intention to treat analysis was used to assess treatment response.

Echocardiography protocol.

Echocardiography was performed using standard commercial equipment (Vivid 7, Vivid i and Vivid e9, General Electric Medical Systems, Milwaukee, WI; ie33, Philips, Andover. MA). Data were stored as DICOM files. In patients with atrial fibrillation, three beats were averaged.

Standard measurements Left ventricular (LV) and RV measurements were performed according to ASE/EACVI guidelines [101] by a single reader for both studies. LV ejection fraction was measured from the Simpson's biplane method from the apical 4- and 2-chamber views. RV end-diastolic area (RVEDA) and RV end-systolic area (RVESA) were measured from an apical RV focused view. Fractional area change (FAC) was calculated as the percentage change between the RVEDA and RVESA. Peak velocities of the early (E) and late (A) diastolic filling were derived from the transmitral inflow pattern. Tissue Doppler imaging was used to determine the peak diastolic early velocity (e') of the lateral and septal mitral annulus from the

apical 4-chamber view. Tricuspid annular plane systolic excursion (TAPSE) was obtained from M-mode measurement of tricuspid annular motion in the apical 4 chamber focused view. The distance the annulus travelled between systole and diastole was measured in cm. Right atrial area (RAA) was traced in a single plane area-length measurement in the 2D apical 4 chamber view during the largest size in systole. PASP was measured from the peak tricuspid regurgitation velocity using the modified Bernoulli equation [29]. Right atrial pressure was derived from the inferior vena cava dimension and distensibility from the subcostal view [44]. Pulmonary vascular resistance was calculated from the RVOT VTI, and tricuspid regurgitant signal using the Abbas method (PVR echo=$TRV/TVI_{RVOT} \times 10 + 0.16$) [47].PV acceleration time (PV AT) is measured from pulsed-wave Doppler at the level of the pulmonary valve leaflets, with a measurement of time from baseline to peak modal velocity. Hemodynamic variables referred to in results are echocardiographically-derived. Tricuspid valve systolic excursion velocity was measured in a subset of patients; these data were not included in the final analysis due to the significant degree of missing data, and risk of bias.

Speckle-tracking strain analysis. Wall motion tracking software (Image-Arena, TomTec Gmbh, Unterschleissheim, Germany) was used to analyse the optimal 2D echocardiographic image in which the whole RV cavity was visualised. The LV measurement package was formatted to track the RV free wall. Velocity vector imaging converts images to a DICOM frame rate of 30fps for analysis. The RV end-diastolic endocardial border was manually traced along the RV septal and RV free wall. These borders were then tracked automatically frame-by-frame throughout the cardiac cycle. Manual adjustments were performed when necessary, and regions excluded if excessive noise or inadequate tracking were present. RV-FWS was calculated from an average of three segmental RV-FWS

Right heart catheterisation. RHC studies were undertaken after premedication and local anesthesia. A 4-lumen 110 cm 7-Fr Swan-Ganz catheter (Edwards Lifesciences, Irvine, CA) was floated to the right heart and resting measurements of right atrial, RV, pulmonary arterial

and PCWP were made at end-expiration using a pressure transducer (21BB, ITL Healthcare, Chelsea Heights, Australia). The transducer was calibrated to atmospheric pressure at the level of the RA and re-checked at intervals to avoid zero drift. CO was determined by thermodilution, using an average of four consecutive values that varied <10%. All hemodynamic monitoring was recorded using a Horizon SE Hemodynamic System (Mennen Medical Ltd., Yavne, Israel) and analysed off-line.

6.3.2 Functional testing.

Functional testing.

A 6MWD test was performed at the time of the echocardiogram, or in close succession to by a research nurse in the majority of patients. The test was done in a quiet hospital hallway and followed a standardised protocol [110]

Analysis. Statistical analysis was performed using standard software (SPSS version 22, IBM, Chicago, IL). RV-FWS was analysed as a positive figure. Changes between baseline and follow-up were calculated as baseline subtracted from follow-up. Paired t-tests were used to compare baseline with follow-up values, using linear regression to assess clinical features associated with 6MWD distance. Multivariable models were selected based on predicted clinical markers. Sequential models were employed to assess the incremental and independent benefit of RV function parameters. Change in model chi-square was used to determine whether the additional markers had an incremental benefit over a clinical model. Bivariate logistic regression was used to assess associates of patients likely to improve, versus decline 6MWD distance. Height and weight was not recorded in a number of patients, with 132 data points being imputed with a mean value. A variability analysis has been reported previously by our group in this same cohort [118].

6.4 Results

6.4.1 Baseline

Patients had an age (62±13 years) and female preponderance (73% women) typical of PAH (Table 6.1). The 6MWD was low (329±131 m), with reduced RV-FWS (17±6%) and increased PVR. In a subgroup of patients before treatment, functional capacity was slightly lower (314±128 m), as was RV FWS (15±6%) with very similar PASP (51±23 mmHg).

Table 6-1. Baseline Characteristics

	Pre Treatment N=90	**All patients N=143**
	Pre Treatment	All patients
	N=79	N=120
Age (years)	64±13	62±13
BMI	30±13	29±13
Sex (female)		
HR (bpm)	74±15	74±15
SBP (mmHg)	124±23	125±23
DBP (mmHg)	73±23	73±11
• PAH subtype		
• Scleroderma	40(51%)	66(55%)
• idiopathic	30(38%)	43(36%)
• CTEPH	3(4%)	5(4%)
• Eisenmenger	2(3%)	3(3%)
Other	4(5%)	4(3%)
• PAH treatment type		
• ERA only	43(54%)	59(49%)
• PDE5 only	12(15%)	17(14%)
• Combined ERA and PDE	24(30%)	44(36%)

BMI, body mass; HR heart rate; SBP, systolic blood pressure; DBP, diastolic blood pressure; PAH, pulmonary arterial hypertension; CTEPH, chronic thromboembolic pulmonary hypertension; ERA, endothelin receptor antagonist; PDE5, phosphodiesterase type 5 inhibitor.

6.4.2 Follow-up.

Over a follow up of 21±15 months (n=119) (Table 6.2), there were improvements in 6MWD distance (24±74 m, p=0.005) RV-FWS (1.3±5.4%, p=0.01) and estimated PVR (-0.38±1.5 Wood units, p=0.006). There was a borderline significant improvements in PASP (-2.4±17.6 mmHg, p=0.07) and LV systolic function (EF 1.5±8.6%, p=0.08).

In selected patients with matched data before and after initiating treatment (n=79, follow up 19±15 months) (Table 2), there were improvements in 6MWD distance (31±80, p=0.003), RV-

FWS (2.5±4.5%, p<0.001), PASP (-2±18 mmHg, p<0.001), or estimated PVR (-0.28±1.5 Wood units, p=0.05). There were no significant changes in LV systolic (EF 2.7±18%, p=0.19) or diastolic function (e' -0.4±1.5 cm/s, p =0.12; E/e' 2.0±7.3; p=0.06). Appendix Figure 6.3-6.5 shows the variability in parameters from visit 1 to visit 2 in all patients.

6.4.3 Echocardiographic features independently associated with exercise capacity.

In patients not on treatment at baseline, RV function markers associated with exercise capacity included RV-FWS, RVEDA, FAC, and LV filling pressures (Table 6.3). In all 119 patients (Table 6.3) age was associated with exercise capacity, as were RV-FWS, RVEDA, TAPSE, LV filling pressures and hemodynamic markers. After long-term follow-up, age, RV-FWS, RV end-diastolic area, RV fractional area change, and LV E/e' were associated with baseline 6MWD performance.

Table 6-2. Baseline and follow

	All patients				Patients initiating treatment			
	Baseline	**Follow up**	**Delta**	**P value**	**Baseline**	**Baseline**	**Follow up**	**Delta**
6MWD (metres)	329±131	353±143	24±74	0.005	314±128	346±146	31±80	0.003
RV free wall (%)	17±6	19±5	1.3±5.4	0.01	15±6	18±6	2.5±4.5	<0.001
PASP (mmHg)	50±24	47±22	-2.4±17.6	0.07	51±23	48±20	-1.7±17.6	<0.001
RVEDA (cm^2)	22±9	22±10	0.5±8.3	0.50	22±9	22±8	-0.77±5.8	0.18
FAC (%)	32±14	35±12	2.4±12.3	0.04	31±14	33±12	1.9±12.3	0.19
RAA (cm^2)	20±8	20±8	0.71±5.8	0.19	19±8	20±8	0.58±5.0	0.32
PVR (W.u)	3.6±1.9	3.2±1.5	-0.38±1.5	0.006	3.8±1.8	3.4±1.7	-0.28±1.5	0.05
TAPSE (cm)	1.9±0.5	1.9±0.6	0.03±0.54	0.54	1.8±0.5	1.9±0.5	0.11±0.46	0.04
PV AT (cm/s)	80±28	80±24	0.06±28.3	0.99	76±25	78±20	1.6±25.7	0.63
RVOT VTI (cm)	12±3.9	12±3.7	0.62±3.3	0.09	11±3.9	12±4.0	0.68±3.4	0.14
LVEDV (ml)	87±33	87±33	-0.05±20.9	0.98	86±38	89±35	2.7±18.3	0.29
EF (%)	61±10	63±9	1.5±8.6	0.08	60±11	62±9	2.7±18.3	0.19
SV (ml)	51±16	52±15	0.88±15	0.60	49±16	51±16	1.8±16	0.41
LAV (ml/m^2)	32±14	35±14	3.2±11.0	0.02	31±14	34±13	3.2±10.5	0.04
e' septal (cm/s)	6±2.2	6±2.2	-0.07±1.7	0.7	6±2.3	5±2.0	-0.35±1.5	0.12
e/e' avg	11±6	13±8	1.2±6.7	0.12	11±5.0	13±9	2.0±7.3	0.06

6MWD, six minute walk distance; RV, right ventricle; PASP, pulmonary artery systolic pressure; RVEDA, right ventricular end diastolic area; FAC, fractional area change; RAA, right atrial area; PVR, pulmonary vascular resistance; TAPSE, tricuspid annular plane systolic excursion; PV AT, pulmonary valve acceleration time; RVOT VTI, right ventricular outflow tract velocity time integral; LVEDV, left ventricular end diastolic volume; EF, ejection fraction; LAV, left atrial volume

Table 6-3 Regression analysis of 6MW distance

	All baseline patients (n=121)		**baseline (not on PAH therapy) (n=79)**		**Follow-up (after PAH therapy, all patients)**	
	Std β (95% CI)	**P value**	**Std β (95% CI)**	**Std β (95% CI)**	**Std β (95% CI)**	**P Value**
Age (years)	-0.41(-5.7;-2.4)	<0.001	-0.26(-5.0;-0.40)	0.02	-0.21(-5.0;0.12)	0.06
BMI	-0.18(-6.6;0.09)	0.06	-0.21(-7.8;0.35)	0.07	-0.16(-7.9;1.4)	0.17
HR (bpm)	-0.09(-2.4;0.86)	0.35	-0.16(-3.3;0.60)	0.17	-0.14(-3.6;0.86)	0.22
RV FWS (%)	0.36(3.7;10.6)	<0.001	0.34(2.8;12.6)	0.003	0.36(3.6;14.7)	0.001
RVEDA (cm^2)	-0.30(-7.5;-2.0)	0.001	-0.26(-6.9;-0.49)	0.03	-0.29(-8.4;-1.1)	0.01
FAC (%)	0.25(0.73;4.2)	0.006	0.25(0.19;4.2)	0.03	0.23(0.06;4.7)	0.05
TAPSE (cm)	0.21(7.1;104.6)	0.03	0.20(-7.2;110.2)	0.09	0.16(-19.2;1113.7)	0.16
PASP (mmHg)	-0.28(-2.5;-0.56)	0.002	-0.20(-2.4;0.20)	0.10	-0.26(-3.0;-0.18)	0.03
PVR (w.u)	-0.29(-35.9;-7.0)	0.004	-0.22(-35.4;2.4)	0.09	-0.29(-45;-3.2)	0.02
PV AT (cm/s)	0.22(0.14;1.8)	0.02	0.07(-0.92;1.7)	0.57	0.16(-0.48;2.5)	0.18
EF (%)	0.07(-1.5;3.4)	0.44	0.11(-1.5;4.1)	0.35	0.11(-1.8;4.7)	0.37
SV (ml)	1.4(-0.33;3.05)	0.11	0.40(-1.6;2.5)	0.70	0.92(-0.72;2.6)	0.27
LAV (ml/m^2)	-0.25(-4.4;-0.44)	0.02	-0.16(-3.9;0.91)	0.22	-0.30(-5.7;-0.51)	0.02
E/e' Average	-0.33(-13.5;-3.0)	0.003	-0.38(-17.3;-3.1)	0.006	-0.49(-22.3;-7.3)	<0.001

6MW, six-minute walk distance; RV, right ventricle; PASP, pulmonary artery systolic pressure; RVEDA, right ventricular end diastolic area; FAC, fractional area change; RAA, right atrial area; PVR, pulmonary vascular resistance; TAPSE, tricuspid annular plane systolic excursion; PV AT, pulmonary valve acceleration time; RVOT VTI, right ventricular outflow tract velocity time integral; LVEDV, left ventricular end diastolic volume; EF, ejection fraction; LAV, left atrial volume

6.4.4 Incremental value of RV function in assessing exercise capacity.

In a sequential linear regression model, clinical parameters (age and BMI) and PASP were associated with 6MWD (R^2=0.33, p<0.001) (Figure 1). The addition of FAC was borderline in significantly adding to the model (Figure 2) (R^2 0.36, p<0.001, F change=0.10), and TAPSE was independent, but did not significantly increase the power of the model (R^2=0.34, p<0.001, F change=0.12). However, RV-FWS added incremental prognostic information (Figure 2) (R^2=0.38, p<0.001, F change=0.005). Appendix 6.6 shows the incremental value of RV-FWS in patients prior treatments, with results replicated.

Figure 6-1. Sequential linear regression model for baseline visit..

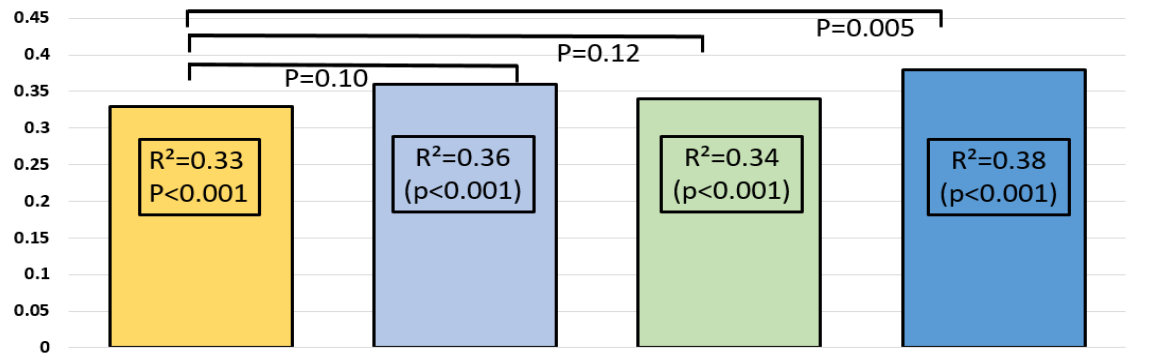

	Clinical		Clinical + FAC		Clinical + TAPSE		Clinical + RVFWS	
	Std β(95%CI)	P	Std β(95%CI)	P value	Std β(95%CI)	P value	Std β(95%CI)	P value
Age	-0.45(-6.0;-2.8)	<0.001	-0.45(-6.1;-2.9)	<0.001	-0.46(-6.0;-2.8)	<0.001	-0.44(-5.9;-2.8)	<0.001
PASP	-0.32(-2.6;-0.85)	<0.001	-0.23(-2.3;-0.23)	0.02	-0.27(-2.4;-0.50)	0.003	-0.22(-2.1;0.28)	0.01
Sex	0.15(-5.2;90.6)	0.08	0.16(0.09;96)	0.05	0.14(-5.7;89.5)	0.08	0.17(3.0;96.2)	0.04
BMI	-0.22(-6.8;-0.96)	0.01	-0.20(-6.6;-0.77)	0.01	-0.21(-6.7;-0.92)	0.01	-0.17(-5.9;-0.12)	0.04
		FAC	0.16(-0.31;3.4)	0.10				
				TAPSE	0.14(-10;83.5)	0.12		
						RVFWS	0.25(1.5;8.4)	0.005

RV free wall strain is the most robust echocardiographic RV function marker in the association of functional capacity

After long-term treatment of pulmonary hypertension patients, age, PASP and BMI significantly associated with exercise capacity in a clinical model (R^2=0.41, p<0.001)

(Figure 6.2). FAC did not add significantly (R^2=0.42, p<0.001, F change p=0.19) and the association of TAPSE (R^2=0.43, p<0.001, F change. p=0.09) with follow-up walking distance reached borderline significance (Figure 6.3). Again, however, RV-FWS showed incremental value in prediction of 6MWD distance (Figure 6.3) (R^2 =0.48, p<0.001, F change p=0.001).

Figure 6-2. Sequential linear regression model for follow-up in all patients.

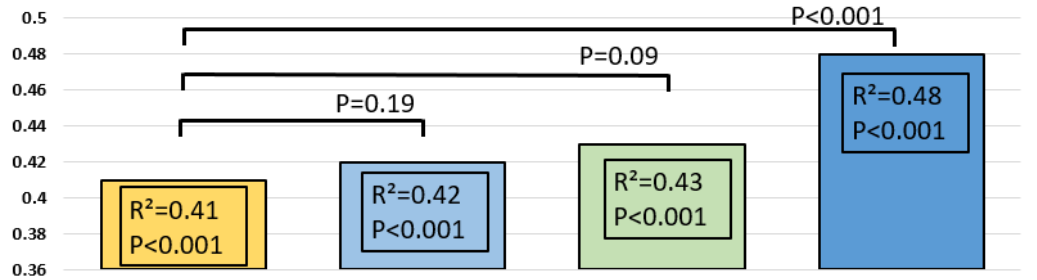

	Clinical		Clinical + FAC		Clinical + TAPSE		Clinical + RVFWS	
	Std β(95%CI)	P value	Std β(95%CI)	P value	Std β(95%CI)	P value	Std β(95%CI)	P value
Age	-0.47(-6.7;-3.3)	<0.001	-0.47(-6.7;-3.3)	<0.001	-0.46(-6.5;-3.2)	<0.001	-0.45(-6.4;-3.2)	<0.001
PASP	-0.50(-4.3;-2.2)	<0.001	-0.45(-4.1;-1.8)	<0.001	-0.47(-4.1;-2.0)	<0.001	-0.38(-3.5;-1.4)	<0.001
Sex	0.13(-9.7;91.0)	0.11	0.14(-5.9;95.1)	0.08	0.12(-12.5;87.5)	0.14	0.15(0.86;96.0)	0.05
BMI	-0.17(-6.4;-0.27)	0.03	-0.16(-6.3;-0.15)	0.04	-0.17(-6.2;-0.19)	0.04	-0.07(-4.4;1.7)	0.38
		FAC	0.12 (-0.66;3.3)	0.19				
				TAPSE	0.14(-5.2;70.7)	0.09		
						RVFWS	0.31(3.8;12.7)	<0.001

Similar to baseline, after long-term treatment, RV free wall strain was the strongest echocardiographic associate of functional capacity in those on long term treatment for pulmonary arterial hypertension

6.4.5 Features associated with a change in 6MW.

Table 6.4 summarises the associations of delta 6MWD with echocardiographic and clinical markers. Delta RV-FWS was the only significant RV function marker associated with change in 6MWD (std β 0.25(95% CI 0.95 to 6.0) p=0.007), as was PASP (std β -0.21 (95% CI -1.7 to -0.10), p=0.03). Change in delta FAC, delta TAPSE and diastolic markers were not significantly associated with a change in 6MWD.

.

Table 6-4. Associations with delta 6MW distance

	Treatment only group		Follow-up all patients	
	Std β (95%CI)	**P value**	**Std β (95%CI)**	**P value**
Sex	-0.15(-64.6;13.5)	0.20	-0.06(-39.4;20.7)	0.54
Baseline Age	-0.02(-1.6;1.3)	0.85	-0.01(-1.1;0.94)	0.88
Delta RV FWS (%)	0.27(0.82;8.8)	0.02	0.25(0.95;6.0)	0.007
Delta PASP (mmHg)	-0.12(-1.6;0.52)	0.31	-0.21(-1.7;-0.10)	0.03
Delta RVEDA (cm^2)	-0.05(-3.9;2.5)	0.66	-0.14(-2.9;0.47)	0.16
Delta RAA (cm^2)	-0.15(-6.0;1.3)	0.20	-0.09(-3.6;1.2)	0.33
Delta FAC (%)	0.14(-0.62;2.4)	0.24	0.03(-0.99;1.3)	0.78
Delta TAPSE (cm)	0.09(-25.6;55.3)	0.47	0.11(-10.3;40.6)	0.24
Delta LAV/BSA (ml/m^2)	0.18(-0.75;3.5)	0.20	0.23(0.001;3.1)	0.05
Delta EF (%)	0.04(-1.8;2.5)	0.76	0.02(-1.5;1.8)	0.85
Delta E/e' average	0.23(-0.71;5.7)	0.12	0.12(-1.3;3.9)	0.33
Delta e' sep (cm/s)	-0.10(-20.7;10.1)	0.49	-0.01(-11.1;9.9)	0.91

RVFWS, right ventricular free wall strain; PASP, pulmonary artery systolic pressure; RVEDA, right ventricular end diastolic area; RAA, right atrial area; FAC, fractional area change; TAPSE, tricuspid annular plane systolic excursion; LAV left atrial volume; BSA, body surface area; EF, ejection fraction.

To distinguish "responders" vs. "non-responders" to pulmonary vasodilator therapy, patients were split into those who increased 6MWD distance (n=45), versus those whom 6MWD distance declined (n=17). There was no significant difference in baseline demographics or RV systolic function. PASP was significantly higher in the group who declined 6MWD distance (p=0.004), as was PV acceleration time (p=0.03) (Table 6.5). Logistic regression showed that baseline PASP was the only significant univariable association of those who decline in 6MWD distance (OR -0.25 (95% CI -1.7 to -0.09), p=0.03) (Table 6.6); baseline RV-FWS was not significant (OR 0.95(95% CI 0.94 to 1.03), p=0.39).

Table 6-5. 6MW responders versus non responders

	Improved 6MW (n=45)	Declined 6MW (n=17)	P value
Age (years)	65±13	62±13	0.42
6MW (m)	311±133	343±79	0.26
RV free wall strain (%)	16.5±5.7	15±5.8	0.39
RVEDA (cm^2)	20±9.5	24±7.8	0.17
RAA (cm^2)	17.4±7.5	20.1±7.5	0.22
FAC (%)	36±13.2	30±12.2	0.10
PASP (mmHg)	41±20	58±18.9	0.004
PVR (w.u)	3.0±1.4	3.3±1.4	0.29
PV AT (cm/s)	85±25.8	68±17.8	0.03
LVEDV (ml)	86±44	82±22	0.78
EF (%)	60±10	60±12	0.88

6MW, six-minute walk; RV right ventricle; RVEDA, right ventricle end diastolic end diastolic area; RAA, right atrial area; FAC, fractional area change; PASP, pulmonary artery systolic pressure; PVR, pulmonary vascular resistance; PV AT pulmonary valve acceleration time; LVEDV, left ventricular end diastolic volume; EF, ejection fraction.

Table 6-6. Bivariate logistic regression for improved versus decline 6MW

	OR (95%CI)	P value
Sex	0.41(0.12;1.3)	0.14
Age at Baseline	0.98(0.94;1.03)	0.42
RV free wall strain (%)	0.95(0.86;1.06)	0.39
RVEDA (cm^2)	-0.19(-3.7;0.32)	0.10
FAC (%)	0.71(-1.03;1.5)	0.71
PASP (mmHg)	-0.25(-1.7;-0.09)	0.03
PVR (w.u)	1.4(0.91;2.1)	0.13
TAPSE (cm)	0.55(0.14;2.1)	0.39
EF (%)	1.005(0.95;1.06)	0.87
E/e'	1.03(0.91;1.2)	0.68

RV, right ventricle; RVEDA, right ventricular end diastolic area; FAC, fractional area change; PASP, pulmonary artery systolic pressure; PVR, pulmonary vascular resistance; TAPSE, tricuspid annular plane systolic excursion; EF, ejection fraction.

Variability analysis. In short, the intraobserver variability of RV-FWS showed an intra-class correlation coefficient of 0.73 (95% CI, 0.44–0.88; $P < .001$) and a mean difference of 1.3±3.2%. Inter-observer variability showed an intra-class correlation coefficient of 0.62 (95% CI, 0.26–0.83; $P < .001$) and a mean difference of 4.5±4.7%.

6.5 Discussion.

The guidelines propose that a 6MWD distance of <300m and TAPSE <1.5cm [10] are useful predictors of outcome. Although baseline TAPSE and 6MWD showed a significant association, changes in TAPSE over time did not associate with 6MWD, in contrast with a significant association with RV-FWS. This study supports recent work emphasising the prognostic power of RV-FWS (2) by showing that RV-FWS associates with exercise performance before and after long-term treatment of PAH. We have looked at patients' naïve to treatment, and have also separately included a cohort of patients on long-term treatment. Our work has shown that changes over time in the 6MWD distance are associated changes in RV free wall strain, with no other RV parameters showing this association. In this respect, RV-FWS was the most robust echocardiographic marker of RV function, independent and incremental to clinical variables in the association of exercise capacity. Importantly, this was true throughout the whole time course of PAH treatment. Changes in exercise capacity were strongly related to changes in RV free wall strain, but not to other RV echocardiographic parameters. Interestingly, patients who were more likely to decline 6MWD distance showed higher PASP levels at baseline.

Despite the strong mortality benefits of pulmonary vasodilators [189], the degree of change of clinical parameters is less well documented. A wide range of responses to pulmonary vasodilator therapy is shown in this and other studies [190]. A number of pivotal studies have shown small, but significant improvements in hemodynamics – for example, 1.6-2.7 mmHg improvements in pulmonary pressure have been reported after treatment [5]. A meta-analysis of intervention trials showed a mean decrease in mPAP of -2.86 mmHg [185] using invasive measures - a magnitude of change is similar

to our findings. However, assessing treatment based on pulmonary pressure does not account for all of the survival benefits from therapy [191]. Accounting for the role of the RV adds to pulmonary pressure for predicting change in exercise capacity.

RV free wall strain.

Although RV function is a more important predictor of outcome, in patients with PAH, much effort is directed towards follow up of PASP. Nonetheless, support for RV-FWS in the most recent guidelines is constrained by lack of evidence (12). RV-FWS measures longitudinal function, which accounts for the predominant aspect of RV contraction [192]. The RV free wall is regarded as superior to RV 6-segment strain for assessing systolic RV function. When compared with controls, the RV septum was not significantly different [193], with this generally lower than the RV free wall (due to tethering associated with the mitral annulus). RV-FWS has been shown to have excellent intra- and inter-observer variation [194,195], with use of the three segment RV-FWS producing more favourable results over segmental analysis that includes the septum.

The association of RV-FWS with exercise capacity is an essential component of the validation of this test. Previously published data [193] involve fewer numbers of patients and lack of information on treatment response. One of the strengths of RV-FWS is that it avoids the pitfalls of translational rocking, as TAPSE can become pseudonormal through translational movement caused by hyperdynamic LV function [196,197]. Previous outcome studies have shown events in treated PAH to be associated with failure to significantly augment RV-FWS [198].

6.6 Limitations.

The gold standard of exercise capacity is maximal cardiopulmonary exercise testing (CPET) was not performed in this study. However, 6MWD distance is widely used in PAH follow-up, and submaximal testing is a useful marker of daily functional capacity. Likewise, the reference standard for RV systolic function is invasive pressure-volume loop assessment [199]. The latter is difficult to perform in a clinical setting and requires specialised equipment. Thus, echocardiography is primarily used for follow up.

This study has used 2D cardiac ultrasound to assess cardiac size and function. Due to the non-geometric nature of the RV, the RV size is often underestimated. 3D volumes have a promising place within the echocardiographic follow up of PAH [108], with better correlations with MRI than are achievable with 2D volumes [81]. The use of 3D right ventricular strain is limited by the technical aspects of achieving adequate frame rate, with studies also shown that there is a steep learning curve for this technique [92]. Some of the most robust echocardiographic markers of mortality in PAH and pericardial effusion, and right atrial size. Both of these are signs of end-stage disease, and thus may not be suitable markers to identify early patient decline. As this was a retrospective analysis of prospectively acquired data, there were some limitations of study design – for example, the times between follow-up studies were variable. Changes in echocardiographic protocols meant that RVS' data has only been collected in recent studies. Patients were excluded if 6MWD was not performed, possibly, these patients could have represented a more advanced cohort, altering outcomes.

6.7 Conclusion.

RV free wall strain is a robust predictor of functional capacity in the standard clinical follow-up assessment of PAH, further supporting the use of this parameter for assessment of RV function in PAH. More studies need to assess the association of these changes with patient outcomes, and how this might be used to individualize therapy.

6.8 Postscript

In this chapter, we have used a surrogate of peak exercise performance, the 6MW test, to determine the association between echocardiographic measures of RV systolic function and patient clinical status. RVFWS independently associated with 6MW distance, incremental to other physiologic predictors.

There has been difficulty in determining a follow-up measure that tracks patient progression in PAH. Although there are some established markers of prognostic significance, outcome measures appear to underestimate treatment benefit. The 6MW test is an example of this. In a recent meta-analysis of 23 trials involving PAH pharmacotherapy, the 6MW distance was the primary or combination endpoint in 17[185]. In PAH, increases in the 6MW distance of > 38 meters [200] are required to have an impact on patient clinical status. Changes to this degree are rarely seen, with some studies showing a difference in the follow-up of > 2 meters able to distinguish survivors, from non-survivors [201]. The change is also less than the re-test reliability of the 6MW test in a stable PAH cohort [182]. The meaningful clinical difference required is also higher than that observed from a recent meta-analysis of improvements in 6MW distance following therapy [202]. Ceiling effects can also be witnessed, with stronger outcome affecting those whom functional capacity is severely reduced [94].

Unfortunately, invasive assessment of pressures also underestimates the survival benefits seen in trials [191]. Newer methods of tracking outcome in patients need to be assessed to determine association with outcome. Of these, measurements of right ventricular size and function may be predictive of outcome throughout follow-up.

RVFWS is influenced by the chronicity of disease, and minimally by the severity of PHT, with RVFWS possibly better than 6MWD for determining functional status.

Speckle tracking can also provide additional information about the LV status, which could play a role in PH.

Figure 6-3 Appendix. Variation in the degree of change in 6MW distance at baseline and follow up

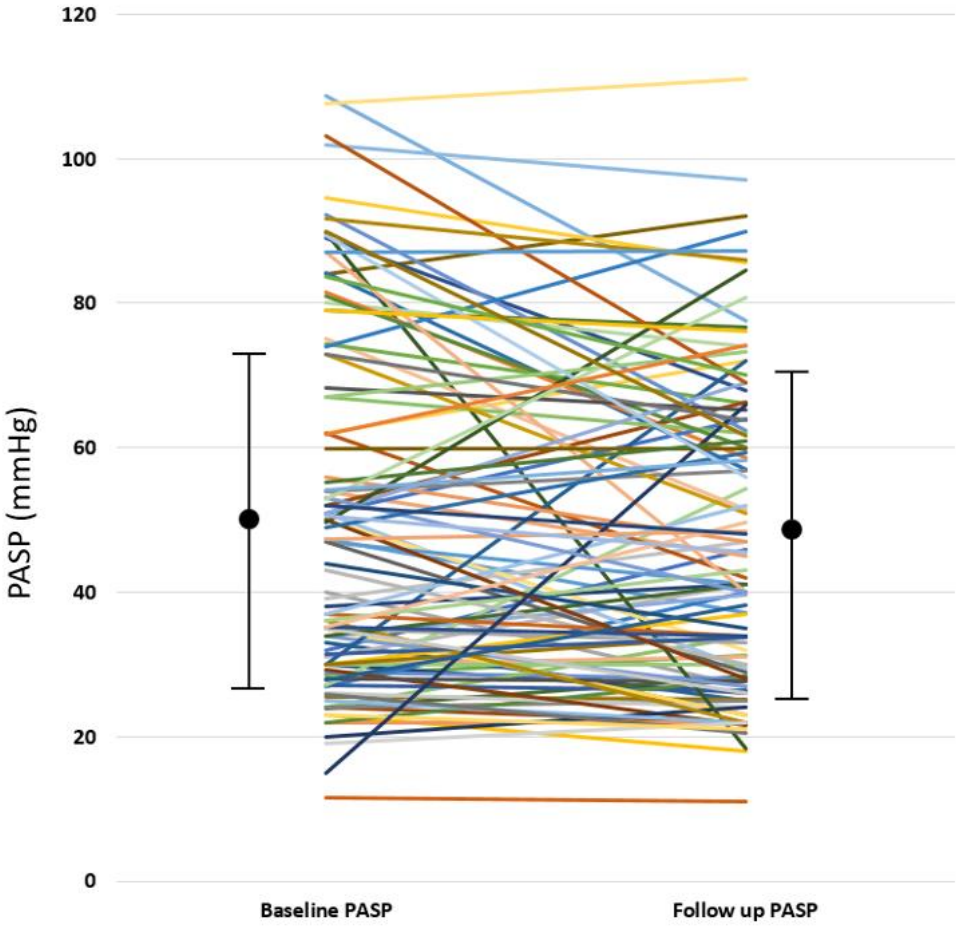

Figure 6-4 Appendix. Variation in the degree of change in RV free wall Strain at baseline and follow up

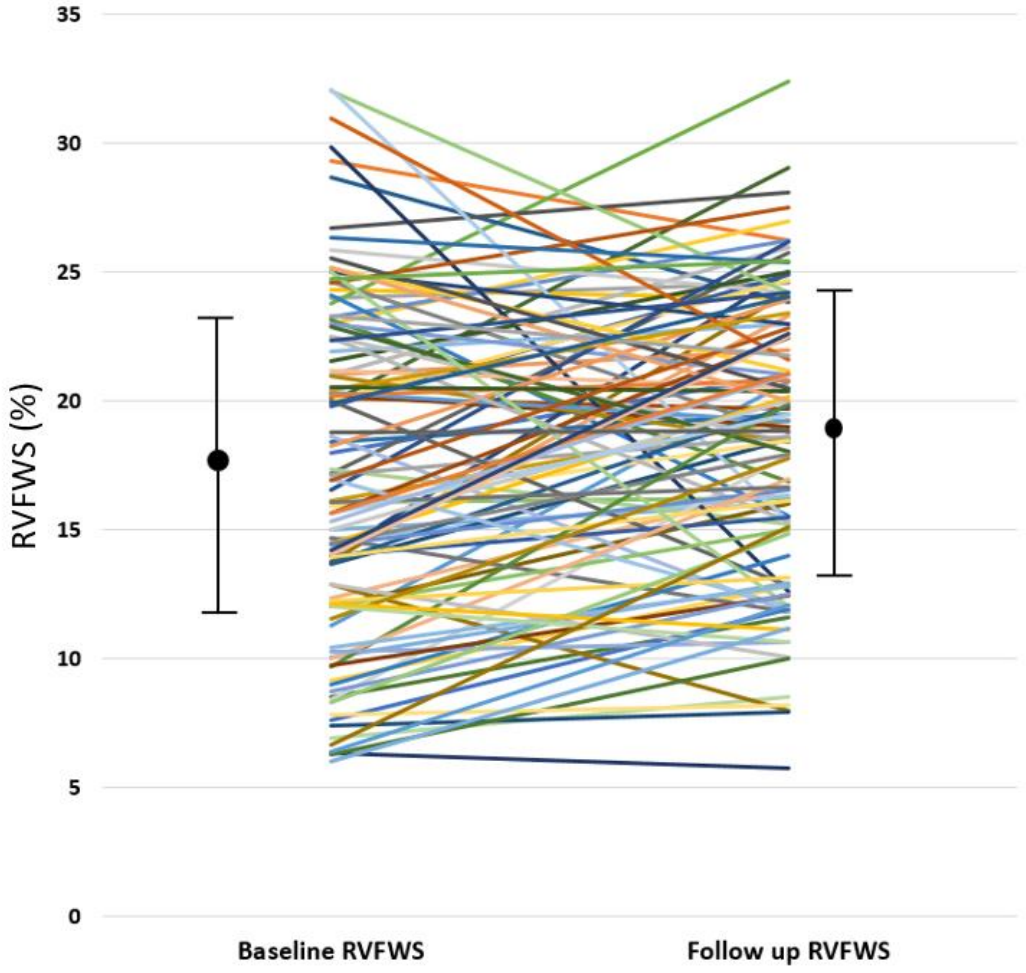

Figure 6-5 Appendix. Variation in the degree of change in Pulmonary artery systolic pressure at baseline and follow up

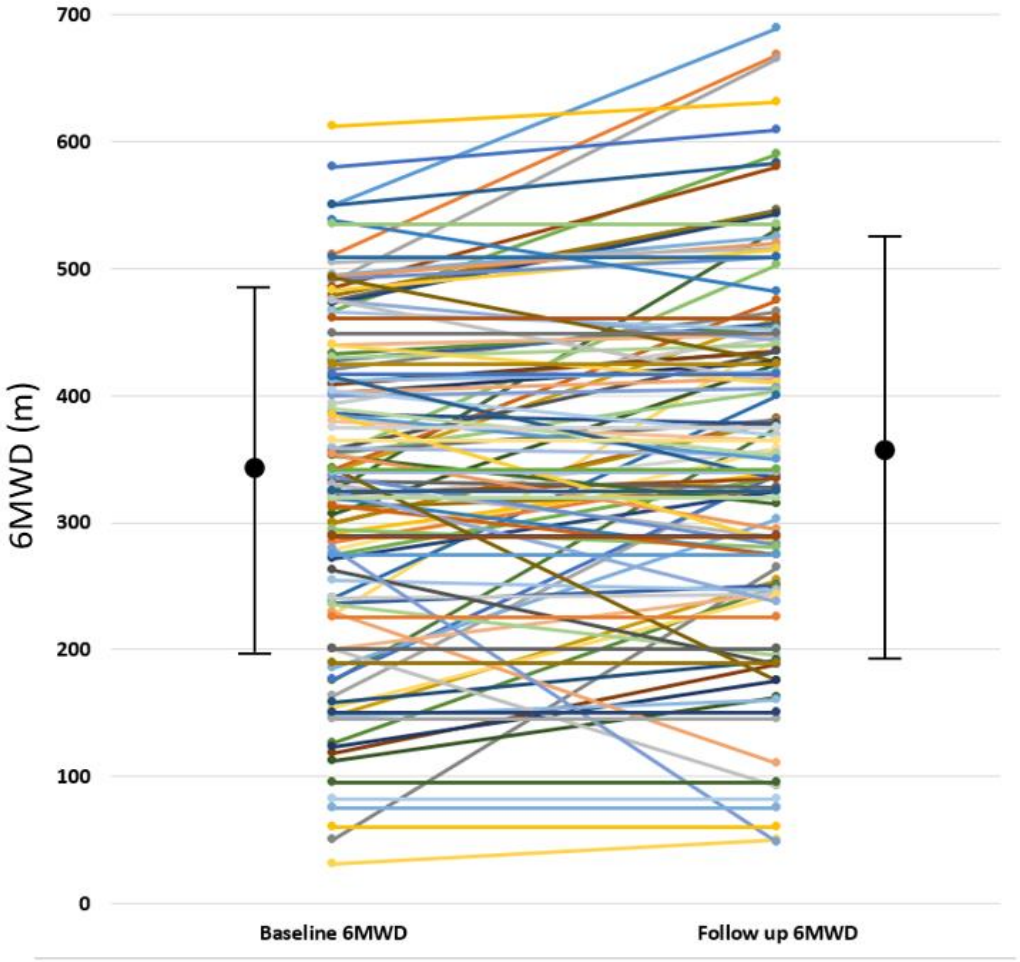

Figure 6-6 Appendix. The incremental predictive ability of RV function markers over clinical parameters before treatment (baseline)

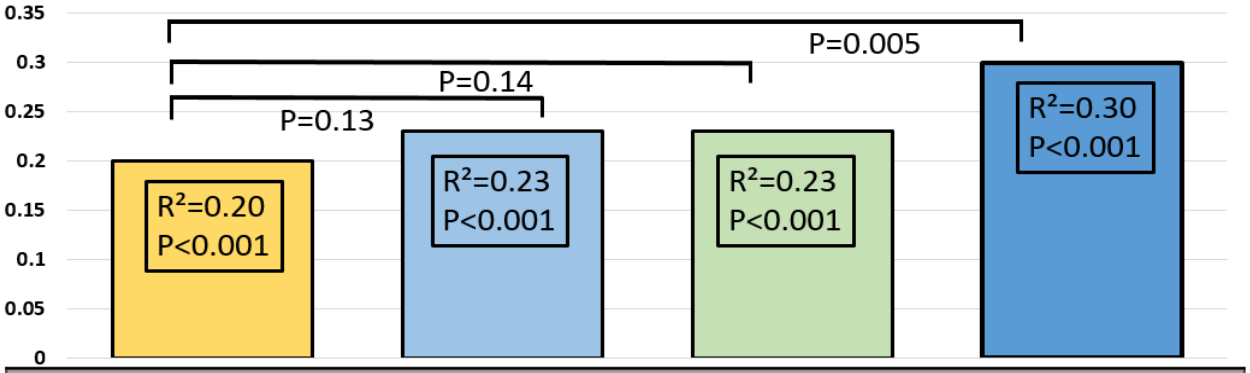

	Clinical		Clinical + FAC		Clinical + TAPSE		Clinical + RVFWS	
	Std β(95%CI)	P value	Std β(95%CI)	P value	Std β(95%CI)	P value	Std β(95%CI)	P value
Age	-0.45(-6.0;-2.8)	<0.001	-0.35(-5.9;-1.3)	0.003	-0.35(-5.9;-1.3)	0.003	-0.36(-5.9;-1.4)	0.002
PASP	-0.32(-2.6;-0.85)	<0.001	-0.14(-2.3;0.70)	0.29	-0.19(-2.4;0.29)	0.12	-0.13(-2.0;0.55)	0.26
Sex	0.15(-5.2;90.6)	0.08	0.19(-12.0;117.9)	0.11	0.16(-19.2;109.8)	0.17	0.23(2.2;127.9)	0.04
BMI	-0.22(-6.8;-0.96)	0.01	-0.22(-7.8;0.11)	0.06	-0.25(-8.3;-0.51)	0.03	-0.21(-7.4;0.16)	0.06
		FAC	0.20(-0.56;4.1)	0.13				
				TAPSE	0.18(-14.6;104.5)	0.14		
						RVFWS	0.34(2.4;12.8)	0.005

Chapter 7

Left and Right Ventricular Function in Systemic Sclerosis

Article published as "Mechanics and Prognostic Value of Left and Right Ventricular Dysfunction in Patients with Systemic Sclerosis" accepted for publication in Aug 2017

Journal of the American College of Cardiology; Cardiovascular Imaging 2017

Makoto Saito*, Leah Wright *, Kazuaki Negishi, Nathan Dwyer, Thomas H Marwick

*Joint first authors

7 Left and right ventricular function in systemic sclerosis; Tools for advanced imaging and prediction of outcome

7.1 Preface; Myocardial imaging for differential diagnosis

Systemic sclerosis (SSC) is an interesting model of PH as identification of patients can occur early in the course of PH. However, these patients are also susceptible to left heart disease - SSC patients are at risk of developing heart failure with preserved EF at higher rates than the general population (ranges of 20-45% are proposed) [203,204]. Incremental to this, the risk of myocardial infarction is increased [205], plus worse survival rates following diagnosis of heart failure preserved EF [206].

A number of different techniques exist to measure fibrosis; the gold standard, invasive cardiac biopsy, is not a viable option for screening patients. CMR is viable [207], but due to expense, it is not a practical option for early disease screening. Increased stiffness in the myocardium is mediated through collagen regulation, with speckle tracking imaging able to detect early changes in the myocardium [208].

Echocardiography is well positioned to be a successful screening tool, with many imaging techniques available. Traditional measures, such as the EF, may not be ideal methods to detect early disease. In SSC, there is a large proportion of focal fibrosis [209], with global measures not detecting such disease patterns. Tissue Doppler utilises the velocity of the myocardium and is particularly useful for detecting abnormalities in myocardial structure[210]. A caveat to this is that measures a traditionally performed in the longitudinal plane, likewise angle dependency may affect results.

Historically, research and clinical interests have focused on LV fibrosis characterisation. However, the RV is also prone to fibrotic infiltration, which can is

associated with increased RV loading conditions[211], but, not entirely. There have been interesting patterns noted in late gadolinium enhancement on MRI in the RV in SSC patients. Studies have shown enhancement at the RV insertion points[211], with a patchy distribution, not linked to classical coronary artery territory supply[212]. Fibrosis patterns support the concept that myocardial disease in SSC is due to microvascular disease as opposed to primary afterload increases due to increased pulmonary artery pressures. Focusing on a patients' haemodynamic profile, as opposed to myocardial characteristics, limits the clinical interpretation of progression of cardiac disease.

Speckle tracking imaging enables measurements of the myocardium not only in the longitudinal plane, but circumferentially[213], and radially[214], with all the different vectors adding substantially to myocardial contraction.

7.2 Abstract

Background: Impairment of myocardial function is a significant potential complication of SSc and associated with poor prognosis. The detection of subclinical LV and RV dysfunction may permit therapeutic intervention. We sought to investigate the prognostic value of both LV and RV deformation in patients with SSc.

Methods and Results: Speckle tracking LV strain parameters (global longitudinal strain (GLS) and global circumferential strain (GCS)) and tricuspid annular peak systolic velocity (Ts') were measured in 112 patients with SSc and 112 age- and gender-matched controls. Subjects were followed for a median of 1.9 years for all-cause admission or death, and the association of the study parameters with outcome was assessed using Cox proportional hazards models. GLS, GCS, and Ts' were significantly impaired in patients with SSc, even without PH, compared to controls. GCS (r^2=0.06, p=0.03) but not GLS (r^2=0.04, p=0.11) was associated with systolic pulmonary artery pressure. During follow-up, comparable numbers of SSc patients (n=45, 40%) and controls (n=38, 34%) had events (p=0.33). In SSc patients, GCS (but not GLS), Ts', and 6MWD were significantly associated with outcome. A model based on age, gender and 6MWD was significantly improved by adding GCS (p=0.03) and additionally by adding Ts' (p=0.03). However, 6MWD and Ts' (but not GCS) were independently associated with outcome.

Conclusion: RV dysfunction was associated with adverse outcome, independent of and incremental to clinical and LV deformation parameters in SSc. Subclinical LV dysfunction appears to have less prognostic relevance than RV dysfunction.

7.3 Background

SSc is a systemic CTD characterised by inflammation, widespread vascular lesions and fibrosis involving various organs including the lungs, skin, gastrointestinal tract, kidneys, and heart [215]. In particular, cardiopulmonary involvement in SSc associates with an unfavourable prognosis [215,216] - particularly PH [217-224]. Although pathologic observations at necropsy have demonstrated myocardial involvement in around 50-80% of patients with SSc [212,225,226], clinical evidence of myocardial dysfunction using conventional diagnostic modalities has not been widely recognised [215,227,228]. New techniques for the assessment of myocardial deformation has proven to be more sensitive than conventional echocardiography for the prediction of outcomes [229]. Several strain studies have demonstrated not only right ventricular (RV) but also left ventricular (LV) dysfunction in SSc, although the severity of LV dysfunction was relatively mild [230], even with the use of sophisticated methods [220-222,224]. The prognostic impact of this observation is unclear, as is its independence from RV dysfunction associated with pulmonary vascular disease, mainly as the LV and RV share several anatomical structures [231,232].

The purpose of this study was to investigate the mechanism of subclinical LV dysfunction, and its prognostic value compared to RV function in patients with SSc.

7.4 Methods

7.4.1 Study design.

We identified 116 consecutive patients with SSc without significant ischemic and valvular heart disease, who underwent echocardiography between July 2005 to June 2014. In patients with multiple echocardiograms, the first report on the system was selected as the baseline. The diagnosis of SSc was based on the American Rheumatism Association's criteria and confirmed by medical records [233]. After the exclusion of 4 patients due to inadequate echocardiographic image quality, 112 age- and gender-

matched control patients without significant cardiac disease (e.g. routine studies before non-cardiac surgery) were identified, then clinical details were confirmed by viewing each medical record. The Tasmanian Health Research Ethics Committee approved the study as a low-risk protocol based on data linkage without the need for individual consent.

7.4.2 Clinical data.

Clinical parameters (comorbidities, medications, vital signs, serum markers) at the time of echocardiography were comprehensively assessed by reviewing each medical record. The data of 6MWD and lung function test at the date closest to the echocardiogram were also collected in patients with SSc.

7.4.3 Echocardiography.

The earliest data stored in the echocardiography database was used for analysis. Transthoracic echocardiography was performed by experienced sonographers using a commercially available ultrasound machine (Vivid 7, Vivid 9, or Vivid I; GE Vingmed, Horten, Norway). Echocardiographic images were digitally recorded and downloaded to an imaging server for offline analysis. All echocardiographic parameters including strain were analysed by a single core reader, blinded to the other data.

Conventional echocardiographic parameters were measured according to the recommendations of the ASE [234,235]. LV volumes and LV ejection fraction (EF) were calculated by the modified Simpson method using 2-dimensional images, and LV volumes were indexed to BSA. LV mass was calculated according to the ASE formula and normalised to BSA. LAV was calculated by the modified Simpson's method using 2-dimensional images and indexed to BSA. The transmitral early diastolic velocity (E) was acquired in the apical 4-chamber view using pulsed-wave Doppler at the level of

the mitral valve tips during diastole. The early diastolic mitral annular tissue velocity (e') was measured in the apical 4-chamber view with the sample volume positioned at both the septal and lateral mitral annulus with the average of these two values calculated. The combined assessment of E and e' was used to calculate E/e'. The peak pressure gradient between RV and RA (TRPG) was measured on the continuous-wave spectral Doppler signal of tricuspid regurgitation. Systolic pulmonary artery pressure (SPAP) was estimated from TRPG and the maximum IVC diameter and its collapsibility [44]. In addition, PVR was also calculated from peak tricuspid regurgitant velocity and RV outflow tract velocity time integral [47].

7.4.4 LV strain and tricuspid annular velocity.

We measured the two global strain parameters (global longitudinal strain (GLS) and global circumferential strain (GCS)) using standard methodologies for speckle tracking (Research Arena, Tomtec, Germany) [236]. After manual tracing of the LV endocardial border, the dedicated software automatically tracked the myocardium throughout the cardiac cycle. Peak values of segmental longitudinal strain were obtained from grayscale–recorded images in the apical 4-chamber, 2-chamber, and long-axis views and GLS was obtained by averaging these peak values [89]. The peak values of the six segmental circumferential strain curves were obtained from the short-axis view at the papillary muscle level and averaged to provide GCS. Similarly, using speckle tracking, tricuspid annular peak systolic and early diastolic velocities (Ts' and Te') were measured from the RV apical 4-chamber view. The mean frame rate was 54±21 frames/s. In the patients with AF, strain parameters were measured if the preceding and pre-preceding intervals were equal [237].

7.4.5 Follow-up.

The primary outcome was unplanned all-cause admission or death after the index echocardiogram. The secondary outcome was heart failure (HF)-specific admission or death. The outcome was confirmed from each medical record. Patients were censored at the time of outcome or the end of study follow-up.

7.4.6 Statistical analysis.

Data were expressed as mean±SD or median (interquartile range). Overall, <5% of observations were missing, with the exception of Ts' and Te' (14%), and lung function parameters (48%). Missing Ts' and e' were imputed from propensity models using parameters without missing data (age, gender, body mass index, systolic blood pressure, HR, LV mass index, e', E/e', LA volume index, GLS, SPAP, diabetes mellitus, serum creatinine, AF, hemoglobin). Other continuous variables (<5%) were imputed using the corresponding mean value. The significance of differences between the groups was assessed using Student's t-test or Mann-Whitney U-test according to the distribution of the study parameters. For categorical variables, the chi-square test or Fisher exact test were used, as appropriate. Univariable linear regression analysis was performed to assess the association between carbon monoxide diffusing capacity of the lungs (%DLCO) and cardiac function parameters. Univariable quadratic regression analysis was used to evaluate the associations between LV strain parameters and SPAP because it had better fit than a simple linear regression model.

Univariable and multivariable Cox proportional-hazards models were used to determine the features associated with the outcomes. The optimal model was selected based on the significant variables in the univariable analysis and clinically relevant parameters. The incremental value of GCS and Ts' were also assessed in 3 modelling steps, using nested models. The first step consisted of fitting a multivariable model of

age, gender, and 6MWD. Then, GCS was included in the second step. Finally, Ts' was included in the third step. The change in overall log-likelihood ratio chi-square was used to assess the increase in predictive power after the addition of GCS and Ts', and Harrell's C statistic was used to evaluate model performance. The receiver operating characteristic (ROC) curve was used to determine the optimal cut-off values of GCS, Ts', and 6MWD for predicting the outcomes. Comparisons of AUC in each parameter were performed with the method proposed by Delong *et al*.[238] Reclassification was evaluated to assess the incremental benefit of adding Ts' to the model based on age, gender, 6MWD and GCS with continuous net reclassification improvement (NRI) methods and integrated diagnostic improvement (IDI) [239,240].

Inter- and intraobserver variabilities were examined for GLS, GCS, and Ts' using the intraclass and interclass correlation coefficients. Measurements were performed in a group of 10 randomly selected subjects by one observer, then repeated on 14 separate days by two observers. Statistical analysis was performed using standard statistical software packages (SPSS software 20.0, SPSS Inc., Chicago, IL and R software ver.3.0.2 (http://cran.r-project.org/)), and statistical significance was defined by $p<0.05$.

7.5 Results

7.5.1 Clinical characteristics.

Table 7.1 summarises the clinical characteristics of the patients with SSc and controls. Patients with SSc had significantly higher HR and prevalence of chronic lung disease, and lower blood pressure and less use of anti-hypertensive agents. About half of the SSc patients were treated with pulmonary vasodilators. The performance of lung function testing was incomplete in SSc patients, but their %DLCO appeared to be more impaired rather than forced vital capacity and forced expiratory volume in one second.

Table 7-1. Baseline characteristics in patients with systemic sclerosis and controls

Variables	Systemic sclerosis (n = 112)	Control (n = 112)	p Value
Age (yrs)	64 (57-71)	64 (57-71)	1.00
Male sex, n (%)	27 (24)	27 (24)	1.00
Body mass index (kg/m^2)	26.9 (23.7-28.4)	27.6 (24.8-29.4)	0.14
Systolic blood pressure (mmHg)	121 (110-135)	128 (118-142)	**0.01**
Diastolic blood pressure (mmHg)	73 (65-79)	75 (70-82)	**0.01**
Heart rate (/min)	74 ± 13	69 ± 12	**<0.01**
Comorbidities			
Hypertension, n (%)	31 (28)	39 (35)	0.31
Diabetes , n (%)	12 (11)	15 (13)	0.53
Atrial fibrillation, n (%)	9 (8)	6 (5)	0.42
Chronic lung disease, n (%)	34 (30)	20 (18)	**0.03**
Serum markers			
Blood urea nitrogen (mmol)	5.8 (4.6-6.7)	5.8 (4.3-6.5)	0.42
Creatinine (mmol/L)	75 (63-86)	75 (64-81)	0.74
Sodium (mmol/L)	139 (137-140)	139 (137-140)	0.95
Hemoglobin (g/L)	133 ± 17	135 ± 15	0.49
Medications			
β blockers, n (%)	7 (6)	9 (8)	0.60
ACEi/ARB, n (%)	13 (12)	28 (25)	**0.02**
Diuretics (loop or thiazide), n (%)	14 (13)	9 (8)	0.20
Endothelin receptor antagonist, n (%)	54 (48)	0 (0)	**<0.01**
PDE5 inhibitor, n (%)	5 (4)	0 (0)	**<0.01**
6-minute walk test			
6 minute walk distance (m)	451 (386-498)	-	NA
Lung function test (n = 58)			
% FVC	98 (81-110)	-	NA
% FEV_1	77 (69-81)	-	NA
% DLco	63 (46-80)	-	NA

Data are expressed as mean±SD or as number (percentage) or median (interquartile range).ACEi indicates Angiotensin-converting enzyme inhibitors; ARB, Angiotensin receptor blockers; PDE5, Phosphodiesterase type 5; %FVC, percent forced vital capacity; % FEV1, percent FEV; % DLco, percent predicted diffusing capacity of the lung for carbon monoxide.

7.5.2 Echocardiographic characteristic

Table 7.2 shows a comparison of echocardiographic parameters, most of which were within the normal range. Although LV volume, EF, and diastolic parameters were not significantly different between the groups, pulmonary haemodynamics, RV function and LV strain parameters were significantly worse in patients with SSc compared to controls. These results were consistent even in SSc patients with SPAP <40mmHg and no administration of drugs for PH (n=44, Appendix Table 7.4). Both longitudinal and circumferential peak strain in the mid-septal segment were significantly more impaired in SSc patients than in controls (longitudinal: -16.5% [IQR -13.0--20.0] vs -19.0% [IQR -16.0--22.0], p<0.01, circumferential: -29.0% [IQR -23.5--36.0] vs -32.0% [IQR 26.5--40.0], p=0.04) (Figure 1).

Figure 7-1. Bull's-eye diagram of a percent difference of left ventricular segmental strain (Longitudinal strain: 18 segments; Circumferential strain: 6 segments) between patients with SSC and controls ((strain in SSc/strain in control) x 100 (%)). Blue segments show a significant deterioration of strain

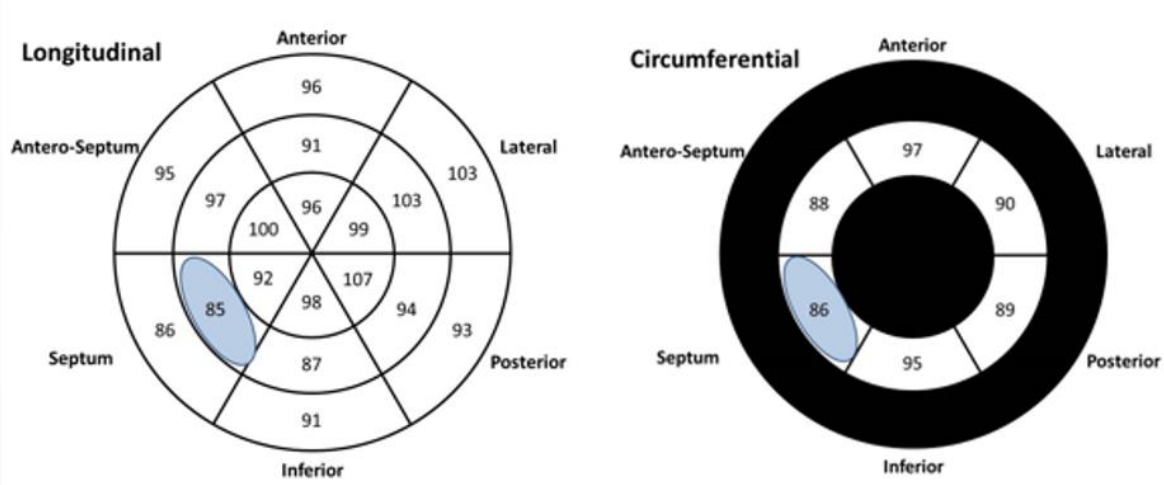

Table 7-2. Echocardiographic characteristics in patients with systemic sclerosis and controls

Variables	Systemic sclerosis (n = 112)	Control (n = 112)	p Value
LV end-diastolic volume index (ml/m^2)	49 ± 13	48 ± 12	0.55
LV end-systolic volume index (ml/m^2)	15 (10-20)	14 (11-17)	0.53
LV ejection fraction (%)	69 ± 9	70 ± 7	0.76
LV mass index (g/m^2)	82 (68-95)	81 (70-97)	0.86
LA volume index (ml/m^2)	32 (27-41)	32 (26-36)	0.27
E/A	1.04 (0.84-1.30)	1.04 (0.85-1.26)	0.84
E velocity deceleration time (ms)	200 (167-232)	196 (166-229)	0.97
e' (cm/s)	8.6 (7.0-10.5)	8.5 (6.5-9.5)	0.07
E/e'	9.1 (7.3-10.6)	9.0 (7.6-10.7)	0.55
TRPG (mmHg)	23 (19-32)	19 (6-25)	**<0.01**
SPAP (mmHg)	27 (22-35)	24 (11-28)	**<0.01**
PVR (Wood units)	1.5 (1.2-1.9)	1.2 (0.9-1.5)	**<0.01**
LV global longitudinal strain (%)	-18.3 ± 3.0	-19.5 ± 2.6	**<0.01**
LV global circumferential strain (%)	-26.9 ± 5.3	-29.5 ± 5.3	**<0.01**
Ts' (cm/s)	6.3 ± 1.9	6.8 ± 1.6	**0.02**
TAe' (cm/s)	-5.4 (-4.1--6.5)	-5.7 (-4.9--6.9)	**0.03**

Data are expressed as mean ± SD or median (interquartile range).LA indicates left atrial; LV, left ventricular; PVR, pulmonary vascular resistance; RV, right ventricular; SPAP, systolic pulmonary artery pressure; Ts', tricuspid annular peak systolic velocity; TAe', tricuspid annular peak early diastolic velocity

There were weak but significant associations of diffusion capacity with SPAP (r^2=0.07, p=0.04), but not PVR (r^2=0.06, p=0.06), Ts' (r^2=0.05, p=0.08), GCS (r^2=0.05, p=0.09), and GLS (r^2=0.01, p=0.46).

In SSc, a quadratic regression demonstrated a significant relationship between GCS and SPAP (r^2=0.06, p=0.03) (Figure 7.2). No significant relationship could be defined between GLS and SPAP (r^2=0.04, p=0.11).

7.5.3 Events.

During follow-up (median 1.9 years [IQR 1.1-3.8]), unplanned all-cause readmission or death occurred in 45 SSc patients (40%) and 38 controls (34%, p=0.33). In the case of SSc patients without PH (n=44), only one patient had an event.

SSc patients (n=20, 18%) were slightly more likely to develop HF-specific readmission or death (secondary outcome) compared to controls (n=11, 10%, p=0.08). In patients with SSc, the common reasons for admission other than HF (n=11) were lung disease (n=5), renal disease (n=3), and ischemic heart disease (n=3).

Figure 7-2. The relationships between global longitudinal strain (7.2a), global circumferential strain (7.2b), and systolic pulmonary artery pressure in patients with SSC. The dotted line shows 95% confidence interval

Figure 7.2a; GLS and PAPs

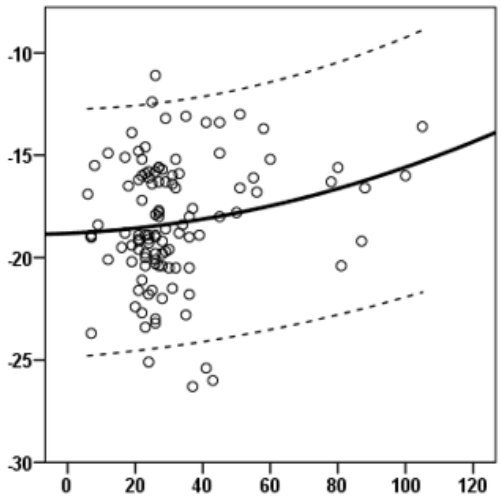

Figure 7.2b; GCS and PAPs

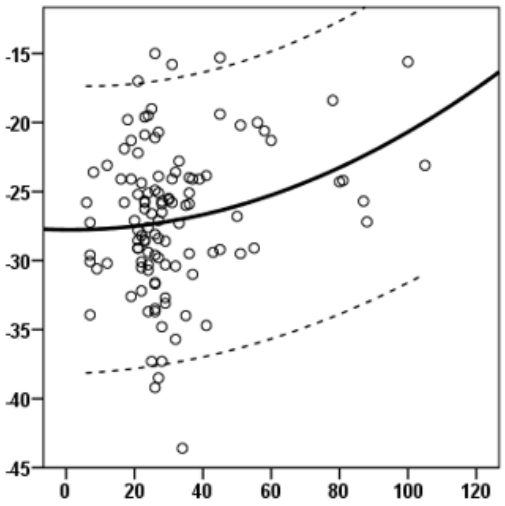

7.5.4 Associations of outcomes.

Table 7.3 shows the univariable Cox regression analyses of the primary outcome in patients with SSc. All-cause admission or death was significantly associated with lower sodium, diuretic use, shorter 6MWD, impaired lung function, LV mass index, SPAP and PVR, GCS and Ts'. LV diastolic function parameters and GLS were not significantly associated with outcome. Similarly, HF-specific admission or death was also associated with the same variables and lower systolic blood pressure (Appendix Table 7.5). In the ROC analysis for predicting the primary outcome, the discriminative ability of 6MWD (AUC=0.79) was significantly larger than that of GCS (AUC=0.65, p=0.04), but not Ts' (AUC=0.68, p=0.09) (Figure 7.3A). There was no significant difference of AUCs between Ts' and GCS (p=0.80). The optimal cut-point for GCS was -25.8% (sensitivity 64%, specificity 67%), for Ts' 6.9 cm/s (sensitivity 84%, specificity 47%), and for 6MWD 433 m (sensitivity 80%, specificity 67%).

Table 7-3. Univariable Cox regression analysis for the association of all-cause admission or death in patients with systemic sclerosis

Variables	Univariable HR (95%CI)	p-Value
Age (yrs)	1.02 (0.99-1.04)	0.26
Male sex, n (%)	1.73 (0.90-3.33)	0.10
Body mass index (kg/m^2)	1.02 (0.96-1.08)	0.55
Systolic blood pressure (mmHg)	0.98 (0.97-1.00)	0.06
Diastolic blood pressure (mmHg)	0.98 (0.95-1.01)	0.21
Heart rate (/min)	1.02 (1.00-1.04)	0.051
Comorbidities		
Hypertension, n (%)	1.12 (0.62-2.03)	0.70
Diabetes , n (%)	0.97 (0.38-2.46)	0.97
Atrial fibrillation, n (%)	1.88 (0.79-4.47)	0.16
Chronic lung disease, n (%)	1.61 (0.88-2.93)	0.12
Serum markers		
Blood urea nitrogen (mmol)	1.01 (0.85-1.20)	0.90
Creatinine (mmol/L)	1.01 (1.00-1.02)	0.18
Sodium (mmol/L)	0.88 (0.80-0.97)	**<0.01**
Hemoglobin (g/L)	1.01 (1.00-1.02)	0.17
Medications		
β blockers, n (%)	0.89 (0.12-6.73)	0.91
ACEi/ARB, n (%)	1.43 (0.41-4.98)	0.58
Diuretics (loop or thiazide), n (%)	2.96 (1.48-5.91)	**<0.01**
Endothelin receptor antagonist, n (%)	0.67 (0.37-1.23)	0.20
PDE5 inhibitor, n (%)	2.83 (0.86-9.33)	0.09
6-minute walk test		
6 minute walk distance (m)	0.99 (0.99-1.00)	**<0.01**
Lung function test (n = 58)		
% FVC	0.98 (0.97-1.00)	**0.03**
% FEV_1	0.97 (0.94-1.00)	0.09
% DLco	0.96 (0.94-0.99)	**<0.01**
Echocardiographic parameters		
LV end-diastolic volume index (ml/m^2)	0.98 (0.95-1.01)	0.13
LV end-systolic volume index (ml/m^2)	1.00 (0.94-1.06)	0.92
LV ejection fraction (%)	0.98 (0.95-1.01)	0.24
LV mass index (g/m^2)	1.02 (1.01-1.03)	**<0.01**
LA volume index (ml/m^2)	0.98 (0.96-1.02)	0.99
E/A	0.65 (0.30-1.45)	0.30
E velocity deceleration time (ms)	1.00 (0.99-1.01)	0.95
e' (cm/s)	0.92 (0.81-1.04)	0.18
E/e'	1.07 (0.96-1.19)	0.21

TRPG (mmHg)	1.02 (1.01-1.03)	**<0.01**
SPAP (mmHg)	1.02 (1.01-1.03)	**<0.01**
PVR (Wood units)	1.69 (1.32-2.16)	**<0.01**
LV global longitudinal strain (%)	1.02 (0.91-1.13)	0.75
LV global circumferential strain (%)	1.09 (1.03-1.16)	**<0.01**
Ts' (cm/s)	0.75 (0.63-0.89)	**<0.01**
TAe' (cm/s)	1.15 (0.97-1.37)	0.11

ACEi; angiotensin-converting-enzyme inhibitor; ARB, Angiotension receptor blockade; PDE5, phosphodiesterase type 5 inhibitor; %FVC, percent forced vital capacity; % FEV1, percent FEV; % DLco, percent predicted diffusing capacity of the lung for carbon monoxide LA indicates left atrial; LV, left ventricular; PVR, pulmonary vascular resistance; RV, right ventricular; SPAP, systolic pulmonary artery pressure;TRPG, tricuspid regurgitation pressure gradient; Ts', tricuspid annular peak systolic velocity; TAe', tricuspid annular peak early diastolic velocity.

ROC analysis for predicting the secondary outcome also showed similar results (Figure 3B). There was a significant difference of AUCs between 6MWD and GCS (p=0.03), but other AUC comparisons were not significant. Addition of Ts' into the model reduced the impact of GCS. In the final model, 6MWD and Ts' were independently associated with outcome.

Figure 7-3. ROC curves for predicting all-cause admission or death (7.3a) and HF-specific admission or death (7.3b) in patients with SSC. GCS indicates global circumferential strain; Ts', tricuspid annular peak systolic velocity; 6MWD, 6-minute walk distance; 95%CI, 95% confidence interval

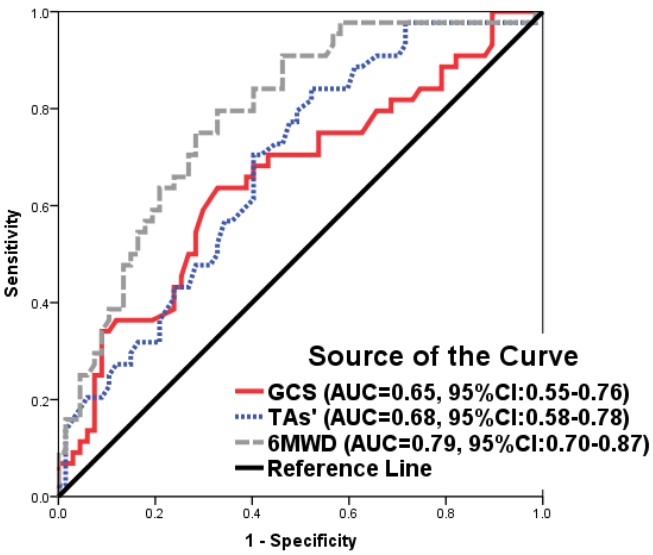

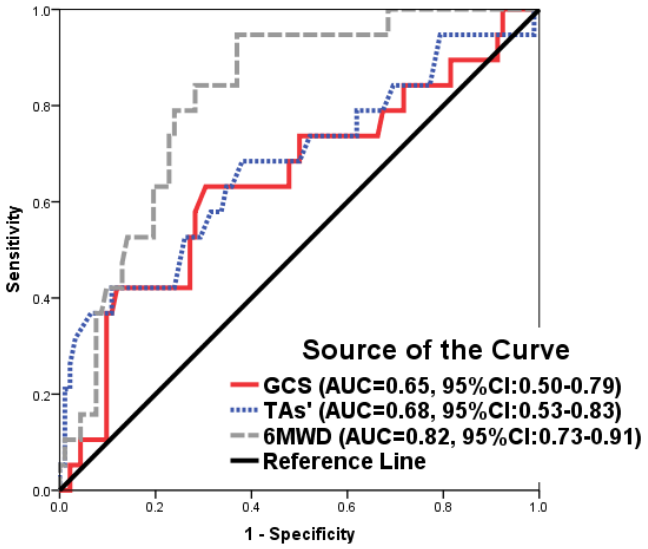

7.5.5 Incremental value and independence of RV and LV function for outcome.

In sequential Cox models for predicting all-cause readmission or death in patients with SSc, the model based on age, gender, and 6MWD was significantly improved by the addition of GCS and further improved by adding Ts' (Figure 7.4). Moreover, the addition of Ts' to the model based on age, gender, 6MWD, and GCS led to a further significant reclassification improvement in the overall group (Continuous NRI: 0.63, p<0.01). However, IDI (0.02) was not significant (p=0.32).

Figure 7-4. Incremental value of Ts' over clinical parameters and GCS as a correlate of all-cause readmission or death in patients with SSC. GCS indicates global circumferential strain; Ts', tricuspid annular peak systolic velocity

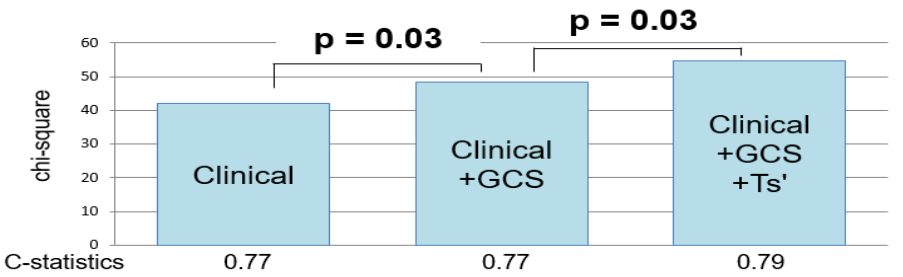

Variable	Model 1 (Clinical) Chi-square=42.0 HR (95%CI), p Value	Model 2 (Clinical+GCS) Chi-square=48.4 HR (95%CI), p Value	Model 3 (Clinical+GCS+Ts') Chi-square=54.7 HR (95%CI), p Value
Age (per 1 year increase)	0.97 (0.94-1.00), p=0.06	0.96 (0.94-0.99), **p=0.02**	0.97 (0.94-1.00), **p=0.03**
Male	2.91 (1.43-5.95), **p<0.01**	2.57 (1.27-5.23), **p<0.01**	2.68 (1.33-5.40), **p<0.01**
6-min walk distance (per 1m increase)	0.99 (0.99-0.99), **p<0.01**	0.99 (0.99-0.99), **p<0.01**	0.99 (0.99-0.99), **p<0.01**
GCS (per 1% increase)		1.08 (1.01-1.16), **p=0.03**	1.04 (0.97-1.12), p=0.28
Ts' (per 1cm/s increase)			0.81 (0.68-0.98), **p=0.03**

7.5.6 Reproducibility.

The intraclass and interclass correlation coefficients were, 0.93 (95%CI 0.72 to 0.98) and 0.92 (95%CI 0.67 to 0.98) for GLS, 0.91 (95%CI 0.67 to 0.98) and 0.93 (95%CI 0.70 to 0.99) for GCS, and 0.86 (95%CI 0.44 to 0.97) and 0.85 (95%CI 0.32 to 0.97) for Ts'. All reproducibility and agreement therefore fell into the good to excellent ranges.

7.6 Discussion

The present study demonstrates the relative prognostic value of RV and LV dysfunction in SSc patients, and points towards a mechanism for linking these features. Similar to previous reports, LV deformation in SSc – while reduced compared with controls - was within the normal range. GCS appeared to be more affected by increased systolic RV pressure and associated with adverse outcome than GLS. The measurement of GCS had an incremental benefit over 6-minute walk test for predicting outcome. However, the association between GCS and outcome appeared to be mediated by RV function, and RV systolic function and 6MWD showed the only independent association with outcome in SSc.

7.6.1 Mechanism of LV dysfunction in SSc.

SSc is a systemic CTD characterised by inflammation and fibrosis involving distinct target organs [215]. Histological studies have shown myocardial fibrosis in up to 80% of patients with SSc [212], and myocardial fibrosis has been considered as the primary mechanism of LV dysfunction. In the present study, a mild deterioration of LV longitudinal and the circumferential strain was observed compared to controls [219-222], consistent with previous observations of impaired LV longitudinal strain in SSc, and thought to be associated with subendocardial myocardial fibrosis [219-222,224,241].

The deterioration of segmental strain in the septal segments, likely affected by both LV and RV function, appeared to contribute to the impairment of global strain. Also, GCS was weakly associated with increased SPAP and reduced diffusion capacity. These results suggest that LV dysfunction could be affected by not only LV myocardial fibrosis but also by RV dysfunction and pulmonary haemodynamics, reflecting ventricular interdependence in patients with SSc. In addition to its association with RV longitudinal systolic deformation, RV pressure overload

influences the IVS and LV geometry. An altercation of the geometry impairs LV torsion and segmental longitudinal and circumferential strain, more for the septum than for the free wall of the LV [231]. These findings are supportive of our observations; in the present study, SSc patients had significantly higher PVR, and half of the patients were treated pulmonary vasodilators, which could minimise the effects of chronic RV pressure overload.

7.6.2 Prognostic value of LV dysfunction in SSc.

RV dysfunction, usually caused by vascular and interstitial lung disease resulting in PH, has frequently been reported, and strongly associated with adverse outcomes in SSc patients [87,215,216,242]. The present study also demonstrated that RV dysfunction associated with adverse outcome, independent of and incremental to functional capacity and LV deformation parameters in SSc. However, LV dysfunction was not independently associated with outcome, implying that RV dysfunction mediated its univariable association. Also, there was only one adverse event in SSc patients without PH. Above all, these results suggest that the predictive power of LV dysfunction seems to be weaker than RV dysfunction in SSc, although this could depend on the severity of PH in the study cohort.

7.7 Study limitations.

Our data should be interpreted in the context of their limitations. First, our observational study carries the risk of unmeasured confounders. However, the prevalence of SSc (50 to 300 cases per 1 million persons) [215] makes a prospective design difficult, and the present study sample was among the largest reported to date [87,219-222]. Second, in this study, half of the patients were already on pulmonary vasodilator therapy, implying that the prognostic impact of RV dysfunction might be attenuated. However, the association with adverse outcome was similar even in SSc

patients without PH. Finally, we did not measure RV global strain, which requires the whole RV to be visible throughout the cardiac cycle. As a surrogate, we measured tricuspid annular velocity using speckle tracking, which is angle-independent and has good reproducibility [44]. In the multivariable analysis, the majority of predictors displayed weak strength of contribution. The inclusion of parameters together could lead to an overstatement of contribution of each parameter in the model.

7.8 Conclusion.

Subclinical LV dysfunction, as well as RV dysfunction, is observed in SSc. The impairment of LV circumferential deformation was associated with adverse outcome and had an incremental benefit over functional capacity for predicting outcome. However, this association was related to RV dysfunction; consequently, RV dysfunction and functional capacity were more strongly associated with clinical events.

7.9 **Appendix**

Appendix Table 7-4. Echocardiographic characteristics in patients with systemic sclerosis without pulmonary hypertension and controls

Variables	**Systemic sclerosis without pulmonary hypertension (n = 44)**	**Control (n = 44)**	**p**
Age (yrs)	60 (52-64)	60 (52-64)	1.00
Male sex, n (%)	11 (25)	11 (25)	1.00
LV end-diastolic volume index (ml/m^2)	48 ± 10	50 ± 13	0.33
LV end-systolic volume index (ml/m^2)	14 (11-20)	15 (11-18)	0.93
LV ejection fraction (%)	68 ± 9	70 ± 7	0.47
LV mass index (g/m^2)	80 (65-94)	78 (68-94)	0.70
LA volume index (ml/m^2)	30 (25-39)	31 (25-36)	0.78
E/A	1.12 (0.92-1.31)	1.15 (0.89-1.43)	0.52
E velocity deceleration time (ms)	181 (156-218)	200 (167-230)	0.20
e' (cm/s)	8.6 (7.4-10.5)	8.6 (7.3-10.7)	0.79
E/e'	8.2 (7.3-10.4)	8.8 (7.3-9.8)	0.92
TRPG (mmHg)	22 (18-25)	16 (5-23)	**<0.01**
SPAP (mmHg)	26 (22-28)	21 (9-26)	**<0.01**
PVR (Wood units)	1.4 (1.2-1.7)	1.1 (0.9-1.4)	**<0.01**
LV global longitudinal strain (%)	-18.6 ± 3.0	-20.0 ± 3.0	**0.03**
LV global circumferential strain (%)	-27.8 ± 5.4	-30.5 ± 5.8	**0.02**
Ts' (cm/s)	6.2 ± 1.6	7.2 ± 1.7	**<0.01**
TAe' (cm/s)	-5.4 (-4.3--6.4)	-6.1 (-5.5--7.3)	**0.03**

Appendix Table 7-5. Association of HF-specific admission or death in patients with systemic sclerosis (univariable Cox regression analysis).

Variables	Univariable HR (95%CI)	p Value
Age (yrs)	1.02 (0.98-1.06)	0.37
Male sex, n (%)	2.05 (0.78-5.38)	0.14
Body mass index (kg/m^2)	1.00 (0.92-1.09)	0.99
Systolic blood pressure (mmHg)	0.96 (0.93-1.00)	**0.01**
Diastolic blood pressure (mmHg)	0.96 (0.91-1.00)	0.058
Heart rate (/min)	1.01 (0.98-1.05)	0.46
Comorbidities		
Hypertension, n (%)	0.82 (0.33-2.03)	0.67
Diabetes , n (%)	1.75 (0.51-6.04)	0.38
Atrial fibrillation, n (%)	2.12 (0.62-7.30)	0.23
Chronic lung disease, n (%)	2.63 (1.09-6.37)	**0.03**
Serum markers		
Blood urea nitrogen (mmol)	0.91 (0.69-1.20)	0.49
Creatinine (mmol/L)	1.00 (0.97-1.03)	0.98
Sodium (mmol/L)	0.90 (0.78-1.03)	0.12
Hemoglobin (g/L)	1.01 (0.98-1.04)	0.58
Medications		
β blockers, n (%)	0.70 (0.09-5.24)	0.73
ACEi/ARB, n (%)	1.77 (0.59-5.34)	0.31
Diuretics (loop or thiazide), n (%)	5.90 (2.41-14.47)	**<0.01**
Endothelin receptor antagonist, n (%)	1.16 (0.47-2.87)	0.75
PDE5 inhibitor, n (%)	2.67 (0.77-9.33)	0.09
6-minute walk test		
6 minute walk distance (m)	0.99 (0.99-1.00)	**<0.01**
Lung function test (n = 58)		
% FVC	0.96 (0.94-0.99)	**<0.01**
% FEV_1	1.02 (0.97-1.08)	0.50
% DLco	0.94 (0.90-0.98)	**<0.01**
Echocardiographic parameters		
LV end-diastolic volume index (ml/m^2)	0.98 (0.94-1.01)	0.12
LV end-systolic volume index (ml/m^2)	1.01 (0.94-1.08)	0.85
LV ejection fraction (%)	0.97 (0.92-1.02)	0.19
LV mass index (g/m^2)	1.02 (1.00-1.04)	**0.02**
LA volume index (ml/m^2)	1.00 (0.97-1.04)	0.90
E/A	0.76 (0.24-2.43)	0.65
E velocity deceleration time (ms)	1.00 (0.99-1.01)	1.00
e' (cm/s)	0.85 (0.70-1.03)	0.10

E/e’	1.11 (0.97-1.28)	0.14
TRPG (mmHg)	1.03 (1.02-1.05)	**<0.01**
SPAP (mmHg)	1.03 (1.02-1.05)	**<0.01**
PVR (Wood units)	1.52 (1.24-1.85)	**<0.01**
LV global longitudinal strain (%)	1.03 (0.89-1.20)	0.68
LV global circumferential strain (%)	1.10 (1.01-1.20)	**0.04**
Ts’ (cm/s)	0.68 (0.51-0.90)	**<0.01**
TAe’ (cm/s)	1.26 (0.97-1.65)	0.09

7.10 Postscript.

The previous chapter shows that LV function is a reliable outcome marker in SSC patients. However, this association was confounded by RV dysfunction; consequently, RV dysfunction and functional capacity were more strongly associated with clinical events. RV dysfunction can manifest through a number of markers – but due to the arrangement of RV fibres, contraction of the RV is comprehensively reflected from EF. Haemodynamic markers are often measured, but the infiltrative process could provoke RV dysfunction despite normal pulmonary pressures. Speckle tracking plays an essential role in this, but other aspects of the echocardiographic exam may be abnormal. No single parameter should be considered in isolation.

As mentioned previously, SSC patients are a unique group in which there is an interplay of left and right heart disease. The distinction between pre versus post capillary hypertension in these patients can often make for complex clinical analysis. The diagnosis of diastolic dysfunction combines tissue Doppler, haemodynamics, and structural changes. Eventually, downstream effects of increased LA pressure will lead to structural abnormalities within the RV. The clear differentiation of left versus right heart disease is difficult in the SSC cohort.

In the forthcoming chapter, we look into how current clinical guidelines work in a population at risk for PHT, and further investigate the use of speckle tracking as a novel tool in preclinical disease differentiation.

Chapter 8

PH Differential Diagnosis; Echocardiography for the differential diagnosis of pre versus postcapillary pulmonary hypertension

Under review as "Echocardiographic Evaluation of Dyspnea in the Context of Diastolic Evaluation Guidelines: Implications for Evaluation of Pulmonary Arterial Hypertension"

Heart, Lung and Circulation

Leah Wright, Nathan Dwyer, Sudhir Wahi, Thomas H Marwick

8 PAH differential diagnosis; Echocardiography for the Differential diagnosis of pre versus postcapillary pulmonary arterial hypertension

8.1 Preface; Differential diagnosis of pre versus postcapillary pulmonary hypertension

Previously the strength of LV versus RV markers for prediction of outcome in SSC was assessed. As mentioned, the pressure is routinely used within this cohort to screen for the presence of pulmonary vascular disease. The importance of determining the cause of raised PA pressure has a substantial impact on clinical follow-up.

PH is divided into Group 1 (increased pulmonary artery resistance) and Group 2 (PH due to left heart disease leading to raised left atrial pressure). Overall, left ventricular related PH is the predominant cause of raised pressures within the general population[7]. The clinical sonographer is faced with the dilemma of determining the pathophysiological basis of raised pulmonary pressures.

Diastolic dysfunction refers to the impaired filling of the heart due to increases in ventricular stiffness. Increased pressures within the left atrium lead to congestion within the pulmonary circulation, creating an increase in pulmonary artery pressure. Guidelines have been published regarding the echocardiographic diagnosis of diastolic dysfunction [243]. The gold standard is through the invasive measurement of the LV relaxation time constant (tau), and PCWP to determine invasive pressures). Guidelines suggest four categories of diastolic dysfunction severity, with the determination based on four criteria; left atrial size, tricuspid jet velocity, tissue velocities, and estimation of LV filling pressures with E/e' ratio [243].

In a PH cohort, the diagnostic accuracy of this algorithm may be altered. Current diagnostic guidelines also do not allude to the diagnostic strength of parameters. This chapter aims to compare strain and other echocardiographic parameters in

differentiating PH type. If diastolic dysfunction criteria are not sufficient, perhaps LV GLS could be helpful in distinguishing pathology.

8.2 Abstract

Background. Treatment selections for PH are dependent on etiology. We sought whether recently published recommendations for non-invasive assessment of PCWP could facilitate the recognition of pulmonary venous hypertension in dyspneic patients undergoing right RHC for evaluation of suspected PH.

Methods. We recruited 157 consecutive patients undergoing RHC with echocardiographic EF >50% (median interval 1 day) for investigation of dyspnea. The proposed algorithm included tricuspid regurgitant maximum velocity (TRV max), tissue Doppler annular velocities (e'), average E/e' and LAV ml/m^2. Bivariate logistic regression, including receiver-operating characteristic (ROC) curves, were used to assess predictive ability using the area under the receiver operator curve (AUC).

Results. Patients with preserved EF and raised PCWP showed significantly increased LAV ml/m^2 and E/e', but not TRV max or average e'. Bivariate logistic regression showed E/e' (OR 0.15 95% CI 0.06-0.38, p<0.001) and LAV ml/m^2 (OR 0.43 95% CI (0.22-0.84), p=0.01) associated with raised PCWP, and LAV and E/e' showed only modest predictive ability for determining raised wedge pressure (AUC=0.64 and 0.69). Only 45% of patients with PCWP≥15 mmHg had >2 abnormal parameters. Alternative markers of post-capillary PH were increased LV mass (AUC=0.60), LV end-diastolic volume (AUC=0.64), impaired GLS (AUC=0.47) and pulmonary to left atrial ratio (ePLAR; AUC=0.73).

Conclusions. The detection of post-capillary PH appears to be better predicted with LV markers than recently recommended algorithms for detecting raised PCWP.

8.3 Background

Echocardiographic assessment of pulmonary artery pressure and LV dysfunction are central to the investigation of dyspnoea [244,245]. PH may be due to changes in the pulmonary arterial bed (pre-capillary PH) [10], or due to increased left atrial pressure (LAP) (post-capillary PH) [10,246]. Elevation of pulmonary venous pressure leads to elevations in right heart pressures; 44-80% of patients with diastolic dysfunction (DD) develop PH [247] in referral and community-based cohorts [248]. The distinction has significant implications, particularly for pulmonary vasodilator therapy [249] that are relatively contraindicated in Group 2 PH

The predictive ability of echocardiographic methods for the differentiation of normal from abnormal filling pressures in heart failure with preserved EF remains controversial [250]. However, new combinations of measurements have been proposed to characterise abnormal LV function. Recent recommendations have proposed that DD may be diagnosed in most patients with a normal EF, by a majority of abnormal average E/e', annular velocities (e'), tricuspid regurgitation velocity (TRV max) and left atrial volume (LAV) index [243]. In patients with impaired EF or myocardial disease, increased LV filling pressure may be recognized if the E/A ratio is >2, or E/A ratio is 0.8-2 (or E/A<0.8 with a peak E velocity of >50 cm/sec) if there is a majority of abnormal average E/e', tricuspid regurgitation velocity (TRV max) and left atrial volume (LAV) index. In our practice, RHC is performed to identify the cause of unexplained dyspnea when this has therapeutic implications, especially in relation to the use of pulmonary vasodilator therapy. Accordingly, we sought whether the accuracy of this new diagnostic algorithm for recognition of raised filling pressures was superior to LV parameters in dyspneic patients undergoing RHC.

8.4 Methods

8.4.1 Patient selection.

Consecutive patients were included if they underwent RHC and echocardiography (median interval 1 day) between July 2003 to April 2015. Patients were retrospectively recruited from the cardiac catheterisation laboratories of the Royal Hobart Hospital (Hobart, Australia) and the Princess Alexandra Hospital (Brisbane, Australia). Patient exclusions are shown in Figure appendix 8.4. Approval was obtained from the Tasmanian Human Research Ethics committee (H0013333) and Metro South Human Research Ethics Committee (HREC 16/QPAH/008).

8.4.2 Echocardiography.

Echocardiography was performed using commercial equipment (Vivid 7, Vivid i and Vivid e9, General Electric Medical Systems, Milwaukee, WI; ie33, Philips, Andover. MA). A single reader performed all LV and RV measurements according to ASE guidelines [101]. LV EF was measured from the apical 4- and 2-chamber views (Simpson's biplane method) [101]. LV mass was calculated from the parasternal long axis (ASE method) [101]. RVEDA and RVESA were calculated from the apical RV focused view; FAC was calculated as the percentage change in RVEDA and RVESA [101] . PASP was measured from the peak TR velocity using the modified Bernoulli equation [29]. RAP was derived from the IVC dimension response to inspiration from the subcostal view [44].

Peak velocities of the early (E) and late (A) diastolic filling were derived from transmitral inflow. Peak diastolic early velocity (e') of the lateral and septal mitral annulus was recorded from the apical 4-chamber view (Pulsed-wave tissue Doppler imaging). E/e' was calculated from early transmitral E wave divided by the average e' to infer LV filling pressures (LVFP) [243]. LAV measurements were performed from the apical 2- and 4- chambers (area-length method) [101]. Recommended parameters were

dichotomized based on ASE guidelines regarding diastolic evaluation with LVEF>50%: 1) Average E/e' >14, 2) Septal e' <7 cm/s or lateral <10 cm/s, 3) TR velocity >2.8 m/s, 4) LAV 34 ml/m^2. DD was defined as >50% positive criteria (Figures 8.1, 8.2 and 8.3). To assess the efficacy of the guidelines for assessing DD, groups were created [243]; Group 1 (E/e'+, e'+, LAV+), Group 2 (E/e'+, e'+, TR+), Group 3 (E/e'+, TR+, LAV+), Group 4 (e'+, TR+, LAV+), Group 5 (All markers +), Group 6 (2 markers+), Group 7 (1+), Group 8 (no +). Furthermore, patients were categorised based on the classification of DD regardless of EF: 1) Normal LAP with grade 1 DD, 2) Indeterminate, 3) Increased LAP and grade 2 DD, 4) Increased LAP, grade 3 DD. Pulmonary to left atrial ratio (ePLAR) was calculated from the peak TR velocity divided by the transmitral E/e' (TR V max/E/e') [251].

Wall motion tracking software that accepted DICOM images (Image-Arena, TomTec Gmbh, Unterschleissheim, Germany,) was used to analyse the apical 4-, 2- and 3-chamber LV views, which were averaged to produce LV global strain (LV GLS). Optimal LV cavity views were selected, with the LV end-diastolic endocardial border manually traced along the myocardium (borders were automatically tracked frame-by-frame). Manual adjustments were performed when necessary, and regions excluded as required (e.g. inadequate tracking). RVFWS was performed from the RV focused view (basal, mid and apical segments averaged).

8.4.3 Right heart catheterisation.

RHC studies were undertaken after premedication and local anesthesia. A 4-lumen 110 cm 7-Fr Swan-Ganz catheter (Edwards Lifesciences, Irvine, CA) was floated to the right heart, and resting measurements of right atrial, right ventricular, pulmonary arterial and PCWP were made at end-expiration using a pressure transducer (21BB, ITL Healthcare, Chelsea Heights, Australia). The transducer was calibrated to

atmospheric pressure at the level of the RA and re-checked at intervals to avoid zero drift. CO was determined by thermodilution, using an average of four consecutive values that varied <10%. Electrocardiographic (ECG) leads were connected to both arms and the left leg, allowing three ECG channels for the timing of signals. All haemodynamic monitoring was recorded using a Horizon SE Haemodynamic System (Mennen Medical Ltd., Yavne, Israel) and subsequently analysed off-line.

Figure 8-1. Diastolic dysfunction interpretation and comparisons with invasive pressure assessment

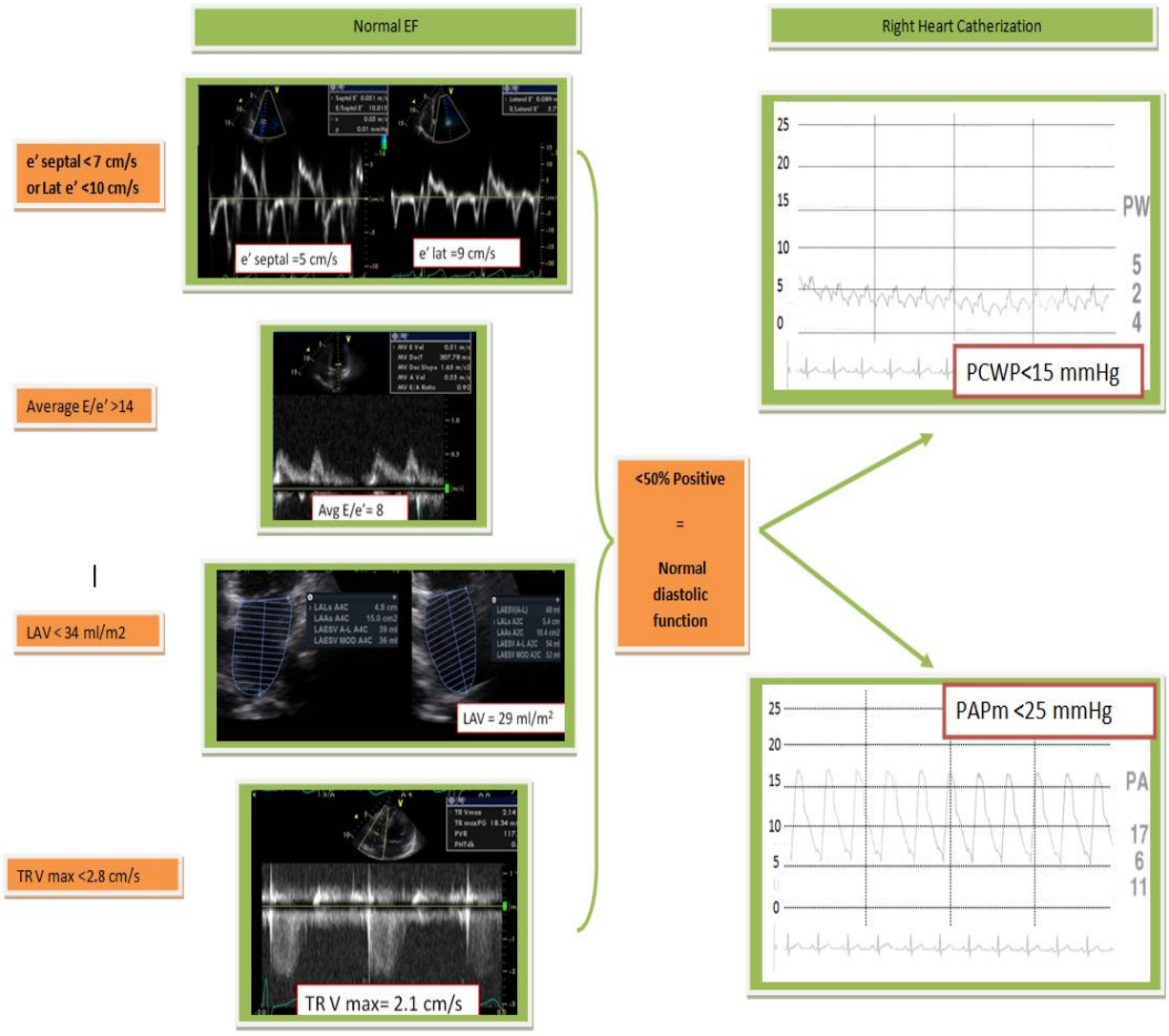

8.1 patient correctly identified as having normal PCWP through echocardiography. Tissue Doppler velocities reduced, although, E/e', LAV indexed and TR v max are all within normal ranges. Diagnosis confirmed with invasive pressure assessment.

Figure 8-2. Incorrect identification of normal PASP

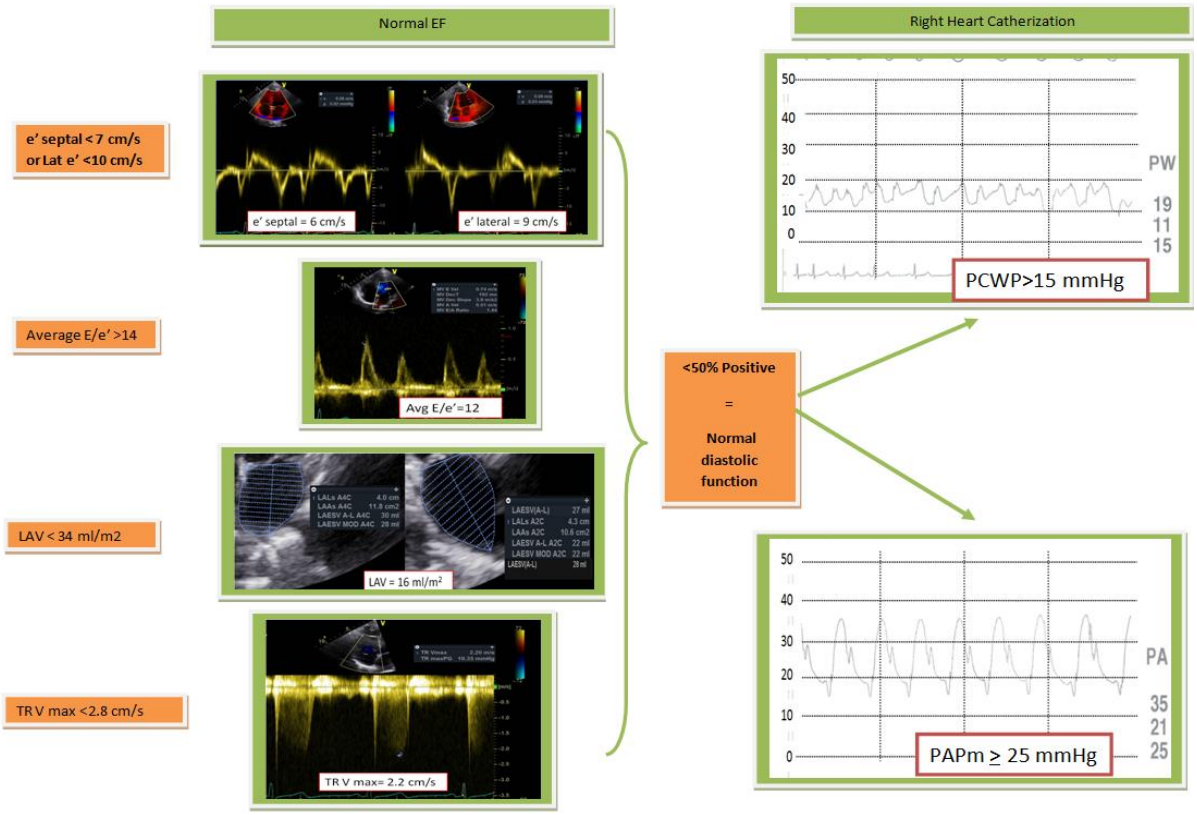

Incorrect echo identification of normal PCWP and normal PASP. Reduced tissue Doppler velocities in the presence of normal E/e', normal LAV indexed and TR V max. The patient shows both raised wedge pressure, and mean pulmonary artery pressure on invasive examination.

8.4.4 Statistical analysis.

Statistical analysis was performed using standard software (SPSS 20.0, IBM, Chicago, IL) Data are presented as mean and standard deviations. Data that were not normally distributed are presented as medians and inter-quartile range. In patients with missing BSA, the group mean was substituted (1.73 in women and 1.96 in men). Student T-test was used to compare parametric data, and the Mann-Whitney U-test used to compare significance, with statistical significance set to $p<0.05$. Bivariate logistic regression was used to compare groups. Receiver operator characteristic (ROC), area under the curve (AUC) was performed with MedCalc Statistical software version 16.8.4 (MedCalc Software bvba, Ostend, Belgium). Youden Index was calculated as sensitivity + specificity.

Figure 8-3. Incorrect identification of normal PCWP, with elevated pulmonary pressures identified.

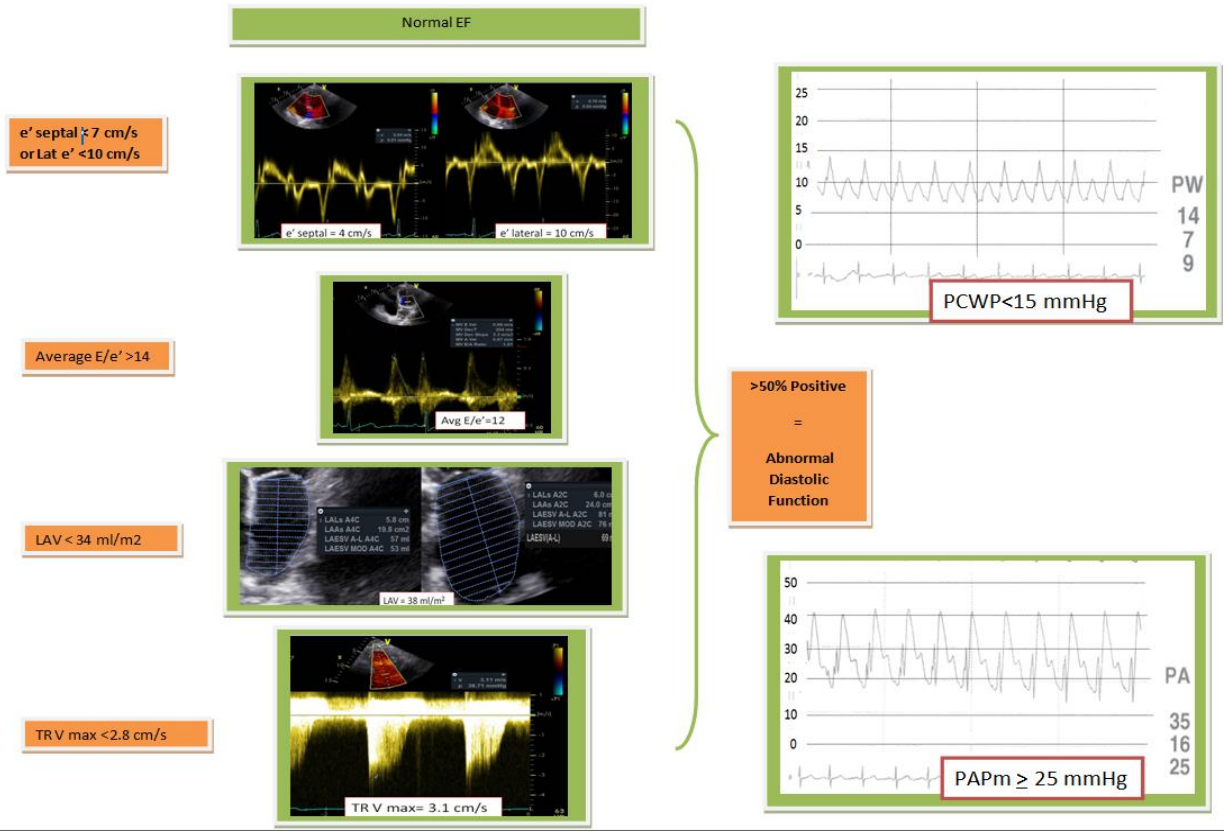

Incorrect identification of normal PCWP, with elevated PASP, correctly identified. Septal tissue Doppler velocities are reduced, increased LAV indexed, with raised TR v max. After the invasive assessment, the subject was found to have normal wedge pressure, with increased mean pulmonary artery pressure

8.5 Results

8.5.1 Patient characteristics.

Of 190 consecutive patients with invasive PCWP and echocardiography (Figure 8.1), 157 had EF >50% (60 with PCWP>15 mmHg, and 97 with PCWP<15 mmHg). AF was present in 3 patients in each PCWP group, and TR v max was not measureable in 8. The 33 patients with EF<50% (Appendix Table 8.4) had significantly greater PCWP ($p<0.001$), LAV ($p=0.001$), E/e' septal ($p=0.03$), and e' septal ($p=0.001$).

Table 8-1. Baseline measurements. Groups are compared with PCWP <15 and ≥15mmHg

	All patients (n=190) Mean (SD)	Median (IQR)	PCWP<15 mmHg(n=97)	PCWP≥15 mmHg (n=60)	P value
Age	62(13.8)	63(55-63)	59(16.0)	65 (11.8)	0.01
Sex (female)	72%(172)		80 (78)	41 (68)	0.07
SBP	126±27	125 (112-134)	123(18)	126 (33)	0.58
DBP	72±10	70 (65-80)	72 (9)	68 (19)	0.38
HR	76±14	75 (66-85)	77 (15)	73 (13)	0.07
BSA	1.8±0.21	1.8 (1.8-1.8)	1.8 (0.15)	1.8 (0.16)	0.03
Invasive					
• PAPs (mmHg)	49±21.5	41 (35-60)	46.6(20.3)	50(20.6)	0.38
• PAPm (mmHg)	33.0±9.5	31 (26-45)	34.1(14.6)	38.0(12.6)	0.08
• PCWP (mmHg)	12.8±4.0	14 (10-16)	10.0(3.0)	18.4(4.0)	<0.001
• Cardiac output	4.8±1.2	4.7 (3.9-6.1)	5.2 (1.5)	5.4 (2.3)	0.59
Echocardiography					
• LV Mass (gm)	160±64.1	148(112-188)	138.6(50.8)	164.3(62.6)	0.009
• LV Mass (gm/m^2)	88.4±34.5	83(64-104)	77.4(26.1)	89.5(34.1)	0.02
• LVEDV (ml)	89.8±45.5	81 (63-97)	75.4(26.2)	90.6(35.1)	0.005
• LVESV (ml)	40.7±34.7	32 (23-43)	29.3(12.0)	34.2(15.6)	0.04
• SV (ml)	50±19.1	46 (38-56)	46(18.0)	52(20)	0.02
• EF (%)	58±12.5	61 (52-66)	62(7.1)	63(7.8)	0.60
• LVGLS (%)	17±4.5	18 (15-20)	19(3.4)	18(3.9)	0.27
Diastology					
• e' septal (cm/s)	5.8±2.2	5 (4-7)	6.1(2.5)	5.8(2.5)	0.44
• e' lat (cm/s)	8.8±3.0	8(6-10)	9.0(3.3)	8.4(2.5)	0.24
• e' average (cm/s)	7.4±2.4	7 (6-9)	8.0(3.3)	7.4(2.9)	0.30
• E/e' septal	13.0±7.8	12 (9-18)	11.1(3.8)	18.1(12.5)	<0.001
• E/e' lateral	8.5±5.4	8(6-12)	8.0(4.2)	11.3(7.5)	0.006
• E/e' avg	10.8±6.4	10(8-14)	9.7(4.2)	15.0(10.9)	0.001
• LAV ml/m2	33.6±15.7	31 (23-49)	30.3(14.9)	42.3(22.3)	<0.001
• Mitral valve E wave	0.67±0.23	0.70 (0.52-0.89)	0.68(0.25)	0.85(0.31)	0.001
• Mitral valve A wave	0.68±0.22	0.71(0.54-0.84)	0.71(0.21)	0.71(0.25)	0.87
• EA ratio	1.1±0.68	0.87 (0.72-1.2)	1.0(0.51)	1.3(0.91)	0.03
• DT cm/s	234±55.1	223 (185-272)	234(55.2)	232(55.9)	0.81
Right side					
• RVEDA (cm^2)	22.5±8.9	21 (14-27)	21.1(7.9)	21.9(8.2)	0.56
• FAC (%)	29.5±13.6	32 (23-40)	31.2(13.4)	33.9(11.6)	0.23
• RV Free wall (%)	16.6±6.1	16(13-21)	17.4(5.9)	17.6(5.5)	0.84
• PASP echo (mmHg)	57.6±25.4	47 (32-66)	50.9(24.6)	52.2(23.6)	0.77
• RAA (cm^2)	20.4±8.0	19 (14-26)	19.2(7.7)	22.1(8.3)	0.04
• PVR (w.u)	3.7±1.8	3.2 (2.2-4.5)	3.8(2.0)	3.2(1.2)	0.15
• Tr Vmax (cm/s)	3.5±0.84	3.1 (2.8-3.9)	3.3(0.80)	3.3(0.79)	0.72

SBP- systolic blood pressure, DBP- Diastolic Blood pressure, Pulmonary artery pressure systolic, PAPm- Pulmonary artery pressure mean, CO- Cardiac Output, PCWP- pulmonary capillary wedge pressure, LVEDV- left ventricular end diastolic volume, LVESV- Left ventricular end-systolic volume, EF – Ejection fraction , LVGLS-left ventricular global longitudinal strain, DT-deceleration time, RVEDA- Right ventricular end-diastolic area, FAC- Fractional area change, RAA- right atrial area, PVR-Pulmonary vascular resistance.

8.5.2 Association of raised PCWP

Patients with preserved EF (n=157) were divided based on invasive PCWP <15 or ≥15 mmHg (Table 8.1). These groups showed differences in E/e' avg (p=0.001), LAV (p<0.001) and LV mass (p=0.02). However, there were no differences between groups in e' (p=0.30), or TR velocity (p=0.72). Table 8.2 shows the strength of the association between echo markers and raised PCWP in a bivariate logistic regression. The strongest associations were raised E/e' and LAV.

Most patients (87%) were categorized as E/A≤0.8 and E>50 cm/s or E/A from 0.8-2.0, and 73 had normal LAP. We were unable to categorize 27% of patients. Table 8.3 summarizes patients with normal EF, according to whether PCWP was ≥15 mmHg or not. Significantly more patients with elevated PCWP had dilated LAV (32% vs 53%, p=0.01) and increased E/e' (11% vs 38%, p<0.001). However, there were no significant differences in septal e' (66% vs 73%, p=0.86), TR velocity (75% vs 77%, p=0.76), LV mass (16% vs 25%, p=0.13) or LV GLS (59% vs 66%, p=0.40).

Table 8-2. Echocardiographic parameters associated with elevated PCWP**.** In this logistic regression, the only significant associations were with E/e' and LA volume

	OR (95%CI)	**p**
e' lateral >10 cm/s	1.0 (0.47;2.1)	1.0
e' septal >7 cm/s	0.73(0.32;1.6)	0.44
Any e' normal	0.85(0.39;1.9)	0.69
E/e' average <14	0.15(0.06;0.38)	<0.001
TR vmax (≤2.8 cm/s)	0.76(0.42;1.9)	0.76
LAV ml/m^2 (≤ 34 ml/m^2)	0.43(0.22;0.84)	0.01
LV mass index gm/m^2 (<115 or 96 gm/m^2 by gender)	0.54(0.24;1.2)	0.14
LV GLS (%) (>19.7%)	0.74(0.37;1.5)	0.40

TR Vmax- Tricuspid jet maximum regurgitant velocity, LAV ml/m^2- left atrial volume ml/m^2, LV mass index – Left ventricular mass index gm/m^2, LV GLS – left ventricular global longitudinal strain

8.5.3 Estimation of raised PCWP.

The discriminant ability of diastolic parameters for PCWP ≥15 mmHg was assessed from ROC curves (Appendix Figure 8.5). Only LAV and average E/e' showed significant but modest predictive ability (AUC 0.61, p=0.03 and AUC 0.64, p=0.007

respectively). In patients with EF >50%, an E/e' >14 had had the highest accuracy (94/134, 70%) and the highest specificity (71/80, 89%), but with a lower sensitivity (23/54, 43%). In contrast, a peak TR velocity >2.8 m/s has a lower accuracy (70/154, 45%) and specificity (24/94, 26%) but higher sensitivity (46/60, 77%). The accuracy of an indexed LAV >34 ml/m^2 was intermediate (93/150, 62%), with a low sensitivity (31/59, 53%) but better specificity (71/80, 89%).

Table 8-3. Echocardiographic features associated with each PCWP group

	Positive for each parameter	**PCWP <15 mmHg**	**PCWP ≥15 mmHg**	**p**
LAV ml/m2	60 (38%)	29 (32%)	31 (53%)	0.01
e' lat <10 cm/s	80 (64%)	48 (64%)	32 (64%)	1.0
e' septal < 7 cm/s	80 (69%)	45 (66%)	35 (73%)	0.44
Any e' abnormal	100 (74%)	59 (73%)	41 (76%)	0.49
E/e' avg>14	32 (24%)	9 (11%)	23 (38%)	<0.001
TR vmax >2.8 cm/s	116 (75%)	70 (75%)	46 (77%)	0.76
Other echo markers				
LV Mass (>115 or 96 gm/m^2 by gender)	19 (19%)	15 (16%)	15 (25%)	0.13
LV GLS (<19.7%)	92 (62%)	55 (59%)	37 (66%)	0.40

No patients categorised into group 3. LAV ml/m^2 – left atrial volume indexed, TR Vmax- Tricuspid valve maximum regurgitant velocity, LV Mass gm/m^2- Left ventricular mass index, LV GLS – left ventricular global longitudinal strain.

The diastolic guidelines correctly identified 106 patients with normal wedge pressure (65% of all 162 patients, regardless of EF), 75 of whom (71%) had PCWP <15 mmHg. They identified 17 patients with increased LAP, of whom 11 (65%) had PCWP ≥15 mmHg. The remaining 39 patients (n=24%) could not be determined using the guidelines (either because of difficulties with attributing an E/A ratio due to AF or E/A fusion), and 20 of these had PCWP ≥15 mmHg.

Pre versus postcapillary pulmonary arterial hypertension. Patients (irrespective of EF) were divided into pre-capillary (PAPm ≥25 mmHg with PCWP <15 mmHg, n=89) versus post-capillary PH (PAPm ≥25 mmHg with PCWP ≥15 mmHg, n=79)) (Appendix Table 8.5). Post-capillary PH patients were significantly older (p=0.02), otherwise clinical variables were similar. LV mass (p=0.001), EDV (p<0.001) and E/e' (p<0.001) were significantly greater in the post-capillary group, and EF (p=0.01) and LV-GLS were lower (p=0.001), but there no differences in tissue Doppler velocities. The post-capillary group showed a significantly larger RA area (p=0.008). ePLAR was significantly different between groups (Appendix Figure 8.6) (p<0.001), and showed modest discrimination (AUC=0.73, p<0.001) (Appendix Figure 8.7); a cut-off of 0.21 m/s (derived from the Youden index) derived showed good sensitivity (92%) and modest specificity (57%). Alternative markers of post-capillary PH were increased LV mass (AUC=0.68, p<0.001), LV EDV (AUC=0.71, p=0.0001), impaired LVGLS (AUC=0.64, p=0.007). Comparison of the AUC showed ePLAR had similar discrimination to LVGLS (p=0.15), LV mass index (p=0.37) and EDV (p=0.75). There were no significant differences between LVGLS and EDV (p=0.23), or LV mass BSA (p=0.50).

Discussion

In this population of dyspneic patients undergoing RHC with preserved EF, non-invasive markers of LVFP (E/e' and LAV) were moderately useful, but other markers proposed in the diastolic function recommendations were non-contributory. Among those with PAH, the recognition of pulmonary venous hypertension was challenging, with LV parameters more effective than estimated LVFP.

Echocardiographic markers of LV filling pressure. The results of this study emphasise the ongoing difficulties associated with the assessment of diastolic function by echocardiography. LV filling is characterised by untwisting and suction, LV relaxation and LV compliance, but the assessment of all of these components are influenced by left atrial pressure [252]. Previous work has shown that an array of parameters have associations with invasive PCWP (isovolumetric relaxation time, atrial filling fraction, deceleration time, and E/A ratio), with the combinations being stronger than individual markers [253]. When assessing reader concordance in the grading of DD, perceived weights given to different markers by reading cardiologists is an important driver of variation. In particular, pseudonormal and restrictive patterns display lower levels of agreement among readers [254]. In response to the complexity of categorising patients, especially in patients with discordant criteria, recommendations have been updated [243]. Previous recommendations suggested e' as a starting point for diastolic assessment, as normal values are unlikely in patients with DD [255]. However, we found no significant difference in e' when comparing the elevated versus normal PCWP groups. Low E/e' values (<8) or high values (>15) seem to be adequate in correctly identifying LVFP, but a significant proportion of patients fall between these categories, requiring additional indices [250].

The accuracy of E/e' is lower in those with normal EF [256], unfortunately, this group is one where the diagnostic challenge of defining LVFP is most important [257-259]. Our results are similar to those derived from meta-analysis [250] and research cohorts [260] that estimate between 24-44% of patients with elevated LVFP had increased E/e'. We found 32% of patients with raised PCWP had increased E/e', while 11% of patients with normal PCWP showed elevated E/e'. A caveat of this is the quality control

required when performing Doppler echocardiography, specifically the acquisition of traces at gentle end expiration (as is performed during RHC readings).

Left atrial measurements are a good indicator of chronically elevated left atrial pressures. However, a dilated left atrium may be a legacy of previously elevated LVFP, or changes may be accelerated in disease conditions such as diabetes mellitus [261] and obesity [262]. The finding that markers of LVFP (E/e' and LAV) displayed the strongest predictive ability in determining raised PCWP is contrary to the equal weightings of LAV, E/e' and TR maximum velocity proposed in recent recommendations. However, E/e' and LAV have only modest predictive ability for determining elevated PCWP. The new process of evaluation of diastolic parameters does not appear to have improved the identification of raised PCWP – at least in patients captures in our practice of RHC - with a significant proportion of patients still categorised as "indeterminate".

The distinction of pre- and post-capillary pulmonary hypertension. There is no evidence to support the use of pulmonary vasodilator therapy in HFpEF [10,263], so the distinction between pre and post-capillary PH is vital for therapeutic decision-making. Invasively, this is performed through assessing PCWP, combined with the mean pulmonary arterial pressure and cardiac output [10]. PH occurs in DD due to passive transmission of LAP. ePLAR has been proposed as a new method in which echocardiography can aid in the non-invasive distinction between pre and postcapillary PH [251]. Although there were significant differences between pre- versus post-capillary PH in our group, the AUC demonstrated only modest discrimination, with significant overlap between cases.

Limitations. While concerns about the new guidelines may be raised about their application in all echocardiograms, this study pertains specifically to individuals undergoing RHC. This test is not performed routinely at our institutions in most patients with dyspnoea. Our centres are referral centres for PAH, and RHC is generally performed in those with suspected PH. Nonetheless, the non-invasive recognition of pulmonary venous hypertension is an important topic in this group.

Second, velocity vector imaging was used to measure strain on archived images at a frame-rate of 30 frames/second. While this approach has been validated, the results for strain may have been different with the use of different software on raw data.

Conclusion. Individual diastolic markers do not have the same predictive ability in determining raised PCWP. LV GLS did not appear to add significantly to discrimination of raised PWCP. Markers of elevated left atrial pressure have modest discriminatory ability for predicting raised PCWP.

8.6 Conclusion

A combined echocardiographic approach offers significant improvement in diagnostic accuracy over single echocardiographic markers. Interestingly, studies have found that RV dilation and dysfunction can occur early in an "at risk cohort", even in the presence of normal pulmonary pressures [264].

8.7 Postscript

Patients within this cohort are considered to have the progressive disease already; once filling pressure has increased, substantial myocardial dysfunction is already present. However, the detection of raised pulmonary pressure by echocardiography is constrained by errors and inconsistencies with TR assessment [31], and the assessment of RAP is a potential source of inaccuracy. RAP is a reliable marker of outcome, and is a highly significant risk stratification marker [42]. There may be a role for speckle tracking to assess changes in PAP throughout the cardiac cycle. Functional assessment of the left atrium with speckle tracking imaging has shown progressive dysfunction as diastolic function progresses [265], highlighting its ability to track the progression of the disease. Potentially, underestimation of patients who present with falsely normal pressure could be identified with speckle tracking. The next chapter addresses whether RA strain can help with one of the other conundrums of PH assessment measurement of RA pressure.

8.8 **Appendix**

Table 8-4 Appendix. Baseline measurements in all 190 patients, divided by groups with EF<50% and ≥50%.

	All patients (n=190) Mean (SD)	Median (IQR)	EF<50% (n=33) Mean (SD)	EF ≥50% (n=157) Mean (SD)	P value
Age	62(13.8)	63(55-63)	65(14.4)	61(14.8)	0.18
Sex (female)	72%(172)		47%(16)	76%(142)	<0.001
SBP	126±27	125 (112-134)	133(14)	124(24)	0.24
DBP	72±10	70 (65-80)	76(11.5)	70(13)	0.19
HR	76±14	75 (66-85)	78(17)	75(21)	0.54
BSA	1.8±0.21	1.8 (1.8-1.8)	1.8(0.10)	1.8(0.15)	0.32
Invasive					
• PAPs (mmHg)	49±21.5	41 (35-60)	39(19)	40 (20)	0.98
• PAPm (mmHg)	33.0±9.5	31 (26-45)	27 (9.0)	30 (18.3)	0.35
• PCWP (mmHg)	12.8±4.0	14 (10-16)	16 (8.0)	13.0 (6.0)	<0.001
• Cardiac output	4.8±1.2	4.7 (3.9-6.1)	4.1 (1.4)	5.3 (2.2)	<0.001
Echocardiography					
• LV Mass (gm)	160±64.1	148 (112-188)	217 (72)	148 (56.7)	<0.001
• LV Mass (gm/m^2)	88.4±34.5	83(64-104)	122 (38.8)	82(30)	<0.001
• LVEDV (ml)	89.8±45.5	81 (63-97)	135 (74)	81 (30.7)	<0.001
• LVESV (ml)	40.7±34.7	32 (23-43)	89.5 (59.5)	31 (13.6)	<0.001
• EF (%)	58±12.5	61 (52-66)	36.8 (11.6)	62 (7.3)	<0.001
• LVGLS (%)	17.3±4.5	18 (15-20)	12.2 (5.3)	18.3 (3.6)	<0.001
Diastology					
• e' septal (cm/s)	5.8±2.2	5 (4-7)	4.4 (1.9)	6.0 (2.5)	0.001
• e' lat (cm/s)	8.8±3.0	8(6-10)	8.1 (3.4)	8.8 (3.0)	0.36
• e' average (cm/s)	7.4±2.4	7 (6-9)	7.4 (4.2)	7.8(3.2)	0.56
• E/e' septal	13.0±7.8	12 (9-18)	19.9(11.5)	14.0 (9.2)	0.03
• E/e' lateral	8.5±5.4	8(6-12)	10.9 (5.6)	9.4 (5.9)	0.22
• E/e' avg	10.8±6.4	10(8-14)	14.5 (7.9)	11.8 (8.0)	0.10
• LAV ml/m2	33.6±15.7	31 (23-49)	63.4 (44.4)	35 (19.1)	0.001
• Mitral valve E wave	0.67±0.23	0.70 (0.52-0.89)	0.74(0.24)	0.75(0.29)	0.91
• Mitral valve A wave	0.68±0.22	0.71(0.54-0.84)	0.63(0.25)	0.71(0.23)	0.17
• EA ratio	1.1±0.68	0.87 (0.72-1.2)	1.2 (0.21)	1.1 (0.70)	0.47
• DT cm/s	234±55.1	223 (185-272)	212 (69)	233 (55)	0.13
Right side					
• RVEDA (cm^2)	22.5±8.9	21 (14-27)	22.8(9.7)	21.4 (8.0)	0.40
• FAC (%)	29.5±13.6	32 (23-40)	30.2 (11.2)	32.2 (12.7)	0.43
• RV Free wall (%)	16.6±6.1	16(13-21)	15.7(7.0)	17.5 (5.7)	0.13
• PASP echo (mmHg)	57.6±25.4	47 (32-66)	48.3 (17.1)	51.4 (24.1)	0.51
• RAA (cm^2)	20.4±8.0	19 (14-26)	26.1 (12.4)	20.3 (8.0)	0.02
• PVR (w.u)	3.7±1.8	3.2 (2.2-4.5)	3.6 (2.1)	3.6 (1.8)	0.94
• Tr Vmax (cm/s)	3.5±0.84	3.1 (2.8-3.9)	3.1 (0.64)	3.3 (0.80)	0.21

SBP- systolic blood pressure, DBP- Diastolic Blood pressure, Pulmonary artery pressure systolic, PAPm- Pulmonary artery pressure mean, CO- Cardiac Output, PCWP- pulmonary capillary wedge pressure, LVEDV- left ventricular end diastolic volume, LVESV- Left ventricular end-systolic volume, EF – Ejection fraction , LVGLS-left ventricular global longitudinal

strain, DT- deceleration time, RVEDA- Right ventricular end-diastolic area, FAC- Fractional area change, RAA- right atrial area, PVR-Pulmonary vascular resistance

Table 8-5 Appendix. Pre versus postcapillary pulmonary hypertension

	Pre-capillary Mean (SD) (n=89)	Post-capillary Mean (SD) (n=79)	P
Age (years)	60(15.3)	65(11.7)	0.02
HR (bpm)	78(15.3)	74(12.7)	0.08
SBP (mmHg)	123(18.2)	127(30)	0.66
DBP (mmHg)	72(9.0)	70(18.7)	0.53
PAPs (mmHg)	53(18.5)	51.5(19.9)	0.69
PAPm (mmHg)	38.2(12.6)	37.9(11.7)	0.90
PCWP (mmHg)	10.5(3.0)	18.9(4.5)	<0.001
• LV Mass (gm)	138(52.9)	178.9(69.6)	<0.001
• LVMI	77.4(27.7)	97.8(38.2)	<0.001
• LVEDV (ml)	73.6(25.0)	103.2(55.3)	<0.001
• LVESV (ml)	29.8(13.1)	51.5(47.2)	<0.001
• EF (%)	60(8.9)	55(15.8)	0.01
• LVGLS (%)	18.1(3.4)	15.6(5.4)	0.001
• e' med (cm/s)	5.8(2.5)	5.2(2.4)	0.17
• e' lat (cm/s)	8.7(3.1)	8.0(2.6)	0.18
• e' average (cm/s)	7.9(3.2)	7.4(3.7)	0.45
• E/e' medial	11.3(4.0)	19.6(12.8)	<0.001
• E/e' lateral	7.7(3.2)	11.6(7.1)	<0.001
• E/e' avg	9.5(3.6)	15.7(10.5)	<0.001
• LA 4 ch (ml)	52.9(21.4)	92.2(66.2)	<0.001
• LA 2 ch (ml)	52.1(21.4)	93.0(64.2)	<0.001
• LAV avg (ml)	52.3(24.5)	91.2(62.2)	<0.001
• LAV ml/m2	28.6(13.4)	50.1(34.2)	<0.001
• EA ratio	0.89(0.38)	1.3(0.87)	0.002
• DT cm/s	237(56.7)	227(63.3)	0.28
• RVEDA (cm^2)	22.4(8.8)	22.9(9.1)	0.68
• FAC (%)	29.7(13.3)	30.9(11.8)	0.56
• RV Free wall (%)	16.8(6.2)	16.2(5.8)	0.53
• PASP echo (mmHg)	55.5(25.0)	53.6(22.4)	0.62
• RAA (cm^2)	20.1(8.3)	24.0(10.0)	0.008
• PVR (w.u)	3.8(2.0)	3.4(0.76)	0.29
• TR Vmax (cm/s)	3.4(0.8)	3.4(0.76)	0.56
• ePLAR	0.35(0.17)	0.24(0.15)	<0.001

HR, heart rate; SBP, systolic blood pressure; DBP, diastolic blood pressure; PAPs, pulmonary artery pressure systolic; PAPm. Pulmonary artery pressure mean; PCWP, pulmonary capillary wedge pressure; LVMI, left ventricular mass index; LVEDV, left ventricular end diastolic volume; LVESV, left ventricular end systolic volume; EF, ejection fraction; LVGLS, left ventricular global longitudinal strain; LA, left atrial; LAV, left atrial volume; DT, deceleration time. RVEDA, right ventricular end diastolic area; FAC, fractional area change; PASP, pulmonary artery systolic pressure; RAA, right atrial area; PVR, pulmonary vascular resistance; TR V max, tricuspid regurgitation max velocity; ePLAR, echocardiographic pulmonary to left atrial ratio.

Figure 8-4 Appendix. Study flow chart

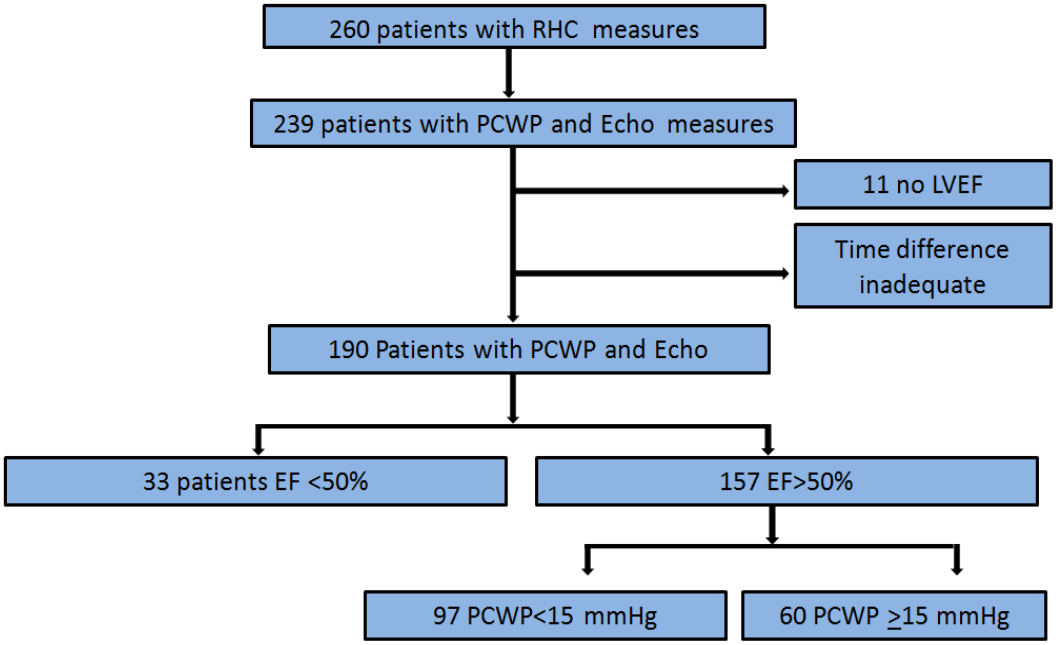

Figure 8-5 Appendix. Discrimination of raised PCWP (≥ or < 15 mmHg) by echocardiographic markers

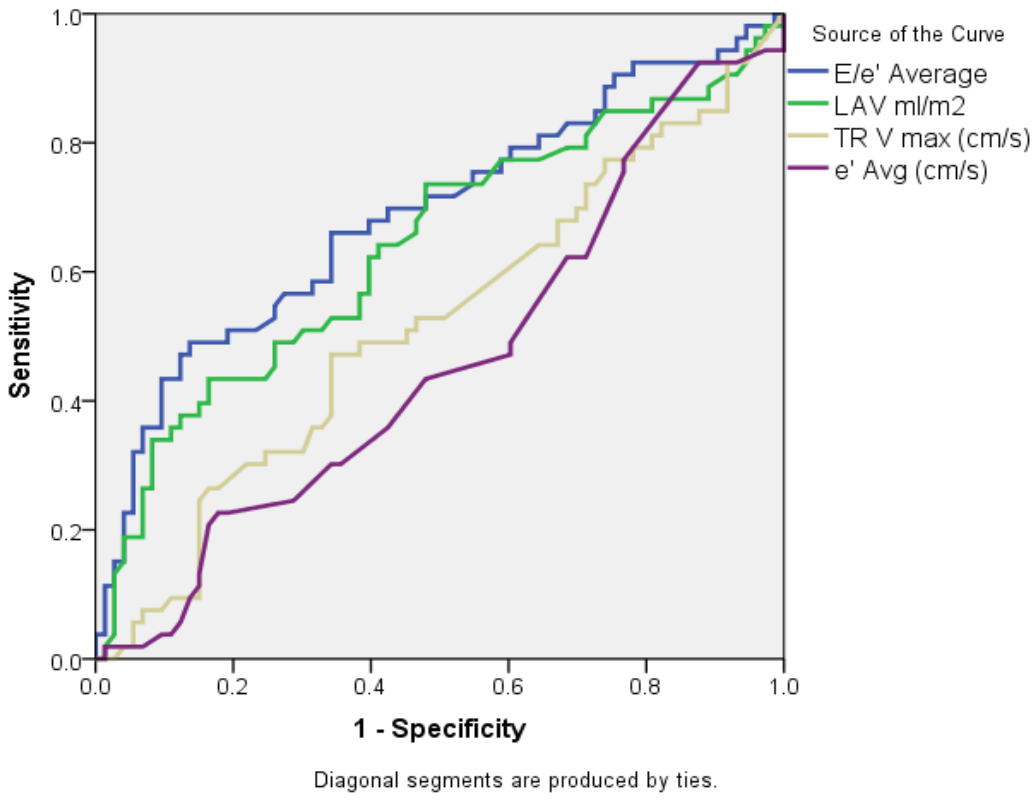

Figure 8-6. Boxplot with median and 95% ranges for normal, precapillary and postcapillary PH ePLAR ranges

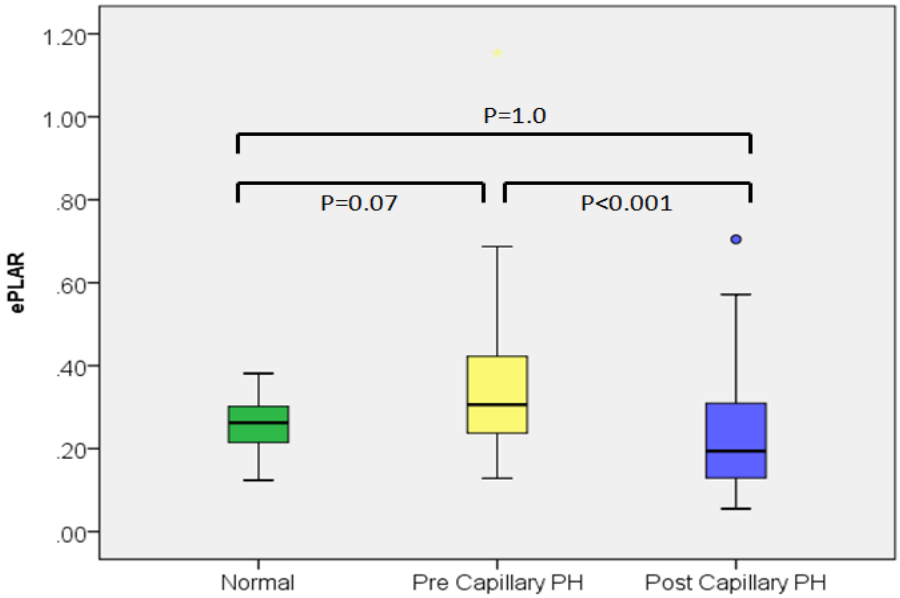

Figure 8-7. Receiver-operating characteristic curves area under the curve using ePLAR to differentiate pre versus postcapillary PH

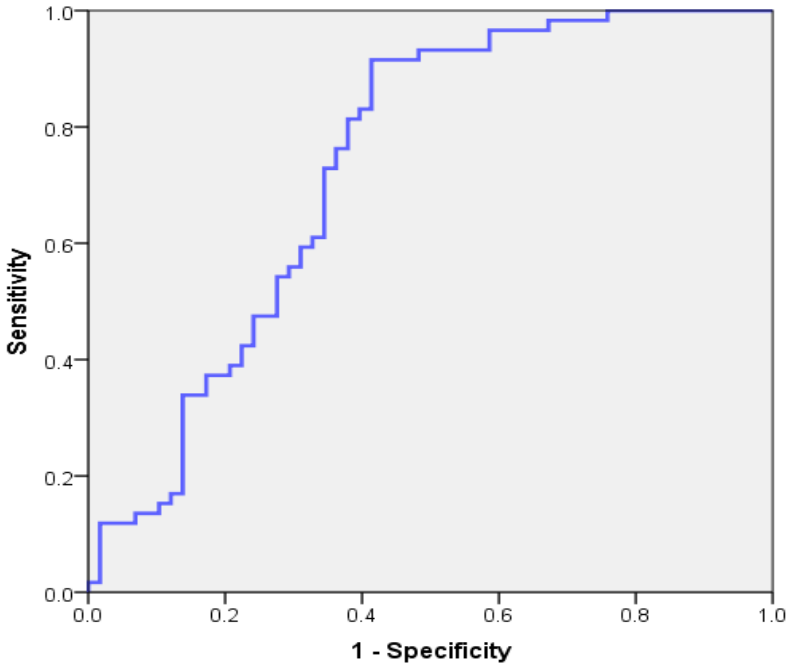

Chapter 9

Right Atrial Pressure Estimation with Echocardiography

Under review as "Right Atrial Pressure Assessment by Echocardiography: Association with Right Atrial Strain"

Echo Research and Practice

Leah M Wright; Nathan Dwyer; Sudhir Wahi; Thomas H. Marwick.

9 Right atrial pressure estimation with echocardiography

9.1 Preface; Right atrial pressure estimation with echocardiography

Previously thought of as a passive structure, the function of the RA has a direct impact on ventricular filling[164]. RAP pressure-volume loop analysis involving a micro-manometer tipped catheter[266] gives a precise measure of changes in volumes and size throughout cardiac contraction (in animals). Changes are intrinsically linked pressures at that specific time point.

RAP assessment with echocardiography plays a fundamental role in clinical risk stratification. A variety of methods can be used to estimate RAP assessment, these range from providing a discrete value from regression equations to the estimation of categorical ranges of values. Assessment protocols are published in standard echocardiography guidelines [101], but the accuracy of these measures is limited. The diagnostic accuracy of echocardiography has been reviewed by a number of authors[267], with sensitivity (the ability of the test to correctly identify disease) and specificity (the ability of the test to correctly identify those without the disease) acceptable for predicting > or < 10 mmHg. Calculation with this method still leaves a large percentage of patients in whom increased RAP may be over or underdiagnosed. Review of RAP techniques in a large validation cohort was only accurate in 34% of cases[268]. IVC diameter varies significantly between RAP invasive ranges, with inadequate visualisation in 19% of patients [268]. A restrictive filling profile, TV E/e' and systolic filling fraction are secondary markers but have not shown to improve RAP estimation accuracy [268], with under-estimation the predominant error. Predictors of this inaccuracy (the difference between echocardiography and invasive RAP) are not defined. Weak, but significant associations include RA EF. RA size, RV function, or BSA did not show a significant association with bias. Novel markers of RA assessment have shown 3DE to be valuable in defining elevated RAP [269], but are not endorsed for

use in recent guidelines. 2D speckle tracking does not require any additional images to be acquired and gives an in-depth view of RA function.

Whether markers of RA function are independent of RV systolic function has been questioned, as close correlations often exist between RA and RV longitudinal strain [270]. The afterload dependence of strain could be used to advantage in the RA, as it influences speckle tracking. Measures of RA elastance have been shown to improve in a chronic pressure overload state, with increases in reservoir function, and declines in conduit function as shown [271]. The incremental value of RA function above standard clinical assessment is not established.

9.2 Abstract

Background. Echocardiographic assessment of RAP from inferior vena cava (RAP_{IVC}) dimension may underestimate catheter-derived pressure (RAP_C). As RA deformation, measured by speckle tracking, is preload-dependent, we hypothesised that RA strain might improve estimation of RAP_C.

Methods. Right atrial strain components (RA reservoir function (ƐR), peak RA ƐCT and RA ƐCD were measured in 125 of 175 patients who had echocardiography and invasive measures of RAP (median difference 1 day). To determine the ability of RA strain measures to differentiate incorrect RAP_{IVC} assessment, categories with RAP_{IVC} values <3, 8 and >15 mmHg were compared with RAP_C groups <3, 4-7, 8-10, 11-14 and >15 mmHg.

Results. Non-invasively determined RAP was significantly lower (p=0.001) than invasively determined RAP_C, with a weak correlation (r=0.35, p<0.001). RA strain components were associated with RA size, RV function and IVC size. In those with invasive RAP >15 mmHg, over half of patients were categorised into the echocardiographic prediction of RAP <10 mmHg. There were no significant differences in RA characteristics that differentiated patients in whom echocardiographic estimation of RAP was inaccurate.

Conclusion. Right atrial strain was significantly different between those with normal versus raised pressure, but it did not identify those with an incorrect echocardiographic assessment of RAP.

9.3 Background

Echocardiographic quantification of right atrial pressure (RAP) is primarily performed through interrogation of inferior vena cava (IVC) size and distensibility [272-274]. The IVC is a compliant vessel and is highly responsive to changes in central venous pressure and volume, as well as changes in intra-thoracic pressure. Consequently, guidelines are based on 3 values (Figure 1); normal IVC size of <2.1 cm defines a RAP of <3 mmHg, RAP >2.1 cm with ≥50% collapsibility suggests RAP of 8 mmHg; patients with IVC >2.1 cm with <50% collapsibility have RAP of 15 mmHg [101]. Although measurement of RA pressure has been removed from recent PAH guidelines[15] due to the level of inaccuracy of echocardiographic assessment, RAP is still a strong prognostic marker

Velocity vector imaging is based upon tracking of individual speckles from frame to frame, and the use of this technique for assessment of myocardial deformation has been validated in numerous studies. While some methods of myocardial strain measurement are vendor-specific, this approach has been used for the analysis of DICOM data from differing ultrasound machines and is, therefore, vendor independent. Velocity vector imaging has been used to assess RA function, with normal ranges published in small cohorts [275]. A number of previous studies have shown that RA strain is reduced in PAH[276], adding to the growing number of markers associated with increased pulmonary artery pressures. RA strain can be broken down into 3 phases (Figure 2); RA ℇR refers to the deformation which occurs from filling of the RA from the venous system. RA ℇCT, measured as the peak deformation post RA contraction. RA ℇCD is the difference between the RA ℇR and RA ℇCT. Timing relative to the QRS is used to conduct measurements, using either P-P or R-R intervals. As RA strain is preload-dependent, increased deformation of the RA during the

reservoir phase could be indicative of increased venous pressure. The aim was to determine whether measures of right atrial strain would aid in the identification of incorrect RAP assessment with echocardiography (RAP_{IVC}). We hypothesised that RA strain would increase before IVC size, and therefore identify those with potential underestimation of RAP.

9.4 Methods.

9.4.1 Patient selection.

Between July 2003 to April 2015, 175 consecutive patients underwent RHC and echocardiography (median difference -1, IQR 26 days. Patients were prospectively recruited from the Royal Hobart Hospital Cardiac Catheterization laboratory (Hobart, Australia) and the Princess Alexandra Hospital Cardiac Catheterization laboratory (Brisbane, Australia). Of these, all right atrial strain components could be measured in 125 patients - 14 patients were excluded due to AF, 1 due to heart block, and the remainder due to insufficient echo images. Institutional Review Board approval was obtained from the Human Research Ethics committee (Tasmania) Network (approval number H0013333) and the Metro South Human Research Ethics Committee (HREC 16/QPAH/008).

9.4.2 Conventional echocardiography

Echocardiography was performed using standard commercial equipment (Vivid 7, Vivid i and Vivid e9, General Electric Medical Systems, Milwaukee, WI; ie33, Philips, Andover. MA). LV and RV measurements were performed according to ASE guidelines [101] by a single reader. LV EF was measured from the Simpson's biplane method from the apical 4- and 2-chamber views [101]. LV mass was calculated from the parasternal long axis linear method, using the ASE method [101]. RVEDA and RVESA were calculated from an apical RV focused view. FAC was calculated as the percentage change between the RVEDA and RVESA [101]. PASP was measured from

the peak tricuspid regurgitation velocity using the modified Bernoulli equation [29]. RAP was derived from the IVC dimension and distensibility from the subcostal view [44]. RAP was given a value of 3 mmHg if IVC size was <2.1cm, the intermediate value of 8 mmHg was given if IVC size was ≥21 cm, with >50% change during respiration. RAP ≥15 mmHg was given to patients with IVC>2.1 cm with a change in respiration <50%. (Figure 9.1). Peak velocities of the early (E) and late (A) diastolic filling were derived from the transmitral inflow pattern. Tissue Doppler imaging was used to determine the peak diastolic early velocity (e') of the lateral and septal mitral annulus from the apical 4-chamber view. E/e' was calculated from early mitral inflow divided by the average annular velocity to infer LV filling pressures [243]. LAV measurements were performed from the apical 2 and 4 chamber views, using the area-length method [101].

Figure 9-1. Echocardiographic assessment of right atrial pressure RAP

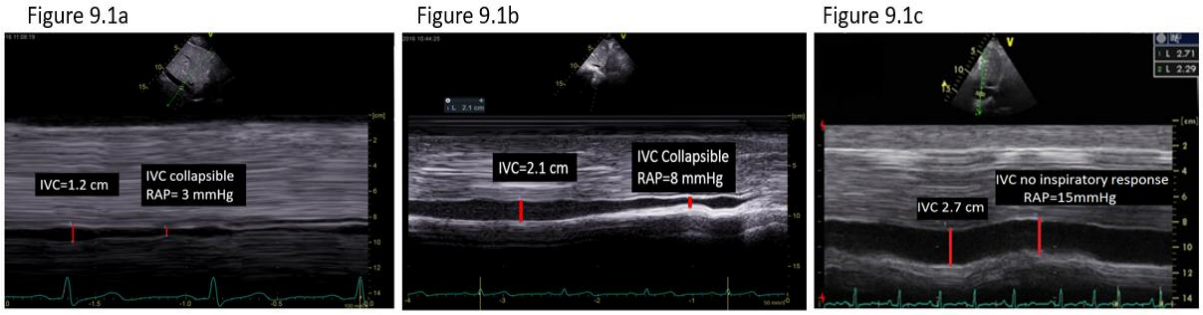

Figure 9.1a, Normal IVC (IVC<2.1cm) and collapsible, RAP= 3mmHg. Figure 9.1b, IVC dilated (>2.1 cm), with >50% collapsibility with inspiration, RAP=8 mmHg.Figure 9.1c, dilated IVC (>2.1cm), with no respiratory collapse, RAP=15 mmHg.

9.4.3 Strain.

Velocity vector imaging was performed with wall motion tracking software (Image-Arena, TomTec Gmbh, Unterschleissheim, Germany). The LV package was used to measure the RA as no specific atrial packages were available.

For each chamber analysed, manual adjustments were performed when necessary, and regions excluded if excessive noise or inadequate tracking was present. For RA strain, P-P gating was used from the RV apical-focused view. RA measurement points (Figure 9.2), peak RA ƐR, was measured as the mean peak of 6 segments of the RA, RA contraction (ƐCT) was measured as 6 segments at peak RA contraction. RA ƐCD was calculated as the difference between RA ƐR and RA ƐCD. LV global longitudinal strain (LVGLS) was performed from the apical 4, 3 and 2 chamber views. The right ventricular free wall (RVWFS) was performed from the RV apical focused view, as the average of the basal, mid and apical segments.

Figure 9-2. Echocardiographic measure of right atrial strain. Speckle tracking right atrial strain measurements

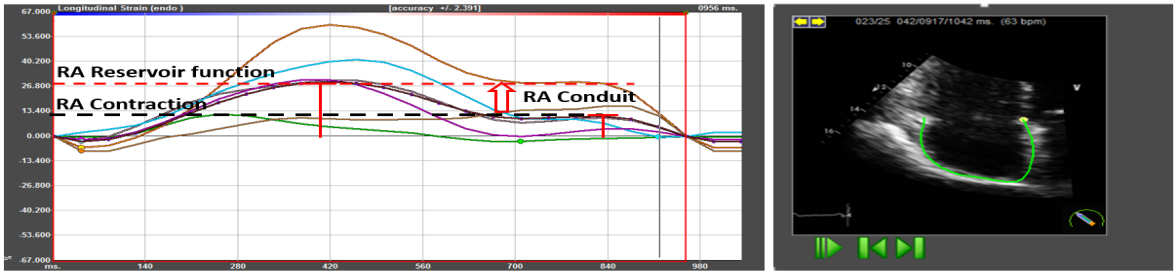

RAƐ Reservoir (RA Ɛ R) function was measured as the peak phase of RA deformation. RAƐ contraction (RAƐ CT) is the peak right atrial deformation point after atrial contraction (p wave). Right atrial conduit function (RAƐ CD) is the difference between RAƐ R and RAƐ CT

9.4.4 Right heart catheterisation.

RHC studies were undertaken after premedication and local anesthesia. A 4-lumen 110 cm 7-Fr Swan-Ganz catheter (Edwards Lifesciences, Irvine, CA) was floated to the right heart, and resting measurements of right atrial, right ventricular, pulmonary arterial and PCWP were made at end-expiration using a pressure transducer (21BB, ITL Healthcare, Chelsea Heights, Australia). The transducer was calibrated to atmospheric pressure at the level of the RA and re-checked at intervals to avoid zero

drift. CO was determined by thermodilution, using an average of four consecutive values that varied <10%. Electrocardiographic (ECG) leads were connected to both arms and the left leg, allowing three ECG channels for the timing of signals. All haemodynamic monitoring was recorded using a Horizon SE Haemodynamic System (Mennen Medical Ltd., Yavne, Israel) and subsequently analysed off-line.

9.4.5 Statistics.

Statistical analysis was performed using standard software (SPSS 20.0, IBM, Chicago, IL) Data that were not normally distributed are presented as medians and inter-quartile range. Receiver operator characteristic curves were used to evaluate the strengths of atrial strain for predicting under-estimation of RAP by echocardiography. Bivariate logistic regression was used to compare groups. The Mann-Whitney U-test was used to compare significance, with statistical significance set to $p<0.05$. To categorise under versus overestimation of RAP with echo, groups were split into the 3 echocardiographic RAP estimation ranges (3, 8 and 15 mmHg). Using invasive RAP measures, groups were then categorised into several subgroups; RAP 4-7, RAP 8-10, RAP 11-14 or RAP>15 mmHg.

9.5 Results

9.5.1 Patient characteristics (Table 9.1).

The 175 patients (median age 64 years, 64% female) included in the study had mild increases in pulmonary pressures and borderline reduced RV function. The RA size was mildly increased, and median RAP_C was 8 mmHg, with RAP_{IVC} was only 3 mmHg ($p<0.001$); the mean difference between invasive and non-invasive measures was 3±5 mmHg. RA strain parameters showed RA ƐR 31±20%, RA ƐCT 12±11% and RA ƐCD 16±14%.

9.5.2 Associations with invasively determined RAP.

There was a weak association between RAP_C and RAP_{IVC} (r=0.35, p<0.001) (Table 9.2). Demographic features such as BSA and sex were associated with RAP_C (Table 9.3). RAP_{IVC} was associated with RA size, RVEDA (β 0.30(0.09; 0.26), p<0.001), RV pressure and RVFWS (β-0.21(-0.30;-0.04), p=0.009). Table 9.3 shows that RA deformation parameters were associated with RAV, RAP_{IVC} but not RAP_C. RA strain parameters were associated with some indices of RV function.

9.5.3 Comparison of echocardiographic and invasive RAP.

Table 9.4 summarises the association between RAP_C values and RAP_{IVC} ranges. In those with echocardiographic RAP 3 mmHg, only 13% RAP_C <3 mmHg. In the RAP_{IVC} 8 mmHg group, echocardiography overestimated 43%. In those with RAP_{IVC} >15 mmHg, half of the patients were categorised into RAP <10 mmHg.

Table 9-1. Baseline demographics

Clinical variables	**Median (IQR) (n=175)**
• Age (years)	64 (18.2)
• Sex (female)	112(64%)
• SBP (mmHg)	127 (30)
• DBP (mmHg)	77 (11)
• Heart rate (bpm)	70 (17)
• BMI	27.2 (9.6)
Invasive measures	
• Right atrial pressure (mmHg)	8 (6)
• Right ventricular systolic pressure (mmHg)	53 (40)
• Mean pulmonary artery pressure (mmHg)	33 (20)
• Pulmonary artery systolic pressure (mmHg)	40.5(32)
RA size and function (n=125)	
• IVC (cm)	1.9(0.8)
• RA ƐR (%)	30.9 (20.4)
• RA ƐCT (%)	12.4 (10.8)
• RA ƐCD (%)	16.1 (13.9)
• Right atrial area (cm^2)	21.1 (12.5)
• Right atrial volume/ BSA (ml/m^2)	34.5 (32.5)
Right ventricular size and function	
• Right ventricular end diastolic area (cm^2)	22.0 (12.0)
• Right ventricular end systolic area (cm^2)	15.4 (10.6)
• FAC (%)	32.6 (17.8)
• TAPSE (cm)	1.8 (0.80)
• RVS' (cm/s)	9.0 (3.0)
• RV free wall strain (%)	16.8 (8.6)
• Right ventricular systolic pressure echo (mmHg)	44.0 (35.8)
• Right atrial pressure echo (mmHg)	3.0 (5)
• Pulmonary vascular resistance (w.u, Abbas method))	3.2 (2.2)
Left ventricular size and function	
• Left ventricular mass (gm)	151.2 (80.7)
• Left ventricular Mass/ BSA (gm/m^2)	89.0 (34.2)
• LVEDV (ml)	85.0 (43.5)
• LVESV (ml)	32.0 (23.3)
• Ejection fraction (%)	61 (14)
• Left atrial volume/BSA (ml)	42 (28)
• MV E (cm/s)	0.71 (0.42)
• MV A (cm/s)	0.69 (0.31)
• MV DT (s)	217 (76)
• e' average (cm/s)	7.0 (3.5)
• e/e' sep	12.1 (9.0)
• e/e' lat	7.9 (6.0)
• E/e' avg	10.2 (7.2)
• LV global longitudinal strain (%)	18.3 (5.4)

SBP, Systolic blood pressure; DBP, diastolic blood pressure;; BMI, body mass index; IVC, inferior vena cava; RA ƐR, right atrial reservoir function; RA ƐCT, right atrial contraction; RA ƐCD, right atrial conduit function; FAC, fractional area change; TAPSE, tricuspid annular plane systolic excursion; RVS', LVEDV, left ventricular end diastolic volume; LVESV, left ventricular end systolic volume; MV E, mitral valve inflow; MV A, Mitral valve atrial contraction inflow;

Table 9-2. Factors associated with invasive right atrial pressure (n=125)

		Std B (95% CI)	p
Clinical features	Age (years)	0.06(-0.03;0.07)	0.45
	HR (bpm)	0.02(-0.05;0.06)	0.76
	BSA	0.22(2.4;11.5)	**0.003**
	Sex	0.20(0.58;3.7)	**0.007**
RA size and function	RAP echocardiography	0.35 (0.25;0.58)	**<0.001**
	RA ƐR (%)	-0.13(-0.09;0.01)	0.13
	RA ƐCT (%)	-0.13(-0.17;0.03)	0.15
	RA ƐCD(%)	-0.10(-0.12;0.03)	0.26
	RAA (cm^2)	0.29(0.08;0.25)	**<0.001**
	RAV/BSA (ml/m^2)	0.24(0.02;0.07)	**0.002**
	IVC (cm)	0.36(1.8;4.3)	**<0.001**
RV size and function	RVEDA (cm^2)	0.30(0.09;0.26)	**<0.001**
	FAC (%)	-0.19(-0.13;-0.02)	**0.01**
	TAPSE (cm)	-0.13(-2.6;0.17)	0.08
	RVSP (mmHg)	0.18(0.006;0.07)	**0.02**
	RV free wall strain (%)	-0.21(-0.30;-0.04)	**0.009**

HR, heart rate; BSA, body surface area; RAP, right atrial pressure; RA ƐR, right atrial reservoir function; RA ƐCT, right atrial contraction; RA ƐCD, right atrial conduit; RAA, right atrial area; RAV, right atrial volume; IVC, inferior vena cava; RVEDA, right ventricular end diastolic area; FAC, fractional area change; TAPSE, tricuspid annular plane systolic excursion; RVSP, right ventricular systolic pressure

To determine whether RA strain measures differentiated patients with correct vs incorrect non-invasive RAP assessment, groups were first split based on 3 distinct RAP_{IVC} values (<3, 8 or >15 mmHg, Table 5). Patients were then categorized based on 5 invasive RAP_C groups (RAP<3 mmHg, 4-7 mmHg, 8-10 mmHg, RAP 11-14 mmHg and >15 mmHg (Table 9.5). Within the RAP 3 group, there were no significant differences in over- vs under-estimated groups in RA size and function, or RV size and function. Similar results were seen in the RAP 8 group, with no significant differences in RA and RV structure and function parameters. There were much smaller numbers present in the RAP>15 mmHg group, but again the groups showed no significant differences.

Table 9-3. Associations with right atrial strain parameters

		RA ℰR	p value	RA ℰCT	p values	RA ℰCD	p value
RA parameters	RAP invasive	-0.13 (-1.6;0.15)	0.13	-0.13 (-0.62;0.10)	0.15	-0.10 (-0.75;0.20)	0.26
	RAP echo	-0.46(-2.6;-1.34)	<0.001	-0.40 (-1.3;-0.53)	<0.001	-0.37 (-1.6;-0.60)	<0.001
	RAV (ml^2)	-0.46(-0.23;-0.11)	<0.001	-0.39(-0.11;-0.05)	<0.001	-0.40(-0.14;-0.06)	<0.001
	RAA (cm^2)	-0.46 (-1.3;-0.65)	<0.001	-0.41(-0.63;-0.27)	<0.001	-0.40(-0.81;-0.34)	<0.001
	IVC size (cm)	-0.41 (-17.6;-7.6)	<0.001	-0.41(-9.1;-3.7)	<0.001	-0.30(-10.5;-2.5)	0.002
	RAV/BSA (ml/m^2)	-0.46 (-0.42;-0.21)	<0.001	-0.39(-0.20;-0.08)	<0.001	-0.40(-0.26;-0.11)	<0.001
RV parameters	RVSP echo	-0.21 (-0.28;0.03)	0.02	-0.09 (-0.10;0.04)	0.35	-0.26(-0.22;-0.04)	0.004
	RVEDA (cm^2)	-0.25(-0.80;-0.15)	0.004	-0.15(-0.34;0.04)	0.11	-0.27(-0.60;-0.13)	0.002
	FAC (%)	0.35(0.24;0.65)	<0.001	0.29(0.08;0.32)	0.001	0.31(0.12;0.43)	0.001
	RVFWS (%)	0.53(1.02;1.8)	<0.001	0.40(0.34;0.86)	<0.001	0.48(0.58;1.2)	<0.001
	RVSP invasive	-0.23(-0.30;-0.03)	0.02	-0.01 (-0.08;0.071)	0.96	-0.34(-0.27;-0.08)	0.001
	HR (bpm)	-0.20(-0.47;-0.04)	0.02	-0.15(-0.23;0.02)	0.09	-0.17(-0.32;0.004)	0.06

RAP, right atrial pressure; RAV, right atrial volume; RAA, right atrial area; IVC, inferior vena cava ; RAV/BSA, right atrial volume/body surface area; RVSP, right ventricular systolic pressure; RVEDA, right ventricular end diastolic area;; FAC, fractional area change; RVFWS, right ventricular free wall strain; HR, heart rate.

Table 9-4. Echocardiographic as compared to invasive RAP groupings

	RAP_{IVC} 3 mmHg	**RAP_{IVC} 8 mmHg**	**RAP_{IVC} >15 mmHg**
RAP <3 mmHg	14(12.8%)	1 (2.5%)	0 (0%)
RAP 4-7 mmHg	43 (39.4%)	13(32.5%)	4 (15.4%)
RAP 8-10 mmHg	27 (24.8%)	9 (22.5%)	9 (34.6%)
RAP 11-14 mmHg	17 (15.6%)	8 (20%)	5 (19.2%)
RAP>15 mmHg	8 (7.3%)	9 (22.5%)	8 (30.8%)

RAP, right atrial pressure, IVC, inferior vena cava

9.5.4 Between reader variability.

Variability measures were performed on 10 patients, and 20 patients for intra-observer variation. For RA ƐR there was a modest, significant association between readers (r=0.68, p=0.03). The same was true for RA ƐCT contraction, with a modest, significant associations (r=0.66, p=0.04), and RA ƐCD (r=0.65, p=0.04). Bland-Altman analysis revealed that scatter increased as mean values increased for all RA strain parameters (Figure 4). ICC analysis revealed there were modest correlations between reads of RA reservoir (ICC 0.68 (0.12-0.91), p=0.01), RA contraction (ICC=0.65(0.08-0.90) p=0.02), and RA conduit function (ICC=0.65(0.08-0.90), p=0.02). Intra-observer correlations were better for RA reservoir (r=0.92, p<0.001) and contractile function (r=0.83, p<0.001). The ICC for intra observer variability was higher than between reader values; with RA ƐR (ICC 0.91 (0.80-0.97) p<0.001), similar to RA ƐCT (0.83(0.62-0.93), p<0.001) and conduit function (0.78(0.52-0.91), p<0.001). The respective mean differences were small (0.24±5.1%, -0.24±4.1% and 0.47±4.9%).

Table 9-5. Non-Invasive RAP as compared to invasive RAP readings and differences in RA strain values

RAP, right atrial pressure; RA ƐR, right atrial reservoir function; RA ƐCT, right atrial contraction; RA ƐCD, right atrial conduit function

RAP = 3 on echo						
	RAP ≤ 3 mmHg (n=12)	RAP 4-7 (n=37)	RAP 8-10 (n=24)	RAP 11-14 (n=12)	RAP>15 (n=7) *6 missing*	P value
RA ƐR	32.8(±12.0)	42.0(±17.7)	35.8(±15.0)	43.7(±19.6)	28.1(±10.7)	0.72
RA ƐCT	14.2(±5.3)	19.5(±10.6)	13.7(±7.5)	19.8(±7.3)	13.6(±7.7)	0.84
RA ƐCD	17.3(±8.7)	23.6(±11.5)	22.7(±12.5)	23.9(±14.7)	12.2(±5.1)	0.88
RAP =8 on echo						
	RAP ≤ 3 mmHg (n=1)	RAP 4-7 (n=9)	RAP 8-10 (n=7)	RAP 11-14 (n=6)	RAP>15 (n=5)	P value
RA ƐR	18.1	30.2(±16.8)	28.1(±22.0)	32.7(±5.5)	21.1(±9.7)	0.10
RA ƐCT	5.5	14.2(±10.4)	11.0(±11.9)	12.7(±6.3)	9.1(±5.7)	0.07
RA ƐCD	12.6	16.0(±9.7)	17.1(±20.1)	20.1(±9.5)	12.0(±5.6)	0.15
RAP= 15 mmHg on echo						
	No patients	RAP 4-7 (n=4)	RAP 8-10 (n=6)	RAP 11-14 (n=4)	RAP>15 (n=2)	P value
RA ƐR		15.2(±5.4)	15.3(±6.0)	13.9(±7.5)	12.1(±5.4)	0.92
RA ƐCT		6.2(±5.5)	6.4(±3.0)	7.8(±6.9)	3.5(±0.28)	0.80
RA ƐCD		8.9(±8.0)	10.3(±5.0)	6.1(±2.2)	8.6(±5.1)	0.73

Figure 9-3. Between reader Pearson's correlation for right atrial strain components. Table 9.3a shows correlation between RA ƐR for 2 readers (r=0.68, p=0.03), 9.3b shows RA ƐCT between readers (r=0.66, p=0.04), with similar results for 9.3c RA ƐCD (r=0.65, p=0. 04)

Figure 9.3a

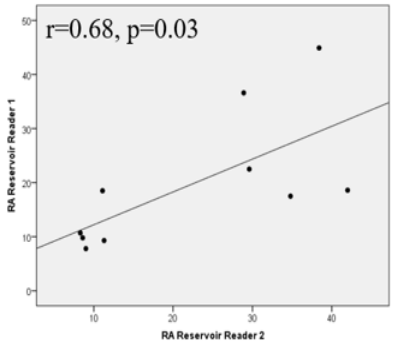

Figure 9.3b

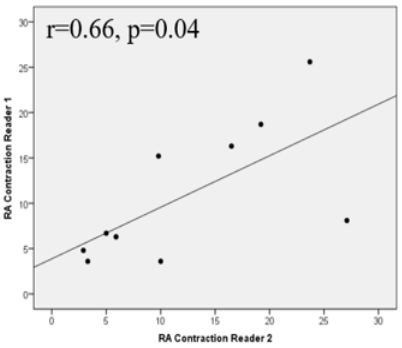

Figure 9.3c

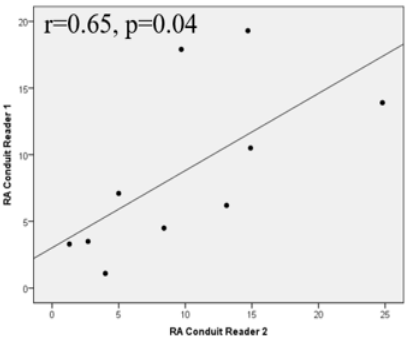

Figure 9-4. 9.4a shows Bland-Altman plot between reader RA ƐR (ICC 0.68 (0.12; 0.91), p=0.01), with a mean difference of -2.6% (±10.5). Table 9.4b shows the RA ƐCT plots (ICC 0.65(0.08; 0.90), p=0.02), with a mean difference of -1.5 %(±6.8).Table 9.4c displaying RA ƐCD shows a similar result (ICC 0.65(0.08; 0.90), p=0.02), with a mean difference of -1.1 %(±5.7)

Figure 9.4a

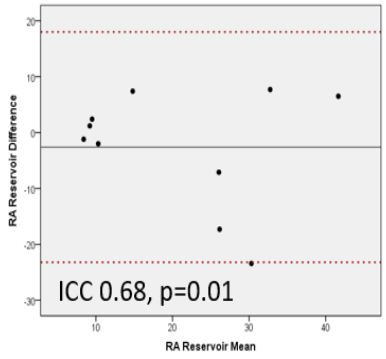

Figure 9.4b

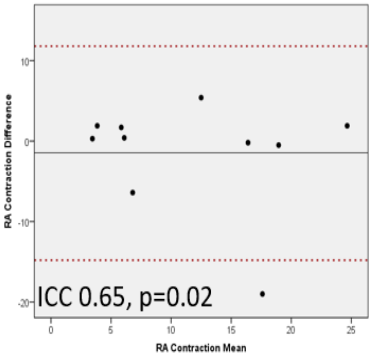

Figure 9.4c

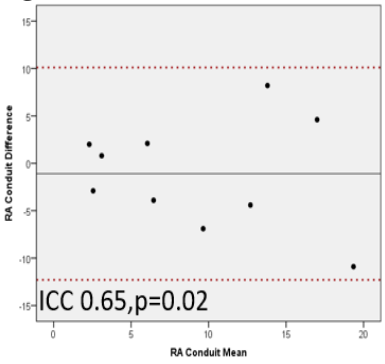

9.6 Discussion

Overall, although there were significant correlations between invasive and non-invasive RAP, there are still a large number of people in which echocardiography underestimates RAP. Overall, RA strain values do not add to the clinical ability to determine underestimation of invasive RAP. Right atrial strain was associated with RV function and non-invasively derived RAP, although associations with invasively derived RAP were lacking. Variability measures for RA deformation appear acceptable for both intra- and inter-variability analysis.

We have found associations with pressures were present, but this did not add to the ability to predict RA pressure. Other studies have replicated the associations with RV invasive pressures and right strain, this adds to the current evidence, but how its superior or additive to current processes' in pulmonary hypertension management are not known. Other work has shown a strong association with right atrial strain in functional capacity and has shown strong associations with PVR and cardiac output [276].

9.6.1 Echocardiographic assessment of RA pressure.

Classical drivers of the miscalculation of RAP using echocardiography can come from patient body size, athletic training (through increased venous return) [277], prominent Eustachian valve, or patients on mechanical ventilation [278]. We excluded patients on mechanical ventilation, and although did not screen for athletic training, this would have been highly unlikely in this cohort. Correcting IVC dimensions for BSA [279] has previously been suggested, although is not routinely performed in clinical practice, and was not used in our cohort. The use of 3D ultrasound could have been combined with strain markers to formulate a composite value for RAP calculation. 3D RAV has been shown to be feasible in healthy control patients [280], and 3D RA volume has been used in conjunction with IVC size to predict RAP, specifically >10 mmHg, in acutely decompensated heart failure patients [269].

9.6.2 Right atrial function within the cardiac cycle.

The RA promotes RV filling, while also minimising pressure within the central venous circulation [266]. As the pulmonary pressure increases, the RV undergoes hypertrophy to adapt to increased afterload, and RV filling becomes increasingly dependent on right atrial contraction. Animal models have demonstrated that the RA can alter its functionality to act as a reservoir or a conduit [281]. It also provides a buffer to

irregularities in atrial filling, and help to prevent acute elevations in RV diastolic pressure, as well as being able to actively respond to an acute increase in pulmonary pressure by increasing RA contractile force. All these findings further justify the need to consider the RA as more than just a static entity in the cardiac cycle. Remodelling occurs within the RA tissue in response to chronic increases in afterload, RA tissue in PAH been shown to have significantly reduced contractile force as compared to controls, with this possibly independent of RV function [282]. RA size itself is a strong predictor of outcome in PAH. Whether or not RA function could be an early determinant or RA size increases is not yet known. Within our cohort, RA size seemed to be a significant driver of RA strain.

9.6.3 Right atrial deformation

RA strain has previously been reported using LV strain packages, with studies showing a reduction of RA strain compared to controls in a variety of disease cohorts [270]. The results of our study contrast with previous work showing a significant negative correlation between peak RA strain and RAP [283], as well as the association of RV invasive pressures and right atrial strain in treatment-naïve patients, in whom RA strain was associated negatively with PVR ($r = -0.46$; $p<0.05$), functional capacity, and cardiac output [276]. It is possible that this heterogeneity relates to the duration of pulmonary hypertension – the development of atrial fibrosis as a consequence of sustained pressure overload may add a vital confounder to the association between atrial strain and pulmonary pressure – but this requires further study.

An interesting group is that of the elite athlete cohort, with studies showing significantly lower RA reservoir function phase, and RA contraction phase against matched controls [284]. The difficulty comes in determining how this value will add in clinical settings. The importance of the association with RA strain and RV free wall

strain should not be overstated. As the RV acts as a "mirror", this association likely due to tethering effects, with other cohorts also showing associations with RV decompensation [270]. Similar associations have been found with mRAP[285] and PASP[276].

9.7 Limitations.

Data were acquired in different echocardiographic machines, although TomTec is vendor independent software. Although having the measures performed on same machines would be optimal, this is often not feasible in a busy echocardiographic lab. All efforts were made to perform the echocardiographic measures in close succession, but the median time difference was 1 day. We acknowledge that changes in patient volumetric status would have occurred during this period.

9.8 Conclusion.

Right atrial strain measures appear to differentiate between patients with PH and associated with markers of RV failure. RAP is an essential diagnostic parameter in PAH. However, right atrial strain parameters did not appear to identify those in which non-invasive techniques are incorrect.

9.9 Postscript

Right atrial size and pressure are markers associated with PHT and right heart failure. Whether this can be used as an early disease marker to track the progression of PAH is unknown. The previous chapter presented our experience in the performance of right atrial deformation in a clinical cohort and its clinical utility in the prediction of RAP.

Strong correlations exist between IVC collapsibility and RHC assessment of RAP[274], but it is pertinent to remember that a highly significant association can still be seen even if individual data points disagree [286]. Other studies have attempted to use other

methods to adjust inaccuracies present, including tricuspid E/e' ratio and diastolic flow predominance in the hepatic veins[46], but these have had a modest effect on accuracy. Precaution should be used when utilising the IVC to estimate the pressure in athletes [277] and ventilated patients[287]. Other clinical and echocardiographic predictors of inaccuracies have not been identified[268].

Chapter 9 shows that right atrial strain appears to be a possible measurement in a PAH cohort. However, although significant associations exist with RAP, this does not differentiate over versus underestimation of RAP. Whether RA strain can facilitate understanding of the clinical progression of PAH, and early detection of clinical decompensation warrants more study.

Patients with SSC constitute a challenging group, as screening for PH is undertaken to identify patients with early disease [288]. Historically, SSC patients have been screened using the echocardiographic measurement of PASP. As previously mentioned, following PASP is not an optimal method of PAH follow-up. At least 50% of pulmonary circulation must be obstructed before a rise in resting PAP is detected[288]. RV strain may be helpful in the pursuit of early diagnosis; before the persistent elevation of PASP, there may be temporal fluctuations that leave a "fingerprint" of myocardial damage. Alternatively, provocative tests are used to identify whether there is some compromise of the pulmonary vascular reserve. The next chapter will investigate whether provocative testing and RV strain provide different information about the preclinical disease.

Chapter 10

RV and PASP response to provocative testing

In preparation for submission

….

10 RV and PASP response to provocative testing

10.1 Preface; Early detection of myocardial disease in systemic sclerosis.

Although the majority of Group 1 PAH is idiopathic, rarer causes such as congenital heart disease and CTD may provide insights into the temporal progression of RV failure. As mentioned previously, the SSC cohort is of particular interest. Routine screening is recommended with echocardiography, to facilitate early detection of PAH (using haemodynamic markers).

PH is one of the most significant causes of morbidity in CTD [289], with high rates of right heart failure. The SSC cohort is characterised by fibrosis and thickening of the central and peripheral organs and can manifest in the cardiac pathophysiology through LV diastolic dysfunction[290]. Both of these conditions present with raised TR jet velocity.

The detection of a ”pre-clinical” phase of cardiovascular fibrosis in SSC could help with early detection of either right and left-sided heart disease. Elevations in pressure due to left versus right heart disease requires substantially different clinical management. Mortality benefits seen through pulmonary artery vasodilator treatment are not witnessed in pulmonary venous hypertension, with no changes in functional status or outcomes seen [291-293]. Echocardiographic markers of myocardial deformation could aid in the early differentiation of pulmonary venous or PAH. When suspicion of disease is high (symptoms combined with risk factors), the treating team may proceed directly to RHC. Further to this, “stress testing” by volume loading used to elucidate raised pressures during invasive assessment can aid in early diagnosis[294].

A combination of a “stress test” with subsequent myocardial imaging may give further insight into temporal progression of disease in an at-risk population.

10.2 Abstract

Background- Early detection of PH in SSC may improve outcomes. "Stress testing" during RHC with a volume challenge is thought to differentiate those with latent cardiac disease. Speckle tracking with echocardiography could identify SSC patients who raise cardiac pressures post stress. We seek to define LV and RV characteristics that are predictive of a pathological response to fluid loading. We hypothesised that speckle tracking of the myocardium would identify SSC patients presenting with raised pressures after stress.

Method. 231 patients were identified who had RHC performed in close succession to echocardiography (median 0 days (-132;-7). 43 symptomatic SSC (age 59±13, 91% women) with no overt PH (PASP 30±6 mmHg with echo) underwent fluid loading (670±320 ml). Echocardiography was performed in close succession to RHC. Associations of abnormal responses was sought and significance set to $p<0.05$.

Results. SSC who underwent fluid loading were significantly younger than the remainder, with less evidence of LV diastolic or LV/RV systolic dysfunction as compared to post- and pre-capillary PH groups. PCWP increased to $\geq$15mmHg in 17 patients after fluid loading, and LV mass was the only echocardiographic marker to predict change in PCWP. TAPSE was a weak, borderline significant association of increased mean pulmonary artery pressure.

Conclusion. LV markers associated with changes in PCWP after fluid loading. RV function showed a weak association with raises in PAPm. Myocardial deformation did not associate with increases in filling pressure after fluid loading.

10.3 Background

Cardiac fibrosis, as determined via biopsy, has shown to be present in a large number of SSC patients. Two critical cardiac sequelae of this are the development of PAH and diastolic dysfunction, and shortness of breath in SSC patients could be attributable to either of these entities. The diagnosis of elevated pulmonary artery pressure is confirmed with RHC, with PCWP measurements used to differentiate the pathological source of elevation. PAH has a substantial mortality risk, thus early detection and intervention with novel treatments can improve patient outcomes and quality of life substantially.

The echocardiographic differentiation between pre versus postcapillary PH is dependent on the integration of measurements of LV diastolic and systolic function, pulmonary haemodynamics and right ventricular assessment. Myocardial deformation imaging could be used to elucidate early progression of the disease.

In SSC patients who present with shortness of breath, the echocardiographic sensitivity to detect early disease is not known. The presence of mild symptoms may already herald advanced obliterative disease. The DETECT algorithm [295] recommends SSC patients with suggestive markers (serum markers, telangiectasia, reduced FVC%/DLCO%, right axis deviation on ECG) should undergo echocardiography. The recommended echocardiographic parameters to raise PAH suspicion are TR V max and RAA. TR V max is in current echocardiographic guidelines for the diagnosis of post-capillary PH[243]. A higher TRV max threshold has been suggested for PAH patients, with a velocity of >3.4 m/s. The use of novel imaging markers using speckle tracking imaging could identify patients most likely to respond to fluid loading.

Physicians may decide to proceed directly to invasive assessment if clinical suspicion is high. Before catheterisation, patients have generally been in a fasting state for ~12 hours, which can lead to a depletion of intravascular volume, and possible underestimation of LV filling pressures[296]. Fluid loading during RHC has been proposed as a method to "unmask" latent PAH. The aims for this chapter are to define LV and RV characteristics that predict a pathological response to fluid loading during RHC.

10.4 Methods.

10.4.1 Patient recruitment.

Consecutive patients undergoing RHC from 2003 to 2013 to investigate dyspnoea or fatigue were studied at the Royal Hobart Hospital and Princess Alexandra Hospital (Queensland, Australia). 236 patients were identified who had RHC performed in close succession to echocardiography (median 0(-132;-7) (figure 1). PAH was defined as PAPm ≥ 25 mm Hg and PCWP of ≤ 15 mm Hg in both groups, as per local Australian prescribing guidelines at the time. Of these, 43 patients (age 59±13, 91% women) with SSC, but no overt PAH (PASP 30±6 mmHg with echo) underwent fluid loading (670±320 ml). We used previously published detection scores from the DETECT algorithm for PAH detection in SSC.

Figure 10-1. Patient flow chart

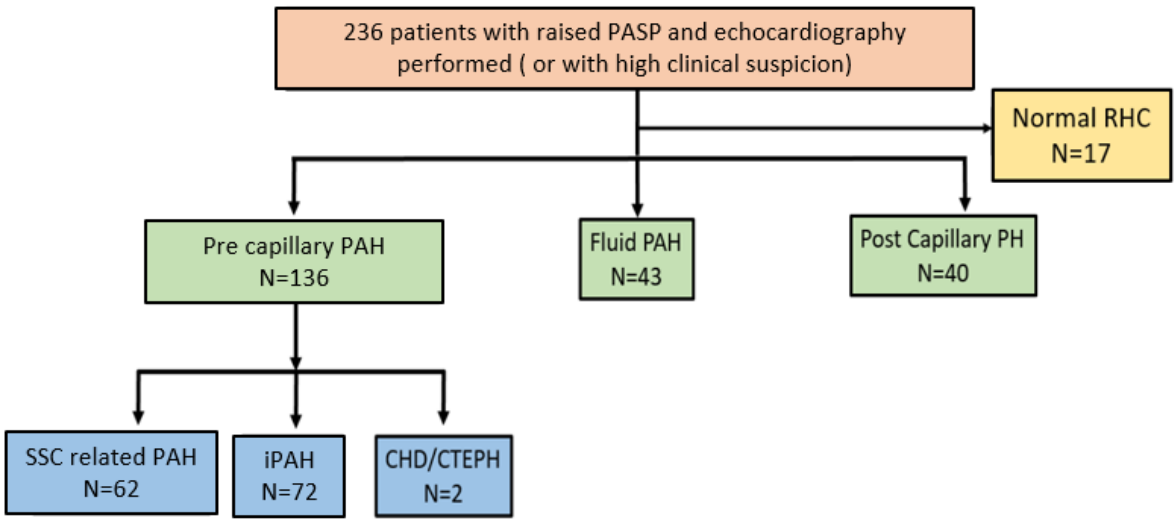

10.4.2 Fluid loading.

Up to 1 litre of normal saline was administered via the venous sheath, usually over a 20-minute period. Haemodynamics were reassessed with every 250 mL volume. The bolus was ceased if the criteria for PH were reached; PCWP > 15 mm Hg, or if the patient became symptomatic.

10.4.3 Echocardiography.

Echocardiography was performed using standard commercial equipment (GE Vivid 7, Vivid i and Vivid e9, Horten, Norway; Philips ie33, Bothell, WA). All measurements were performed by a single reader, using standard views.

Standard measurements. LV and RV measurements were performed according to ASE guidelines [101] by a single reader for both studies. The measurement technique for the systolic and diastolic function has been described previously in the methods chapter.

10.4.4 Statistical analysis

Statistical analysis was performed using SPSS (IBM, version 21). An independent samples t-test was used to compare groups. A paired-sample t-test was used to compare patients before and after fluid loading during RHC. Univariable logistic

regression was used to assess association with raised invasive PCWP. Patients were split based on raised PCWP post fluid ≥15 mmHg. Associations of increased PCWP were sought using binary logistic regression. The significance level was set to $p<0.05$.

10.5 Results.

10.5.1 Baseline data

Echocardiographic data are shown in Table 10.1. The 43 patients with SSC who underwent fluid loading were significantly younger than the remainder, with less evidence of LV diastolic dysfunction. Left ventricular systolic markers were not significantly different. The post-capillary PH group showed evidence of impaired right ventricular function with standard RV function measures and RVFWS.

Table 10-1. Baseline clinical and echocardiographic values of fluid load PAH

	Fluid PAH (n=43)	Post cap PH (n=40)	P value
Age (years)	58(16.0)	68 (19.7)	0.04
PAPs (mmHg)	26 (4.6)	45 (29.5)	0.004
PAPm (mmHg)	17 (3.5)	30 (18.5)	<0.001
PCWP (mm	7 (2.9)	19(8.3)	<0.001
6MWD (meters)	398 (152)	NA	
HR (bpm)	70 (17)	75 (20)	0.01
LV Mass (gm)	132 (46.1)	199 (113.6)	0.47
LV EDV (ml)	75 (23)	110 (86.8)	0.66
LV ESV (ml)	31 (12)	47(69.5)	0.82
SV (ml)	47 (13)	60 (28)	0.13
EF (%)	61 (11)	56 (28)	0.55
MV EA ratio	1.0 (0.47)	1.2 (1.5)	0.59
MV DT (cm/s)	238 (87)	186 (66)	0.63
e septal (cm/s)	7.0 (4)	5.0(4.8)	<0.001
e lat (cm/s)	10 (6.5)	8(4.8)	0.006
E/e med	9 (4.7)	19(12.1)	0.001
E/e lat	7 (4.4)	12(7.5)	0.03
LAV (ml)	44.3 (16.5)	111(85.4)	0.04
LV GLS %	19.2 (3.6)	15.0(12.3)	0.30
TAPSE (cm)	2.1 (0.70)	1.5(1.2)	0.006
RV EDA (cm^2)	14.0 (5.0)	21.2(8.1)	<0.001
RVSP (mmHg)	26 (7.3)	40 (28.8)	<0.001
RAA (cm^2)	14 (4.5)	24(10.0)	<0.001
RVFWS %	21.9 (9.2)	17.1(10.1)	0.002
RV FAC %	39 (16)	28 (15.7)	0.19

PAPs, pulmonary artery systolic pressure; PAPm, pulmonary artery pressure mean; PCWP, pulmonary capillary wedge pressure; 6MWD, six-minute walk distance; HR, heart rate; LV, left ventricle; LVEDV, left ventricular end diastolic volume; LVESV, left ventricular end systolic volume; EF, ejection fraction; MV EA, mitral valve early to atrial inflow ratio; MV DT, mitral valve deceleration time; LAV, left atrial volume, LV GLS, left ventricular global longitudinal strain; TAPSE, tricuspid annular plane systolic excursion; RVEDA, right ventricular end diastolic area; RVSP, right ventricular systolic pressure; RAA, right atrial area; RVFWS, right ventricular free wall strain; FAC, fractional area change.

10.5.2 Fluid loading response

Fluid loading significantly increased PCWP, PADP, PAPm, and PCWP (Table 10.2).

Figure 10.2 shows the individual response to fluid loading. Although the mean

pressures all significantly increased, there was a significant amount of individual variation present. 17 patients elevated PCWP≥15 mmHg.

Table 10-2. Invasive haemodynamic response to fluid loading

	Pre fluid	Post fluid	Delta	P value
PAPs (mmHg)	26.1 (±4.6)	37.2 (±4.6)	11.0 (±4.0)	<0.001
PAPd (mmHg)	9.2 (±3.3)	18.3 (±3.1)	9.1 (±4.2)	<0.001
PAPm (mmHg)	16.8 (±3.5)	26.4 (±4.0)	10.2 (±3.4)	<0.001
PCWP (mmHg)	7.1 (±2.9)	13.9 (±2.7)	6.9 (±3.1)	<0.001

PAPs, pulmonary artery pressure systolic; PAPd, Pulmonary artery diastolic pressure; PAPm, pulmonary artery pressure; PCWP, pulmonary capillary wedge pressure.

Figure 10-2. Individual variation in response to fluid load for PAPm, PAPs, PADP and PCWP.

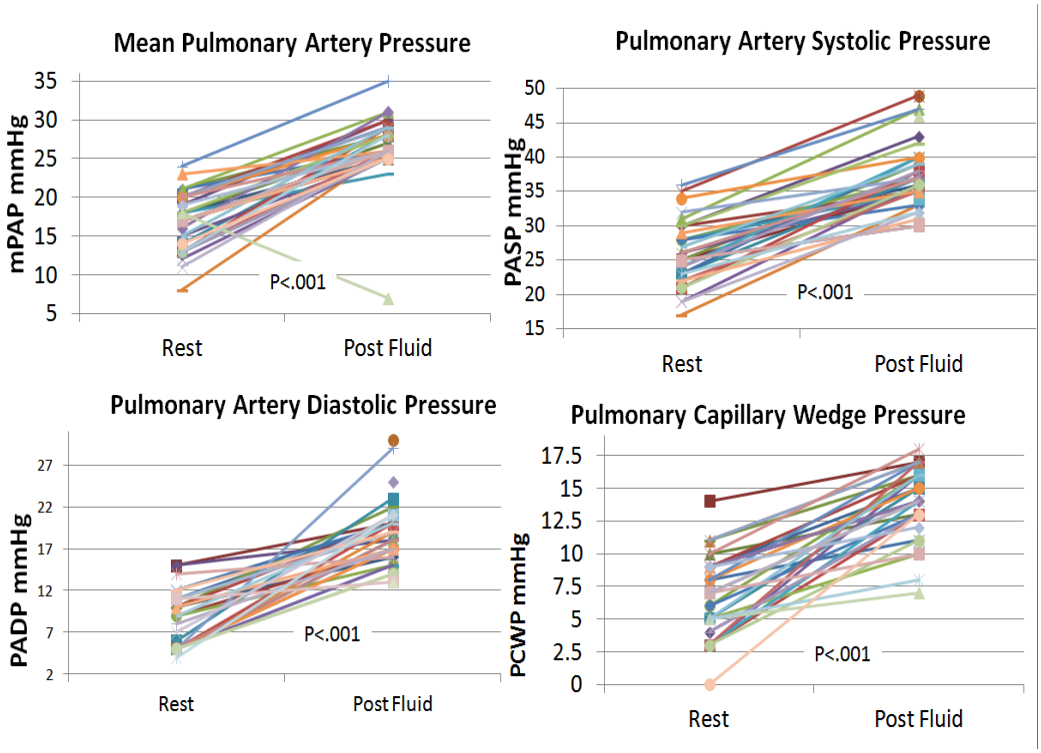

10.5.3 Echocardiographic characteristics of fluid response group

Groups were split based on PCWP elevations of >15 mmHg (Table 10.3). Systolic function measures did not show any significance. Similarly, diastolic function was not different. LV GLS was not different, with LA strain parameters also not significant. Right ventricular markers were also not statically significant between the two groups.

Table 10-3. Echocardiographic comparison of PCWP response to fluid loading

PAPs, pulmonary artery systolic pressure; PCWP, pulmonary capillary wedge pressure; PAPm, pulmonary artery mean pressure; LV, left ventricle; LVEDV, left ventricle end diastolic volume; EF, ejection fraction; MV E, mitral valve early inflow; MV A, mitral valve atrial contraction; MV DT, mitral valve deceleration time; LAV, left atrial volume; LA, left atrium; GLS,

	PCWP < 15 mmHg after fluid	**PCWP>15 mmHg after fluid**	**P value**
	Mean (SD)	**Mean (SD)**	
PAPs (mmHg)	26(±3.7)	27(±5.8)	0.43
PCWP (mmHg)	6(±2.3)	8(±3.3)	0.08
PAPm (mmHg)	16(±2.8)	17 (±4.2)	0.42
Age (years)	59(±10.6)	57(±16.3)	0.70
LV Mass (gm)	130.3(±32.6)	132.4(±26.7)	0.83
LV EDV (ml)	76.2(±16.0)	81.3(±22.6)	0.41
LV EF (%)	58(±10.3)	61(±7.3)	0.22
SV (ml)	43.5(±10.2)	49.7(±13.7)	0.11
MV E (cm/s)	0.65(±0.13)	0.74(±0.19)	0.10
MV A (cm/s)	0.66(±0.20)	0.66(±0.18)	0.95
MV DT (cm/s)	237(±48.8)	245(±43.2)	0.62
e' septal (cm/s)	8.3(±3.2)	8.2(±2.8)	0.98
e' lateral (cm/s)	10.5(±4.0)	10.8(±3.9)	0.89
e' avg (cm/s)	9.6(±3.7)	10.0(±3.7)	0.78
E/e' med	8.5(±2.8)	9.9(±2.3)	0.25
E/e' lat	7.0(±4.0)	7.6(±2.7)	0.69
E/e avg	7.7(±3.6)	8.3(±2.6)	0.57
LAV (ml)	46.3(±11.5)	48.4(±16.7)	0.66
LA reservoir (%)	30.8(±10.0)	32.4(±7.7)	0.58
LA contraction (%)	12.9(±4.8)	13.0(±3.2)	0.95
LA conduit (%)	17.9(±7.6)	19.4(±6.4)	0.51
LV GLS (%)	18.0(±2.7)	19.2(±3.3)	0.23
RV FAC (%)	36.4(±10.5)	41.2(±7.3)	0.11
PASP echo	30.4(±7.2)	28.4(±4.0)	0.34
RAA (cm^2)	14.6(±3.0)	14.4(±3.4)	0.80
RVEDA (cm^2)	14.5(±3.6)	13.9(±3.3)	0.63
RVFWS (%)	20.6(±5.8)	23.2(±5.7)	0.17

global longitudinal strain; FAC, fraction area change; PASP, pulmonary artery systolic pressure; RAA, right atrial area; RVEDA, right ventricular end diastolic area; RVFWS, right ventricular free wall strain.

10.5.4 Univariate associates of changes in pulmonary haemodynamics after fluid load.

Data were assessed as continuous variables, with the pre-measure subtracted from post fluid values for PCWP, PADP and PAPm. LV mass associated with increased delta PCWP and delta PAPm. TAPSE was of borderline significance for association with raised PAPm. PADP did not show any significant associations with echocardiographic makers. Patients were then split into groups based on whether post fluid PCWP increased > 15 mmHg. Bivariate logistic regression showed similar results, with no baseline invasive or echocardiographic variables predicting those who increased PCWP > 15 mmHg (Table 10.4).

10.5.4.1 Detection of Pulmonary Arterial hypertension based on DETECT guidelines

Current PAH detection algorithms in SSC suggest the use of right atrial size and TR jet velocity for detection of PAH. The categorisation of DETECT parameters (TR V max >2.8 or RAA> 16 cm^2) and association with increases in PAPm (as a continuous variable) was assessed. The degree of change in PAPm did not show a significant relationship with baseline TR Vmax >2.8 (Std β -0.08(-4.4; 2.9) p=0.68), or with RAA >16 cm^2 (Std β -0.18(-3.6; 1.1) p=0.30). RV dysfunction value of <20% was also not a significant predictor or delta PAPm (Std β 0.04(-2.3;2.8)p=0.83).

Echocardiographic measures of increased LV filling pressures (septal e', LAV and E/e') were ineffective for predicting raised PCWP, but measures of structural change showed significant univariable associations with LVEDV and LV mass. Patients were then split into groups based on whether post fluid PCWP increased to >15 mmHg. Bivariable logistic regression showed no baseline invasive or echocardiographic variables predicting those who increased PCWP >15 mmHg (Table 10.4).

10.5.5 ROC characteristics for pre versus post capillary pulmonary hypertension

We compared three groups; SSC-PAH, SSC-symptomatic (normal resting haemodynamics but elevated pressure after fluid load) and post-capillary PH. In the symptomatic SSC and SSC PAH, LAV was a significant discriminator (AUC 0.63 (0.51; 0.74) p=0.04), with the SSC PAH group showing significantly larger LA volume. TR Vmax (AUC 0.80(0.70; 0.89) p<0.001) and RAA (AUC 0.76(0.66; 0.85) p<0.001) also had significant discriminatory ability. RVFWS had modest predictive ability (AUC 0.69(0.58; 0.80) p=0.002), but LV GLS was not significant (AUC 0.44(0.32; 0.55) p=0.30).

The SSC symptomatic group was difficult to distinguish from the post-capillary PH group, RV FWS (AUC 0.65(0.55;0.75), p=0.007) discriminated disease type, but not LV GLS (AUC 0.57(0.47;0.68), p=0.18). RAA (AUC 0.41(0.31; 0.51) p=0.09), TR V max (AUC 0.66(0.56; 0.75) p=0.003) and LAV were not significant (AUC0.54 (0.43; 0.65) p=0.48).

Finally, the pre versus capillary pulmonary hypertension groups were compared for the ability for echocardiography to discriminate cause of raised pulmonary pressure. TR Vmax was not significant in predicting pre from post-capillary PH (AUC 0.50(0.39; 0.62), p=0.95), RAA was significant, but this trended towards the post-capillary group having larger RAA (AUC 0.71 (0.61;0.82), p<0.001), RV free wall was not significant (AUC 0.42(0.29;0.55), p=0.22). LV GLS showed significant but modest predictive ability (AUC 0.64 (0.51;0.77), p=0.02), and LA volume was a strong discriminatory marker (AUC 0.83(0.74;0.92), p<0.001).

Table 10-4 Echocardiographic associates of delta invasive haemodynamic pressures

	Delta PAPm		Delta PCWP		Delta PADP	
	Std β (95%CI)	**P value**	**Std β (95%CI)**	**P value**	**Std β (95%CI)**	**P value**
Age (years)	-0.10(-0.11;0.06)	0.57	0.19(-0.04;0.12)	0.30	-0.19(-0.18;0.06)	0.30
LAV (mls)	-0.18(-0.13;0.045)	0.32	-0.20(-0.12;0.04)	0.30	-0.25(-0.19;0.04)	0.19
LV mass (gm)	-0.34(-0.08;-0.002)	0.04	-0.41(-0.08;-0.009)	0.02	-0.28(-0.09;0.01)	0.11
e' avg (cm/s)	-0.10(-0.44;0.28)	0.64	-0.35(-0.58;0.07)	0.12	0.08(-0.72;0.94)	0.78
E/e' avg	-0.03(-0.53;0.46)	0.88	0.24(-0.24;0.66)	0.33	-0.23(-1.0;0.37)	0.35
E/e' lat	-0.04(-0.44;0.38)	0.88	0.16(-0.33;0.64)	0.51	-0.26(-0.94;0.27)	0.26
LV GLS (%)	-0.26(-0.63;0.08)	0.13	-0.11(-0.47;0.27)	0.57	0.01(-0.48;0.52)	0.94
LVEDV	-0.24(-0.10;0.02)	0.15	-0.36(-0.11;-0.003)	0.04	-0.21(-0.13;0.03)	0.25
EF (%)	0.07(-0.10;0.15)	0.70	0.15(-0.07;0.17)	0.41	0.03(-0.15;0.18)	0.87
RAV	0.004(-0.09;0.10)	0.98	0.01(-0.09;0.10)	0.94	-0.17(-0.18;0.07)	0.35
TAPSE (cm)	-0.29(-5.0;0.28)	0.08	-0.22(-4.1;0.93)	0.21	-0.10(-4.4;2.5)	0.59
RVEDA (cm^2)	-0.26(-0.63;0.07)	0.12	-0.23(-0.52;0.11)	0.20	-0.22(-0.70;0.16)	0.21
RVSP (mmHg)	-0.05(-0.24;0.18)	0.80	-0.09(-0.26;0.16)	0.64	-0.16(-0.40;0.17)	0.41
RV FAC (%)	0.006(-0.12;0.12)	0.97	0.08(-0.09;0.15)	0.66	0.11(-0.12;0.21)	0.56
RV free wall	-0.19(0.31;0.09)	0.28	-0.21(-0.31;0.09)	0.26	-0.10(-0.33;0.19)	0.60

PAPm, pulmonary artery pressure mean; PCWP, pulmonary capillary wedge pressure; PADP, pulmonary artery diastolic pressure; LAV, left atrial volume; LV, left ventricle; GLS, global longitudinal strain; EDV, end diastolic volume; EF, ejection fraction; RAV, right atrial volume; TAPSE, tricuspid annular plane systolic excursion; RV, right ventricle; EDA, end diastolic area; FAC, fractional area change;

10.6 Discussion.

SSC patients are a unique group who have a high chance of presenting with latent pulmonary vascular disease. Echocardiographic markers did not have a strong association with the prediction of post fluid loaded elevations in RHC. LV mass was the only echocardiographic marker to show significance for predicting PCWP increases, with right heart function also bordering on significance for detecting increased PAPm. SSC specific baseline detection algorithms variables (TR V max, and RAA) did not predict patients who elevated PAPm post fluid.

Prior work on fluid loading has been done in a number of settings, with the clinical applicability of this technique still being defined. Some reasons for this could are postulated. Firstly, correct protocols for this procedure are still to be defined, and the response of "normal" patients to fluid loading is unclear. Fujimoto and colleagues [297] used a fluid challenge of 2 litres in healthy individuals. Interestingly, they found both age and sex associated with increased PCWP response. Another study suggested that infusion of 500 ml of fluid over 5-10 minutes [298] is sufficient, and suggested increasing upper limits of normal after saline infusion to include PCWP $\geq$18 mmHg. Recent guidelines state [130] that although fluid loading of 400 ml over 5 to 10 minutes is safe, and can help to distinguish PAH from LV diastolic dysfunction, standardisation is required before its use in clinical practice can be endorsed. Our study limited the amount of fluid given to ~ 1 litre, which is in line with previous studies.

Recent guideline reviews [130] suggests the SSC population to be a specific group in which the term "borderline" may be helpful, as this could identify a subgroup of patients likely to progress to PAPm> 25mm Hg. "Borderline" PH has not been added to the guidelines, as evidence that this term would be helpful in the left heart sided

PH population is lacking. Unfortunately, in our sample, echocardiography did not have a strong association with elevations of PASP/EDP after fluid challenge. Echocardiographic guidelines now recommend echocardiographic values be indexed for body surface area. Measures were not routinely performed when the majority of these studies were undertaken hence values have not been indexed due to lack of data.

Higher survival rates have been shown in SSC-PAH patients diagnosed through a detection program [299], highlighting the importance of early detection and intervention. Echocardiographic components of these algorithms are related to haemodynamic markers (TR v max), and dilation of the RA. Diastolic guidelines highlight the importance of TR v max in post-capillary PH. In our SSC group, TR v max was not a significant discriminator between the PAH vs PH post capillary groups, with RAA significantly trending towards being larger in the post capillary PH group. Both markers had significant discriminatory ability in SSC PAH compared to the SSC fluid loaded group, with RV strain showing modest discriminatory ability. We feel some of these contradictions highlight issues with simplifying the diagnostic pathway to simple echocardiographic haemodynamic markers. If early detection is such a strong outcome marker, echocardiographic markers which differentiate pathological basis of pressure changes should be incorporated.

Exercise is also a popular stressor used in during RHC. Although exercise pressures are not in current guidelines for PAH diagnosis, exercise echocardiography has been used to screen for potential diastolic dysfunction[300]. The predictive ability of echocardiography for predicting exercise-induced PH could also be assessed in the SSC cohort.

Screening of SSC patients offers a chance to detect early onset of PH. Structural changes of the myocardium (LV mass) associated with an increment of filling pressure after fluid loading, but myocardial deformation did not aid in the differentiation of this cohort. Strain did not appear useful to identify to the preclinical phase of SSC related heart disease.

10.7 Conclusion

Early detection of PH through fluid loading can be performed safely in an SSC cohort, but the ability of echocardiographic parameters to detect responders has not been shown. Whether early disease treatment should be established based on fluid loading response also is not known. Likewise, the prognostic significance of a fluid loading response in regards to PAH outcome is unknown.

10.8 Postscript

Echocardiography permits assessment of myocardial function along with haemodynamics. In SSC, changes are not only due to pressure elevations, but also to intrinsic fibrotic changes in the myocardium. Early pharmaceutical intervention can improve patient symptom status, but physicians must also consider side effect risk to patients [301].

Although echocardiography was not predictive of fluid response, exercise could be a more appropriate stressor of the pulmonary vasculature in regards to PAH symptom development. The up triation of treatment is primarily guided by changes in functional class [10]. In SSC, there is increased risk of developing left heart disease thus echocardiography can reveal the underlying pathology that might provoke disease.

There are other tools which may be better for tracking outcome. Increased pressure depends on pulmonary vascular properties; impaired vascular function could detect early changes in the SSC population. The next chapter will evaluate the value of vascular function.

Chapter 11

Early detection; Microvascular and Pulmonary vascular disease

In preparation for submission

11 Early detection – microvascular function and pulmonary vascular disease

11.1 Preface

SSC is an interesting model of PH because it provides an opportunity to observe a phase when pulmonary pressures are healthy, despite pulmonary vascular changes. Echocardiography is a widely used non-invasive screening tool in SSC, and vital in patient risk stratification. As discussed, conventional echocardiographic markers are primarily indicators of late-stage disease. Other non-invasive methods exist which could be used to assess disease status.

Screening with echocardiography is recommended if patients present symptomatically, the presence of TR velocity > 2.5 m/s is used to refer patients for invasive measures [302]. This elevation in PA pressure only occurs after a significant amount of the pulmonary vascular bed is destroyed. Algorithms for early detection have also included right atrial size [295], although this is a marker of end-stage disease progression.

Histological samples suggest small vessel associated disease in the connective disease cohort [303]. Although direct assessment of the pulmonary vasculature is possible with MRI, this has limited feasibility for clinical follow-up. Other methods include single-photon emission computed tomography which measures lung perfusion, and absolute quantification of pulmonary blood flow, but due to radiation dosage, repeated use for clinical follow-up is not recommended. Direct measurement of vascular function is a practical way in which patients with vascular disease are identified.

A number of different peripheral measures of vascular dysfunction exist. Assessment can be split into micro or macrovascular function (cut off 100 microns). Vascular

function has been used in the association of left-sided heart disease, but limited work has been done with microvascular function and right-sided echocardiographic parameters.

11.2 Abstract

Background. SSC is a multi-organ disease that presents with sclerodactyly, digital ulceration and exercise impairment related to interstitial lung disease, pulmonary vascular disease as well as systolic and diastolic heart failure. We sought to characterise associations between central and peripheral dysfunction in SSC, with the hypothesis that macrovascular disease would be more closely related to traditional CVD endpoints, while microvascular disease would be related to subclinical cardiac dysfunction.

Methods. We identified 88 patients diagnosed with SSC - 21 with diffuse disease (26%), and 35 (38%) on treatment for PAH. Assessment of microvascular function was performed with brachial flow-mediated dilatation (FMD), peripheral artery tonometry (PAT) and laser Doppler flowmetry (LDF) in response to a 5 minute period of occlusive hyperaemia. Echocardiography assessed pulmonary artery pressure, LV and RV function.

Results. Traditional CVD risk factors did not show associations with macrovascular disease, with microvascular function having modest correlations with disease duration. Macrovascular function appeared associated with LV mass and RV size, and in the PAH group, the microvascular function associated with RV function.

Conclusion. Microvascular disease appears related to RV function in PAH. The macrovascular disease appears to relate to traditional heart disease factors such as LV mass. Endothelial function markers do not appear to be interchangeable in assessing patient outcome.

11.3 Background

SSC is a multisystem autoimmune disease which invariably leads to vascular damage and fibrosis in heart, lungs and other internal organs. Vascular disease can manifest as ischemia of the peripheral extremities, PAH, and secondary Raynaud's phenomenon. Although a rare disease (~242 cases per million adults) [304], this presents a significant burden; 1 and 3 year survival rates in CTD-related PAH are significantly lower than in idiopathic PAH [305]. SSC patients have repeated follow-up visits involving multiple specialists, and SSC associated with serious adverse events during PAH treatment [306].

Peripheral disease subtypes include limited cutaneous (features on the face, forearms and lower legs), or the less common diffuse cutaneous sclerosis (upper arms, thighs and trunks). Peripheral digit amputation is needed in ~15% [307]. Vascular damage occurs at a micro and macro-vascular level, both peripherally and centrally. The cause of death is predominantly heart and lung disease related [308]. Nonfatal outcomes are based on peripheral diseases, such as ulcer rates and amputations, or central CVD outcomes such as PAH development, and LV dysfunction. This combination of peripheral and central disease creates a complex disease phenotype, and the disease trajectory is highly individualised. However, better characterisation of the underlying disease processes might facilitate interventions to improve mortality rates, which have been unchanged over the past few decades [308]. We hypothesise that microvascular and macrovascular disease will be associated with left-sided cardiac function, while microvascular will be associated with peripheral disease, and right-sided function.

11.4 Methods

11.4.1 Study group.

We recruited 88 patients from the Tasmanian scleroderma database. Written informed consent was provided, and the Human Research Ethics Committee (Tasmania)

Network approved the study (H14301). Studies were performed at two sites, Menzies Institute of Medical Research (Hobart) and Launceston General Hospital (Launceston). Patients were asked to refrain from caffeine and nicotine for at least 6 hours before testing and had no heavy meals before testing (a light breakfast was allowed 4 hours before testing). Patients were tested in a climate controlled room (~ 24 ºC) after patients had been lying supine for >15 minutes. Patients with PAH were diagnosed with invasive RHC and had been stable on PAH therapy for at least 1 year (n=34). Patients treated with vasodilator therapy (mean duration 7.1±3.3 years) did not refrain from PH medication before the studies.

We excluded patients with acute myocardial infarction within 3 months but did not selectively exclude patients with diabetes mellitus, CAD, hypercholesterolemia, hypertension or history of valve repair.

11.4.2 Total skin scores.

Rodnan's skin scores were performed by a specialist rheumatology physician or nurse [309]. By skin involvement, diffuse cutaneous sclerosis was classified as skin involvement proximal to the elbows and skin. Limited cutaneous sclerosis included skin involvement distal to the elbow and knees.

11.4.3 Brachial flow-mediated dilatation.

Studies were performed according to published guidelines [103], using standard equipment (Philips iu22, Phillips Healthcare, Bothell, WA and Vivid I, General Electric Medical Systems, Milwaukee, WI). A single expert sonographer performed all studies. A cuff was placed on the forearm; an ECG tracing was obtained with 3 beat acquisitions used. Full methods detailed in chapter 2 methodology.

11.4.4 Finger plethysmography.

Peripheral artery tonometry (PAT) measurements were obtained with plethysmography (Endopat 2000, Haifa, Israel). All jewellery was removed before testing. Testing followed recommend guidelines [104], and hyperemic measurements were performed simultaneously with brachial FMD measurements. The index finger was used for the majority of testing (94%); if this finger was not available (due to digit amputation, or open wounds), the next finger with no open wounds was used-usually the ring finger (3.4%), with the 3rd and 5th digit for use for 1 patient each. Full methods detailed in chapter 2.

11.4.5 Laser Doppler Flow-mediated dilatation:

Laser Doppler probes (CP1, Moor Instruments, UK) were placed on the subcutaneous tissues on the dorsal side of the forearm. The skin was shaved and wiped with alcohol. Probes were fixed lightly with medical tape to the same arm as was used for brachial FMD and Endopat-2000. Measurement of data was performed according to the methodology of Roustit *et al.* [106]. The full methodology is detailed in chapter 2.

11.5 Echocardiography.

Echocardiograms were obtained in the closest possible temporal proximity to the vascular studies and measurements were performed according to guidelines[101] Left ventricular free wall strain (LV GLS; Velocity vector imaging, Tomtec GmbH, Unterschlessheim, Germany) was performed in 3 apical images; right ventricular (RV) strain was performed on the RV free wall. PASP was measured from the tricuspid jet regurgitation signal, plus RAP (determined from IVC distensibility). Peak velocities of the early (E) and late (A) diastolic filling were derived from spectral Doppler of transmitral inflow. Tissue Doppler imaging was used to determine the peak diastolic early velocity (e') of the lateral and septal mitral annulus from the apical 4-chamber

view. Standard ranges of echocardiographic parameters [101] were used to identify studies as normal or abnormal.

11.5.1 Statistical analysis.

Sample size calculations were powered for the primary hypothesis that FMD and PAT ratio was higher in patients treated than untreated. Work will be the first observational trial to characterise the difference in endothelial function in SSc patients with and without pulmonary hypertension treatments, so the effect sizes are estimated from previous observations of a PAT ratio difference of 0.4 (between SSc controls and SSc-PAH patients) and a clinically meaningful 7% increase in FMD[310]. With an anticipated effect size of 0.68, a power of 0.8 and a type I error of 5% (two-tailed) we will need a minimum of 35 patients per group to demonstrate a difference in endothelial function. This study is not powered to identify differences in endothelial function between types of PAH therapies but will be hypothesis generating.

Data were analysed with standard statistical software (SPSS version 21, IBM, Chicago, IL). Baseline data are presented as mean or median and standard deviation or inter-quartile ranges. Brachial FMD, resting LDF, peak LDF, PASP, E/e' and LV mass/BSA were log-transformed to obtain normality. Mann-Whitney U-test was used to assess significance between groups (p-value set to <0.05). Logistic regression was used to assess associations, with bivariate regression used for dichotomous variables.

11.6 Results

Baseline characteristics. Of 88 patients (median age 63 years, IQR 55-68), 21 (26%) had diffuse SSC (Table 11.1). The median time since diagnosis of SSC was 11 years (IQR6-18), and the median Rodnan's skin score was 6 (IQR 2-12). Although 25 patients had previous or active skin ulceration (28%), only 4 patients had previous

digit amputation (5%). Dyslipidemia was the most prominent cardiovascular risk factor (20%), with small numbers with a history of CAD (10%), and diabetes (7%).

PAH had previously been diagnosed in 34 (38%), although most of these patients (92%) showed normal PASP by echocardiography (25 mmHg). Most of these patients were treated with endothelin receptor antagonists (30%), or phosphodiesterase type 5 inhibitors (8%). Groups showed standard medians for vascular and echocardiographic markers (Table 11.2).

LV and RV dysfunction (Table 11.3) were present in a minority of patients - 28% displayed reduced RV radial contraction (RV FAC <35%), with 12% of patients showing reduced RV longitudinal function (RV free wall strain <16%).

There were low levels of overt LV systolic dysfunction (2 patients displayed LV EF <50%), although 40% of patients displayed reduced global longitudinal strain (LV GLS <19.7%). Stroke volume of <60 ml was present in 75% of patients.

A similar proportion of patients displayed markers of diastolic dysfunction; 48% showed increased LV filling pressures (E/e'>8), and 37% showed increased LA size (LAV indexed > 34 ml/m^2).

Table 11-1. Patient baseline demographics

	Group (N=88)
Age (years)	63(55-68)
Disease Duration (years)	11 (8.0)
Sex (female)	76%(68)
SSC limited (vs. Diffuse)	75%(67)
SBP (mmHg)	128 (21)
HR (bpm)	71 (13)
Diagnosed PAH	35(38%)
Medications	

- **Any ERA**	27(30%)
- **Any PDE5**	7(8%)
Statin	19(78%)
Diuretic	6 (7%)
ARB	22(25%)
BB	7(8%)
CCB	25(28%)
ACEI	16(18%)
Diabetes	7%(6)
Coronary Disease	10%(9)
Dyslipidaemia	20%(18)
DBP (mmHg)	72 (14)
BMI	26.4 (6.3)
Skin Score	4.5 (7)

Abbreviations. BMI, body mass index; BSA, body surface area; ERA, endothelin receptor antagonists; PDE5, phosphodiesterase type 5 inhibitor; DBP, diastolic blood pressure; SBP, systolic blood pressure; HR, heart rate; SSc, systemic sclerosis; TCP02, transcutaneous tissue oximetry

Table 11-2. Vascular and echocardiographic function

Vascular function (n=88)	**Median (IQR)**		
• **Baseline LDF (PU)**	42.5(48.6)		
• **Peak LDF (PU)**	147.6(82.5)		
• **Peak-Baseline LDF (PU)**	91.4(68.9)		
• **FMD (%)**	2.9 (4.9)		
• **Log Reactive Hyperaemia**	0.51(0.75)		
Echocardiography (n=75)	Median (IQR)	Normal	Abnormal
• **PASPe(mmHg)**	25.2 (9.4)	65(91.5%)	6 (8.5%)
• **LV Mass/BSA (gm/m^2)**	111.9(43.1)	61(69%)	12 (14%)
• **SV (ml)**	53 (21)	18 (25%)	53 (75%)
• **LVEF (%)**	60(13)	71(97%)	2(3%)
• **LAV/BSA (ml/m^2)**	32.7(11.5)	46(52%)	27(30%)
• **e' septal (cm/s)**	6.0(4)	30(43%)	40 (57%)
• **E/e' average**	8.4(3.2)	38(55%)	31(45%)
• **LV GLS (%)**	20.3(2.9)	44(49%)	29(40%)
• **RVEDA/BSA (cm^2/m^2)**	9.1(2.1)	68(92%)	6 (8%)
• **RAV/BSA (ml/m^2)**	22.3(11.9)	49(66%)	25(34%)
• **TAPSE (cm)**	2.1(0.53)	65(88%)	9(12%)
• **RVFAC (%)**	39.2(11.9)	53(60%)	21(28%)
• **RV free wall strain (%)**	23.1(4.9)	62(84%)	12(16%)

PU, Perfusion units; LAV, left atrial volume; LDF, laser Doppler flow; LV, left ventricular; LVEF, left ventricular ejection fraction; LVGLS, left ventricular global longitudinal strain; PASPe, pulmonary artery systolic pressure via echocardiography; RV, right ventricular; RVEDA, right ventricular end-diastolic area; RVFAC, right ventricular fractional area change; TAPSE, tricuspid annular plane systolic excursion

11.6.1 Associations of vascular function.

Vascular function measures did not have significant associations with SSC characteristics such as the presence of PAH, diffuse versus limited SSC and history of peripheral ulcers (Table 11.4), although PAT and disease duration did show weak associations (std β-0.24(-7.2;0.02), p=0.05). Traditional CVD risk factors did not show any significant associations with vascular function makers (Table 11.1, Appendix).

Table 11-3. Vascular function markers and SSC disease status

	History of ulcers		Disease duration		Rodnans skin score (log)		Diffuse Vs. limited (bivariate)	
	Std β (95%CI)	**P value**	**Std β (95%CI)**	**P value**	**Std β (95%CI)**	**P value**	**HR (95%CI)**	**P value**
Brachial FMD (log)	1.5(0.47;5.0)	0.48	0.12(-2.2;6.4)	0.33	-0.08(-0.35;0.18)	0.54	0.79(0.24;2.6)	0.69
PAT (log)	0.83(0.29;2.4)	0.72	**-0.24(-7.2;0.02)**	**0.05**	-0.23(-0.34;0.02)	0.09	1.2(0.41;3.7)	0.71
Baseline LDF (log)	1.5(0.32;7.3)	0.59	0.13(-2.5;9.1)	0.26	0.11(-0.16;0.42)	0.38	0.53(0.10;2.9)	0.47
Peak LDF (log)	1.9(0.13;28.1)	0.64	0.13(-4.4;15.30	0.27	-0.006(-0.53;0.51)	0.96	1.9(0.11;33.5)	0.65
Peak-Baseline LDF	1.0(0.99;1.01)	0.995	0.01(-0.04;0.04)	0.92	-0.08(-0.003;0.001)	0.51	1.01(0.99;1.02)	0.41
Linear regression for vascular and echocardiography								
	LV mass		**LV GLS**		**E/e' avg**		**LAV/BSA**	
	Std β (95%CI)	**P value**	**Std β (95%CI)**	**P value**	**Std β (95%CI)**	**P value**	**Std β (95%CI)**	**P value**
Brachial FMD (log)	**-0.36(-28.7;-5.8)**	**0.004**	-0.05(-2.0;1.4)	0.73	0.04(-1.6;2.3)	0.75	0.04(-0.46;0.61)	0.78
PAT (log)	-0.14(-15.5;4.5)	0.28	0.09(-0.88;1.8)	0.50	**0.26(0.06;3.4)**	**0.04**	-0.09(-6.0;3.0)	0.50
Baseline LDF (log)	0.03(-15.2;19.9)	0.79	-0.03(-2.4;1.9)	0.83	-0.09(-3.6;1.8)	0.49	0.15(-3.0;12.4)	0.23
Peak LDF	-0.10(-42.4;18.4)	0.43	-0.06(-4.3;2.8)	0.66	-0.21(-8.4;0.63)	0.09	0.02(-12.1;14.6)	0.85
Baseline-Peak LDF	-0.17(-0.21;0.04)	0.18	-0.03(-0.02;0.01)	0.81	**-0.25(-0.04;0.00003)**	**0.05**	-0.14(-0.09;0.02)	0.26

FMD; Flow-mediated dilatation; PAT, peripheral arterial tone; LDF, laser Doppler flowmetry; LV, left ventricle; GLS, global longitudinal strain; LAV/BSA left atrial volume to body surface area.

Table 11-4. Vascular markers and RV function

	FAC		RV free wall strain		RVEDA/BSA		RAV/BSA	
	Std β (95%CI)	P value	Std β (95%CI)	P value	Std β (95%CI)	P value	Std β (95%CI)	P value
Brachial FMD (log)	0.08(-3.2;6.3)	0.51	-0.13(-3.6;1.2)	0.31	-0.27(-2.3;-0.08)	0.04	-0.22(-10.2;0.57)	0.08
PAT (log)	0.25(0.06;7.3)	0.05	0.13(-1.006;3.1)	0.31	-0.09(-1.1;0.52)	0.47	-0.03(-5.1;4.2)	0.85
Baseline LDF (log)	-0.13(-9.5;2.9)	0.30	0.04(-2.9;4.1)	0.74	-0.03(-2.07;1.7)	0.82	-0.06(-9.5;5.9)	0.64
Peak LDF (log)	-0.14(-16.8;4.7)	0.26	0.03(-5.3;6.8)	0.80	-0.11(-4.7;1.7)	0.36	-0.15(-21.4;5.0)	0.22
Peak-Baseline LDF	-0.15(-0.07;0.02)	0.24	-0.04(-0.03;0.02)	0.77	-.10(-0.02;0.008)	0.41	-0.15(-0.09;0.02)	0.23
Restricted to PAH treatment group only								
	FAC		**RV free wall strain**		**RVEDA/BSA**		**RAV/BSA**	
	Std β (95%CI)	P value	Std β (95%CI)	P value	Std β (95%CI)	P value	Std β (95%CI)	P value
Brachial FMD (log)	-0.09(-0.02;0.01)	0.63	-0.01(-4.1;3.9)	0.96	-0.41(-4.2;0.38)	0.02	-0.22(-17.3;4.3)	0.23
PAT (log)	-0.41(0.003;0.06)	0.03	0.40(0.18;5.6)	0.04	-0.29(-2.3;0.33)	0.14	-0.07(-9.6;6.7)	0.71
Baseline LDF (log)	0.12(-6.4;12.0)	0.54	0.09(-3.6;5.8)	0.65	-0.23(-6.0;1.5)	0.22	-0.23(-21.4;5.0)	0.21
Peak LDF (log)	0.17(-6.9;18.5)	0.36	0.21(-2.9;9.9)	0.27	-0.14(-7.1;3.4)	0.47	-0.18(-27.4;9.6)	0.34
Peak-Baseline LDF	0.12(-0.04;0.08)	0.55	0.11(-0.02;0.04)	0.58	0.02(-0.02;0.03)	0.92	-0.06(-0.10;0.07)	0.76

FMD; Flow-mediated dilatation; PAT, peripheral arterial tone; LDF, laser Doppler flowmetry; FAC, fractional area change; RVEDA/BSA, right ventricular end diastolic area/ body service area; RAV/BSA, right atrial volume/ body service area

11.6.2 Vascular function and echocardiographic findings.

Brachial FMD was associated with indexed LV mass (std β-0.36[-28.7;-5.8], p=0.004), but not with LVGLS, or diastolic markers (Table 10.3). LV filling pressures showed a weakly significant association with microvascular function measures (baseline-peak LDF std β-0.25[-0.04;0.00003], p=0.05; PAT std β 0.26[0.06;3.4], p=0.04). RV structure showed a mildly significant association with brachial FMD (RVEDA cm/m^2 std β -0.41[-4.2; 0.38], p=0.04). RV radial function as measured with RV FAC showed a moderate association with microvascular function (std β-0.25 [0.06;7.3], p=0.05),

In order to correct for treatment with vasodilators, assessment of RV function parameters was restricted to those on active treatment for PAH. This showed a moderate, significant association with brachial FMD and PASP (r=0.52, p<0.001), RAV/BSA (r=0.40, p=0.02) and RVEDA/BSA (r-0.49, p=0.04). There were moderately significant associations with PAT and RV free wall strain (Table 4) (r=0.40, p=0.04) and FAC (r=0.41, p=0.03) (Figure 11.1).

Figure 11-1. Associations with RV function parameters and microvascular function.

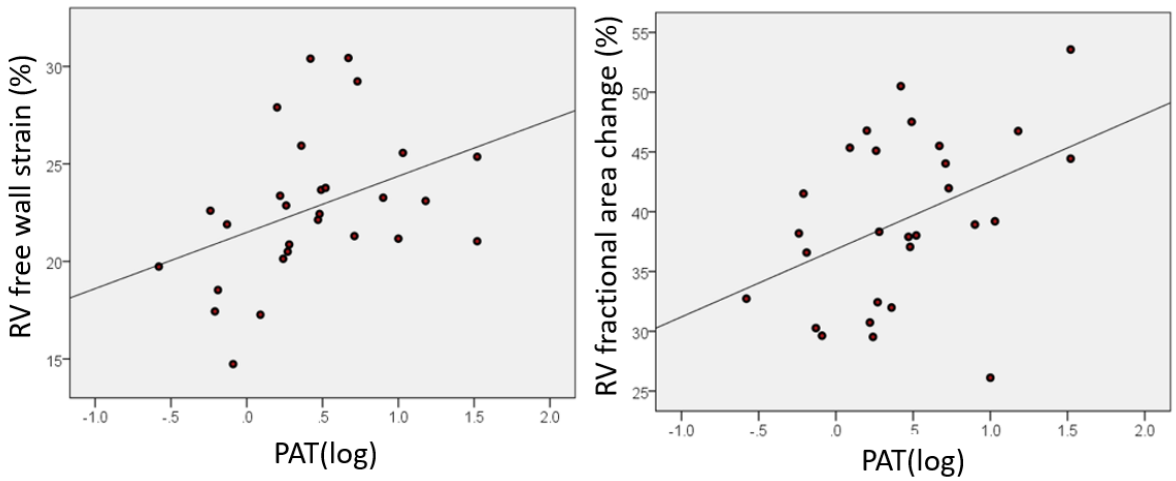

PAT shows moderate significant correlation with RVFWS (r=0.40, p=0.04) and FAC (r=0.41, p=0.03)

11.7 Discussion

The results of this study with patients with SSC showed that LV mass and macrovascular dysfunction appeared related, whereas microvascular function showed only a minor association with diastolic dysfunction. Traditional CVD risk factors did not seem strongly associated with the vascular function. Digital microvascular function showed moderate associations with RV function in both FAC and RV free wall strain.

11.7.1 Vascular function measures.

The heterogeneity of systemic SSC creates a wide variation in the description of cohorts in the literature. Fibro-proliferative disease in the vasculature, combined with underlying risk factors [311], has led to the proposal of the term 'accelerated atherosclerosis' in SSC. Our groups had small rates of associated chronic disease, but groups did seem to have reduced vascular function as compared to normal ranges. We did not measure carotid IMT in our cohort (a popular surrogate for CVD risk), although there is no consensus about the value of this parameter [312].

Our findings on the association of brachial FMD and LV mass has been shown in a population-based cohort [313]. This association was also witnessed in this group of SSC patients with multiple risk factors, suggesting trials targeting LV structure might include brachial FMD as a surrogate marker of vascular function. Brachial flow-mediated dilatation (FMD) [102] has been used as a measure of atherosclerotic risk and macrovascular disease in SSC in a large number of trials [314]. Its previous use in SSc [315] suggested value in differentiation between diffuse and limited entities [315], although this differentiation was not shown in our findings.

LDF relies on the Doppler shift of the red blood cells in the microvasculature, with this expressed in perfusion units, although a variety of different methodologies have

been proposed [316,317]. Its use is mainly limited to the research domain, with studies into the relation of outcome in CVD and SSC not yet performed. We showed weak, significant associations with diastolic function and markers. We feel more work should be performed in this area before results are extrapolated.

A primary strength of PAT measures is the relative level of operator independence as compared to brachial FMD [104]. The prediction of CV events is similar between EndoPAT and FMD [318], with prognostic information available in a variety of disease cohorts [318]. Nonetheless, within the SSC population, we have found this measure to have some limitations. Due to the nature of the disease, there are difficulties performing measures on the same finger (active ulcers and amputations). If this measure is to be used for an SSC cohort, these reproducibility issues should be addressed. Interestingly, although brachial FMD and Endo-PAT 2000 measured endothelial function, clinical correlates did differ in population-based cohorts [319] and did not seem significantly related [320].

11.7.2 Echocardiography in systemic sclerosis.

Echocardiography has been adopted as a tool for both clinical and research outcomes in SSC. Cardiac involvement in SSC can manifest in a number of mechanisms.

Fibrosis may present as myocardial damage, fibrosis of the conduction system or pericardial disease [217]. Clinically, diastolic dysfunction is the most frequently observed manifestation of cardiac involvement [321] and present in 17% of patients, with significant mortality due to heart disease [322]. There was a significant number of patients with reduced GLS within our cohort, but impaired systolic function rates were low. Diastolic dysfunction showed similar results, with large numbers showing markers of raised LV filling pressures. There has been limited work on the association of

peripheral and cardiac manifestations of SSC [323]. Left-sided cardiac disease (LV GLS) has shown an association with brachial FMD in a small number of SSC patients [324].

The clinical focus has been placed mainly on detection of pulmonary pressures with tricuspid regurgitation, but as shown in outcome in PAH trials, RV strain is a strong predictor of outcome [77]. We are looking to track this cohort over time, to determine if RV strain in SSC has similar findings. RV dysfunction in SSC-PAH could occur primarily as a response to afterload increases [325], but work with the novel parameter isovolumetric acceleration, which is a load-independent marker of RV function, has shown this to be impaired in patients without PAH-induced SSC [87].

11.7.3 Limitations.

The SSc population in this study was a highly heterogeneous group, with patients displaying a wide range of skin and internal organ involvement. Patients also had a history of traditional cardiovascular disease risk factors, with a significant proportion having diabetes and small numbers with prior myocardial infarction. However, this population truly reflects the interplay between different comorbidities in SSc [326]. An omission from this chapter is the echocardiographic measurement of flow. Brachial flow-mediated dilatation with the flow was measured, but evidence shows markers are not a robust substitute for cardiac flow[327] thus have not been included in the paper.

Conclusion.

Vascular function and echocardiography both have an essential role in the characterisation of disease status. Micro and macrovascular function in SSC appears to have different traditional and echocardiographic associations. PAH and microvascular disease appear related to RV function measures, while macrovascular disease relates to LV structural heart disease.

11.8 Postscript

SSC patients with worse PAH have worse outcomes than their idiopathic PAH counterparts, even in the presence of less severe haemodynamic profiles [328]. It is difficult though to decide how accurate early prediction markers are, and whether early treatment should be initiated in the presence of impaired vascular function. Vascular dysfunction can present as a number of comorbidities associated with SSC, and differentiating the cause of dysfunction is not possible.

Sequential follow-up of patients, as opposed to detection at a single time point is also important. There is limited information on the variability of vascular function measures over follow-up. Issues with skin thickening and fluctuations in weather conditions can drastically change peripheral vascular status. Tests should be replicable and disease-specific. Although microvascular tests can be performed non-invasively, patient functional status is what physicians use to guide treatment.

Previously in this thesis, we have attempted to identify early disease markers through speckle tracking of the myocardium. However, we have not shown a clear marker for early cardiac disease in this cohort. It is likely that early detection and screening for PH offers substantial benefits, novel techniques need to be assessed in large registry data to establish how tools can impact survival.

11.1 Appendix

Table 11-5. Bivariate logistic regression and traditional cardiovascular disease risk factors

	History CAD		**History of HTN**		**History of Type 2 diabetes**		**History Dyslipidaemia**	
	Std β (95%CI)	P value	Std β (95%CI)	P value	Std β (95%CI)	P value	Std β (95%CI)	P value
Brachial FMD (log)	0.47(0.10;2.3)	0.36	**0.95(0.32;2.8)**	**0.92**	**1.09(0.13;8.8)**	**0.94**	**0.46(0.13;1.6)**	**0.23**
Log PAT	0.44(0.11;1.8)	0.25	**1.2(0.48;2.9)**	0.72	**0.52(0.11;2.5)**	0.42	**-0.03(-5.1;4.2)**	**0.85**
Baseline LDF (log)	2.1(0.20;22.4)	0.54	**1.2(0.29;4.8)**	0.83	**0.44(0.03;6.9)**	0.56	**1.5(0.26;8.2)**	0.67
Peak LDF	0.44(0.009;23.1)	0.69	**0.09(0.007;1.1)**	0.06	**0.01(0.001;1.3)**	0.06	**0.34(0.02;6.2)**	0.34
Baseline-Peak LDF	0.99(0.98;1.01)	0.42	**0.99(0.98;0.998)**	0.03	**0.98(0.96;1.005)**	0.12	**1.0(0.99;1.01)**	0.67

12 **Conclusion**

This thesis aimed to determine the role of advanced imaging techniques in PAH follow-up. From this thesis, I have been able to draw a number of conclusions about the use of speckle tracking in the assessment of the RV. Chapter 3 details the importance of baseline measures, specifically of the right ventricle using RV free wall strain. When correcting for changes over time, RVFWS was the only RV function measures which displayed superiority. Finding that changes over time do not predict outcome appears counterintuitive but provides practical advice for clinicians in the follow up of pulmonary hypertension. Limitations in techniques involved in this paper could have weakened the results. Our use of averaging changes over visits could lead to dilution of this effect. There is variability in technical factors of echocardiography such as imaging windows, and tracing of the myocardium. The optimal research protocol would use prospectively acquired data, with images capture on the same ultrasound machine. PAH is a rare disease with low incidence rates. Therefore prospective recruitment of patients is time consuming and would require multiple sites. Disease registries are the most powerful tool available to detect predictors of outcome. Registries do not have access to the level of echocardiographic data which is available in our cohort. Our paper also has strength in the use of a sole sonographer for echocardiographic measures decreasing inter-variability error. Our use of the novel echocardiographic RVFWS has not been compared in great detail to traditional outcome markers. Comparison of traditional systolic markers is essential to understand the role which novel markers have in improving clinical follow up of PAH.

CMR is the optimal scanning method, but its cost restricts wide spread use in clinical follow-up. Throughout follow up, patients treatment regimens were accelerated or

reduced in line with symptom statues. This was not accounted for over clinical follow-up but has an impact on the magnitude of changes.

Chapter 4 addresses the impact which RV afterload has on the measurement of RV systolic function. Animal studies and invasive pressure-volume loop work define how vital the afterload to systolic function relationship is. There is no ideal way to account for the relationship bedside. The study results show that RVFWS is robust in differentiating 10 and 15% changes in pressure over time. Measurement of invasive pressure at the time of echocardiographic study would be ideal, but difficult to achieve in practice. Work performed in this chapter is considered as a "proof of concept", and highlights areas of interest in the clinical field which require more work. There are numerous concepts to considering when identifying the effect of afterload on RVFWS (pulsatile load, previous RV infarct or disease, pathophysiology flow through the ventricle), but concise measurement of these in a clinical cohort with non-invasive means would be complicated. A second validation cohort to test regression equation would increase the strength of this work.

Clinical applicability of findings is an essential aspect of the thesis. The chapter on pulmonary embolism answers a crucial diagnostic dilemma encountered in clinical practice; the differentiation of RV failure cause. In this chapter, RV failure in cohorts was matched for pressure assessment. A secondary matching technique would be through the pulmonary vascular resistance which would take into account flow through the ventricle. Due to the acquisition of pulmonary embolism scans during a critical care period, scans did not have flow measured, physicians instead ask for a targeted study to assess the presence of embolism and comments on RV size and function. Unfortunately, this is a reality of using retrospective data from a clinical cohort.

Although the mean differences for the Bland-Altman analysis are small, there appears to be some bias present with higher values showing increased mean differences between reads. Clinical applicability is a strong focus of the work which I have performed. Work in the pulmonary embolism cohort shows work can be translated to the bedside during routine clinical practice.

Two chapters in this thesis have presented work on the longitudinal follow up of the PAH cohort. In Australia, six monthly visits are mandated. Within our data, the timing of follow up was not six month for all patients. The reasons for this a multifaceted. Firstly, only two tests were required to be performed. Primarily, this was an echocardiogram or 6MWD. If patients had a RHC done, they are not required to have both non-invasive tests performed. Treating teams can apply for an exemption if one measure is not available (for example an injury means no 6MWD can be performed). There were also limitations with echocardiographic databases, or some studies performed off-site. These are limitations of the retrospective nature of this work, but we feel it does not limit the strength of our findings.

Chapter 7 details differentiation of left versus right heart disease in the systemic sclerosis cohort. Again, the retrospective nature of the paper leads to issues in the collection of clinical data. An example of this is the lack of DLCO% available in this cohort. The DLCO is a robust outcome predictor. In this chapter, the focus was on the novel LV function markers of circumferential strain, which was not assessed in our other cohorts. Models showed a significant association between GCS and PASP but with a weak R squared value suggesting there may be limited applicability in an individual patient setting. The use of multivariable

The control cohort for this paper had high all-cause readmission or death occurred in 38% of the matched patient which is high for a matched group. The control cohort had high readmission rates, associated with the high incidence of COPD. The high rates of readmission present also relate to patients being recruited Tasmanian echocardiography databases, thus had a select bias for having an echocardiographic study performed. In this sense, they are not a pure control cohort as they have a clinical indication for echocardiography. A more accurate control cohort would have been from a community subgroup. The SSC cohort constituted of those with treated pulmonary arterial hypertension hence TR Vmax levels would be lower than in a treatment naïve cohort. The levels of PAH in the SSC group also add bias, as patients have already been diagnosed. A subgroup analysis was performed on those without PAH treatment, and results still hold true. A limitation of this paper is the omission of RVFWS thus it could not be included analysis with the LV GCS. As RVFWS is a marker of early cardiac disease, this would have been a more appropriate comparison as opposed to RVS' and TAPSE.

The distinction between pre versus postcapillary pulmonary hypertension is addressed in chapter 8. The cohort consisted of a large percentage of diagnosed PAH. In the normal screening population, rates of increased TR V max would be significantly lower in a population-based cohort. Cause of pulmonary hypertension has a drastic impact on the follow up required for the presenting patient. If diastolic dysfunction cannot be measured and accurately assessed, the need for invasive measures of patient haemodynamics is required. Work in this chapter shows further work needs to be done in this area to improve the sensitivity and specificity of LV filling pressure assessment with echocardiography.

The utility of RA function for clinical decision making has not been previously assessed. Although normal ranges have are quoted, research translation into clinical practice has not occurred. Our work has attempted to bridge this gap and determine the use RA strain in improving the sensitivity of echocardiographic estimation of RAP. Other work has been performed using secondary markers to improve the sensitivity of echocardiography. Secondary markers include tricuspid E/e, hepatic vein and superior vena cava flow. These markers were not routinely collected in our cohort, and we were not able to include these into the sensitivity and specificity analysis. The study did not show any significant increase in sensitivity with RA strain. Reasons for this could be differentiated into two main categories, physiological reasons or errors with the calculation of right atrial strain. Our cohort is not equipped to fully delve into the differentiation of these reasons. The gold standard would involve sonomicrometry of the right atrium, with simultaneous measures of right atrial pressure. Errors seen in clinical practice relate to image quality (adequate visualisation of the right atrial border), heart rate and consistencies with region tracking.

The fluid loading chapter presents a cohort of clinical interest in attempting to find early onset markers of pulmonary hypertension. The majority of these patients had systemic sclerosis. As mentioned in previous chapters this cohort can present with pre or post capillary pulmonary hypertension. It is hard to differentiate the cause of the raised pressure hence this group have not been included in the WHO pulmonary hypertension guidelines as a PH subtype. To determine the natural history of patients who present with raise pressure with fluid, they would need to be tracked over time and monitored for invasive changes. A control group of age-matched patients without SSC undergoing fluid loading to show how changes compare against a

healthy cohort would have been an interesting addition to the thesis. Research work now shows exercise is the preferred method of stress for diagnosing early changes in the pulmonary vasculature.

In the final chapter presented vascular function in systemic sclerosis. Dichotomization of normal versus abnormal was based on conservative values of decreased function. By using these ranges, it reflects the early stage of cardiac disease which is more applicable when assessing microvascular changes. Cardiac stroke volume was significantly reduced in a large percentage of patients. Invasive measures of cardiac output are the gold standard, once diagnosed with PAH, we did not have a significant number of sequential invasive studies performed to add values into our analysis. Instead, the echocardiographic calculation was used. Measures were calculated as LVEDV-LVESV. As mentioned in the introduction statements, changes in morphology during PAH significantly alter LV geometry, which would have significantly hampered the success SV in our analysis. Stroke volume ranges are from a composites of large data sets. Our paper has a high percentage of women and a mean age of 63. Both of these factors lead to a reduction in stroke volume and overestimation of patients with impaired function.

An interesting study design would be to follow microvascular changes over time and determine what outcome this has on cardiac parameters. As mentioned previously in the thesis, the SSC cohort is highly heterogeneous thus determining casualty based on changes would require intense monitoring of changes in a variety of organs.

In conclusion, RV strain imaging is predictive of outcome in PAH- importantly, this is incremental and independent of PASP.

1) The time course/chronicity of the disease seem to be a better clue to the underlying cause of RV dysfunction than afterload increase

2) RV free wall strain appears to be robust in the face of standard minor clinical fluctuations in PASP, more so then traditional 2D systolic function markers.

3) RV free wall strain was also independent of pulmonary pressure for prediction of 6MW distance.

The use of strain in PH is not limited to the assessment of RV dysfunction but can be used in RA pressure estimation, LV function in SSC and in distinguishing pre from post-capillary pulmonary hypertension. We have found that in a group with a high rate of PAH, current guidelines do not offer strong guidance on the differentiation of LV and pulmonary vascular aetiologies for PH. Although RA speckle tracking was associated with RAP, it did not appear to add in the correction of pressure assessment. Speckle tracking imaging also shows potential in systemic CTD, exposing unique fibrosis patterns in the LV.

I have examined three methods for the detection of early disease, including strain combined with volume loading of the LV and vascular function markers. The vascular function had associations with echocardiographic LV and RV parameters, but heterogeneity in this population hinder its use as a strong discriminative marker. Speckle tracking echocardiography does not appear to detect elevations of invasive PCWP.

Future studies to progress the understanding of echocardiographic follow up in PAH should include the use of 3D imaging to accurately measure volume and chamber size.

Echocardiographic measures of flow are viable, but within the data presented did not show significance to outcome of 6MWD.

Assessment of PAH patients symptom status needs to go beyond the 6MWD. Exercise echocardiography, ideally with a supine bike using light exercise protocols, is well poised to assess haemodynamics simultaneously with exercise. A crucial aspect is if RVFW strain remains an accurate measure during exercise. Failure to augment RV function during exercise is an important predictor of status, titration of medications based on findings would add value to the clinical utility of RVFWS. From a technical standpoint, RVFWS currently is using the left ventricular strain package. Work from industry to determine if optimisation of algorithms for the RV should be made. Two concepts to work on are the thickness of the tracking segment and also the impact which the curvatures of the RV have on the algorithm.

In conclusion, new echocardiographic markers of RV systolic function offer a significant increment of prognostic information in PAH. The measurement of RV free wall strain should be integrated into clinical decision-making.

13 References

1. D'Alonzo GE, Barst RJ, Ayres SM, et al. Survival in patients with primary pulmonary hypertension. Results from a national prospective registry. *Annals of internal medicine.* 1991;115(5):343-349.
2. Benza RL, Miller DP, Barst RJ, Badesch DB, Frost AE, McGoon MD. An evaluation of long-term survival from time of diagnosis in pulmonary arterial hypertension from the REVEAL Registry. *Chest.* 2012;142(2):448-456.
3. Simonneau G, Gatzoulis MA, Adatia I, et al. Updated clinical classification of pulmonary hypertension. *J Am Coll Cardiol.* 2013;62(25 Suppl):D34-41.
4. Abramson SV, Burke JF, Kelly JJ, Jr., et al. Pulmonary hypertension predicts mortality and morbidity in patients with dilated cardiomyopathy. *Annals of internal medicine.* 1992;116(11):888-895.
5. Galie N, Rubin L, Hoeper M, et al. Treatment of patients with mildly symptomatic pulmonary arterial hypertension with bosentan (EARLY study): a double-blind, randomised controlled trial. *Lancet.* 2008;371(9630):2093-2100.
6. Lavie CJ, Hebert K, Cassidy M. Prevalence and severity of Doppler-detected valvular regurgitation and estimation of right-sided cardiac pressures in patients with normal two-dimensional echocardiograms. *Chest.* 1993;103(1):226-231.
7. Strange G, Playford D, Stewart S, et al. Pulmonary hypertension: prevalence and mortality in the Armadale echocardiography cohort. *Heart.* 2012;98(24):1805-1811.
8. Bshouty Z. Vascular compromise and hemodynamics in pulmonary arterial hypertension: model predictions. *Can Respir J.* 2012;19(3):209-215.
9. Allanore Y, Meune C, Vonk MC, et al. Prevalence and factors associated with left ventricular dysfunction in the EULAR Scleroderma Trial and Research group (EUSTAR) database of patients with systemic sclerosis. *Ann Rheum Dis.* 2010;69(1):218-221.
10. Galie N, Humbert M, Vachiery JL, et al. 2015 ESC/ERS Guidelines for the diagnosis and treatment of pulmonary hypertension: The Joint Task Force for the Diagnosis and Treatment of Pulmonary Hypertension of the European Society of Cardiology (ESC) and the European Respiratory Society (ERS): Endorsed by: Association for European Paediatric and Congenital Cardiology (AEPC), International Society for Heart and Lung Transplantation (ISHLT). *Eur Heart J.* 2016;37(1):67-119.
11. McLaughlin VV, Sitbon O, Badesch DB, et al. Survival with first-line bosentan in patients with primary pulmonary hypertension. *Eur Respir J.* 2005;25(2):244-249.
12. Gabler NB, French B, Strom BL, et al. Race and sex differences in response to endothelin receptor antagonists for pulmonary arterial hypertension. *Chest.* 2012;141(1):20-26.
13. Ling Y, Johnson MK, Kiely DG, et al. Changing demographics, epidemiology, and survival of incident pulmonary arterial hypertension: results from the pulmonary hypertension registry of the United Kingdom and Ireland. *Am J Respir Crit Care Med.* 2012;186(8):790-796.
14. McLaughlin VV, Badesch DB, Delcroix M, et al. End points and clinical trial design in pulmonary arterial hypertension. *J Am Coll Cardiol.* 2009;54(1 Suppl):S97-107.
15. Galie N, Hoeper MM, Humbert M, et al. Guidelines for the diagnosis and treatment of pulmonary hypertension: the Task Force for the Diagnosis and Treatment of Pulmonary Hypertension of the European Society of Cardiology (ESC) and the European Respiratory Society (ERS), endorsed by the International Society of Heart and Lung Transplantation (ISHLT). *Eur Heart J.* 2009;30(20):2493-2537.
16. Raymond RJ, Hinderliter AL, Willis PW, et al. Echocardiographic predictors of adverse outcomes in primary pulmonary hypertension. *J Am Coll Cardiol.* 2002;39(7):1214-1219.

17. Montani D, Savale L, Natali D, et al. Long-term response to calcium-channel blockers in non-idiopathic pulmonary arterial hypertension. *Eur Heart J.* 2010;31(15):1898-1907.
18. Brittain EL, Pugh ME, Wheeler LA, et al. Prostanoids but not oral therapies improve right ventricular function in pulmonary arterial hypertension. *JACC Heart failure.* 2013;1(4):300-307.
19. Langleben D, Brock T, Dixon R, Barst R, group S-s. STRIDE 1: effects of the selective ET(A) receptor antagonist, sitaxsentan sodium, in a patient population with pulmonary arterial hypertension that meets traditional inclusion criteria of previous pulmonary arterial hypertension trials. *J Cardiovasc Pharmacol.* 2004;44 Suppl 1:S80-84.
20. Humbert M, Barst RJ, Robbins IM, et al. Combination of bosentan with epoprostenol in pulmonary arterial hypertension: BREATHE-2. *Eur Respir J.* 2004;24(3):353-359.
21. Galie N, Beghetti M, Gatzoulis MA, et al. Bosentan therapy in patients with Eisenmenger syndrome: a multicenter, double-blind, randomized, placebo-controlled study. *Circulation.* 2006;114(1):48-54.
22. Channick RN, Simonneau G, Sitbon O, et al. Effects of the dual endothelin-receptor antagonist bosentan in patients with pulmonary hypertension: a randomised placebo-controlled study. *Lancet.* 2001;358(9288):1119-1123.
23. Sastry BK, Narasimhan C, Reddy NK, Raju BS. Clinical efficacy of sildenafil in primary pulmonary hypertension: a randomized, placebo-controlled, double-blind, crossover study. *J Am Coll Cardiol.* 2004;43(7):1149-1153.
24. Singh TP, Rohit M, Grover A, Malhotra S, Vijayvergiya R. A randomized, placebo-controlled, double-blind, crossover study to evaluate the efficacy of oral sildenafil therapy in severe pulmonary artery hypertension. *Am Heart J.* 2006;151(4):851 e851-855.
25. Badesch DB, Champion HC, Sanchez MA, et al. Diagnosis and assessment of pulmonary arterial hypertension. *J Am Coll Cardiol.* 2009;54(1 Suppl):S55-66.
26. Berger M, Haimowitz A, Vantosh A, Berdoff RL, Goldberg E. Quantitative Assessment of Pulmonary-Hypertension in Patients with Tricuspid Regurgitation Using Continuous Wave Doppler Ultrasound. *Journal of the American College of Cardiology.* 1985;6(2):359-365.
27. Yock PG, Popp RL. Noninvasive estimation of right ventricular systolic pressure by Doppler ultrasound in patients with tricuspid regurgitation. *Circulation.* 1984;70(4):657-662.
28. Bech-Hanssen O, Selimovic N, Rundqvist B, Wallentin J. Doppler Echocardiography Can Provide a Comprehensive Assessment of Right Ventricular Afterload. *J Am Soc Echocardiog.* 2009;22(12):1360-1367.
29. Lafitte S, Pillois X, Reant P, et al. Estimation of pulmonary pressures and diagnosis of pulmonary hypertension by Doppler echocardiography: a retrospective comparison of routine echocardiography and invasive hemodynamics. *Journal of the American Society of Echocardiography : official publication of the American Society of Echocardiography.* 2013;26(5):457-463.
30. Attaran RR, Ramaraj R, Sorrell VL, Movahed MR. Poor correlation of estimated pulmonary artery systolic pressure between echocardiography and right heart catheterization in patients awaiting cardiac transplantation: results from the clinical arena. *Transplant Proc.* 2009;41(9):3827-3830.
31. Fisher MR, Forfia PR, Chamera E, et al. Accuracy of Doppler echocardiography in the hemodynamic assessment of pulmonary hypertension. *Am J Respir Crit Care Med.* 2009;179(7):615-621.

32. D'Alto M, Romeo E, Argiento P, et al. Accuracy and precision of echocardiography versus right heart catheterization for the assessment of pulmonary hypertension. *Int J Cardiol.* 2013;168(4):4058-4062.
33. Galie N, Hinderliter AL, Torbicki A, et al. Effects of the oral endothelin-receptor antagonist bosentan on echocardiographic and doppler measures in patients with pulmonary arterial hypertension. *J Am Coll Cardiol.* 2003;41(8):1380-1386.
34. Amsallem M, Sternbach JM, Adigopula S, et al. Addressing the Controversy of Estimating Pulmonary Arterial Pressure by Echocardiography. *Journal of the American Society of Echocardiography : official publication of the American Society of Echocardiography.* 2016;29(2):93-102.
35. Granstam SO, Bjorklund E, Wikstrom G, Roos MW. Use of echocardiographic pulmonary acceleration time and estimated vascular resistance for the evaluation of possible pulmonary hypertension. *Cardiovasc Ultrasound.* 2013;11:7.
36. Tossavainen E, Soderberg S, Gronlund C, Gonzalez M, Henein MY, Lindqvist P. Pulmonary artery acceleration time in identifying pulmonary hypertension patients with raised pulmonary vascular resistance. *Eur Heart J Cardiovasc Imaging.* 2013;14(9):890-897.
37. Arkles JS, Opotowsky AR, Ojeda J, et al. Shape of the right ventricular Doppler envelope predicts hemodynamics and right heart function in pulmonary hypertension. *Am J Respir Crit Care Med.* 2011;183(2):268-276.
38. Abbas AE, Fortuin FD, Schiller NB, Appleton CP, Moreno CA, Lester SJ. Echocardiographic determination of mean pulmonary artery pressure. *The American journal of cardiology.* 2003;92(11):1373-1376.
39. Pyxaras SA, Pinamonti B, Barbati G, et al. Echocardiographic evaluation of systolic and mean pulmonary artery pressure in the follow-up of patients with pulmonary hypertension. *European journal of echocardiography : the journal of the Working Group on Echocardiography of the European Society of Cardiology.* 2011;12(9):696-701.
40. Ristow B, Ali S, Ren X, Whooley MA, Schiller NB. Elevated pulmonary artery pressure by Doppler echocardiography predicts hospitalization for heart failure and mortality in ambulatory stable coronary artery disease: the Heart and Soul Study. *J Am Coll Cardiol.* 2007;49(1):43-49.
41. Ristow B, Ahmed S, Wang L, et al. Pulmonary regurgitation end-diastolic gradient is a Doppler marker of cardiac status: data from the Heart and Soul Study. *Journal of the American Society of Echocardiography : official publication of the American Society of Echocardiography.* 2005;18(9):885-891.
42. Austin C, Alassas K, Burger C, et al. Echocardiographic Assessment of Estimated Right Atrial Pressure and Size Predicts Mortality in Pulmonary Arterial Hypertension. *Chest.* 2015;147(1):198-208.
43. Forfia PR, Fisher MR, Mathai SC, et al. Tricuspid annular displacement predicts survival in pulmonary hypertension. *Am J Respir Crit Care Med.* 2006;174(9):1034-1041.
44. Rudski LG, Lai WW, Afilalo J, et al. Guidelines for the echocardiographic assessment of the right heart in adults: a report from the American Society of Echocardiography endorsed by the European Association of Echocardiography, a registered branch of the European Society of Cardiology, and the Canadian Society of Echocardiography. *Journal of the American Society of Echocardiography : official publication of the American Society of Echocardiography.* 2010;23(7):685-713; quiz 786-688.
45. Nath J, Vacek JL, Heidenreich PA. A dilated inferior vena cava is a marker of poor survival. *Am Heart J.* 2006;151(3):730-735.

46. Nagueh SF, Kopelen HA, Zoghbi WA. Relation of mean right atrial pressure to echocardiographic and Doppler parameters of right atrial and right ventricular function. *Circulation.* 1996;93(6):1160-1169.
47. Abbas AE, Fortuin FD, Schiller NB, Appleton CP, Moreno CA, Lester SJ. A simple method for noninvasive estimation of pulmonary vascular resistance. *J Am Coll Cardiol.* 2003;41(6):1021-1027.
48. Dahiya A, Vollbon W, Jellis C, Prior D, Wahi S, Marwick T. Echocardiographic assessment of raised pulmonary vascular resistance: application to diagnosis and follow-up of pulmonary hypertension. *Heart.* 2010;96(24):2005-2009.
49. Abbas AE, Franey LM, Marwick T, et al. Noninvasive assessment of pulmonary vascular resistance by Doppler echocardiography. *Journal of the American Society of Echocardiography : official publication of the American Society of Echocardiography.* 2013;26(10):1170-1177.
50. Tonelli AR, Conci D, Tamarappoo BK, Newman J, Dweik RA. Prognostic value of echocardiographic changes in patients with pulmonary arterial hypertension receiving parenteral prostacyclin therapy. *Journal of the American Society of Echocardiography : official publication of the American Society of Echocardiography.* 2014;27(7):733-741 e732.
51. Nath J, Demarco T, Hourigan L, Heidenreich PA, Foster E. Correlation between right ventricular indices and clinical improvement in epoprostenol treated pulmonary hypertension patients. *Echocardiography.* 2005;22(5):374-379.
52. Rajagopalan N, Simon MA, Suffoletto MS, et al. Noninvasive estimation of pulmonary vascular resistance in pulmonary hypertension. *Echocardiography.* 2009;26(5):489-494.
53. Kusunose K, Tsutsui RS, Bhatt K, et al. Prognostic value of RV function before and after lung transplantation. *JACC Cardiovasc Imaging.* 2014;7(11):1084-1094.
54. Vitarelli A, Mangieri E, Terzano C, et al. Three-dimensional echocardiography and 2D-3D speckle-tracking imaging in chronic pulmonary hypertension: diagnostic accuracy in detecting hemodynamic signs of right ventricular (RV) failure. *Journal of the American Heart Association.* 2015;4(3):e001584.
55. Thomas JD, Popovic ZB. Assessment of left ventricular function by cardiac ultrasound. *J Am Coll Cardiol.* 2006;48(10):2012-2025.
56. De Maria AN, Raisinghani A. Comparative overview of cardiac output measurement methods: has impedance cardiography come of age? *Congest Heart Fail.* 2000;6(2):60-73.
57. Wetterslev M, Moller-Sorensen H, Johansen RR, Perner A. Systematic review of cardiac output measurements by echocardiography vs. thermodilution: the techniques are not interchangeable. *Intensive Care Med.* 2016;42(8):1223-1233.
58. van Wolferen SA, van de Veerdonk MC, Mauritz GJ, et al. Clinically significant change in stroke volume in pulmonary hypertension. *Chest.* 2011;139(5):1003-1009.
59. Deboeck G, Taboada D, Hagan G, et al. Maximal cardiac output determines 6 minutes walking distance in pulmonary hypertension. *PLoS One.* 2014;9(3):e92324.
60. Someya F, Mugii N, Oohata S. Factors relating to impaired stroke volume during the 6-minute walk test in patients with systemic sclerosis. *Clin Exp Rheumatol.* 2016;34 Suppl 100(5):152-156.
61. Morishita T, Miyaji K, Akao I, et al. The ratio of the atrial areas reflects the clinical status of patients with pulmonary arterial hypertension. *J Med Ultrason.* 2009;36(4):201-206.
62. Sebbag I, Rudski LG, Therrien J, Hirsch A, Langleben D. Effect of chronic infusion of epoprostenol on echocardiographic right ventricular myocardial performance index

and its relation to clinical outcome in patients with primary pulmonary hypertension. *The American journal of cardiology.* 2001;88(9):1060-1063.
63. Borges AC, Knebel F, Eddicks S, et al. Right ventricular function assessed by two-dimensional strain and tissue Doppler echocardiography in patients with pulmonary arterial hypertension and effect of vasodilator therapy. *The American journal of cardiology.* 2006;98(4):530-534.
64. Hinderliter AL, Willis PWt, Barst RJ, et al. Effects of long-term infusion of prostacyclin (epoprostenol) on echocardiographic measures of right ventricular structure and function in primary pulmonary hypertension. Primary Pulmonary Hypertension Study Group. *Circulation.* 1997;95(6):1479-1486.
65. Wilkins MR, Paul GA, Strange JW, et al. Sildenafil versus Endothelin Receptor Antagonist for Pulmonary Hypertension (SERAPH) study. *Am J Respir Crit Care Med.* 2005;171(11):1292-1297.
66. Peacock AJ, Crawley S, McLure L, et al. Changes in right ventricular function measured by cardiac magnetic resonance imaging in patients receiving pulmonary arterial hypertension-targeted therapy: the EURO-MR study. *Circulation Cardiovascular imaging.* 2014;7(1):107-114.
67. Eysmann SB, Palevsky HI, Reichek N, Hackney K, Douglas PS. Two-dimensional and Doppler-echocardiographic and cardiac catheterization correlates of survival in primary pulmonary hypertension. *Circulation.* 1989;80(2):353-360.
68. Gan CT, Lankhaar JW, Westerhof N, et al. Noninvasively assessed pulmonary artery stiffness predicts mortality in pulmonary arterial hypertension. *Chest.* 2007;132(6):1906-1912.
69. van Wolferen SA, Marcus JT, Boonstra A, et al. Prognostic value of right ventricular mass, volume, and function in idiopathic pulmonary arterial hypertension. *Eur Heart J.* 2007;28(10):1250-1257.
70. McCrory DC, Coeytaux RR, Schmit KM, et al. 2013.
71. Fijalkowska A, Kurzyna M, Torbicki A, et al. Serum N-terminal brain natriuretic peptide as a prognostic parameter in patients with pulmonary hypertension. *Chest.* 2006;129(5):1313-1321.
72. Sano H, Tanaka H, Motoji Y, et al. Right Ventricular Function and Right-Heart Echocardiographic Response to Therapy Predict Long-term Outcome in Patients With Pulmonary Hypertension. *Can J Cardiol.* 2015;31(4):529-536.
73. Ghio S, Pazzano AS, Klersy C, et al. Clinical and prognostic relevance of echocardiographic evaluation of right ventricular geometry in patients with idiopathic pulmonary arterial hypertension. *The American journal of cardiology.* 2011;107(4):628-632.
74. Mathai SC, Sibley CT, Forfia PR, et al. Tricuspid annular plane systolic excursion is a robust outcome measure in systemic sclerosis-associated pulmonary arterial hypertension. *J Rheumatol.* 2011;38(11):2410-2418.
75. Yeo TC, Dujardin KS, Tei C, Mahoney DW, McGoon MD, Seward JB. Value of a Doppler-derived index combining systolic and diastolic time intervals in predicting outcome in primary pulmonary hypertension. *The American journal of cardiology.* 1998;81(9):1157-1161.
76. Brierre G, Blot-Souletie N, Degano B, Tetu L, Bongard V, Carrie D. New echocardiographic prognostic factors for mortality in pulmonary arterial hypertension. *European journal of echocardiography : the journal of the Working Group on Echocardiography of the European Society of Cardiology.* 2010;11(6):516-522.
77. Fine NM, Chen L, Bastiansen PM, et al. Outcome prediction by quantitative right ventricular function assessment in 575 subjects evaluated for pulmonary hypertension. *Circulation Cardiovascular imaging.* 2013;6(5):711-721.

78. Sachdev A, Villarraga HR, Frantz RP, et al. Right ventricular strain for prediction of survival in patients with pulmonary arterial hypertension. *Chest.* 2011;139(6):1299-1309.
79. Mahapatra S, Nishimura RA, Oh JK, McGoon MD. The prognostic value of pulmonary vascular capacitance determined by Doppler echocardiography in patients with pulmonary arterial hypertension. *Journal of the American Society of Echocardiography : official publication of the American Society of Echocardiography.* 2006;19(8):1045-1050.
80. Nagaya N, Nishikimi T, Uematsu M, et al. Plasma brain natriuretic peptide as a prognostic indicator in patients with primary pulmonary hypertension. *Circulation.* 2000;102(8):865-870.
81. Grapsa J, O'Regan DP, Pavlopoulos H, Durighel G, Dawson D, Nihoyannopoulos P. Right ventricular remodelling in pulmonary arterial hypertension with three-dimensional echocardiography: comparison with cardiac magnetic resonance imaging. *European journal of echocardiography : the journal of the Working Group on Echocardiography of the European Society of Cardiology.* 2010;11(1):64-73.
82. Lang RM, Badano LP, Mor-Avi V, et al. Recommendations for cardiac chamber quantification by echocardiography in adults: an update from the American Society of Echocardiography and the European Association of Cardiovascular Imaging. *Eur Heart J Cardiovasc Imaging.* 2015;16(3):233-270.
83. Yoshifuku S, Otsuji Y, Takasaki K, et al. Pseudonormalized Doppler total ejection isovolume (Tei) index in patients with right ventricular acute myocardial infarction. *The American journal of cardiology.* 2003;91(5):527-531.
84. Badesch DB, Abman SH, Simonneau G, Rubin LJ, McLaughlin VV. Medical therapy for pulmonary arterial hypertension: updated ACCP evidence-based clinical practice guidelines. *Chest.* 2007;131(6):1917-1928.
85. Pavelescu A, Naeije R. Effects of epoprostenol and sildenafil on right ventricular function in hypoxic volunteers: a tissue Doppler imaging study. *European journal of applied physiology.* 2012;112(4):1285-1294.
86. Maffessanti F, Gripari P, Tamborini G, et al. Evaluation of right ventricular systolic function after mitral valve repair: a two-dimensional Doppler, speckle-tracking, and three-dimensional echocardiographic study. *Journal of the American Society of Echocardiography : official publication of the American Society of Echocardiography.* 2012;25(7):701-708.
87. Schattke S, Knebel F, Grohmann A, et al. Early right ventricular systolic dysfunction in patients with systemic sclerosis without pulmonary hypertension: a Doppler Tissue and Speckle Tracking echocardiography study. *Cardiovasc Ultrasound.* 2010;8:3.
88. Vogel M, Schmidt MR, Kristiansen SB, et al. Validation of myocardial acceleration during isovolumic contraction as a novel noninvasive index of right ventricular contractility: comparison with ventricular pressure-volume relations in an animal model. *Circulation.* 2002;105(14):1693-1699.
89. Stanton T, Leano R, Marwick TH. Prediction of all-cause mortality from global longitudinal speckle strain: comparison with ejection fraction and wall motion scoring. *Circulation Cardiovascular imaging.* 2009;2(5):356-364.
90. Freed BH, Tsang W, Bhave NM, et al. Right ventricular strain in pulmonary arterial hypertension: a 2D echocardiography and cardiac magnetic resonance study. *Echocardiography.* 2015;32(2):257-263.
91. Roca GQ, Campbell P, Claggett B, et al. Impact of lowering pulmonary vascular resistance on right and left ventricular deformation in pulmonary arterial hypertension. *Eur J Heart Fail.* 2015;17(1):63-73.

92. Portnoy SG, Rudski LG. Echocardiographic evaluation of the right ventricle: a 2014 perspective. *Curr Cardiol Rep.* 2015;17(4):21.
93. Bustamante-Labarta M, Perrone S, De La Fuente RL, et al. Right atrial size and tricuspid regurgitation severity predict mortality or transplantation in primary pulmonary hypertension. *Journal of the American Society of Echocardiography : official publication of the American Society of Echocardiography.* 2002;15(10 Pt 2):1160-1164.
94. Benza RL, Miller DP, Gomberg-Maitland M, et al. Predicting survival in pulmonary arterial hypertension: insights from the Registry to Evaluate Early and Long-Term Pulmonary Arterial Hypertension Disease Management (REVEAL). *Circulation.* 2010;122(2):164-172.
95. Naeije R, Manes A. The right ventricle in pulmonary arterial hypertension. *Eur Respir Rev.* 2014;23(134):476-487.
96. Vanderpool RR, Pinsky MR, Naeije R, et al. RV-pulmonary arterial coupling predicts outcome in patients referred for pulmonary hypertension. *Heart.* 2015;101(1):37-43.
97. Brown KA, Ditchey RV. Human right ventricular end-systolic pressure-volume relation defined by maximal elastance. *Circulation.* 1988;78(1):81-91.
98. Kuehne T, Yilmaz S, Steendijk P, et al. Magnetic resonance imaging analysis of right ventricular pressure-volume loops: in vivo validation and clinical application in patients with pulmonary hypertension. *Circulation.* 2004;110(14):2010-2016.
99. Sanz J, Garcia-Alvarez A, Fernandez-Friera L, et al. Right ventriculo-arterial coupling in pulmonary hypertension: a magnetic resonance study. *Heart.* 2012;98(3):238-243.
100. Knight DS, Grasso AE, Quail MA, et al. Accuracy and reproducibility of right ventricular quantification in patients with pressure and volume overload using single-beat three-dimensional echocardiography. *Journal of the American Society of Echocardiography : official publication of the American Society of Echocardiography.* 2015;28(3):363-374.
101. Lang RM, Badano LP, Mor-Avi V, et al. Recommendations for cardiac chamber quantification by echocardiography in adults: an update from the American Society of Echocardiography and the European Association of Cardiovascular Imaging. *Journal of the American Society of Echocardiography : official publication of the American Society of Echocardiography.* 2015;28(1):1-39 e14.
102. Celermajer DS, Sorensen KE, Gooch VM, et al. Non-invasive detection of endothelial dysfunction in children and adults at risk of atherosclerosis. *Lancet.* 1992;340(8828):1111-1115.
103. Corretti MC, Anderson TJ, Benjamin EJ, et al. Guidelines for the ultrasound assessment of endothelial-dependent flow-mediated vasodilation of the brachial artery: a report of the International Brachial Artery Reactivity Task Force. *J Am Coll Cardiol.* 2002;39(2):257-265.
104. Axtell AL, Gomari FA, Cooke JP. Assessing endothelial vasodilator function with the Endo-PAT 2000. *J Vis Exp.* 2010(44).
105. Valentini G, Leonardo G, Moles DA, et al. Transcutaneous oxygen pressure in systemic sclerosis: evaluation at different sensor temperatures and relationship to skin perfusion. *Arch Dermatol Res.* 1991;283(5):285-288.
106. Roustit M, Simmons GH, Baguet JP, Carpentier P, Cracowski JL. Discrepancy between simultaneous digital skin microvascular and brachial artery macrovascular post-occlusive hyperemia in systemic sclerosis. *J Rheumatol.* 2008;35(8):1576-1583.
107. Zamanian RT, Kudelko KT, Sung YK, Perez VJ, Liu J, Spiekerkoetter E. Current clinical management of pulmonary arterial hypertension. *Circ Res.* 2014;115(1):131-147.

108. van de Veerdonk MC, Kind T, Marcus JT, et al. Progressive right ventricular dysfunction in patients with pulmonary arterial hypertension responding to therapy. *J Am Coll Cardiol.* 2011;58(24):2511-2519.
109. van de Veerdonk MC, Marcus JT, Westerhof N, et al. Signs of right ventricular deterioration in clinically stable patients with pulmonary arterial hypertension. *Chest.* 2015;147(4):1063-1071.
110. ATS statement: guidelines for the six-minute walk test. *American journal of respiratory and critical care medicine.* 2002;166(1):111-117.
111. Shapiro S, Traiger GL, Turner M, McGoon MD, Wason P, Barst RJ. Sex differences in the diagnosis, treatment, and outcome of patients with pulmonary arterial hypertension enrolled in the registry to evaluate early and long-term pulmonary arterial hypertension disease management. *Chest.* 2012;141(2):363-373.
112. Vonk Noordegraaf A, Westerhof BE, Westerhof N. The Relationship Between the Right Ventricle and its Load in Pulmonary Hypertension. *J Am Coll Cardiol.* 2017;69(2):236-243.
113. Vonk-Noordegraaf A, Haddad F, Chin KM, et al. Right heart adaptation to pulmonary arterial hypertension: physiology and pathobiology. *J Am Coll Cardiol.* 2013;62(25 Suppl):D22-33.
114. Shimony A, Fox BD, Langleben D, Rudski LG. Incidence and significance of pericardial effusion in patients with pulmonary arterial hypertension. *Can J Cardiol.* 2013;29(6):678-682.
115. McLaughlin VV, Archer SL, Badesch DB, et al. ACCF/AHA 2009 expert consensus document on pulmonary hypertension a report of the American College of Cardiology Foundation Task Force on Expert Consensus Documents and the American Heart Association developed in collaboration with the American College of Chest Physicians; American Thoracic Society, Inc.; and the Pulmonary Hypertension Association. *J Am Coll Cardiol.* 2009;53(17):1573-1619.
116. Mazurek JA, Vaidya A, Mathai SC, Roberts JD, Forfia PR. Follow-up tricuspid annular plane systolic excursion predicts survival in pulmonary arterial hypertension. *Pulm Circ.* 2017;7(2):361-371.
117. Giusca S, Dambrauskaite V, Scheurwegs C, et al. Deformation imaging describes right ventricular function better than longitudinal displacement of the tricuspid ring. *Heart.* 2010;96(4):281-288.
118. Wright L, Negishi K, Dwyer N, Wahi S, Marwick TH. Afterload Dependence of Right Ventricular Myocardial Strain. *Journal of the American Society of Echocardiography : official publication of the American Society of Echocardiography.* 2017;30(7):676-684 e671.
119. McLaughlin VV, Gaine SP, Howard LS, et al. Treatment goals of pulmonary hypertension. *J Am Coll Cardiol.* 2013;62(25 Suppl):D73-81.
120. Jenkins C, Chan J, Bricknell K, Strudwick M, Marwick TH. Reproducibility of right ventricular volumes and ejection fraction using real-time three-dimensional echocardiography: comparison with cardiac MRI. *Chest.* 2007;131(6):1844-1851.
121. Leibundgut G, Rohner A, Grize L, et al. Dynamic assessment of right ventricular volumes and function by real-time three-dimensional echocardiography: a comparison study with magnetic resonance imaging in 100 adult patients. *Journal of the American Society of Echocardiography : official publication of the American Society of Echocardiography.* 2010;23(2):116-126.
122. Muraru D, Onciul S, Peluso D, et al. Sex- and Method-Specific Reference Values for Right Ventricular Strain by 2-Dimensional Speckle-Tracking Echocardiography. *Circulation Cardiovascular imaging.* 2016;9(2):e003866.

123. Souza R, Channick RN, Delcroix M, et al. Association between six-minute walk distance and long-term outcomes in patients with pulmonary arterial hypertension: Data from the randomized SERAPHIN trial. *PLoS One.* 2018;13(3):e0193226.
124. Savarese G, Paolillo S, Costanzo P, et al. Do changes of 6-minute walk distance predict clinical events in patients with pulmonary arterial hypertension? A meta-analysis of 22 randomized trials. *J Am Coll Cardiol.* 2012;60(13):1192-1201.
125. Spruijt OA, Di Pasqua MC, Bogaard HJ, et al. Serial assessment of right ventricular systolic function in patients with precapillary pulmonary hypertension using simple echocardiographic parameters: A comparison with cardiac magnetic resonance imaging. *J Cardiol.* 2017;69(1):182-188.
126. Lee WT, Ling Y, Sheares KK, Pepke-Zaba J, Peacock AJ, Johnson MK. Predicting survival in pulmonary arterial hypertension in the UK. *Eur Respir J.* 2012;40(3):604-611.
127. Humbert M, Sitbon O, Yaici A, et al. Survival in incident and prevalent cohorts of patients with pulmonary arterial hypertension. *Eur Respir J.* 2010;36(3):549-555.
128. Mathai SC, Hassoun PM, Puhan MA, Zhou Y, Wise RA. Sex differences in response to tadalafil in pulmonary arterial hypertension. *Chest.* 2015;147(1):188-197.
129. Macchia A, Marchioli R, Tognoni G, et al. Systematic review of trials using vasodilators in pulmonary arterial hypertension: why a new approach is needed. *Am Heart J.* 2010;159(2):245-257.
130. Hoeper MM, Bogaard HJ, Condliffe R, et al. Definitions and diagnosis of pulmonary hypertension. *J Am Coll Cardiol.* 2013;62(25 Suppl):D42-50.
131. Donal E, Bergerot C, Thibault H, et al. Influence of afterload on left ventricular radial and longitudinal systolic functions: a two-dimensional strain imaging study. *European journal of echocardiography : the journal of the Working Group on Echocardiography of the European Society of Cardiology.* 2009;10(8):914-921.
132. Plana JC, Galderisi M, Barac A, et al. Expert consensus for multimodality imaging evaluation of adult patients during and after cancer therapy: a report from the American Society of Echocardiography and the European Association of Cardiovascular Imaging. *Eur Heart J Cardiovasc Imaging.* 2014;15(10):1063-1093.
133. Authors/Task Force M, Galie N, Humbert M, et al. 2015 ESC/ERS Guidelines for the diagnosis and treatment of pulmonary hypertension: The Joint Task Force for the Diagnosis and Treatment of Pulmonary Hypertension of the European Society of Cardiology (ESC) and the European Respiratory Society (ERS)Endorsed by: Association for European Paediatric and Congenital Cardiology (AEPC), International Society for Heart and Lung Transplantation (ISHLT). *Eur Heart J.* 2015.
134. Greiner S, Jud A, Aurich M, et al. Reliability of noninvasive assessment of systolic pulmonary artery pressure by Doppler echocardiography compared to right heart catheterization: analysis in a large patient population. *Journal of the American Heart Association.* 2014;3(4).
135. Pirat B, McCulloch ML, Zoghbi WA. Evaluation of global and regional right ventricular systolic function in patients with pulmonary hypertension using a novel speckle tracking method. *The American journal of cardiology.* 2006;98(5):699-704.
136. Fukuda Y, Tanaka H, Sugiyama D, et al. Utility of right ventricular free wall speckle-tracking strain for evaluation of right ventricular performance in patients with pulmonary hypertension. *Journal of the American Society of Echocardiography : official publication of the American Society of Echocardiography.* 2011;24(10):1101-1108.
137. Reichek N. Right ventricular strain in pulmonary hypertension: flavor du jour or enduring prognostic index? *Circulation Cardiovascular imaging.* 2013;6(5):609-611.

138. Quinones MA, Gaasch WH, Alexander JK. Influence of acute changes in preload, afterload, contractile state and heart rate on ejection and isovolumic indices of myocardial contractility in man. *Circulation.* 1976;53(2):293-302.
139. Bossone E, D'Andrea A, D'Alto M, et al. Echocardiography in pulmonary arterial hypertension: from diagnosis to prognosis. *Journal of the American Society of Echocardiography : official publication of the American Society of Echocardiography.* 2013;26(1):1-14.
140. Cho EJ, Jiamsripong P, Calleja AM, et al. Right ventricular free wall circumferential strain reflects graded elevation in acute right ventricular afterload. *Am J Physiol Heart Circ Physiol.* 2009;296(2):H413-420.
141. Thavendiranathan P, Poulin F, Lim KD, Plana JC, Woo A, Marwick TH. Use of myocardial strain imaging by echocardiography for the early detection of cardiotoxicity in patients during and after cancer chemotherapy: a systematic review. *J Am Coll Cardiol.* 2014;63(25 Pt A):2751-2768.
142. Koo TK, Li MY. A Guideline of Selecting and Reporting Intraclass Correlation Coefficients for Reliability Research. *J Chiropr Med.* 2016;15(2):155-163.
143. Bartelds B, Borgdorff MA, Smit-van Oosten A, et al. Differential responses of the right ventricle to abnormal loading conditions in mice: pressure vs. volume load. *Eur J Heart Fail.* 2011;13(12):1275-1282.
144. Bellofiore A, Chesler NC. Methods for measuring right ventricular function and hemodynamic coupling with the pulmonary vasculature. *Ann Biomed Eng.* 2013;41(7):1384-1398.
145. Voelkel NF, Quaife RA, Leinwand LA, et al. Right ventricular function and failure: report of a National Heart, Lung, and Blood Institute working group on cellular and molecular mechanisms of right heart failure. *Circulation.* 2006;114(17):1883-1891.
146. Petitjean C, Rougon N, Cluzel P. Assessment of myocardial function: a review of quantification methods and results using tagged MRI. *J Cardiovasc Magn Reson.* 2005;7(2):501-516.
147. Brimioulle S, Wauthy P, Ewalenko P, et al. Single-beat estimation of right ventricular end-systolic pressure-volume relationship. *Am J Physiol Heart Circ Physiol.* 2003;284(5):H1625-1630.
148. Takeuchi M, Igarashi Y, Tomimoto S, et al. Single-beat estimation of the slope of the end-systolic pressure-volume relation in the human left ventricle. *Circulation.* 1991;83(1):202-212.
149. Brittain EL, Hemnes AR, Keebler M, Lawson M, Byrd BF, 3rd, Disalvo T. Right ventricular plasticity and functional imaging. *Pulm Circ.* 2012;2(3):309-326.
150. Lankhaar JW, Westerhof N, Faes TJ, et al. Quantification of right ventricular afterload in patients with and without pulmonary hypertension. *Am J Physiol Heart Circ Physiol.* 2006;291(4):H1731-1737.
151. Borgdorff MA, Bartelds B, Dickinson MG, Steendijk P, de Vroomen M, Berger RM. Distinct loading conditions reveal various patterns of right ventricular adaptation. *Am J Physiol Heart Circ Physiol.* 2013;305(3):H354-364.
152. Tedford RJ. Determinants of right ventricular afterload (2013 Grover Conference series). *Pulm Circ.* 2014;4(2):211-219.
153. Tan JL, Prati D, Gatzoulis MA, Gibson D, Henein MY, Li W. The right ventricular response to high afterload: comparison between atrial switch procedure, congenitally corrected transposition of the great arteries, and idiopathic pulmonary arterial hypertension. *Am Heart J.* 2007;153(4):681-688.
154. van Wolferen SA, Boonstra A, Marcus JT, et al. Right ventricular reverse remodelling after sildenafil in pulmonary arterial hypertension. *Heart.* 2006;92(12):1860-1861.

155. Berman M, Gopalan D, Sharples L, et al. Right ventricular reverse remodeling after pulmonary endarterectomy: magnetic resonance imaging and clinical and right heart catheterization assessment. *Pulm Circ.* 2014;4(1):36-44.
156. Szabo G, Soos P, Bahrle S, et al. Adaptation of the right ventricle to an increased afterload in the chronically volume overloaded heart. *Ann Thorac Surg.* 2006;82(3):989-995.
157. Farsalinos KE, Daraban AM, Unlu S, Thomas JD, Badano LP, Voigt JU. Head-to-Head Comparison of Global Longitudinal Strain Measurements among Nine Different Vendors: The EACVI/ASE Inter-Vendor Comparison Study. *Journal of the American Society of Echocardiography : official publication of the American Society of Echocardiography.* 2015;28(10):1171-1181, e1172.
158. Risum N, Ali S, Olsen NT, et al. Variability of global left ventricular deformation analysis using vendor dependent and independent two-dimensional speckle-tracking software in adults. *Journal of the American Society of Echocardiography : official publication of the American Society of Echocardiography.* 2012;25(11):1195-1203.
159. Jamal F, Bergerot C, Argaud L, Loufouat J, Ovize M. Longitudinal strain quantitates regional right ventricular contractile function. *Am J Physiol Heart Circ Physiol.* 2003;285(6):H2842-2847.
160. Park JH, Kusunose K, Kwon DH, et al. Relationship between Right Ventricular Longitudinal Strain, Invasive Hemodynamics, and Functional Assessment in Pulmonary Arterial Hypertension. *Korean Circ J.* 2015;45(5):398-407.
161. Chung L, Farber HW, Benza R, et al. Unique predictors of mortality in patients with pulmonary arterial hypertension associated with systemic sclerosis in the REVEAL registry. *Chest.* 2014;146(6):1494-1504.
162. Shiraev TP, Omari A, Rushworth RL. Trends in pulmonary embolism morbidity and mortality in Australia. *Thromb Res.* 2013;132(1):19-25.
163. Sanchez O, Trinquart L, Colombet I, et al. Prognostic value of right ventricular dysfunction in patients with haemodynamically stable pulmonary embolism: a systematic review. *Eur Heart J.* 2008;29(12):1569-1577.
164. Gaynor SL, Maniar HS, Bloch JB, Steendijk P, Moon MR. Right atrial and ventricular adaptation to chronic right ventricular pressure overload. *Circulation.* 2005;112(9 Suppl):I212-218.
165. Dias CA, Assad RS, Caneo LF, et al. Reversible pulmonary trunk banding. II. An experimental model for rapid pulmonary ventricular hypertrophy. *J Thorac Cardiovasc Surg.* 2002;124(5):999-1006.
166. Rudski LG, Lai WW, Afilalo J, et al. Guidelines for the echocardiographic assessment of the right heart in adults: a report from the American Society of Echocardiography endorsed by the European Association of Echocardiography, a registered branch of the European Society of Cardiology, and the Canadian Society of Echocardiography. *Journal of the American Society of Echocardiography : official publication of the American Society of Echocardiography.* 2010;23(7):685-713; quiz 786-688.
167. Kasper W, Konstantinides S, Geibel A, Tiede N, Krause T, Just H. Prognostic significance of right ventricular afterload stress detected by echocardiography in patients with clinically suspected pulmonary embolism. *Heart.* 1997;77(4):346-349.
168. McConnell MV, Solomon SD, Rayan ME, Come PC, Goldhaber SZ, Lee RT. Regional right ventricular dysfunction detected by echocardiography in acute pulmonary embolism. *The American journal of cardiology.* 1996;78(4):469-473.
169. Casazza F, Bongarzoni A, Capozi A, Agostoni O. Regional right ventricular dysfunction in acute pulmonary embolism and right ventricular infarction. *European journal of echocardiography : the journal of the Working Group on Echocardiography of the European Society of Cardiology.* 2005;6(1):11-14.

170. Kurzyna M, Torbicki A, Pruszczyk P, et al. Disturbed right ventricular ejection pattern as a new Doppler echocardiographic sign of acute pulmonary embolism. *The American journal of cardiology.* 2002;90(5):507-511.
171. Goldhaber SZ, Visani L, De Rosa M. Acute pulmonary embolism: clinical outcomes in the International Cooperative Pulmonary Embolism Registry (ICOPER). *Lancet.* 1999;353(9162):1386-1389.
172. Pirat B, McCulloch ML, Zoghbi WA. Evaluation of global and regional right ventricular systolic function in patients with pulmonary hypertension using a novel speckle tracking method. *Am J Cardiol.* 2006;98(5):699-704.
173. Kjaergaard J, Schaadt BK, Lund JO, Hassager C. Quantification of right ventricular function in acute pulmonary embolism: relation to extent of pulmonary perfusion defects. *European journal of echocardiography : the journal of the Working Group on Echocardiography of the European Society of Cardiology.* 2008;9(5):641-645.
174. Chung T, Emmett L, Mansberg R, Peters M, Kritharides L. Natural history of right ventricular dysfunction after acute pulmonary embolism. *Journal of the American Society of Echocardiography : official publication of the American Society of Echocardiography.* 2007;20(7):885-894.
175. Lopez-Candales A, Edelman K, Candales MD. Right ventricular apical contractility in acute pulmonary embolism: the McConnell sign revisited. *Echocardiography.* 2010;27(6):614-620.
176. Platz E, Hassanein AH, Shah A, Goldhaber SZ, Solomon SD. Regional right ventricular strain pattern in patients with acute pulmonary embolism. *Echocardiography.* 2012;29(4):464-470.
177. Rajagopal S, Forsha DE, Risum N, et al. Comprehensive assessment of right ventricular function in patients with pulmonary hypertension with global longitudinal peak systolic strain derived from multiple right ventricular views. *Journal of the American Society of Echocardiography : official publication of the American Society of Echocardiography.* 2014;27(6):657-665 e653.
178. Smith BC, Dobson G, Dawson D, Charalampopoulos A, Grapsa J, Nihoyannopoulos P. Three-dimensional speckle tracking of the right ventricle: toward optimal quantification of right ventricular dysfunction in pulmonary hypertension. *J Am Coll Cardiol.* 2014;64(1):41-51.
179. Mauritz GJ, Vonk-Noordegraaf A, Kind T, et al. Pulmonary endarterectomy normalizes interventricular dyssynchrony and right ventricular systolic wall stress. *J Cardiovasc Magn Reson.* 2012;14:5.
180. Arena R, Lavie CJ, Milani RV, Myers J, Guazzi M. Cardiopulmonary exercise testing in patients with pulmonary arterial hypertension: an evidence-based review. *J Heart Lung Transplant.* 2010;29(2):159-173.
181. Taichman DB, McGoon MD, Harhay MO, et al. Wide variation in clinicians' assessment of New York Heart Association/World Health Organization functional class in patients with pulmonary arterial hypertension. *Mayo Clin Proc.* 2009;84(7):586-592.
182. Mainguy V, Malenfant S, Neyron AS, et al. Repeatability and responsiveness of exercise tests in pulmonary arterial hypertension. *Eur Respir J.* 2013;42(2):425-434.
183. Nishio R, Tanaka H, Tsuboi Y, et al. Differences in hemodynamic parameters and exercise capacity between patients with pulmonary arterial hypertension and chronic heart failure. *J Cardiopulm Rehabil Prev.* 2012;32(6):379-385.
184. Tonelli AR, Arelli V, Minai OA, et al. Causes and circumstances of death in pulmonary arterial hypertension. *Am J Respir Crit Care Med.* 2013;188(3):365-369.
185. Galie N, Manes A, Negro L, Palazzini M, Bacchi-Reggiani ML, Branzi A. A meta-analysis of randomized controlled trials in pulmonary arterial hypertension. *Eur Heart J.* 2009;30(4):394-403.

186. Miyamoto S, Nagaya N, Satoh T, et al. Clinical correlates and prognostic significance of six-minute walk test in patients with primary pulmonary hypertension. Comparison with cardiopulmonary exercise testing. *Am J Respir Crit Care Med.* 2000;161(2 Pt 1):487-492.
187. Nickel N, Golpon H, Greer M, et al. The prognostic impact of follow-up assessments in patients with idiopathic pulmonary arterial hypertension. *Eur Respir J.* 2012;39(3):589-596.
188. Farber HW, Miller DP, McGoon MD, Frost AE, Benton WW, Benza RL. Predicting outcomes in pulmonary arterial hypertension based on the 6-minute walk distance. *J Heart Lung Transplant.* 2015;34(3):362-368.
189. Humbert M, Sitbon O, Chaouat A, et al. Survival in patients with idiopathic, familial, and anorexigen-associated pulmonary arterial hypertension in the modern management era. *Circulation.* 2010;122(2):156-163.
190. Addetia K, Bhave NM, Tabit CE, et al. Sample size and cost analysis for pulmonary arterial hypertension drug trials using various imaging modalities to assess right ventricular size and function end points. *Circulation: Cardiovascular Imaging.* 2014;7(1):115-124.
191. Steele P, Strange G, Wlodarczyk J, et al. Hemodynamics in pulmonary arterial hypertension (PAH): do they explain long-term clinical outcomes with PAH-specific therapy? *BMC Cardiovasc Disord.* 2010;10:9.
192. Brown SB, Raina A, Katz D, Szerlip M, Wiegers SE, Forfia PR. Longitudinal shortening accounts for the majority of right ventricular contraction and improves after pulmonary vasodilator therapy in normal subjects and patients with pulmonary arterial hypertension. *Chest.* 2011;140(1):27-33.
193. Fukuda Y, Tanaka H, Sugiyama D, et al. Utility of right ventricular free wall speckle-tracking strain for evaluation of right ventricular performance in patients with pulmonary hypertension. *Journal of the American Society of Echocardiography : official publication of the American Society of Echocardiography.* 2011;24(10):1101-1108.
194. Wright L, Dwyer N, Power J, Kritharides L, Celermajer D, Marwick TH. Right Ventricular Systolic Function Responses to Acute and Chronic Pulmonary Hypertension: Assessment with Myocardial Deformation. *Journal of the American Society of Echocardiography : official publication of the American Society of Echocardiography.* 2016;29(3):259-266.
195. Lord RN, George K, Jones H, Somauroo J, Oxborough D. Reproducibility and feasibility of right ventricular strain and strain rate (SR) as determined by myocardial speckle tracking during high-intensity upright exercise: a comparison with tissue Doppler-derived strain and SR in healthy human hearts. *Echo Res Pract.* 2014;1(1):31-41.
196. van Kessel M, Seaton D, Chan J, et al. Prognostic value of right ventricular free wall strain in pulmonary hypertension patients with pseudo-normalized tricuspid annular plane systolic excursion values. *Int J Cardiovasc Imaging.* 2016;32(6):905-912.
197. Motoji Y, Tanaka H, Fukuda Y, et al. Association of Apical Longitudinal Rotation with Right Ventricular Performance in Patients with Pulmonary Hypertension: Insights into Overestimation of Tricuspid Annular Plane Systolic Excursion. *Echocardiography.* 2016;33(2):207-215.
198. Motoji Y, Tanaka H, Fukuda Y, et al. Efficacy of right ventricular free-wall longitudinal speckle-tracking strain for predicting long-term outcome in patients with pulmonary hypertension. *Circ J.* 2013;77(3):756-763.
199. Simon MA. Assessment and treatment of right ventricular failure. *Nat Rev Cardiol.* 2013;10(4):204-218.

200. Mathai SC, Puhan MA, Lam D, Wise RA. The minimal important difference in the 6-minute walk test for patients with pulmonary arterial hypertension. *Am J Respir Crit Care Med.* 2012;186(5):428-433.
201. Groepenhoff H, Vonk-Noordegraaf A, van de Veerdonk MC, Boonstra A, Westerhof N, Bogaard HJ. Prognostic relevance of changes in exercise test variables in pulmonary arterial hypertension. *PLoS One.* 2013;8(9):e72013.
202. Liu HL, Chen XY, Li JR, et al. Efficacy and Safety of Pulmonary Arterial Hypertension-specific Therapy in Pulmonary Arterial Hypertension: A Meta-analysis of Randomized Controlled Trials. *Chest.* 2016;150(2):353-366.
203. Fox BD, Shimony A, Langleben D, et al. High prevalence of occult left heart disease in scleroderma-pulmonary hypertension. *Eur Respir J.* 2013;42(4):1083-1091.
204. Avouac J, Airo P, Meune C, et al. Prevalence of pulmonary hypertension in systemic sclerosis in European Caucasians and metaanalysis of 5 studies. *J Rheumatol.* 2010;37(11):2290-2298.
205. Man A, Zhu Y, Zhang Y, et al. The risk of cardiovascular disease in systemic sclerosis: a population-based cohort study. *Ann Rheum Dis.* 2013;72(7):1188-1193.
206. Bourji KI, Kelemen BW, Mathai SC, et al. Poor survival in patients with scleroderma and pulmonary hypertension due to heart failure with preserved ejection fraction. *Pulm Circ.* 2017;7(2):409-420.
207. Rodriguez-Reyna TS, Morelos-Guzman M, Hernandez-Reyes P, et al. Assessment of myocardial fibrosis and microvascular damage in systemic sclerosis by magnetic resonance imaging and coronary angiotomography. *Rheumatology (Oxford).* 2015;54(4):647-654.
208. Kang SJ, Lim HS, Choi BJ, et al. Longitudinal strain and torsion assessed by two-dimensional speckle tracking correlate with the serum level of tissue inhibitor of matrix metalloproteinase-1, a marker of myocardial fibrosis, in patients with hypertension. *Journal of the American Society of Echocardiography : official publication of the American Society of Echocardiography.* 2008;21(8):907-911.
209. Ntusi NA, Piechnik SK, Francis JM, et al. Subclinical myocardial inflammation and diffuse fibrosis are common in systemic sclerosis--a clinical study using myocardial T1-mapping and extracellular volume quantification. *J Cardiovasc Magn Reson.* 2014;16:21.
210. Shan K, Bick RJ, Poindexter BJ, et al. Relation of tissue Doppler derived myocardial velocities to myocardial structure and beta-adrenergic receptor density in humans. *J Am Coll Cardiol.* 2000;36(3):891-896.
211. Hartke LP, Gilkeson RC, O'Riordan MA, Siwik ES. Evaluation of right ventricular fibrosis in adult congenital heart disease using gadolinium-enhanced magnetic resonance imaging: initial experience in patients with right ventricular loading conditions. *Congenit Heart Dis.* 2006;1(5):192-201.
212. Follansbee WP, Miller TR, Curtiss EI, et al. A controlled clinicopathologic study of myocardial fibrosis in systemic sclerosis (scleroderma). *J Rheumatol.* 1990;17(5):656-662.
213. Fernandes VR, Edvardsen T, Rosen BD, et al. The influence of left ventricular size and global function on regional myocardial contraction and relaxation in an adult population free of cardiovascular disease: a tagged CMR study of the MESA cohort. *J Cardiovasc Magn Reson.* 2007;9(6):921-930.
214. Covell JW. Tissue structure and ventricular wall mechanics. *Circulation.* 2008;118(7):699-701.
215. Gabrielli A, Avvedimento EV, Krieg T. Scleroderma. *The New England journal of medicine.* 2009;360(19):1989-2003.

216. Komocsi A, Vorobcsuk A, Faludi R, et al. The impact of cardiopulmonary manifestations on the mortality of SSc: a systematic review and meta-analysis of observational studies. *Rheumatology (Oxford).* 2012;51(6):1027-1036.
217. Kahan A, Allanore Y. Primary myocardial involvement in systemic sclerosis. *Rheumatology (Oxford).* 2006;45 Suppl 4:iv14-17.
218. Allanore Y, Meune C, Kahan A. Outcome measures for heart involvement in systemic sclerosis. *Rheumatology (Oxford).* 2008;47 Suppl 5:v51-53.
219. Cusma Piccione M, Zito C, Bagnato G, Oreto G, Di Bella G, Carerj S. Role of 2D strain in the early identification of left ventricular dysfunction and in the risk stratification of systemic sclerosis patients. *Cardiovasc Ultrasound.* 2013;11:6.
220. Spethmann S, Dreger H, Schattke S, et al. Two-dimensional speckle tracking of the left ventricle in patients with systemic sclerosis for an early detection of myocardial involvement. *Eur Heart J Cardiovasc Imaging.* 2012;13(10):863-870.
221. Mele D, Censi S, La Corte R, et al. Abnormalities of left ventricular function in asymptomatic patients with systemic sclerosis using Doppler measures of myocardial strain. *Journal of the American Society of Echocardiography : official publication of the American Society of Echocardiography.* 2008;21(11):1257-1264.
222. Kepez A, Akdogan A, Sade LE, et al. Detection of subclinical cardiac involvement in systemic sclerosis by echocardiographic strain imaging. *Echocardiography.* 2008;25(2):191-197.
223. D'Andrea A, Stisi S, Bellissimo S, et al. Early impairment of myocardial function in systemic sclerosis: non-invasive assessment by Doppler myocardial and strain rate imaging. *European journal of echocardiography : the journal of the Working Group on Echocardiography of the European Society of Cardiology.* 2005;6(6):407-418.
224. Spethmann S, Rieper K, Riemekasten G, et al. Echocardiographic follow-up of patients with systemic sclerosis by 2D speckle tracking echocardiography of the left ventricle. *Cardiovasc Ultrasound.* 2014;12:13.
225. D'Angelo WA, Fries JF, Masi AT, Shulman LE. Pathologic observations in systemic sclerosis (scleroderma). A study of fifty-eight autopsy cases and fifty-eight matched controls. *The American journal of medicine.* 1969;46(3):428-440.
226. Bulkley BH, Ridolfi RL, Salyer WR, Hutchins GM. Myocardial lesions of progressive systemic sclerosis. A cause of cardiac dysfunction. *Circulation.* 1976;53(3):483-490.
227. Steen VD, Medsger TA, Jr. Severe organ involvement in systemic sclerosis with diffuse scleroderma. *Arthritis and rheumatism.* 2000;43(11):2437-2444.
228. Deswal A, Follansbee WP. Cardiac involvement in scleroderma. *Rheumatic diseases clinics of North America.* 1996;22(4):841-860.
229. Kalam K, Otahal P, Marwick TH. Prognostic implications of global LV dysfunction: a systematic review and meta-analysis of global longitudinal strain and ejection fraction. *Heart.* 2014.
230. Yingchoncharoen T, Agarwal S, Popovic ZB, Marwick TH. Normal ranges of left ventricular strain: a meta-analysis. *Journal of the American Society of Echocardiography : official publication of the American Society of Echocardiography.* 2013;26(2):185-191.
231. Puwanant S, Park M, Popovic ZB, et al. Ventricular geometry, strain, and rotational mechanics in pulmonary hypertension. *Circulation.* 2010;121(2):259-266.
232. Friedberg MK, Redington AN. Right versus left ventricular failure: differences, similarities, and interactions. *Circulation.* 2014;129(9):1033-1044.
233. Preliminary criteria for the classification of systemic sclerosis (scleroderma). Subcommittee for scleroderma criteria of the American Rheumatism Association Diagnostic and Therapeutic Criteria Committee. *Arthritis and rheumatism.* 1980;23(5):581-590.

234. Nagueh SF, Appleton CP, Gillebert TC, et al. Recommendations for the evaluation of left ventricular diastolic function by echocardiography. *Journal of the American Society of Echocardiography : official publication of the American Society of Echocardiography.* 2009;22(2):107-133.
235. Lang RM, Bierig M, Devereux RB, et al. Recommendations for chamber quantification: a report from the American Society of Echocardiography's Guidelines and Standards Committee and the Chamber Quantification Writing Group, developed in conjunction with the European Association of Echocardiography, a branch of the European Society of Cardiology. *Journal of the American Society of Echocardiography : official publication of the American Society of Echocardiography.* 2005;18(12):1440-1463.
236. Mor-Avi V, Lang RM, Badano LP, et al. Current and evolving echocardiographic techniques for the quantitative evaluation of cardiac mechanics: ASE/EAE consensus statement on methodology and indications endorsed by the Japanese Society of Echocardiography. *Journal of the American Society of Echocardiography : official publication of the American Society of Echocardiography.* 2011;24(3):277-313.
237. Kusunose K, Yamada H, Nishio S, et al. Index-beat assessment of left ventricular systolic and diastolic function during atrial fibrillation using myocardial strain and strain rate. *Journal of the American Society of Echocardiography : official publication of the American Society of Echocardiography.* 2012;25(9):953-959.
238. DeLong ER, DeLong DM, Clarke-Pearson DL. Comparing the areas under two or more correlated receiver operating characteristic curves: a nonparametric approach. *Biometrics.* 1988;44(3):837-845.
239. Pencina MJ, D'Agostino RB, Sr., D'Agostino RB, Jr., Vasan RS. Evaluating the added predictive ability of a new marker: from area under the ROC curve to reclassification and beyond. *Statistics in medicine.* 2008;27(2):157-172; discussion 207-112.
240. Pencina MJ, D'Agostino RB, Sr., Steyerberg EW. Extensions of net reclassification improvement calculations to measure usefulness of new biomarkers. *Statistics in medicine.* 2011;30(1):11-21.
241. Geyer H, Caracciolo G, Abe H, et al. Assessment of myocardial mechanics using speckle tracking echocardiography: fundamentals and clinical applications. *Journal of the American Society of Echocardiography : official publication of the American Society of Echocardiography.* 2010;23(4):351-369; quiz 453-355.
242. Matias C, Isla LP, Vasconcelos M, et al. Speckle-tracking-derived strain and strain-rate analysis: a technique for the evaluation of early alterations in right ventricle systolic function in patients with systemic sclerosis and normal pulmonary artery pressure. *J Cardiovasc Med (Hagerstown).* 2009;10(2):129-134.
243. Nagueh SF, Smiseth OA, Appleton CP, et al. Recommendations for the Evaluation of Left Ventricular Diastolic Function by Echocardiography: An Update from the American Society of Echocardiography and the European Association of Cardiovascular Imaging. *Journal of the American Society of Echocardiography : official publication of the American Society of Echocardiography.* 2016;29(4):277-314.
244. Bossone E, D'Andrea A, D'Alto M, et al. Echocardiography in pulmonary arterial hypertension: from diagnosis to prognosis. *J Am Soc Echocardiogr.* 2013;26(1):1-14.
245. Karnani NG, Reisfield GM, Wilson GR. Evaluation of chronic dyspnea. *Am Fam Physician.* 2005;71(8):1529-1537.
246. Gerges C, Gerges M, Lang MB, et al. Diastolic pulmonary vascular pressure gradient: a predictor of prognosis in "out-of-proportion" pulmonary hypertension. *Chest.* 2013;143(3):758-766.

247. Guazzi M, Gomberg-Maitland M, Arena R. Pulmonary hypertension in heart failure with preserved ejection fraction. *J Heart Lung Transplant.* 2015;34(3):273-281.
248. Lam CS, Roger VL, Rodeheffer RJ, Borlaug BA, Enders FT, Redfield MM. Pulmonary hypertension in heart failure with preserved ejection fraction: a community-based study. *J Am Coll Cardiol.* 2009;53(13):1119-1126.
249. Cheng CP, Ukai T, Onishi K, et al. The role of ANG II and endothelin-1 in exercise-induced diastolic dysfunction in heart failure. *Am J Physiol Heart Circ Physiol.* 2001;280(4):H1853-1860.
250. Sharifov OF, Schiros CG, Aban I, Denney TS, Gupta H. Diagnostic Accuracy of Tissue Doppler Index E/e' for Evaluating Left Ventricular Filling Pressure and Diastolic Dysfunction/Heart Failure With Preserved Ejection Fraction: A Systematic Review and Meta-Analysis. *Journal of the American Heart Association.* 2016;5(1).
251. Scalia GM, Scalia IG, Kierle R, et al. ePLAR - The echocardiographic Pulmonary to Left Atrial Ratio - A novel non-invasive parameter to differentiate pre-capillary and post-capillary pulmonary hypertension. *Int J Cardiol.* 2016;212:379-386.
252. Notomi Y, Thomas JD. Presto untwisting and legato filling. *JACC Cardiovasc Imaging.* 2009;2(6):717-719.
253. Mulvagh S, Quinones MA, Kleiman NS, Cheirif J, Zoghbi WA. Estimation of left ventricular end-diastolic pressure from Doppler transmitral flow velocity in cardiac patients independent of systolic performance. *J Am Coll Cardiol.* 1992;20(1):112-119.
254. Unzek S, Popovic ZB, Marwick TH, Diastolic Guidelines Concordance I. Effect of recommendations on interobserver consistency of diastolic function evaluation. *JACC Cardiovasc Imaging.* 2011;4(5):460-467.
255. Oh JK, Park SJ, Nagueh SF. Established and novel clinical applications of diastolic function assessment by echocardiography. *Circulation Cardiovascular imaging.* 2011;4(4):444-455.
256. Santos M, Rivero J, McCullough SD, et al. E/e' Ratio in Patients With Unexplained Dyspnea: Lack of Accuracy in Estimating Left Ventricular Filling Pressure. *Circ Heart Fail.* 2015;8(4):749-756.
257. Rivas-Gotz C, Khoury DS, Manolios M, Rao L, Kopelen HA, Nagueh SF. Time interval between onset of mitral inflow and onset of early diastolic velocity by tissue Doppler: a novel index of left ventricular relaxation: experimental studies and clinical application. *J Am Coll Cardiol.* 2003;42(8):1463-1470.
258. Nagueh SF, Mikati I, Kopelen HA, Middleton KJ, Quinones MA, Zoghbi WA. Doppler estimation of left ventricular filling pressure in sinus tachycardia. A new application of tissue doppler imaging. *Circulation.* 1998;98(16):1644-1650.
259. Ommen SR, Nishimura RA, Appleton CP, et al. Clinical utility of Doppler echocardiography and tissue Doppler imaging in the estimation of left ventricular filling pressures: A comparative simultaneous Doppler-catheterization study. *Circulation.* 2000;102(15):1788-1794.
260. Penicka M, Bartunek J, Trakalova H, et al. Heart failure with preserved ejection fraction in outpatients with unexplained dyspnea: a pressure-volume loop analysis. *J Am Coll Cardiol.* 2010;55(16):1701-1710.
261. Kadappu KK, Boyd A, Eshoo S, et al. Changes in left atrial volume in diabetes mellitus: more than diastolic dysfunction? *Eur Heart J Cardiovasc Imaging.* 2012;13(12):1016-1023.
262. Stritzke J, Markus MR, Duderstadt S, et al. The aging process of the heart: obesity is the main risk factor for left atrial enlargement during aging the MONICA/KORA (monitoring of trends and determinations in cardiovascular disease/cooperative research in the region of Augsburg) study. *J Am Coll Cardiol.* 2009;54(21):1982-1989.

263. Hoendermis ES, Liu LC, Hummel YM, et al. Effects of sildenafil on invasive haemodynamics and exercise capacity in heart failure patients with preserved ejection fraction and pulmonary hypertension: a randomized controlled trial. *Eur Heart J.* 2015;36(38):2565-2573.
264. Hilde JM, Skjorten I, Grotta OJ, et al. Right ventricular dysfunction and remodeling in chronic obstructive pulmonary disease without pulmonary hypertension. *J Am Coll Cardiol.* 2013;62(12):1103-1111.
265. Singh A, Addetia K, Maffessanti F, Mor-Avi V, Lang RM. LA Strain for Categorization of LV Diastolic Dysfunction. *JACC Cardiovasc Imaging.* 2017;10(7):735-743.
266. Maniar HS, Prasad SM, Gaynor SL, Chu CM, Steendijk P, Moon MR. Impact of pericardial restraint on right atrial mechanics during acute right ventricular pressure load. *Am J Physiol Heart Circ Physiol.* 2003;284(1):H350-357.
267. Brennan JM, Blair JE, Goonewardena S, et al. Reappraisal of the use of inferior vena cava for estimating right atrial pressure. *Journal of the American Society of Echocardiography : official publication of the American Society of Echocardiography.* 2007;20(7):857-861.
268. Magnino C, Omede P, Avenatti E, et al. Inaccuracy of Right Atrial Pressure Estimates Through Inferior Vena Cava Indices. *The American journal of cardiology.* 2017.
269. Patel AR, Alsheikh-Ali AA, Mukherjee J, et al. 3D echocardiography to evaluate right atrial pressure in acutely decompensated heart failure correlation with invasive hemodynamics. *JACC Cardiovasc Imaging.* 2011;4(9):938-945.
270. Querejeta Roca G, Campbell P, Claggett B, Solomon SD, Shah AM. Right Atrial Function in Pulmonary Arterial Hypertension. *Circulation Cardiovascular imaging.* 2015;8(11):e003521; discussion e003521.
271. Miller MJ, McKay RG, Ferguson JJ, et al. Right atrial pressure-volume relationships in tricuspid regurgitation. *Circulation.* 1986;73(4):799-808.
272. Kircher BJ, Himelman RB, Schiller NB. Noninvasive estimation of right atrial pressure from the inspiratory collapse of the inferior vena cava. *The American journal of cardiology.* 1990;66(4):493-496.
273. Mintz GS, Kotler MN, Parry WR, Iskandrian AS, Kane SA. Real-time inferior vena caval ultrasonography: normal and abnormal findings and its use in assessing right-heart function. *Circulation.* 1981;64(5):1018-1025.
274. Moreno FL, Hagan AD, Holmen JR, Pryor TA, Strickland RD, Castle CH. Evaluation of size and dynamics of the inferior vena cava as an index of right-sided cardiac function. *The American journal of cardiology.* 1984;53(4):579-585.
275. Padeletti M, Cameli M, Lisi M, Malandrino A, Zaca V, Mondillo S. Reference values of right atrial longitudinal strain imaging by two-dimensional speckle tracking. *Echocardiography.* 2012;29(2):147-152.
276. Saha SK, Soderberg S, Lindqvist P. Association of Right Atrial Mechanics with Hemodynamics and Physical Capacity in Patients with Idiopathic Pulmonary Arterial Hypertension: Insight from a Single-Center Cohort in Northern Sweden. *Echocardiography.* 2016;33(1):46-56.
277. Goldhammer E, Mesnick N, Abinader EG, Sagiv M. Dilated inferior vena cava: a common echocardiographic finding in highly trained elite athletes. *Journal of the American Society of Echocardiography : official publication of the American Society of Echocardiography.* 1999;12(11):988-993.
278. Beigel R, Cercek B, Luo H, Siegel RJ. Noninvasive evaluation of right atrial pressure. *Journal of the American Society of Echocardiography : official publication of the American Society of Echocardiography.* 2013;26(9):1033-1042.
279. Taniguchi T, Ohtani T, Nakatani S, et al. Impact of Body Size on Inferior Vena Cava Parameters for Estimating Right Atrial Pressure: A Need for Standardization?

Journal of the American Society of Echocardiography : official publication of the American Society of Echocardiography. 2015;28(12):1420-1427.
280. Peluso D, Badano LP, Muraru D, et al. Right atrial size and function assessed with three-dimensional and speckle-tracking echocardiography in 200 healthy volunteers. *Eur Heart J Cardiovasc Imaging.* 2013;14(11):1106-1114.
281. Gaynor SL, Maniar HS, Prasad SM, Steendijk P, Moon MR. Reservoir and conduit function of right atrium: impact on right ventricular filling and cardiac output. *Am J Physiol Heart Circ Physiol.* 2005;288(5):H2140-2145.
282. Bening C, Leyh R. Right atrial contractile dynamics are impaired in patients with postcapillary pulmonary hypertension. *Exp Ther Med.* 2016;12(2):792-798.
283. Sakata K, Uesugi Y, Isaka A, et al. Evaluation of right atrial function using right atrial speckle tracking analysis in patients with pulmonary artery hypertension. *J Echocardiogr.* 2016;14(1):30-38.
284. D'Ascenzi F, Cameli M, Padeletti M, et al. Characterization of right atrial function and dimension in top-level athletes: a speckle tracking study. *Int J Cardiovasc Imaging.* 2013;29(1):87-94.
285. Fukuda Y, Tanaka H, Ryo-Koriyama K, et al. Comprehensive Functional Assessment of Right-Sided Heart Using Speckle Tracking Strain for Patients with Pulmonary Hypertension. *Echocardiography.* 2016;33(7):1001-1008.
286. Bunce C. Correlation, agreement, and Bland-Altman analysis: statistical analysis of method comparison studies. *Am J Ophthalmol.* 2009;148(1):4-6.
287. Jue J, Chung W, Schiller NB. Does inferior vena cava size predict right atrial pressures in patients receiving mechanical ventilation? *Journal of the American Society of Echocardiography : official publication of the American Society of Echocardiography.* 1992;5(6):613-619.
288. Lau EM, Manes A, Celermajer DS, Galie N. Early detection of pulmonary vascular disease in pulmonary arterial hypertension: time to move forward. *Eur Heart J.* 2011;32(20):2489-2498.
289. Clements PJ, Tan M, McLaughlin VV, et al. The pulmonary arterial hypertension quality enhancement research initiative: comparison of patients with idiopathic PAH to patients with systemic sclerosis-associated PAH. *Ann Rheum Dis.* 2012;71(2):249-252.
290. Lambova S. Cardiac manifestations in systemic sclerosis. *World J Cardiol.* 2014;6(9):993-1005.
291. Zile MR, Bourge RC, Redfield MM, Zhou D, Baicu CF, Little WC. Randomized, double-blind, placebo-controlled study of sitaxsentan to improve impaired exercise tolerance in patients with heart failure and a preserved ejection fraction. *JACC Heart failure.* 2014;2(2):123-130.
292. Redfield MM, Chen HH, Borlaug BA, et al. Effect of phosphodiesterase-5 inhibition on exercise capacity and clinical status in heart failure with preserved ejection fraction: a randomized clinical trial. *JAMA.* 2013;309(12):1268-1277.
293. Borlaug BA, Lewis GD, McNulty SE, et al. Effects of sildenafil on ventricular and vascular function in heart failure with preserved ejection fraction. *Circ Heart Fail.* 2015;8(3):533-541.
294. Grignola JC. Hemodynamic assessment of pulmonary hypertension. *World J Cardiol.* 2011;3(1):10-17.
295. Coghlan JG, Denton CP, Grunig E, et al. Evidence-based detection of pulmonary arterial hypertension in systemic sclerosis: the DETECT study. *Ann Rheum Dis.* 2014;73(7):1340-1349.
296. Robbins IM, Hemnes AR, Pugh ME, et al. High prevalence of occult pulmonary venous hypertension revealed by fluid challenge in pulmonary hypertension. *Circ Heart Fail.* 2014;7(1):116-122.

297. Fujimoto N, Borlaug BA, Lewis GD, et al. Hemodynamic responses to rapid saline loading: the impact of age, sex, and heart failure. *Circulation.* 2013;127(1):55-62.
298. D'Alto M, Romeo E, Argiento P, et al. Echocardiographic prediction of pre- versus postcapillary pulmonary hypertension. *Journal of the American Society of Echocardiography : official publication of the American Society of Echocardiography.* 2015;28(1):108-115.
299. Humbert M, Yaici A, de Groote P, et al. Screening for pulmonary arterial hypertension in patients with systemic sclerosis: clinical characteristics at diagnosis and long-term survival. *Arthritis and rheumatism.* 2011;63(11):3522-3530.
300. Maor E, Grossman Y, Balmor RG, et al. Exercise haemodynamics may unmask the diagnosis of diastolic dysfunction among patients with pulmonary hypertension. *Eur J Heart Fail.* 2015;17(2):151-158.
301. Simonneau G, Galie N, Jansa P, et al. Long-term results from the EARLY study of bosentan in WHO functional class II pulmonary arterial hypertension patients. *Int J Cardiol.* 2014;172(2):332-339.
302. Khanna D, Gladue H, Channick R, et al. Recommendations for screening and detection of connective tissue disease-associated pulmonary arterial hypertension. *Arthritis and rheumatism.* 2013;65(12):3194-3201.
303. Dorfmuller P, Humbert M, Perros F, et al. Fibrous remodeling of the pulmonary venous system in pulmonary arterial hypertension associated with connective tissue diseases. *Hum Pathol.* 2007;38(6):893-902.
304. Mayes MD, Lacey JV, Jr., Beebe-Dimmer J, et al. Prevalence, incidence, survival, and disease characteristics of systemic sclerosis in a large US population. *Arthritis and rheumatism.* 2003;48(8):2246-2255.
305. Condliffe R, Howard LS. Connective tissue disease-associated pulmonary arterial hypertension. *F1000Prime Rep.* 2015;7:06.
306. Rhee RL, Gabler NB, Praestgaard A, Merkel PA, Kawut SM. Adverse Events in Connective Tissue Disease-Associated Pulmonary Arterial Hypertension. *Arthritis Rheumatol.* 2015;67(9):2457-2465.
307. Muangchan C, Canadian Scleroderma Research G, Baron M, Pope J. The 15% rule in scleroderma: the frequency of severe organ complications in systemic sclerosis. A systematic review. *J Rheumatol.* 2013;40(9):1545-1556.
308. Elhai M, Meune C, Avouac J, Kahan A, Allanore Y. Trends in mortality in patients with systemic sclerosis over 40 years: a systematic review and meta-analysis of cohort studies. *Rheumatology (Oxford).* 2012;51(6):1017-1026.
309. Clements PJ, Lachenbruch PA, Seibold JR, et al. Skin thickness score in systemic sclerosis: an assessment of interobserver variability in 3 independent studies. *J Rheumatol.* 1993;20(11):1892-1896.
310. Peled N, Shitrit D, Fox BD, et al. Peripheral arterial stiffness and endothelial dysfunction in idiopathic and scleroderma associated pulmonary arterial hypertension. *J Rheumatol.* 2009;36(5):970-975.
311. Soriano A, Afeltra A, Shoenfeld Y. Is atherosclerosis accelerated in systemic sclerosis? Novel insights. *Curr Opin Rheumatol.* 2014;26(6):653-657.
312. Stefania LM, Raluca IM, Carmen MM, Mircea C, Dragos V. Atherosclerosis in Systemic Sclerosis: a Modern Controversy. *Maedica (Buchar).* 2015;10(3):248-256.
313. Hasegawa T, Boden-Albala B, Eguchi K, et al. Impaired flow-mediated vasodilatation is associated with increased left ventricular mass in a multiethnic population. The Northern Manhattan Study. *Am J Hypertens.* 2010;23(4):413-419.
314. Meiszterics Z, Timar O, Gaszner B, et al. Early morphologic and functional changes of atherosclerosis in systemic sclerosis-a systematic review and meta-analysis. *Rheumatology (Oxford).* 2016;55(12):2119-2130.

315. Takahashi T, Asano Y, Amiya E, et al. Clinical correlation of brachial artery flow-mediated dilation in patients with systemic sclerosis. *Mod Rheumatol.* 2014;24(1):106-111.
316. Grattagliano V, Iannone F, Praino E, et al. Digital laser doppler flowmetry may discriminate "limited" from "diffuse" systemic sclerosis. *Microvasc Res.* 2010;80(2):221-226.
317. Roustit M, Blaise S, Millet C, Cracowski JL. Reproducibility and methodological issues of skin post-occlusive and thermal hyperemia assessed by single-point laser Doppler flowmetry. *Microvasc Res.* 2010;79(2):102-108.
318. Matsuzawa Y, Kwon TG, Lennon RJ, Lerman LO, Lerman A. Prognostic Value of Flow-Mediated Vasodilation in Brachial Artery and Fingertip Artery for Cardiovascular Events: A Systematic Review and Meta-Analysis. *Journal of the American Heart Association.* 2015;4(11).
319. Schnabel RB, Schulz A, Wild PS, et al. Noninvasive vascular function measurement in the community: cross-sectional relations and comparison of methods. *Circulation Cardiovascular imaging.* 2011;4(4):371-380.
320. Hamburg NM, Palmisano J, Larson MG, et al. Relation of brachial and digital measures of vascular function in the community: the Framingham heart study. *Hypertension.* 2011;57(3):390-396.
321. Meier FM, Frommer KW, Dinser R, et al. Update on the profile of the EUSTAR cohort: an analysis of the EULAR Scleroderma Trials and Research group database. *Ann Rheum Dis.* 2012;71(8):1355-1360.
322. Tyndall AJ, Bannert B, Vonk M, et al. Causes and risk factors for death in systemic sclerosis: a study from the EULAR Scleroderma Trials and Research (EUSTAR) database. *Ann Rheum Dis.* 2010;69(10):1809-1815.
323. D'Andrea A, Bellissimo S, Scotto di Uccio F, et al. Associations of right ventricular myocardial function with skin and pulmonary involvement in asymptomatic patients with systemic sclerosis. *Ital Heart J.* 2004;5(11):831-839.
324. D'Andrea A, Stisi S, Caso P, et al. Associations between left ventricular myocardial involvement and endothelial dysfunction in systemic sclerosis: noninvasive assessment in asymptomatic patients. *Echocardiography.* 2007;24(6):587-597.
325. Pigatto E, Peluso D, Zanatta E, et al. Evaluation of right ventricular function performed by 3D-echocardiography in scleroderma patients. *Reumatismo.* 2015;66(4):259-263.
326. Ngian GS, Sahhar J, Proudman SM, Stevens W, Wicks IP, Van Doornum S. Prevalence of coronary heart disease and cardiovascular risk factors in a national cross-sectional cohort study of systemic sclerosis. *Ann Rheum Dis.* 2012;71(12):1980-1983.
327. Weber U, Glassford NJ, Eastwood GM, Bellomo R, Hilton AK. A pilot study of the relationship between Doppler-estimated carotid and brachial artery flow and cardiac index. *Anaesthesia.* 2015;70(10):1140-1147.
328. Chung L, Liu J, Parsons L, et al. Characterization of connective tissue disease-associated pulmonary arterial hypertension from REVEAL: identifying systemic sclerosis as a unique phenotype. *Chest.* 2010;138(6):1383-1394.